

Univerzita Karlova v Praze
Lékařská fakulta v Plzni

ANALÝZA A IDENTIFIKACE PROTEINŮ PŘI ORGÁNOVÝCH
DYSFUNKCÍCH POMOCÍ PROTEOMICKÝCH METOD

Zdeněk Tůma
Dizertační práce



Plzeň 2016

ABSTRAKT

Proteomika se zabývá hromadným studiem proteinů a jejich vlastností, především struktury a funkce. V medicíně bývá využívána pro analýzu fungování tkání a orgánů ve zdraví a nemoci a hledání biomarkerů. Metody zahrnují přípravu vzorku, separační techniky a hmotnostní spektrometrii. Protože neexistuje univerzální metoda pro analýzu libovolného biologického vzorku, proto analytické techniky vyžadují optimalizaci pro konkrétní typ vzorku a požadované výstupy.

Cílem práce bylo vytvořit metodické postupy a vyhodnotit proteomické výsledky ve dvou výzkumných rovinách: experimentální a klinické. První část práce obsahuje experimenty využívající proteomiku pro studium změny proteomu plazmy v klinicky relevantním prasečím modelu sepse vyvolané peritonitidou. Proteomické analýzy byly rovněž výchozí metodologickou strategií v experimentech zaměřených na fyziologii ledvin a patofyziologii akutního poškození ledvin v průběhu sepse. Analýzou biopsií ledvin byl sledován časový průběh změn proteomu způsobený sepsí a chirurgickým zásahem. Ve druhé části dizertační práce jsou zahrnuty práce zabývající se biokompatibilitou mimotělních očišťovacích metod. Byla připravena metoda pro analýzu proteinů interagujících s povrchem kapilár hemodialyzátorů a s adsorbenty systému náhrady funkce jater. Analýzou proteinů adsorbovaných na polysulfonové kapiláry dialyzátorů byla identifikována aktivace komplementu jako proces významný v biokompatibilitě dialyzátorů.

Klíčová slova

Proteom; Mitochondrie; Sepse; Elektroforéza; Hmotnostní spektrometrie; Biokompatibilita; Ledviny

ABSTRACT

Proteomics is the large-scale study of proteins, particularly their structures and functions. Proteomics has been utilized in medicine for investigation of disease mechanisms and biomarker discovery. Instrumental methods cover sample preparation, protein and peptide separation and mass spectrometry. At present, there is no proteomic method that can be used as universal for every sample. Analytical methods need to be adapted and optimized for certain samples.

The aim of this work was to create methodic procedures and to interpret results of experimental and clinical research. The first part of the thesis includes experiments utilizing proteomics to study changes in the plasma proteome clinically relevant porcine model of sepsis-induced peritonitis. Proteomic analyzes were also starting methodological strategies in experiments aimed at kidney physiology and pathophysiology of acute kidney injury during sepsis. Renal biopsies were analyzed in order to study the time course of proteome changes caused by sepsis and surgery. The second part of the thesis contains experiments studying biocompatibility. A method for elution of proteins interacting with adsorbents used in extracorporeal liver support system and with hemodialyzer capillaries was prepared. Analysis of proteins adsorbed to polysulfone capillaries identified complement activation as an important process involved in hemodialyzer biocompatibility.

Keywords

Proteome; Mitochondria; Sepsis; Electrophoresis; Mass spectrometry; Biocompatibility; Kidney

Prohlašuji, že tuto dizertační práci jsem vypracoval samostatně. Veškerou literaturu a ostatní prameny, z nichž jsem při přípravě čerpal, řádně cituji a dále uvádím v seznamu literatury. Současně souhlasím se zapůjčováním této práce.

Zdeněk Tůma

Datum:

Podpis: Zdeněk Tůma

Přehled použitých zkratk

2-DE	Dvojměrná gelová elektroforéza
AKI	Akutní poškození ledvin (acute kidney injury)
ANOVA	Analýza variance (analysis of variance)
ATP	Adenosintrifosfát
BN-PAGE	Nativní polyakrylamidová elektroforéza za přítomnosti Coomassie (blue-native polyacrylamide gel electrophoresis)
E/P	Poměr intenzity skvrn na gelech eluátů a plazmy
EDTA	Etylendiamintetraoctová kyselina
ESI	Ionizace elektrosprejem
ETS	Mitochondriální elektrontransportní systém
FPSA	Frakcionovaná separace plazmy a adsorpce
HABP	Protein vázající hyaluronan (hyaluronan binding protein)
CHAPS	3-[3-(cholamidopropyl) dimethylamonio]-1- propansulfonát
IEF	Izoelektrická fokusace
IPG	Imobilizovaný gradient pH
kDa	Kilodalton
LC-MS	Kapalinová chromatografie-hmotnostní spektrometrie
MALDI	Ionizace laserem za přítomnosti matrice (matrix-assisted laser desorption and ionization)
MAM	Membrány asociované s mitochondriemi
MASP	Manózu vázající lektin (MBL), MBL asociovaná serinová proteáza (MBL-associated serine protease)
MW	Molekulová hmotnost (molecular weight)
NHE-RF3	Na ⁺ /H ⁺ exchange regulatory cofactor 3
PCA	Analýza hlavních složek (principal component analysis)
pI	Izoelektrický bod
PMF	Peptidové mapování (peptide mass fingerprinting)
SDS	Dodecylsírán sodný
SELDI	Surface Enhanced Laser Desorption and Ionisation
SRM/MRM	Monitorování vybraných reakcí (selected reaction monitoring/multiple reaction monitoring)
SWATH	Sekvenční akvizice všech fragmentových spekter (Sequential Window Acquisition of all Theoretical Mass Spectra)
TOF	Analyzátor doby letu (time of flight)

Obsah

1. Úvod	6
2. Původní práce.....	8
2.1. Původní vědecké práce	8
2.2. Původní přehledové práce	9
2.3. Práce navazující na studovanou problematiku	9
3. Současný stav problematiky.....	10
3.1. Biologické vzorky využitelné pro proteomiku	10
3.2. Analytické metody v proteomice	12
3.3. Využití a potenciál proteomiky v medicíně	15
4. Legální a etické aspekty studií.....	16
5. Cíle studií.....	16
6. Experimentální práce	17
6.1. Analýza proteomu mitochondrií v ledvinách (studie I).....	17
6.2. Proteom plazmy v časně fázi sepse (studie II).....	19
6.3. Proteom tkáně ledvin v průběhu sepse (studie III)	21
7. Klinické studie	23
7.1. Interaktom systému pro náhradu funkce jater (studie IV)	23
7.2. Analýza interakce krve s kapilárami dialyzátorů.....	25
7.3. Proteomická analýza aktivace komplementu při kontaktu krve s kapilárami dialyzátorů (studie VI).....	27
8. Závěry	28
8.1. Experimentální studie	28
8.2. Klinické studie	28
9. Podpora	29
10. Poděkování.....	29
11. Literatura	30
12. Přílohy	36

1. Úvod

Dysfunkce orgánů jsou komplexní a závažné stavy nastávající v důsledku akutních a chronických onemocnění. Porozumění mechanismům, identifikace biomarkerů a validace účinků léčby může pomoci k vývoji specifické léčby a zlepšení prognózy pacientů [Wang et al. 2006].

Proteomika je soubor technik, přístupů a konceptů, které usilují o kvantitativní a kvalitativní popis a porovnání proteomu. Jako proteom se označuje kompletní sada proteinů včetně jejich izoform a posttranslačních modifikací nacházející se v konkrétním okamžiku v daném organismu, tkáni nebo buňce. Moderní proteomické technologie umožňují identifikaci a kvantitativní hodnocení velkého množství proteinů (v ideálním případě všech proteinů přítomných ve vzorku) a umožňují získat podstatně více informací, než metody zaměřené na sledování definované sady analytů [Bohra et al. 2013].

V současnosti se proteomika v medicíně uplatňuje v oblastech výzkumu fyziologie tkání, orgánů ve zdraví a nemoci, hledání a validaci biomarkerů, a pro vývoj nových léků. Při výzkumu fyziologického a patofyziologického fungování tkání a orgánů je snaha identifikovat co nejvíce proteinů přítomných v daném systému, prozkoumat jejich strukturu a vzájemné interakce a navrhnout fungování metabolických drah. Pomocí metod pro relativní kvantifikaci je možné porovnat expresi proteinů mezi několika stavy, případně v různých časových okamžicích. Nástroje bioinformatiky umožňují zasadit výsledky do kontextu a navrhnout modely fungování metabolických drah. V případě hledání biomarkerů je podstatnou částí standardizace metod, kvantifikace relativní i absolutní pomocí syntetických vnitřních standardů. Aplikace proteomiky při experimentech na modelových organismech pak může přispět k pochopení mechanismů chorob, k identifikaci biomarkerů a testování nových způsobů léčby.

První oddíl dizertační práce obsahuje experimentální práce zabývající se proteomem mitochondrií v ledvinách [I], proteomem plazmy [II] a tkáně [III] na zvířecím modelu sepse, druhý oddíl se zabývá analýzou biofilmu proteinů u mimotělních eliminačních metod [IV-VI], a ve třetím oddílu jsou pak zahrnuty další práce využívající metody proteomiky a práce s mitochondriemi.

Tématem první práce je analýza proteomu mitochondrií v ledvinách [I]. Mitochondrie jsou důležitými dodavateli energie pro procesy aktivního transportu látek v ledvinách. Změny mitochondriálního metabolismu ledvin jsou pozorovány při chorobách (např. sepse, akutní selhání ledvin, diabetes) nebo při působení xenobiotik. V přiložené studii jsme se zajímali o proteom mitochondrií ledvin a prokázali rozdíly odpovídající fyziologickým funkcím kůry a dřeně ledvin.

Další práce se zabývá analýzou plazmy při sepsi indukované peritonitidou na praseti [II]. Podíl autora dizertace je v přípravě vzorků a provádění separace proteinů pomocí elektroforézy. Pomocí analýz založených na dvojrozměrné elektroforéze byly v plazmě prasat s navozenou peritonitidou hledány proteiny, jejichž zastoupení se změnilo vlivem peritonitidy.

Proteom biopsií ledvin v průběhu sepse je popsán v práci [III]. Podíl autora dizertace je v přípravě vzorků, provádění separace proteinů pomocí elektroforézy a analýze výsledků. Byly analyzovány biopsie ledvin odebrané ve dvou časových bodech v průběhu sepse. Porovnáním proteomu biopsií septických zvířat a zvířat kontrolní skupiny, která podstoupila anestezii a operační zákrok, byly nalezeny proteiny specificky reagující na sepsi.

Práce [IV-VI] se týkají analýzy biokompatibility materiálů používaných k dialyzačním metodám. V první případové studii [IV] byly analyzovány proteiny adsorbované na kolony systému náhrady jater Prometheus. Podíl autora dizertace je ve vypracování metody pro získání proteinů adsorbovaných na očišťovací kolony a provedení separace a identifikace proteinů. Byly získány profily proteinů odlišné na koloně s neutrálně nabitou pryskyřicí a na koloně s anexamem. Některé z identifikovaných proteinů bylo možné dát do souvislosti s procesy probíhajícími při poškození jater.

Studie [V] popisuje analýzu proteinů adsorbovaných na stěny kapilár dialyzátoru při hemodialýze. Cílem bylo popsat spektrum proteinů, které se podílí na reakci krve s umělým povrchem. Pro zkoumání proteinů adsorbovaných na stěny kapilár byla připravena metoda eluce. Mezi adsorbovanými proteiny byly identifikovány proteiny účastníci se aktivace koagulační kaskády, komplementu a adheze leukocytů. Poznání mechanismu těchto procesů může posloužit k vývoji kompatibilnějších materiálů a prevenci chronického zánětu vyvolaného opakovaným kontaktem krve s umělým povrchem dialyzátoru [Bonomini et al. 2015].

Studie [VI] využívá metodiku vyvinutou v předcházející práci a aplikuje ji na rozsáhlejší soubor pacientů. Proteiny adsorbované na kapiláry byly zkoumány u souboru 16 pacientů léčených dialýzou a ve vzorcích plazmy byly stanoveny hladiny parametrů systémové biokompatibility. Proteomická analýza poskytla data pro potvrzení lektinové dráhy komplementu způsobené kontaktem krve s dialyzační membránou.

Z prací navazujících na studovanou problematiku jsou zařazeny práce studující vliv propolisů na mitochondrie ve spermích, ve které bylo využito stanovení aktivity mitochondriálních enzymů ke standardizaci respirometrických dat a práce zabývající se charakterizací bakteriálních cefalosporinů, kde byla použita hmotnostní spektrometrie pro identifikaci bakteriálních proteinů.

2. Původní práce

Tato dizertační práce vychází z komentovaného souboru původních experimentálních prací a přehledového článku, jejichž seznam je uveden níže.

2.1. Původní vědecké práce

2.1.1. Experimentální

- I. TŮMA, Zdeněk; KUNCOVÁ, Jitka; MAREŠ, Jan; MATĚJOVIČ, Martin. Mitochondrial proteomes of porcine kidney cortex and medulla: foundation for translational proteomics. *Clin Exp Nephrol*. 2016, 20, s. 39-49. **IF 2,020**
- II. THONGBOONKERD, Visith; CHIANGJONG, Wararat; MAREŠ, Jan; MORAVEC, Jiří; TŮMA, Zdeněk; KARVUNIDIS, Thomas; SINCHAIKUL, Supachok; CHEN, Shui-Tein; OPATRNÝ, Karel Jr.; MATĚJOVIČ, Martin. Altered plasma proteome during an early phase of peritonitis-induced sepsis. *Clin Sci (Lond)*, 2009, 116, s. 721-730. **IF 5,598**
- III. MATĚJOVIČ, Martin; TŮMA, Zdeněk; MORAVEC, Jiří; VALEŠOVÁ, Lenka; SÝKORA, Roman; CHVOJKA, Jiří; BENEŠ, Jan; MAREŠ, Jan. Renal proteomic responses to severe sepsis and surgical trauma: dynamic analysis of porcine tissue biopsies. *Shock*, 2016. **IF 3,045**

2.1.2. Klinické

- IV. MAREŠ, Jan; THONGBOONKERD, Visith; TŮMA, Zdeněk; MORAVEC, Jiří; MATĚJOVIČ, Martin. Specific adsorption of some complement activation proteins to polysulfone dialysis membranes during hemodialysis. *Kidney international*. 2009,76, s. 404-413. **IF 8,563**
- V. MAREŠ, Jan; RICHTROVÁ, Pavlína; HRIČINOVÁ, Alena; TŮMA, Zdeněk; MORAVEC, Jiří; LYSÁK, Daniel; MATĚJOVIČ, Martin. Proteomic profiling of blood-dialyzer interactome reveals involvement of lectin complement pathway in hemodialysis-induced inflammatory response. *Proteomics Clin Appl*, 2010, 4, s. 829-838. **IF 2,956**
- VI. MAREŠ, Jan; THONGBOONKERD, Visith; TŮMA, Zdeněk; MORAVEC, Jiří; KARVUNIDIS, Thomas; MATĚJOVIČ, Martin. Proteomic analysis of proteins bound to adsorption units of extracorporeal liver support system under clinical conditions. *J Proteome Res*, 2009, 8, s. 1756-1764. **IF 4,245**

2.2.Původní přehledové práce

- VII. TŮMA, Zdeněk; KUNCOVÁ, Jitka; MAREŠ, Jan; GRUNDMANOVÁ, Martina; MATĚJOVIČ, Martin. Proteomic approaches to the study of renal mitochondria. *Biomed Pap Med Fac Univ Palacky Olomouc Czech Repub*, 2016, doi: 10.5507/bp.2016.012. **IF 1,200**

2.3.Práce navazující na studovanou problematiku

- VIII. ČEDÍKOVÁ, Miroslava; MIKLÍKOVÁ, Michaela; STACHOVÁ, Lenka; GRUNDMANOVÁ, Martina; TŮMA, Zdeněk; VĚTVIČKA, Václav; ZECH, Nicolas; KRÁLÍČKOVÁ, Milena; KUNCOVÁ, Jitka. Effects of the Czech propolis on sperm mitochondrial function. *Evid Based Complement Alternat Med*, 2014, s. 248768. **IF 1,880**
- IX. PAPAGIANNITSIS, Constantinos; KOTSAKIS, Stathis; TŮMA, Zdeněk; GNIADKOWSKI, Marek; MIRIAGOU, Vivi; HRABÁK, Jaroslav. Identification of CMY-2-Type Cephalosporinases in Clinical Isolates of Enterobacteriaceae by MALDI-TOF MS. *Antimicrob Agents Chemother*, 2014, 58, s. 2952-2957. **IF 4,476**

3. Současný stav problematiky

Proteomika se snaží analyzovat strukturu a kvantitu ideálně všech proteinů obsažených v konkrétním okamžiku v daném organismu, tkáni nebo buňce. Využívá k tomu biochemické separační metody, hmotnostní spektrometrii a bioinformatické nástroje. Pro experimenty zabývající se analýzou metabolických drah, sledování vlivu léčiv a navrhování personalizovaných terapií a hledání biomarkerů v současnosti neexistuje jedna univerzální proteomická metoda aplikovatelná na jakýkoliv biologický materiál. Pro experimenty je proto nezbytné vybrat a přizpůsobit z mnoha způsobů přípravy vzorku, separačních a hmotnostně spektrometrických metod ty, které poskytnou optimální výsledky vzhledem ke studovanému problému.

Výraznou složkou metodik proteomiky je hmotnostní spektrometrie. Vynález technik schopných ionizovat velké, netěkavé a termolabilní molekuly proteinů a peptidů pomocí ionizace laserem za přítomnosti matrice - MALDI [Karas et al. 1988] a ionizace elektrospřejem -ESI [Yamashita et al. 1984]) umožnil využití hmotnostní spektrometrie k analýze struktury proteinů a posttranslačních modifikací. Pro identifikaci proteinů byla vyvinuta metoda peptidového mapování (peptide mass fingerprinting, PMF), kdy jsou měřeny hmotnosti peptidů připravených proteolytickým štěpením izolovaných proteinů a hledána jejich shoda s teoretickými hodnotami odvozenými ze sekvencí známých proteinů [Thiede et al. 2005]. Tandemová hmotnostní spektrometrie, při které je iont peptidu v hmotnostním spektrometru fragmentován a následně změřena hmotnost fragmentů, je nepostradatelný nástroj pro detailní analýzu aminokyselinové sekvence a případných modifikací [Cottrell 2011]. V současnosti jsou používány a rozvíjeny metody kvantitativní analýzy proteomů pomocí hmotnostní spektrometrie. Jejich parametry jsou dostatečné k tomu, aby bylo možné kvantifikovat proteiny s dostatečnou specificitou v komplexních směsích v dynamickém rozsahu až 5 řádů [Liebler et al. 2013].

Proteomika urazila cestu od publikování seznamů identifikovaných proteinů k detailní vysokovýkonné kvantitativní charakterizaci proteomů a integraci s dalšími metodami (např. genomika [Cesnik et al. 2016], metabolomika [Klawitter et al. 2008]). Cílená analýza pomocí hmotnostní spektrometrie je vhodná pro identifikaci biomarkerů a jejich validaci [Liu et al. 2013].

3.1. Biologické vzorky využitelné pro proteomiku

Proteomika je v medicíně využívána pro zkoumání mechanismů chorob a patologických stavů, zkoumání odpovědi na léčbu a v identifikaci biomarkerů. Protože v současnosti neexistuje univerzální metoda pro analýzu kompletního proteomu určitého systému, je nutné pro maximální využití potenciálu proteomiky pečlivě naplánovat experiment. Proteomická analýza zahrnuje výběr biologického materiálu, aplikaci analytických metod pro separaci proteinů a peptidů, identifikaci proteinů pomocí hmotnostní spektrometrie a interpretaci výsledků. Techniky pro zpracování velmi malých množství vzorků s řádově mikrogramovými množstvími proteinů mohou umožnit analýzu proteomu tkáňových biopsií [Feist et al. 2015].

3.1.1. Tělní tekutiny

Tělní tekutiny představují důležitý zdroj proteinů, jejichž výhody oproti vzorkům tkání nebo biopsiím spočívají v nižší invazivitě odběru a snadnějším zpracování. Pomocí proteomiky bylo analyzováno široké spektrum tekutin (plazma, moč [Thongboonkerd et al. 2006], sliny [Amado et al. 2013], mozkomíšní mok [Kroksveen et al. 2011], broncholavážní tekutina a další).

Plazma a sérum představují dobře dostupný materiál. Proteom plazmy zahrnuje kromě abundantních proteinů (např. albumin, transferin) také proteiny vylučované tkáněmi, imunoglobuliny, proteinové a peptidové hormony a cytokiny [Anderson et al. 2002, Nanjappa et al. 2014]. Proteom plazmy a séra je ovlivněn mnoha preanalytickými faktory, zejména volbou antikoagulantu, variabilitou času srážení, hemolýzou, rychlostí a časem centrifugace, teplotou uložení a opakovanými cykly zmrazení a rozmrazení vzorku [Tuck et al. 2009, Pasella et al. 2013]. Proto je důležitá standardizace těchto kroků, obzvláště pro snížení technické variability při mezilaboratorních multicentrických studiích [Rai et al. 2005]. Sérum je kvalitativně odlišné od plazmy v tom, že převážná část fibrinogenu je přeměněna na sraženinu fibrinu a spolu s destičkami odstraněna. Proteom séra je ovlivněn zejména dobou srážení, rychlostí odstředování odstranění fibrinové sraženiny, teplotou skladování a použitými zkumavkami pro sběr materiálu [Lundblad 2003]. Rozsah koncentrací individuálních proteinů v plazmě dosahuje 10-12 řádů a abundantní proteiny plazmy (např. albumin, transferin) představují více než 99% hmotnostního podílu proteinů v plazmě. Techniky odstraňující abundantní proteiny jsou využívány pro zlepšení detekce ostatních proteinů plazmy [Dayon et al. 2013].

Moč obsahuje proteiny po ultrafiltraci plazmy a proteiny pocházející z orgánů účastnících se na její tvorbě a vylučování (ledviny a močový trakt). Proteom moči poskytuje informace o fyziologii a patofyziologii ledvin a močového ústrojí, a může být využit pro detekci biomarkerů jejich chorob [Rodriguez-Suarez et al. 2014]. Podobně jako u plazmy, přítomnost abundantních proteinů znesnadňuje detekci proteinů s nízkými koncentracemi [Kushnir et al. 2009]. Složení proteomu moči se mění v závislosti na čase odběru, dietě, tělesné zátěži a zdravotním stavu [Nagaraj et al. 2011]. Zpracování moči před proteomickou analýzou obvykle vyžaduje odstranění iontů solí pomocí SPE, precipitace nebo dialýzy [Thongboonkerd et al. 2006]. Významný zdroj biomarkerů představují také peptidy v moči [Coon et al. 2008].

Zvláštní případ představují tekutiny z mimotělních očišťovacích metod. Hemodialyzát a hemodiafiltrát mohou poskytnout informaci o uremických toxinech hromadících se v krvi při poruše funkce ledvin [Walden et al. 2007]. Komplikací je to, že obsahují proteiny ve velmi nízké koncentraci a naopak koncentrace elektrolytů (solí) je poměrně vysoká; vyžadují tedy zakonzentrování a odstranění elektrolytů např. dialýzou nebo precipitací organickými rozpouštědly.

3.1.2. Tkáně

Analýzou tkání můžeme zachytit změny metabolických a signálních drah způsobené nemocí a vytipovat proteiny vhodné jako cíle terapie. Získání tkáně je invazivní proces a dostupnost vzorků tkání od pacientů je tedy omezená. Jako zdroj materiálu jsou důležité tkáně zvířat (modely chorob). S vývojem citlivějších analytických metod je možné analyzovat biopsie [Guo et al. 2015].

Zpracování tkání pro proteomické analýzy zahrnuje homogenizaci tkáně a extrakci proteinů. Použité metody do jisté míry závisí na analytické technice použité pro další práci. V případě zkoumání rozpustných proteinových komplexů je nutné pracovat s detergenty, které jsou schopny solubilizovat komplexy bez disociace (např. N-dodecyl-beta-D-maltosid). Pro většinu aplikací využívajících dvojrozměrné elektroforézy jsou využívány pufrы obsahující denaturující a redukční činidla [Shaw et al. 2003]. Membránové proteiny jsou obtížně dostupné a pro jejich získání jsou nutné komplikované solubilizační postupy [Rabilloud 2009]. Při přípravě vzorku pro metody založené na spojení kapalinové chromatografie a hmotnostní spektrometrie pak je cílem proteolyticky rozštěpit proteiny vzorku na peptidy s co největším účinkem [Wisniewski et al. 2009].

3.1.3. Subcelulární organely

Protože počet individuálních proteinů a dynamický rozsah jejich koncentrací překračuje možnosti stávajících analytických metod, proto je vhodné snížit komplexitu vzorku. Častým způsobem je izolace subcelulárních organel [Andreyev et al. 2010]. Analýzou izolovaných organel lze dosáhnout lepšího pokrytí jejich proteomu, protože jsou odstraněny abundanční proteiny (např. cytoplazmy). Příkladem hojně používaného postupu je separace mitochondrií pomocí diferenciální centrifugace. Metoda je založena na rozdílu hustot organel. Provádí se jako série centrifugačních kroků, při nichž sedimentují jednotlivé organely [Graham 2001]. Dalšími možnostmi izolace organel jsou imunopurifikace a separace pomocí magnetických mikročástic. Separace organel byla zatím využita při analýze proteomu mitochondrií [Jiang et al. 2012], peroxisomů [Kikuchi et al. 2004], buněčného jádra [Korfali et al. 2012] a mikrosomů [Peng et al. 2012]. Při izolaci subcelulárních organel je důležitá standardizace izolačního postupu a je také vhodné provést kontrolu čistoty organel [Satori et al. 2013]. Při analýzách proteomů takto izolovaných subcelulárních organel jsou často nacházeny proteiny pocházející z jiných organel. Jsou známy případy spojení organel, např. membrány asociované s mitochondriemi (mitochondria associated membranes, MAM), kdy pomocí proteinových komplexů dochází ke spojení mitochondrií a endoplazmatického retikula [Raturi et al. 2013]. Metody a aplikace proteomiky na analýzu mitochondrií v ledvinách jsou shrnuty v přehledovém článku VII.

3.2. Analytické metody v proteomice

Proteomika spoléhá na spojení separačních metod, hmotnostní spektrometrie a bioinformatických přístupů pro analýzu dat. V separačních metodách využívaných proteomikou jsou hojně zastoupeny gelové elektroforézy a kapalinová chromatografie. Pro hmotnostní spektrometrii jsou vyvíjeny spektrometry, které umožňují stále rychlejší identifikaci a citlivější detekci proteinů.

3.2.1. Metody založené na gelových elektroforézách.

Elektroforetické separace představují podstatnou část technik využívaných v proteomice. Dvojměrná elektroforéza (2-DE) je kombinací separace pomocí izoelektrické fokusace (IEF) a elektroforézy na polyakrylamidovém gelu (SDS-PAGE) a představuje jednu z hojně používaných technik. Po vizualizaci pomocí barviva selektivně se vázajícího na molekuly proteinů se proteiny zobrazí jako skvrny, jejichž poloha na gelu je určena hmotností a izoelektrickým bodem daného proteinu a intenzita skvrny je pak úměrná množství proteinu. Rozlišení se počítá na stovky až tisíce proteinových skvrn [Magdeldin et al. 2014]. Porovnáním obrazů gelů pro sérii vzorků lze pak zjistit relativní změnu proteinů [Rabilloud et al. 2010]. Po zpracování více vzorků v sérii lze pomocí specializovaných programů porovnávat intenzitu skvrn a tím zjistit, jak se množství daných proteinů mění [Chevalier 2010]. Porovnáním obrazů gelů pomocí specializovaných programů lze porovnávat intenzitu proteinových skvrn a tím zjistit, jak se relativní koncentrace daných proteinů v jednotlivých vzorcích mění [Chevalier 2010, Rabilloud et al. 2010]. Začlenění vnitřního standardu do elektroforetické separace zvyšuje reprodukovatelnost. Uspořádání DIGE, kdy vzorky a vnitřní standard jsou označeny fluorescenčními barvivy a separovány na jednom gelu, zvyšuje reprodukovatelnost separace [O'Connell et al. 2009]. Mezi výhody dvojměrná elektroforézy patří uváděny robustnost a kompatibilita s dalšími kroky (např. imunochemická detekce, identifikace pomocí hmotnostní spektrometrie). Významnými nevýhodami jsou obtíže při separaci proteinů s extrémními hodnotami izoelektrických bodů a hydrofobních proteinů, úzký dynamický rozsah detekce proteinů a náročnost na čas a práci [Magdeldin et al. 2014].

Mezi další metody využívající separaci na gelu patří nativní elektroforéza (BN-PAGE). Principem je separace v přítomnosti barviva Coomassie, které se reverzibilně váže na proteiny a uděluje jim záporný náboj. Touto separací je možné získat nativní proteinové komplexy a zkoumat jejich podjednotkové složení [Wittig et al. 2008].

Identifikace vybraných proteinů (např. těch, u kterých je zjištěna změna exprese) může pak být provedena pomocí proteolytického štěpení proteinů v gelu [Shevchenko et al. 2006] a analýzy vzniklých peptidů pomocí hmotnostní spektrometrie [Aebersold et al. 2001].

3.2.2. Metody založené na kapalinových chromatografiích

Postupy využívající on-line spojení kapalinového chromatografu a hmotnostního spektrometru jsou používány s rostoucí tendencí. Proteiny jsou bez předchozí separace podrobeny proteolytickému štěpení, vzniklé peptidy jsou separovány kapalinovým chromatografem. Následně jsou okamžitě analyzovány hmotnostním spektrometrem připojeným na výstup chromatografické kolony. Pomocí hmotnostního spektrometru jsou změřeny hmotnosti peptidů a získána jejich fragmentační spektra. K identifikaci pak slouží fragmentační data a na základě přiřazení aminokyselinových sekvencí k peptidům jsou pak identifikovány proteiny. Informace o proteinech je odvozována z peptidů. Tato akvizice fragmentačních spekter je klíčová pro identifikaci a kvantifikaci proteinů [Bateman et al. 2014]. Pro složité směsi proteinů, kdy separace na chromatografii nedostačuje a dochází k překryvu piků peptidů, byly vyvinuty metody využívající vícerozměrné chromatografické separace [Zhang et al. 2010].

3.2.3. Využití proteinových čipů

Proteinové čipy představují rychlou metodu pro analýzu velkého množství analytů současně [Sutandy et al. 2013]. Jejich potenciál je v rychlém screeningu definované sady proteinů. Proteinové čipy mají využití při sledování změn exprese proteinů, protein-proteinových interakcí, hledání a validaci biomarkerů [Ramachandran et al. 2008]. Metody využívající detekci pomocí hmotnostního spektrometru (Surface Enhanced Laser Desorption and Ionisation, SELDI), využívají různé typy povrchů, na nichž jsou zachytávány proteiny požadovaných vlastností. Zachycené molekuly jsou pak analyzovány pomocí hmotnostního spektrometru MALDI-TOF. Jejich využití je pro hledání a validaci biomarkerů [Muthu et al. 2016].

3.2.4. Hmotnostní spektrometrie v proteomice

Hmotnostní spektrometrie je zásadní součástí proteomických metod. S vynálezem a rozvojem tzv. měkkých ionizačních technik ionizace laserem za přítomnosti matrice (MALDI) [Karas et al. 1988] a ionizace elektrosprejem (ESI) [Yamashita et al. 1984] bylo možné využít hmotnostní spektrometrii pro studium struktury biomolekul včetně proteinů. Hmotnostní spektrometrie je využívána pro analýzu aminokyselinové sekvence proteinů včetně případných posttranslačních modifikací a pro kvantitativní analýzy. V současnosti existuje široká škála spektrometrů využívajících ionizaci MALDI nebo ESI ve spojení s různými analyzátory (kvadrupól, iontová past, orbitrap, analyzátor doby letu) [Holcapek et al. 2012].

Metoda peptidového mapování (peptide mass fingerprinting, PMF) je nejčastěji používaná pro proteiny separované pomocí gelových elektroforéz. Gelové skvrny obsahující protein jsou specificky štěpeny proteázou a hmotnosti výsledných proteolytických peptidů jsou měřeny na hmotnostním spektrometru [Shevchenko et al. 2006]. Hmotnosti těchto peptidů jsou pak porovnávány s hmotnostmi peptidů odvozených ze známých sekvencí proteinů [Aebersold et al. 2001]. Tandemová hmotnostní spektrometrie spočívá ve fragmentaci peptidového prekurzoru a měření hmotnosti fragmentů. Hmotnostní spektra fragmentů pak poskytnou detailní informace o aminokyselinovém složení peptidu a případných modifikacích [Cottrell 2011].

Při využití vysokoúčinné kapalinové chromatografie je fragmentace peptidů pomocí tandemové hmotnostní spektrometrie klíčová jak pro identifikaci proteinů, tak i pro jejich kvantifikaci [Michalski et al. 2011]. Značení proteinů nebo peptidů pomocí izotopických sloučenin je prováděno před separací a hmotnostně spektrometrickou analýzou [Zhou et al. 2014]. Postupy využívající MS data bez značení sledují intenzitu signálu prekurzoru nebo počet fragmentačních spekter daného peptidu jako míru relativní kvantity [Bantscheff et al. 2007]. Tyto způsoby nejsou cílené na určitý protein a snaží se kvantifikovat co nejvíce peptidů/proteinů v analyzovaném vzorku.

Pro identifikaci proteinů jsou po změření hmotnostního spektra vybrány prekurzory s intenzitou nad určitým prahem, je spuštěna jejich fragmentace a zaznamenána data [Wu et al. 2002]. Takto však nejsou pokryty málo abundantní peptidy. Metody využívající fragmentaci prekurzorů v širším rozsahu hmotností (např. sekvenční akvizice všech fragmentových spekter, SWATH) umožňují zachytit teoreticky fragmenty všech peptidů, které vstupují do hmotnostního spektrometru. Při těchto experimentech není předem definován prekurzor a k fragmentaci jsou brány prekurzory v určitém rozsahu hmotností. Výsledkem jsou digitální mapy fragmentačních spekter, které lze

opakovaně interpretovat [Liu et al. 2013]. Hmotnostně spektrometrickými metodami monitorování vybraných reakcí (SRM/MRM) lze cíleně stanovit peptidy s velmi vysokou citlivostí, která je na úrovni detekce pomocí imunochemických metod a tím přesně kvantifikovat peptidové fragmenty vznikající v hmotnostním spektrometru [Lange et al. 2008]. Pro hledání a validaci biomarkerů je podstatná schopnost cíleně a specificky kvantifikovat peptidy vybraného proteinu pomocí hmotnostní spektrometrie [Law et al. 2013]. Absolutní kvantifikace pomocí hmotnostní spektrometrie je možná s použitím izotopově značeného syntetického peptidu jako vnitřního standardu [Bantscheff et al. 2007].

3.3. Využití a potenciál proteomiky v medicíně

Jednou z oblastí je zjišťování mechanismu chorob a působení toxických látek. Analýza proteomu zachytí údaje o změně zastoupení proteinů v průběhu patologického stavu. Ze změn expresí proteinů zapojených v metabolických drahách lze usuzovat na jejich průběh, aktivaci nebo potlačení [Bugger et al. 2009]. Pomocí bioinformatických nástrojů je možné proteiny se změněnou expresí graficky přímo „mapovat“ nebo přiřadit do známých metabolických a regulačních drah a tak vytvářet modely metabolismu při patologických stavech [Husi et al. 2013]. Další zpřesnění mechanismů a modelů metabolických drah lze dosáhnout kombinací proteomických a metabolických dat [Go et al. 2014]. Schopnost proteomiky v rychlém, přesném a reprodukovatelném kvantifikaci velkého množství proteinů může přispět k realizaci personalizované medicíny tím, že poskytne výkonné diagnostické přístupy založené na monitorování molekulárních fenotypů pacientů [Del Boccio et al. 2016].

Proteomika má velký potenciál v hledání biomarkerů. S tím kontrastuje fakt, že dosud velmi málo markerů nalezených pomocí proteomiky je využíváno pro klinickou diagnostiku [Zhang et al. 2010]. Příčinou mohou být nedostatky v designu dosud provedených proteomických studií. Při provádění proteomických analýz zaměřených na identifikaci biomarkerů je klíčové naplánovat kroky analýzy (definice klinického problému, sběr a zpracování vzorků, získání a analýza dat a validace výsledků) [Heegaard et al. 2015]. S rozvojem technologie hmotnostních spektrometrů a zlepšováním jejich citlivosti a reprodukovatelnosti je rozvíjeno využití hmotnostní spektrometrie namísto imunochemických metod pro validaci proteinových biomarkerů [Addona et al. 2011]. Studie využívající proteomiku pro výzkum biomarkerů lze najít v širokém spektru oborů [Colvin et al. 2015, Shao et al. 2015, Schanstra et al. 2015]. Velkou oblast představují studie zabývající se výzkumem biomarkerů karcinomů [Sallam 2015].

4. Legální a etické aspekty studií

Všechny experimentální práce byly řádně schváleny etickou komisí při Lékařské fakultě UK v Plzni.

Protokoly klinických studií byly schváleny etickou komisí při FN v Plzni a Lékařské fakultě UK v Plzni a od všech pacientů zahrnutých do studií byl získán informovaný souhlas s účastí ve studiích.

5. Cíle studií

Mechanismy ve zdraví a nemoci pomocí proteomiky

- Vypracovat metodiku proteomické analýzy mitochondriálních proteinů pomocí kombinace centrifugační separace mitochondrií, dvojrozměrné gelové elektroforézy a hmotnostně spektrometrické identifikace proteinů. Použít proteomiku pro analýzu plazmy a tkáně u prasečích modelů sepse.

Klinické studie

- Izolovat proteiny adsorbované na umělé materiály a identifikovat proteiny specificky interagující s membránami mimotělních hemopurifikačních metod.

6. Experimentální práce

6.1. Analýza proteomu mitochondrií v ledvinách (studie I)

6.1.1. Design studie

Studie byla určena k analýze proteomu mitochondrií kůry a dřeně ledvin prasete. Pro analýzu byly použity ledviny z šesti zdravých prasat. Z každé ledviny byl vyříznut vzorek kůry a dřeně a pomocí diferenciální centrifugace byly připraveny příslušné mitochondriální frakce. Proteiny mitochondriálních frakcí byly separovány na dvojrozměrné elektroforéze (2-DE) a pomocí analýzy obrazů byly hledány proteinové skvrny, jejichž intenzita se lišila více než dvojnásobně mezi mitochondriální frakcí kůry a dřeně. Tyto skvrny byly vyříznuty z gelů, proteiny v nich obsažené byly identifikovány pomocí trypsinového štěpení a hmotnostní spektrometrie. Pro detekci čistoty mitochondriálních frakcí a pro ověření proteomických výsledků byl použit Western blotting.

6.1.2. Výsledky a diskuse

Mitochondrie byly izolovány pomocí diferenciální centrifugace a pomocí western blottingu byla zkoumána přítomnost frakcí jiných subcelulárních organel. Bylo zjištěno, že připravené mitochondriální frakce obsahují malou část proteinů cytosolu a jádra. Na elektroforetických gelech mitochondriálních frakcí bylo detekováno 635 proteinových skvrn. Dále bylo hodnoceno 343 z nich, které se vyskytovaly na více než 90% elektroforetických gelů. 161 z nich se statisticky významně lišilo mezi frakcemi kůry a dřeně. 81 z nich s více než dvojnásobným rozdílem v intenzitě bylo identifikováno pomocí hmotnostní spektrometrie. Z nich pak 41 skvrn obsahovalo mitochondriální proteiny; ve zbylých byly identifikovány proteiny, u nichž byla uvedena lokalizace v endoplazmatickém retikulu, cytoplazmě, peroxisomech a cytoskeletu. Pro validaci proteomických dat byla provedena analýza několika vybraných proteinů pomocí Western blottingu. Data byla v dobré shodě s daty získanými pomocí proteomiky.

V mitochondriálních frakcích kůry ledvin byly větším množstvím detekovány enzymy zapojené v beta-oxidaci, metabolismu aminokyselin, a glukoneogenezi. Tyto procesy jsou charakteristické pro proximální tubulus a odpovídají velkému zastoupení mitochondrií v proximálním tubulu. Naše data se shodovala s dřívějšími pracemi, které uvádí beta oxidaci jako převažující zdroj energie pro procesy aktivního transportu v proximálním tubulu. Proximální tubulus je místem reabsorpce aminokyselin z primární moči. Aminokyseliny jsou využívány jako zdroj energie nebo v syntetických drahách. Glukoneogeneze v kůře ledvin využívá substráty (aminokyseliny a laktát) resorbované v proximálním tubulu.

Spektrum proteinů hojnějších v mitochondriálních frakcích dřeně ledvin zahrnovalo proteiny zapojené v elektrontransportním systému (ETS), enzymy citrátového cyklu a mitochondriální poriny. U některých enzymů citrátového cyklu byla dříve publikována jejich zvýšená exprese při adaptaci buněk na hypoxii. Byla popsána zvýšená exprese pyruvátdehydrogenázy a zvýšená aktivita 2-oxoglutarátdehydrogenázy při hypoxii [Dukhande et al. 2011]. Dále byla dříve zjištěna zvýšená exprese podjednotky 5B cytochrom c oxidázy v reakci na hypoxii [Trueblood et al. 1988].

Proto se domníváme, že zvýšení exprese některých podjednotek ETS systému může souviset s adaptací mitochondrií dřeně na prostředí s nižší dostupností kyslíku.

Ačkoliv mitochondriální proteom představuje podmnožinu proteomu tkáně a tedy elektroforéza by nemusela být limitována přítomností abundantních proteinů, použití 2-DE pro studium mitochondrií je limitováno horší detekcí hydrofobních proteinů. Mezi limitace studie patří také výběr tkáně. Rozdělení ledviny na kůru a dřeň představuje nejjednodušší způsob redukce komplexity. Pro detailnější popis populací mitochondrií v ledvinách by bylo nutné izolovat segmenty nefronu. Mitochondriální frakce obsahovaly proteiny z jiných subcelulárních organel. Tyto organely mohly být izolovány spolu s mitochondriemi nebo asociovány s mitochondriální membránou [Lebiedzinska et al. 2009]. Komplexy obsahující proteiny patřící do jiných subcelulárních organel jsou nacházeny v mitochondriích připravených pomocí centrifugace v hustotním gradientu [Reifschneider et al. 2006] a mohou tedy být součástí mitochondriálního proteomu, ačkoliv jsou lokalizovány na jiné organele.

6.2. Proteom plazmy v časně fázi sepse (studie II)

6.2.1. Design studie

Ve studii byl zkoumán proteom plazmy při sepsi indukované peritonitidou na praseti. Během experimentu byla monitorována hemodynamika, výměna kyslíku, oxidativní a nitrosativní stres a další parametry. Vzorky plazmy pro proteomickou analýzu byly odebrány ve dvou časových bodech: před započítím sepse a 12 hodin po indukci sepse. Proteiny plazmy byly separovány na dvojrozměrné elektroforéze (2-DE). Bylo provedeno srovnání obrazů gelů za účelem nalezení proteinů, jejichž kvantita byla ovlivněna sepsí. Tyto proteiny byly vyříznuty z gelů, štěpeny trypsinem a identifikovány pomocí hmotnostní spektrometrie a bylo zjišťováno jejich zapojení v patofyziologických procesech.

6.2.2. Výsledky a diskuse

Proteiny plazmy byly nejprve separovány pomocí 2-DE v rozsahu hodnot izoelektrických bodů (pI) 3 až 10. Bylo zjištěno, že velká většina proteinů byla zobrazena v oblasti odpovídající pI 4 až 7. Pro dosažení lepšího rozlišení byly k analýze vzorků plazmy použity IPG stripky s rozsahem hodnot pI 4-7. Po provedení separace bylo na každém gelu zobrazeno přibližně 1500 proteinových skvrn. Porovnáním obrazů gelů plazmy před započítím sepse a po 12 hodinách byly zjištěny změny relativních intenzit u 36 proteinových skvrn; ty byly vyříznuty z gelů a byla provedena identifikace pomocí hmotnostní spektrometrie MALDI-TOF/TOF. Některé proteiny byly identifikovány ve více skvrnách pravděpodobně z důvodu přítomnosti různých izoform daného proteinu nebo možných posttranslačních modifikací [Deng et al. 2012]. Celkem bylo identifikováno 22 proteinů ve 30 skvrnách se vzestupem intenzity a 5 proteinů v 6 skvrnách s poklesem intenzity způsobeném sepsí. Dále bylo pomocí softwaru Pathway Tools zkoumáno, jakých metabolických procesů se tyto proteiny účastní. Většina proteinů byla zapojena v odpovědi na zánět, a některé v oxidativním a nitrosativním stresu.

Význam některých proteinů lze dobře zasadit do kontextu současných poznatků o patofyziologii sepse. Protein CD14 je komponent vrozeného imunitního systému a funguje jako koreceptor při detekci bakteriálního lipopolysacharidu. Již dříve byl doložen vzrůst hladiny tohoto proteinu u pacienta se sepsí. Haptoglobin patří mezi proteiny akutní fáze a je zapojen v odpovědi na oxidativní stres jako scavenger radikálů. Také váže hemoglobin uvolněný z erytrocytů a tím inhibuje jeho oxidativní aktivitu. Hemopexin je další protein působící při oxidativním stresu jako protizánětlivá molekula a scavenger radikálů, který váže hem a transportuje jej do jater. Zvýšená hladina haptoglobinu v plazmě byla zjištěna u pacientů v sepsi [Kalenka et al. 2006] a zvýšená hladina hemopexinu v plazmě byla popsána na myším modelu sepse [Ren et al. 2007]. Je možné, že zvýšená hladina haptoglobinu při sepsi má ochranný efekt u pacientů majících zvýšenou hladinu volného hemoglobinu v plazmě [Janž et al. 2013].

Mezi limitace studie patří skutečnosti, že analýza proteomu plazmy byla provedena pouze v jednom časovém bodě po indukci sepse. Analýza vzorků odebíraných ve více časových bodech by mohla poskytnout detailnější informace o dynamice průběhu sepse. Použití plazmy pro proteomiku je také komplikováno omezeným dynamickým rozsahem detekce proteinů separovaných na 2-DE, kdy dochází k zamaskování málo abundantních proteinů hojnými proteiny

plazmy. Přesto studie poskytuje první literární analýzu proteomu plazmy u klinicky relevantního, velkého zvířecího modelu sepse.

6.3. Proteom tkáně ledvin v průběhu sepse (studie III)

6.3.1. Design studie

V této studii byl sledován proteom ledvin v průběhu sepse. Ve studii bylo použito 12 prasat, u kterých byla indukována sepsis intravenózní infúzí živých bakterií a 5 zvířat v kontrolní skupině, která podstoupila pouze anestezii a operační zásah. Ve třech časových bodech (před počátkem sepse, po 12 hodinách a po 22 hodinách od indukce sepse) byly odebrány biopsie kůry ledvin. Proteiny byly z biopsií extrahovány pufrům obsahujícím solubilizační činidla obsahující chaotropní látky (močovinu, thiomočovinu) a detergent (3-[(3-cholamidopropyl)dimethylamonio]propan-1-sulfonát, CHAPS) a dále separovány pomocí 2D elektroforézy (2-DE). Byla provedena analýza obrazů gelů za účelem získání hodnot relativních intenzit proteinových skvrn. Zajímali jsme se o proteiny, jejichž exprese se měnila v důsledku sepse a o proteiny, na jejichž expresi měla vliv anestezie s chirurgickým zásahem. Pro redukci počtu proměnných a pro usnadnění dalšího statistického zpracování byla nejprve použita explorativní analýza a pomocí t-testu hledány spoty, které se statisticky významně lišily mezi počátkem a některým z časových bodů experimentu. Tyto proteinové skvrny byly vybrány k identifikaci pomocí hmotnostní spektrometrie MALDI-TOF/TOF.

Pro vyhodnocení multidimenzionálních dat bylo použito hierarchické shlukování. Rozdíly mezi skupinami byly vyhodnoceny pomocí analýzy rozptylu (ANOVA).

6.3.2. Výsledky a diskuse

Akutní poškození ledvin je jednou z nejčastějších a prognosticky závažných orgánových dysfunkcí způsobených sepsí. Bližší pochopení jeho složité patogeneze brání nedostupnost molekulárních analýz tkáně ledvin od pacientů. Perspektivní cestou je proto analýza dynamických změn renální proteomu na modelu, který má vysoký translační potenciál do klinické medicíny. Prase je považováno za dobrý modelový organismus pro genetickou a fyziologickou podobnost s člověkem [Bendixen 2014].

Protože samotná operace a anestezie mohou ovlivnit proteom ledvin, je důležité nejdříve definovat vliv těchto intervencí na renální proteom. Jako kontrolní skupina byla proto použita v tomto experimentu zvířata, u kterých byl proveden pouze chirurgický inzult.

Analýza rozdílů v proteomech kontrolní skupiny ukázala změny oproti výchozímu stavu. Poté byly zkoumány rozdíly v proteomech septické skupiny. V kontrolní skupině bylo nalezeno 62 proteinových skvrn, které byly v nějakém bodě změněny oproti výchozímu stavu a v nich bylo identifikováno 11 proteinů, u septické skupiny pak 106 skvrn vykazujících změnu a obsahujících 29 proteinů. Na data bylo aplikováno hierarchické shlukování, pomocí něž byla data separována do clusterů odpovídajících kontrolní a septické skupině. To znamená, že chirurgický inzult sám o sobě způsobil detekovatelnou změnu proteomu, kterou lze odlišit od vlivu sepse.

Ve skupině změněných proteinů u kontrolní skupiny byly identifikovány proteiny fungující v drahách stresu endoplazmatického retikula a oxidativního stresu, mitochondriálního energetického metabolismu, tubulárního transportu a signalizace imunitní a zánětlivé odpovědi.

Pro nalezení proteinů, jejichž změna je vyvolaná pouze sepsí, byla použita analýza ANOVA. Jako vstupní data byly použity hodnoty skvrn, které se statisticky významně lišily mezi počátkem a

některým z časových bodů experimentu. Bylo nalezeno 20 proteinových skvrn, jejichž intenzita byla změněna jen v septické skupině nebo vykazovala odlišné chování mezi septickou a kontrolní skupinou. Proteiny se změněnou expresí byly chaperony opravující proteiny, mitochondriální proteiny, proteiny zapojené v procesech stresu endoplazmatického retikula a oxidativním stresu.

Významnou částí proteinů podléhajících změnám u septické skupiny jsou mitochondriální proteiny. Zvýšené množství mitochondriální ATP-syntázy zjištěné naším experimentem je v protikladu s některými studiemi [Porta et al. 2006, May et al. 2012] a může být chápáno jako argument proti selhávání bioenergetiky v brzké fázi sepse. Další potenciálně zajímavou skutečností je vzrůstající exprese proteinu NHE-RF3 (Na⁺/H⁺ exchange regulatory cofactor 3). Tento enzym je důležitý pro regulaci exprese a aktivity některých membránových receptorů a transportérů v renálních tubulech.

Použití biopsií namísto celé ledviny je výhodné pro sledování změn proteomu v několika časových bodech během sepse. Použití biopsií však může vnášet zkreslení. Ledvina je složena z několika druhů buněk a zastoupení různých typů buněk mezi biopsiemi může být variabilní. Poškození ledvin v průběhu AKI také není uniformní a v ledvině mohou existovat oblasti hypoxických nefronů vedle zdravých oblastí [Matejovic et al. 2016]. Detailnější analýza by vyžadovala separaci jednotlivých druhů buněk a využití citlivějších analytických technik (např. LC-MS). Přesto je práce první svého druhu, která ukazuje na rozsáhlý a dynamicky se chovající tkáňový proteom ledvin v průběhu sepse a přináší nové, hypotézu generující výsledky.

7. Klinické studie

7.1. Interaktom systému pro náhradu funkce jater (studie IV)

7.1.1. Design studie

Cílem studie bylo vyvinout techniku pro analýzu proteinů zachycených v adsorpčních kolonách systému pro náhradu funkce jater (Prometheus, Fresenius Medical Care, DE). Systém Prometheus nahrazuje detoxikační funkci jater pomocí spojení frakcionované separace plazmy a adsorpce (FPSA) s high-flux hemodialýzou [Santoro et al. 2006]. Separovaná plazma je pak vedena přes kolonu obsahující vysoce porézní neutrálně nabitou pryskyřici s velkým vnitřním povrchem (Prometh1) a kolonu s aniontovou pryskyřicí (anexem) sloužící pro adsorpci toxinů z albuminu (Prometh2).

Ve studii byly zkoumány proteiny adsorbované na kolony Prometh1 a Prometh2 po proceduře provedené u pacienta s akutním chronickým selháním jater. Před počátkem procedury byla odebrána plazma. Po ukončení procedury byly obě kolony vyprázdněny, promyty PBS pufrem a napuštěny elučními roztoky. Pro kolonu Prometh1 byl použit roztok dodecylsírany sodného (SDS) a pro Prometh2 pak roztok kyseliny octové. Po 30minutové inkubaci byly roztoky vypuštěny a připraveny pro analýzu. Proteiny obsažené v těchto eluátech byly separovány na 2-DE. Pomocí analýzy obrazů byly zjištěny hodnoty izoelektrického bodu a molekulové hmotnosti, porovnány obrazy plazmy a eluátů, a intenzity skvrn byly použity k hodnocení adsorpce proteinů. Vybrané skvrny byly vyříznuty z gelů, štěpeny trypsinem a proteiny pak identifikovány pomocí hmotnostní spektrometrie MALDI-TOF/TOF.

7.1.2. Výsledky a diskuse

Pro studii byl přizpůsoben postup eluce proteinů z umělých povrchů [Ishikawa et al. 2006]. Rostoky pro uvolnění proteinů z povrchů kolon byly vybírány s ohledem na charakter materiálu adsorpčních kolon. Pro neutrální kolonu Prometh1, kde jsme očekávali více hydrofobních proteinů, byl použit roztok SDS a pro kolonu Prometh2 s anexem byl použit kyseliny octové.

Na polyakrylamidových 2-DE gelech Prometh1 bylo detekováno 148 proteinových skvrn, na gelech Prometh2 pak 163 skvrn. Většina z nich se nacházela v oblasti pI 4,8-6,8 a hmotnosti 30-150 kDa. Obrazy gelů v obou eluátech se mezi sebou významně lišily; 38 skvrn mělo odlišnou abundanci, a 64 skvrn vykazovalo odlišné zastoupení při srovnání gelů eluátů a plazmy.

Pro hodnocení adsorpce proteinů na materiál kolon byl použit poměr intenzity skvrn na gelech eluátů a plazmy (E/P). Na gelech Prometh1 byla hodnota E/P vyšší než 2,0 u 33 skvrn a nižší než 0,5 u 53 skvrn; na gelech Prometh2 pak mělo 32 skvrn hodnotu E/P vyšší než 2,0 a 71 hodnotu E/P nižší než 0,5. Z rozložení parametrů molekulové hmotnosti a izoelektrického bodu vyplývá, že proteiny s vyšší hmotností se adsorbovaly více na Prometh1 a proteiny s nižším pI výrazněji na Prometh2. Selektivní adsorpce proteinů by se částečně dala vysvětlit fyzikálními vlastnostmi proteinů a materiálu kolon. V eluátu kolony Prometh2 převládaly proteiny s nízkým izoelektrickým bodem (negativně nabitě proteiny), což odpovídá tomu, že kolona byla pokryta anexem. V eluátu z kolony Prometh1 se nacházely proteiny s vyšší molekulovou hmotností. Vysvětlení není úplně jasné, možná hrála roli větší afinita pryskyřice obsažené v Prometh1 k hydrofobním proteinům.

Pomocí hmotnostní spektrometrie bylo identifikováno 72 skvrn z Prometh1, které obsahovaly 18 proteinů a 93 skvrn z Prometh2, které obsahovaly 30 proteinů. Proteiny s nejvyšším poměrem E/P a tedy nejintenzivnější adsorpcí byly transthyretin, trypsin-2, prothrombin, protein vázající hyaluronan (HABP), a protein vázající retinol byly nalezeny na Prometh2. U některých proteinů bylo možné dohledat potenciální důsledky jejich eliminace. Transthyretin, který byl zjištěn jako hojně se adsorbující na Prometh2, váže v plazmě tyroxin a jeho hladina bývá snižena během dysfunkce jater. Protein vázající retinol vytváří komplex s bílkovinou transportujícím vitamin A, jeho snížená hodnota může být markerem malnutrice.

Protein vázající hyaluronan (HABP) byl nalezen jako výrazně se adsorbující na Prometh2. Tento protein je zapojen v kaskádě procesů přestavby jaterní tkáně při poškození jater. Při poškození jater byla pozorována přeměna prekursoru HABP na aktivní formu rozštěpením na lehký a těžký řetězec [Choi-Miura et al. 2001]. Bylo navrženo, že aktivovaný HABP může účinkovat v kaskádě přestavby tkáně následující po poškození jater. Na gelu Prometh2 byl HABP detekován ve skvrně odpovídající hmotnosti lehkého řetězce. V hmotnostním spektru pak byly nalezeny peptidy se sekvencí odpovídající tomuto lehkému řetězci.

Tento experiment byl navržen za účelem sestavení metody získání proteinů a jejich identifikace, proto nebylo možné udělat detailnější závěry o klinických důsledcích odstraňování proteinů.

7.2. Analýza interakce krve s kapilárami dialyzátorů (studie V)

7.2.1. Design studie

Cílem studie bylo vyvinout metodu získání proteinů adsorbovaných na membránu, provést proteomickou analýzu a hledat proteiny zapojené v procesu interakce krve s umělým povrchem kapilár dialyzátoru. Do studie bylo zahrnuto 5 pacientů léčených v dialyzačním středisku FN v Plzni (věk 58-82 let, doba jejich léčení dialýzou 5-42 měsíců). Od každého pacienty byly ze tří po sobě následujících procedur odebrány dialyzátory a plazma. Po ukončení hemodialýzy byl dialyzátor propláchnut roztokem Plasmalyte. Poté byl do dialyzátoru napuštěn roztok ethylendiamintetraoctové kyseliny (EDTA) ve fosfátovém pufru a recirkulován pomocí čerpadla. Roztok byl vypuštěn a do dialyzátoru byl napuštěn 40% roztok kyseliny octové a recirkulován pomocí čerpadla. Po recirkulaci byl roztok vypuštěn a použit k proteomické analýze. Po zakoncentrování a dialýze byly proteiny obsažené v plazmě, roztoku EDTA a roztoku kyseliny octové separovány pomocí 2-DE. Analýza obrazů gelů byla provedena za účelem porovnání zastoupení a relativní kvantitativní proteinů v těchto třech materiálech. Vybrané proteiny vykazující rozdíly v zastoupení byly identifikovány pomocí hmotnostní spektrometrie MALDI-TOF/TOF.

7.2.2. Výsledky a diskuse

Pro získání proteinů adsorbovaných na membrány byla použita metoda zahrnující sekvenci proplachů dialyzátoru. Nejprve byly odstraněny zbytky plazmy roztokem Plasmalyte. K odstranění adheovaných buněk byl pak aplikován roztok EDTA ve fosfátovém pufru [Grooteman et al. 1996] který je uváděn jako účinný v uvolnění adheovaných leukocytů. K uvolnění proteinů byl použit roztok kyseliny octové.

Koncentrace proteinů v EDTA proplachu a v kyselině octové byly vyšší než v roztoku Plasmalyte, kterým byl propláchnut dialyzátor na konci procedury. To znamenalo, že oba tyto roztoky uvolňují proteiny. Proto pro ověření kvality eluce proteinů byly analyzovány proteiny obsažené v EDTA proplachu, a srovnány s plazmou a eluátem v kyselině octové. Spoty detekované na gelech eluátu byly přítomné na EDTA proplachu a jejich intenzita se nelišila od plazmy. Tím bylo ověřeno, že v eluátu se nachází proteiny uvolněné z kapilár dialyzátoru.

Pro ověření efektivity elučního procesu byl na dvou dialyzátorech proveden pokus se sekvenční elucí roztokem SDS. První dialyzátor byl eluován postupně 40% kyselinou octovou následovanou 10% SDS, druhý dialyzátor stejnými roztoky v opačném pořadí. Množství proteinů získaných za použití pořadí roztoků kyselina octová-SDS byly 9,33 a 0,014 mg. Při opačném pořadí roztoků (SDS-kyselina octová) bylo získáno 6,99 a 2,85 mg proteinů. To dokazuje vhodnost použití roztoku kyseliny octové pro uvolnění maximálního množství proteinů z polysulfonové membrány. Výhoda kyseliny octové pro disociaci elektrostatických vazeb mezi proteiny a membránou ve srovnání s jinými rozpouštědly může být teoreticky přičítána potlačení povrchové negativity polysulfonové membrány acetátovými ionty.

Elektroforéza byla provedena v rozsahu hodnot pI 3-10 a molekulových hmotností 10-200 kDa. Po provedené elektroforéze byly na obrazech gelů hledány proteiny, které vykazovaly adsorpci na stěny kapilár, jako kritérium byl použit poměr intenzit proteinové skvrny na gelu s proteiny eluátu a odpovídající skvrny na gelu s proteiny plazmy (E/P). Proteinové skvrny vyskytující se na gelech u

všech pacientů (celkem 84) byly pak vybrány k identifikaci. Celkem bylo identifikováno 23 proteinů pocházejících z plazmy a erytrocytů.

Některé studie ukazují, že proteiny adsorbované na kapiláry nalezené v našem experimentu jsou zapojeny v interakci krve s umělým materiálem. Jsou to proteiny podílející se na aktivaci komplementu (komplement C3, ficolin-2, klusterin, MASP-1, MASP-2, komplement faktor H a komplement faktor H-related protein 1), proteiny zapojené v procesu srážení krve (fibrinogen, antitrombin a beta-2-glykoprotein-1), a protein zprostředkující adhezi a aktivaci leukocytů (amyloid P). Tyto proteiny vykazovaly vysokou hodnotu E/P, byly tedy ve velkém množství adsorbovány na povrch kapilár.

Srovnání hodnot izoelektrických bodů a molekulových hmotností odečtených z pozice skvrn na gelech s teoretickými hodnotami danými sekvencí proteinů ukázalo některé rozdíly. Ty by se daly vysvětlit komigrací abundančních proteinů (albuminu a hemoglobinu) a proteinů s podobnou molekulovou hmotností a izoelektrickým bodem. Nižší hmotnost u skvrn obsahujících komplement-3 a proteázy MASP1 a MASP2 odpovídala přítomnosti těchto proteinů jako aktivních forem vzniklých proteolytickým štěpením jejich prekurzorů. Ficolin-2 je protein z rodiny lektinů, tvoří komplexy s proteázami MASP 1 a 2. Po vazbě na buněčnou stěnu bakterií štěpí proteázy MASP a iniciuje lektinovou dráhu komplementu.

V rámci této studie byla vyvinuta a ověřena metoda eluce proteinů adsorbovaných na kapiláry dialyzátorů. Porovnání proteomu plazmy a adsorbovaných proteinů umožnilo nalezení proteinů specificky interagujících s materiálem kapilár. Výsledkem je nová hypotéza, že lektinová dráha přispívá k aktivaci komplementu při kontaktu krve s polysulfonovou membránou.

7.3. Proteomická analýza aktivace komplementu při kontaktu krve s kapilárami dialyzátorů (studie VI)

7.3.1. Design studie

Cílem studie bylo poskytnout vhled do procesů indukce zánětu a aktivace leukocytů a komplementu při hemodialýze. Do studie bylo zahrnuto 16 pacientů léčených v dialyzačním středisku Fakultní nemocnice v Plzni hemodialýzou s použitím polysulfonových dialyzátorů. Byly odebrány vzorky plazmy na začátku, po 15 minutách a po 4 hodinách od začátku hemodialýzy z proximálního i distálního portu (na vstupu a na výstupu z dialyzátoru). Po skončení hemodialýzy byly dialyzátory odpojeny a pro získání proteinů adsorbovaných na kapiláry byl použit protokol vyvinutý a publikovaný v předchozí práci (studie V). Plazma a eluát proteinů byly analyzovány pomocí 2-DE a proteiny byly identifikovány pomocí štěpení v gelu a hmotnostní spektrometrie MALDI-TOF/TOF. Koncentrace ficolinu, C5a a trombin/antitrombinu byly sledovány pomocí ELISA. Ve vzorcích plazmy byly stanoveny hladiny parametrů systémové biokompatibility (CD11b, CD14, CD15, CD62L, CD63 a CD66b).

7.3.2. Výsledky a diskuze

Eluáty proteinů byly analyzovány pomocí 2-DE a na obrazech gelů bylo detekováno 217 proteinových skvrn, přičemž 164 skvrn bylo přítomno u alespoň 50% pacientů a 42 přítomno u každého pacienta. Obrazy gelů eluátu byly porovnány s obrazy gelů plazmy a u 112 z nich se intenzity významně lišily od odpovídajících skvrn v plazmě. Pro každý spot byl vypočten poměr intenzity v eluátu a plazmě (E/P) jako míra vazby daného proteinu na membránu kapilár. Pro redukci komplexity dat byla provedena analýza hlavních složek (PCA). Proteinové spoty byly podle dvou hlavních složek rozděleny do tří skupin. Proteiny byly dále identifikovány pomocí hmotnostní spektrometrie. Abundantní proteiny plazmy vykazovaly přibližně stejnou kvantitu na gelech plazmy a eluátu byly seskupeny v první skupině. V další skupině byly seskupeny intracelulární enzymy pocházející z lyzovaných erytrocytů zachycených v dialyzátoru. Třetí skupina proteinů byly proteiny plazmy s výrazně vyšší kvantitou na gelech eluátů. U těchto jsme předpokládali selektivní adsorpci díky specifické interakci s vnitřním povrchem kapilár. Tyto proteiny bylo možné zařadit do významných fyziologických procesů. Mezi nimi byly lektinová a alternativní dráha komplementu (ficolin 2, proteázy MASP, properdin), adheze buněk na substráty (tropomyosiny, aktiny, caldesmon, vinculin).

Pro další ověření identity proteinů bylo provedeno srovnání naměřené molekulové hmotnosti s teoretickou hodnotou. U proteinových skvrn obsahujících proteiny MASP-1, MASP-2 a komplement C3 bylo zjištěno, že se nachází na oblasti s menší molekulovou hmotností, než by odpovídalo teoretickým hodnotám. Detailním ověřením výsledků hmotnostní spektrometrie byla nalezena sekvence odpovídající jejich formám vzniklým proteolytickou aktivací.

Analýzou koncentrace v krvi na vstupu a na výstupu byla potvrzena ztráta ficolinu 2 a MASP-2 v průběhu dialýzy. Protože jsou tyto proteiny důležitými komponenty v imunitě, jejich ztráta může znamenat vyšší riziko infekce pro pacienta. Proteomická analýza tedy poskytla data pro potvrzení lektinové dráhy komplementu spuštěné vazbou ficolinu-2 na membránu kapilár dialyzátoru.

8. Závěry

8.1. Experimentální studie

Analýza proteomu mitochondrií ledvin prasete ukázala rozdíly v mitochondriálních enzymech mezi kůrou a dřeně ledviny. Zastoupení enzymů v kůře ledviny odpovídá procesům odehrávajícím se v proximálním tubulu (beta oxidace, absorpce aminokyselin, glukoneogeneze), proteom mitochondrií dřeně nasvědčuje optimalizaci mitochondriálního metabolismu pro práci v prostředí s nízkou dostupností kyslíku.

Analýza proteomu plazmy při sepsi indukované peritonitidou byla provedena pomocí dvojrozměrné gelové elektroforézy. Ačkoliv dvojrozměrná gelová elektroforéza poskytuje jen limitovanou informaci o proteomu plazmy, byly identifikovány některé proteiny související s detekcí bakteriálního lipopolysacharidu, s oxidativním stresem a proteiny vázající volný hem.

Proteom biopsií ledvin prasat s indukovanou sepsí poskytl informaci o změnách v průběhu časné fáze sepse. Použití biopsií ze dvou časových okamžiků ukázalo dynamické změny některých proteinů. Zařazením skupiny operovaných prasat jako kontroly byl ukázán vliv chirurgického zásahu na proteom ledvin. Proteiny se změněnou expresí u septických prasat byly chaperony opravující proteiny, proteiny mitochondrií, proteiny zapojené v procesech stresu endoplazmatického retikula a oxidativním stresem.

8.2. Klinické studie

Byly popsány proteiny, které interagují s materiály adsorpčních kolon systému Prometheus. Materiály kolon vykazovaly rozdílnou afinitu k proteinům. Některé proteiny spojené s dysfunkcí jater se hojně adsorbovaly na materiál kolon, což může být významné pro zdravotní stav pacientů podstupujících léčbu.

Byla připravena metoda pro získávání proteinů z povrchů kapilár hemodialyzátorů a použita pro izolaci proteinů adsorbovaných na polysulfonových kapilárách. Mezi proteiny reagujícími s polysulfonovým povrchem byly proteiny podílející se na aktivaci komplementu, adhezi a aktivaci leukocytů a srážení krve.

Tato metoda byla dále použita při zkoumání procesů indukce zánětu a aktivace leukocytů a komplementu při hemodialýze. Bylo potvrzeno, že adsorpce ficolinu-2 je spouštěčem lektinové dráhy aktivace komplementu a vede k leukopenii. Ficolin-2 je důležitou složkou komplementu a jeho odstraňování při dialýze může vést ke snížení imunity pacientů. Tyto postupy a výsledky je možné použít pro další studium biokompatibility dialyzátorů.

9. Podpora

Studie obsažené v této práci byly podporovány:

- výzkumným záměrem MSM 0021620819: Náhrada a podpora funkce některých životně důležitých orgánů,
- Programem rozvoje vědních oborů Univerzity Karlovy – PRVOUK (P36),
- OP VaVPI Biomedicínské centrum (2.1.00/03.0076),
- Projektem specifického výzkumu č. 260175/2015 Univerzity Karlovy v Praze,
- Národním programem udržitelnosti (NPU I) č. LO1503 Ministerstva školství, mládeže a tělovýchovy ČR.

10. Poděkování

V souvislosti s tvorbou této dizertační práce bych chtěl poděkovat svému školiteli MUDr. Martinovi Matějovičovi, Ph.D., za vedení, podporu během mého studia a vytvoření podmínek pro zpracování dizertační práce. Velmi si cením jeho trpělivosti a důvěry v moji práci, které mi dodaly motivaci dizertační práci dokončit.

Dále děkuji kolegům doc. MUDr. Jitce Kuncové, Ph.D. a MUDr. Janu Marešovi, Ph.D. za všestrannou pomoc, cenné rady a připomínky.

Velký dík patří mému rodině za podporu, trpělivost a povzbuzení.

11. Literatura

ADDONA, T. A., et al. A pipeline that integrates the discovery and verification of plasma protein biomarkers reveals candidate markers for cardiovascular disease. *Nat Biotechnol.* 2011, 29, s. 635-643.

AEBERSOLD, R., et al. Mass spectrometry in proteomics. *Chem Rev.* 2001, 101, s. 269-295.

AMADO, F. M., et al. One decade of salivary proteomics: current approaches and outstanding challenges. *Clin Biochem.* 2013, 46, s. 506-517.

ANDERSON, N. L., et al. The human plasma proteome: history, character, and diagnostic prospects. *Mol Cell Proteomics.* 2002, 1, s. 845-867.

ANDREYEV, A. Y., et al. Application of proteomic marker ensembles to subcellular organelle identification. *Mol Cell Proteomics.* 2010, 9, s. 388-402.

BANTSCHIEFF, M., et al. Quantitative mass spectrometry in proteomics: a critical review. *Anal Bioanal Chem.* 2007, 389, s. 1017-1031.

BATEMAN, N. W., et al. Maximizing peptide identification events in proteomic workflows using data-dependent acquisition (DDA). *Mol Cell Proteomics.* 2014, 13, s. 329-338.

BENDIXEN, E. Animal models for translational proteomics. *Proteomics Clin Appl.* 2014, 8, s. 637-639.

BOHRA, R., et al. Proteomics and metabolomics in renal transplantation-quo vadis? *Transpl Int.* 2013, 26, s. 225-241.

BONOMINI, M., et al. Proteomic Investigations into Hemodialysis Therapy. *Int J Mol Sci.* 2015, 16, s. 29508-29521.

BUGGER, H., et al. Tissue-specific remodeling of the mitochondrial proteome in type 1 diabetic akita mice. *Diabetes.* 2009, 58, s. 1986-1997.

CESNIK, A. J., et al. Human Proteomic Variation Revealed by Combining RNA-Seq Proteogenomics and Global Post-Translational Modification (G-PTM) Search Strategy. *J Proteome Res.* 2016, 15, s. 800-808.

COLVIN, K. L., et al. Proteomics of pulmonary hypertension: could personalized profiles lead to personalized medicine? *Proteomics Clin Appl.* 2015, 9, s. 111-120.

COON, J. J., et al. CE-MS analysis of the human urinary proteome for biomarker discovery and disease diagnostics. *Proteomics Clin Appl.* 2008, 2, s. 964-973.

COTTRELL, J. S. Protein identification using MS/MS data. *J Proteomics*. 2011, 74, s. 1842-1851.

DAYON, L., et al. Proteomics of human plasma: A critical comparison of analytical workflows in terms of effort, throughput and outcome. *EuPA Open Proteomics*. 2013, 1, s. 8-16.

DEL BOCCIO, P., et al. Integration of metabolomics and proteomics in multiple sclerosis: From biomarkers discovery to personalized medicine. *Proteomics Clin Appl*. 2016, 10, s. 470-484.

DENG, X., et al. The challenge to quantify proteins with charge trains due to isoforms or conformers. *Electrophoresis*. 2012, 33, s. 263-269.

DUKHANDE, V. V., et al. Chronic hypoxia-induced alterations of key enzymes of glucose oxidative metabolism in developing mouse liver are mTOR dependent. *Mol Cell Biochem*. 2011, 357, s. 189-197.

FEIST, P., et al. Proteomic challenges: sample preparation techniques for microgram-quantity protein analysis from biological samples. *Int J Mol Sci*. 2015, 16, s. 3537-3563.

GO, Y. M., et al. Integrated redox proteomics and metabolomics of mitochondria to identify mechanisms of cd toxicity. *Toxicol Sci*. 2014, 139, s. 59-73.

GRAHAM, J. M. Purification of a crude mitochondrial fraction by density-gradient centrifugation. *Curr Protoc Cell Biol*. 2001, Chapter 3, s. Unit 3 4.

GROOTEMAN, M. P., et al. Ex vivo elution of hemodialyzers. An additional criterion for the assessment of bioincompatibility. *Blood Purif*. 1996, 14, s. 421-430.

GUO, T., et al. Rapid mass spectrometric conversion of tissue biopsy samples into permanent quantitative digital proteome maps. *Nat Med*. 2015, 21, s. 407-413.

HEEGAARD, N. H., et al. Important options available--from start to finish--for translating proteomics results to clinical chemistry. *Proteomics Clin Appl*. 2015, 9, s. 235-252.

HOLCAPEK, M., et al. Recent developments in liquid chromatography-mass spectrometry and related techniques. *J Chromatogr A*. 2012, 1259, s. 3-15.

HUSI, H., et al. A combinatorial approach of Proteomics and Systems Biology in unravelling the mechanisms of acute kidney injury (AKI): involvement of NMDA receptor GRIN1 in murine AKI. *BMC Syst Biol*. 2013, 7, s. 110.

CHEVALIER, F. Highlights on the capacities of "Gel-based" proteomics. *Proteome Sci*. 2010, 8, s. 23.

CHOI-MIURA, N. H., et al. Hepatic injury-specific conversion of mouse plasma hyaluronan binding protein to the active hetero-dimer form. *Biol Pharm Bull*. 2001, 24, s. 892-896.

ISHIKAWA, I., et al. Proteomic analysis of serum, outflow dialysate and adsorbed protein onto dialysis membranes (polysulfone and pmma) during hemodialysis treatment using SELDI-TOF-MS. *Am J Nephrol*. 2006, 26, s. 372-380.

JANZ, D. R., et al. Association between haptoglobin, hemopexin and mortality in adults with sepsis. *Crit Care*. 2013, 17, s. R272.

JIANG, Y., et al. Comparative mitochondrial proteomics: perspective in human diseases. *J Hematol Oncol*. 2012, 5, s. 11.

KALENKA, A., et al. Changes in the serum proteome of patients with sepsis and septic shock. *Anesth Analg*. 2006, 103, s. 1522-1526.

KARAS, M., et al. Laser desorption ionization of proteins with molecular masses exceeding 10,000 daltons. *Anal Chem*. 1988, 60, s. 2299-2301.

KIKUCHI, M., et al. Proteomic analysis of rat liver peroxisome: presence of peroxisome-specific isozyme of Lon protease. *J Biol Chem*. 2004, 279, s. 421-428.

KLAWITTER, J., et al. A metabonomic and proteomic analysis of changes in IMCD3 cells chronically adapted to hypertonicity. *Nephron Physiol*. 2008, 109, s. p1-10.

KORFALI, N., et al. The nuclear envelope proteome differs notably between tissues. *Nucleus*. 2012, 3, s. 552-564.

KROKSVEEN, A. C., et al. Proteomics of human cerebrospinal fluid: discovery and verification of biomarker candidates in neurodegenerative diseases using quantitative proteomics. *J Proteomics*. 2011, 74, s. 371-388.

KUSHNIR, M. M., et al. A depletion strategy for improved detection of human proteins from urine. *J Biomol Tech*. 2009, 20, s. 101-108.

LANGE, V., et al. Selected reaction monitoring for quantitative proteomics: a tutorial. *Mol Syst Biol*. 2008, 4, s. 222.

LAW, K. P., et al. Recent advances in mass spectrometry: data independent analysis and hyper reaction monitoring. *Expert Rev Proteomics*. 2013, 10, s. 551-566.

LEBIEDZINSKA, M., et al. Interactions between the endoplasmic reticulum, mitochondria, plasma membrane and other subcellular organelles. *Int J Biochem Cell Biol*. 2009, 41, s. 1805-1816.

LIEBLER, D. C., et al. Targeted quantitation of proteins by mass spectrometry. *Biochemistry*. 2013, 52, s. 3797-3806.

LIU, Y., et al. Mass spectrometric protein maps for biomarker discovery and clinical research. *Expert Rev Mol Diagn.* 2013, 13, s. 811-825.

LUNDBLAD, R. L. Considerations for the Use of Blood Plasma and Serum for Proteomic Analysis. *The Internet Journal of Genomics and Proteomics.* 2003, 1, s.

MAGDELDIN, S., et al. Basics and recent advances of two dimensional- polyacrylamide gel electrophoresis. *Clin Proteomics.* 2014, 11, s. 16.

MATEJOVIC, M., et al. Renal Hemodynamics in AKI: In Search of New Treatment Targets. *J Am Soc Nephrol.* 2016, 27, s. 49-58.

MAY, C. N., et al. Renal bioenergetics during early gram-negative mammalian sepsis and angiotensin II infusion. *Intensive Care Med.* 2012, 38, s. 886-893.

MICHALSKI, A., et al. More than 100,000 detectable peptide species elute in single shotgun proteomics runs but the majority is inaccessible to data-dependent LC-MS/MS. *J Proteome Res.* 2011, 10, s. 1785-1793.

MUTHU, M., et al. Tracing the voyage of SELDI-TOF MS in cancer biomarker discovery and its current depreciation trend – need for resurrection? *TrAC Trends in Analytical Chemistry.* 2016, 76, s. 95-101.

NAGARAJ, N., et al. Quantitative analysis of the intra- and inter-individual variability of the normal urinary proteome. *J Proteome Res.* 2011, 10, s. 637-645.

NANJAPPA, V., et al. Plasma Proteome Database as a resource for proteomics research: 2014 update. *Nucleic Acids Res.* 2014, 42, s. D959-965.

O'CONNELL, K., et al. Proteomic DIGE analysis of the mitochondria-enriched fraction from aged rat skeletal muscle. *Proteomics.* 2009, 9, s. 5509-5524.

PASELLA, S., et al. Pre-analytical stability of the plasma proteomes based on the storage temperature. *Proteome Sci.* 2013, 11, s. 10.

PENG, F., et al. Proteomic and bioinformatics analyses of mouse liver microsomes. *Int J Proteomics.* 2012, 2012, s. 832569.

PORTA, F., et al. Effects of prolonged endotoxemia on liver, skeletal muscle and kidney mitochondrial function. *Crit Care.* 2006, 10, s. R118.

RABILLOUD, T. Membrane proteins and proteomics: love is possible, but so difficult. *Electrophoresis.* 2009, 30 Suppl 1, s. S174-180.

RABILLOUD, T., et al. Two-dimensional gel electrophoresis in proteomics: Past, present and future. *J Proteomics*. 2010, 73, s. 2064-2077.

RAI, A. J., et al. HUPO Plasma Proteome Project specimen collection and handling: towards the standardization of parameters for plasma proteome samples. *Proteomics*. 2005, 5, s. 3262-3277.

RAMACHANDRAN, N., et al. Applications of protein microarrays for biomarker discovery. *Proteomics Clin Appl*. 2008, 2, s. 1444-1459.

RATURI, A., et al. Where the endoplasmic reticulum and the mitochondrion tie the knot: the mitochondria-associated membrane (MAM). *Biochim Biophys Acta*. 2013, 1833, s. 213-224.

REIFSCHNEIDER, N. H., et al. Defining the mitochondrial proteomes from five rat organs in a physiologically significant context using 2D blue-native/SDS-PAGE. *J Proteome Res*. 2006, 5, s. 1117-1132.

REN, Y., et al. The alterations of mouse plasma proteins during septic development. *J Proteome Res*. 2007, 6, s. 2812-2821.

RODRIGUEZ-SUAREZ, E., et al. Urine as a source for clinical proteome analysis: from discovery to clinical application. *Biochim Biophys Acta*. 2014, 1844, s. 884-898.

SALLAM, R. M. Proteomics in cancer biomarkers discovery: challenges and applications. *Dis Markers*. 2015, 2015, s. 321370.

SANTORO, A., et al. Prometheus system: a technological support in liver failure. *Transplant Proc*. 2006, 38, s. 1078-1082.

SATORI, C. P., et al. Bioanalysis of eukaryotic organelles. *Chem Rev*. 2013, 113, s. 2733-2811.

SHAO, S., et al. Mass spectrometry-based proteomic quest for diabetes biomarkers. *Biochim Biophys Acta*. 2015, 1854, s. 519-527.

SHAW, M. M., et al. Sample preparation for two-dimensional gel electrophoresis. *Proteomics*. 2003, 3, s. 1408-1417.

SHEVCHENKO, A., et al. In-gel digestion for mass spectrometric characterization of proteins and proteomes. *Nat Protoc*. 2006, 1, s. 2856-2860.

SCHANSTRA, J. P., et al. Proteomic urinary biomarker approach in renal disease: from discovery to implementation. *Pediatr Nephrol*. 2015, 30, s. 713-725.

SUTANDY, F. X., et al. Overview of protein microarrays. *Curr Protoc Protein Sci*. 2013, Chapter 27, s. Unit 27 21.

THIEDE, B., et al. Peptide mass fingerprinting. *Methods*. 2005, 35, s. 237-247.

THONGBOONKERD, V., et al. Systematic evaluation of sample preparation methods for gel-based human urinary proteomics: quantity, quality, and variability. *J Proteome Res*. 2006, 5, s. 183-191.

TRUEBLOOD, C. E., et al. Differential regulation of the two genes encoding *Saccharomyces cerevisiae* cytochrome c oxidase subunit V by heme and the HAP2 and REO1 genes. *Mol Cell Biol*. 1988, 8, s. 4537-4540.

TUCK, M. K., et al. Standard operating procedures for serum and plasma collection: early detection research network consensus statement standard operating procedure integration working group. *J Proteome Res*. 2009, 8, s. 113-117.

WALDEN, M., et al. (2007). Proteomics of Human Dialysate and Ultrafiltrate Fluids Yielded by Renal Replacement Therapy. Proteomics of Human Body Fluids: Principles, Methods, and Applications. V. Thongboonkerd. Totowa, NJ, Humana Press Inc.: 509-520.

WANG, X., et al. Better understanding of organ dysfunction requires proteomic involvement. *J Proteome Res*. 2006, 5, s. 1060-1062.

WISNIEWSKI, J. R., et al. Universal sample preparation method for proteome analysis. *Nat Methods*. 2009, 6, s. 359-362.

WITTIG, I., et al. Features and applications of blue-native and clear-native electrophoresis. *Proteomics*. 2008, 8, s. 3974-3990.

WU, C. C., et al. Shotgun proteomics: tools for the analysis of complex biological systems. *Curr Opin Mol Ther*. 2002, 4, s. 242-250.

YAMASHITA, M., et al. Electrospray Ion-Source - Another Variation on the Free-Jet Theme. *Journal of Physical Chemistry*. 1984, 88, s. 4451-4459.

ZHANG, X., et al. Multi-dimensional liquid chromatography in proteomics--a review. *Anal Chim Acta*. 2010, 664, s. 101-113.

ZHANG, Z., et al. The road from discovery to clinical diagnostics: lessons learned from the first FDA-cleared in vitro diagnostic multivariate index assay of proteomic biomarkers. *Cancer Epidemiol Biomarkers Prev*. 2010, 19, s. 2995-2999.

ZHOU, Y., et al. Recent advances in stable isotope labeling based techniques for proteome relative quantification. *J Chromatogr A*. 2014, 1365, s. 1-11.

12. Přílohy

TŮMA, Zdeněk; KUNCOVÁ, Jitka; MAREŠ, Jan; MATĚJOVIČ, Martin. Mitochondrial proteomes of porcine kidney cortex and medulla: foundation for translational proteomics. *Clin Exp Nephrol*. 2016, 20, s. 39-49.

THONGBOONKERD, Visith; CHIANGJONG, Wararat; MAREŠ, Jan; MORAVEC, Jiří; TŮMA, Zdeněk; KARVUNIDIS, Thomas; SINCHAIKUL, Supachok; CHEN, Shui-Tein; OPATRNY, Karel Jr.; MATĚJOVIČ, Martin. Altered plasma proteome during an early phase of peritonitis-induced sepsis. *Clin Sci (Lond)*, 2009, 116, s. 721-730.

MATĚJOVIČ, Martin; TŮMA, Zdeněk; MORAVEC, Jiří; VALEŠOVÁ, Lenka; SÝKORA, Roman; CHVOJKA, Jiří; BENEŠ, Jan; MAREŠ, Jan. Renal proteomic responses to severe sepsis and surgical trauma: dynamic analysis of porcine tissue biopsies. *Shock*, 2016.

MAREŠ, Jan; THONGBOONKERD, Visith; TŮMA, Zdeněk; MORAVEC, Jiří; MATĚJOVIČ, Martin. Specific adsorption of some complement activation proteins to polysulfone dialysis membranes during hemodialysis. *Kidney international*. 2009, 76, s. 404-413.

MAREŠ, Jan; RICHTROVÁ, Pavlína; HRIČINOVÁ, Alena; TŮMA, Zdeněk; MORAVEC, Jiří; LYSÁK, Daniel; MATĚJOVIČ, Martin. Proteomic profiling of blood-dialyzer interactome reveals involvement of lectin complement pathway in hemodialysis-induced inflammatory response. *Proteomics Clin Appl*, 2010, 4, s. 829-838.


MAREŠ, Jan; THONGBOONKERD, Visith; TŮMA, Zdeněk; MORAVEC, Jiří; KARVUNIDIS, Thomas; MATĚJOVIČ, Martin. Proteomic analysis of proteins bound to adsorption units of extracorporeal liver support system under clinical conditions. *J Proteome Res*, 2009, 8, s. 1756-1764.

TŮMA, Zdeněk; KUNCOVÁ, Jitka; MAREŠ, Jan; GRUNDMANOVÁ, Martina; MATĚJOVIČ, Martin. Proteomic approaches to the study of renal mitochondria. *Biomed Pap Med Fac Univ Palacky Olomouc Czech Repub*, 2016, doi: 10.5507/bp.2016.012.

ČEDÍKOVÁ, Miroslava; MIKLÍKOVÁ, Michaela; STACHOVÁ, Lenka; GRUNDMANOVÁ, Martina; TŮMA, Zdeněk; VĚTVIČKA, Václav; ZECH, Nicolas; KRÁLÍČKOVÁ, Milena; KUNCOVÁ, Jitka. Effects of the Czech propolis on sperm mitochondrial function. *Evid Based Complement Alternat Med*, 2014, s. 248768.

PAPAGIANNITSIS, Constantinos; KOTSAKIS, Stathis; TŮMA, Zdeněk; GNIADKOWSKI, Marek; MIRIAGOU, Vivi; HRABÁK, Jaroslav. Identification of CMY-2-Type Cephalosporinases in Clinical Isolates of Enterobacteriaceae by MALDI-TOF MS. *Antimicrob Agents Chemother*, 2014, 58, s. 2952-2957.

Mitochondrial proteomes of porcine kidney cortex and medulla: foundation for translational proteomics

Zdenek Tuma¹  · Jitka Kuncova^{1,2} · Jan Mares^{1,3} · Martin Matejovic^{1,3}

Received: 7 November 2014 / Accepted: 2 June 2015
© Japanese Society of Nephrology 2015

Abstract

Background Emerging evidence has linked mitochondrial dysfunction to the pathogenesis of many renal disorders, including acute kidney injury, sepsis and even chronic kidney disease. Proteomics is a powerful tool in elucidating the role of mitochondria in renal pathologies. Since the pig is increasingly recognized as a major mammalian model for translational research, the lack of physiological proteome data of large mammals prompted us to examine renal mitochondrial proteome in porcine kidney cortex and medulla

Methods Kidneys were obtained from six healthy pigs. Mitochondria from cortex and medulla were isolated using differential centrifugation and proteome maps of cortical and medullar mitochondria were constructed using two-dimensional gel electrophoresis (2DE). Protein spots with significant difference between mitochondrial fraction of renal cortex and medulla were identified by mass spectrometry.

Results Proteomic analysis identified 81 protein spots. Of these spots, 41 mitochondrial proteins were statistically

different between renal cortex and medulla ($p < 0.05$). Protein spots containing enzymes of beta oxidation, amino acid metabolism, and gluconeogenesis were predominant in kidney cortex mitochondria. Spots containing tricarboxylic acid cycle enzymes and electron transport system proteins, proteins maintaining metabolite transport and mitochondrial translation were more abundant in medullar mitochondria.

Conclusion This study provides the first proteomic profile of porcine kidney cortex and medullar mitochondrial proteome. Different protein expression pattern reflects divergent functional metabolic role of mitochondria in various kidney compartments. Our study could serve as a useful reference for further porcine experiments investigating renal mitochondrial physiology under various pathological states.

Keywords Mitochondria · Pig kidney · Proteomics · Two-dimensional electrophoresis

Abbreviations

2DE Two-dimensional electrophoresis
KM Kidney medulla
KC Kidney cortex
TCA Tricarboxylic acid cycle
ETS Electron transport system
ROS Reactive oxygen species

Electronic supplementary material The online version of this article (doi:10.1007/s10157-015-1135-x) contains supplementary material, which is available to authorized users.

✉ Zdenek Tuma
zdenek.tuma@lfp.cuni.cz

¹ Faculty of Medicine in Plzen, Biomedical Center, Charles University in Prague, alej Svobody, 1655/76, Plzen, Czech Republic

² Department of Physiology, Charles University Medical School, Plzen, Czech Republic

³ Department of Internal Medicine I, Charles University Medical School and Teaching Hospital, Plzen, Czech Republic

Introduction

Kidney shows extreme metabolic activity and adequate energy supply is a prerequisite of its multiple functions. Removing waste products of metabolism, regulation of water, electrolytes and acid–base balance and reabsorption

of compounds from glomerular filtrate are performed by specialized segments of nephron. Mitochondria in nephrons are important as energy suppliers for active transport processes [1]. Differences in activities of mitochondrial enzymes along the nephron suggest variations in content and specialization of mitochondria in nephron segments [2]. Mitochondrial dysfunction has increasingly been recognized as an important element in a broad spectrum of renal diseases [3]. Mitochondrial dysfunction is a key contributor to renal tubular cell death during acute kidney injury (AKI) [4, 5]. In sepsis and multiorgan dysfunction syndrome, mitochondrial dysfunction has been proposed as a crucial cellular event and mitochondria could be a target for therapy with compounds that improve their function [6, 7]. Therefore, a precise knowledge of mitochondrial physiology and response of mitochondria to pathologic stimuli is important to better understand the mechanisms of diseases.

Proteomics has been used to better understand the physiology and pathophysiology of the kidney, unraveling of pathogenic mechanisms of diseases, and for drug and biomarker research [8]. The tissue heterogeneity is challenging issue in investigation of renal proteome in health and disease. Using gel-based proteomic analysis, differences between rat kidney cortex and medulla proteomes [9] and between human kidney cortex, medulla and glomerulus proteomes were examined [10] and altered levels of mitochondrial proteins between these parts of kidney were detected. Proteomic samples of whole tissue represent complex mixtures of proteins with large dynamic range of concentrations that exceeds capacity and dynamic range of available separation methods. For investigation of specific subcellular organelle proteome, it can be advantageous to reduce sample complexity by separating the organelle of interest, e.g. differential centrifugation [11]. Proteome of renal mitochondria was investigated in various rodent models of diabetes [12], acidosis [13] and in renal tubular cells exposed to calcium oxalate [14] to detect specific response of mitochondria to pathologic conditions. Nevertheless, it should be acknowledged that data identified in rodent models might not necessarily be germane to human physiology, thus requiring cautious interpretation and series of subsequent verification steps in large animal models. Therefore, the aim of this study was to examine mitochondrial proteome of porcine kidney cortex and medulla under physiological conditions. Gel-based proteomic analysis was used as an unbiased attempt to analyze proteomes of mitochondrial fraction of kidney cortex and medulla prepared by differential centrifugation. Due to very similar cardiovascular and renal physiology to humans, pig as model organism is increasingly being used in biomedical research for studying sepsis [15], AKI [16] or for improvement of kidney transplantation process [17].

Very recently, the pig has also been introduced as one of the most promising animal models from a proteomic and translational perspective [18]. To our knowledge, this is the first analysis of differences in mitochondrial proteins between pig kidney cortex and medulla.

Methods

Experimental subjects

Six domestic piglets (Farm Mladotice, Czech Republic) with a comparable body weight (mean weight 24 kg, range 21.3–28.3 kg, age 50–60 days, 3 males and 3 females) were studied. All experiments were conducted in accordance with the relevant Guidelines of the Czech Ministry of Agriculture for Scientific Experimentation on Animals and the European Directive for the Protection of Vertebrate Animals Used for Experimental and Other Scientific Purposes (86/609/EEC) and were approved by the University Committee for Experiments on Laboratory Animals (Charles University, Czech Republic).

The piglets were premedicated intramuscularly with atropine 1.5 mg and azaperon 1.0 mg/kg. Anesthesia was induced with intravenous propofol (1–2 mg/kg) and ketamine (2 mg/kg). Animals were intubated and mechanically ventilated with tidal volumes 8–10 ml/kg, positive end-expiratory pressure 0.6 kPa and FiO₂ 0.4. Respiratory rate was adjusted to maintain normocapnia (arterial carbon dioxide tension 4.0–5.0 kPa). During surgical procedure continuous infusions of fentanyl (10–15 µg/kg/h), thiopental (10 mg/kg/h), and pancuronium (4–6 mg/h) were administered.

A left nephrectomy was performed through a midline laparotomy. The ureter, renal artery, and vein were isolated, ligated, and sharp dissection was used to excise the renal mass. The resected kidney was immediately placed into the ice-cold Tyrode solution and transported into the laboratory within 5 min. In longitudinal section of kidney, renal cortex and pyramids could be macroscopically recognized (Fig. 1). Approximately 1 g of renal cortex and renal medullar pyramids was taken for isolation of mitochondria.

Isolation of mitochondria

Albumin, potassium chloride, ethylenediamine tetraacetic acid (EDTA), urea, thiourea, CHAPS detergent, TRIS base, glycerol, sodium dodecylsulfate (SDS), dithiothreitol (DTT), and iodoacetamide (IAA) were purchased from Sigma (Steinheim, Germany). Carrier ampholytes and Simply Blue stain were purchased from Invitrogen (Carlsbad, USA).

For isolation of mitochondria, differential centrifugation was used [19]. Tissues were put in isolation buffer (IB;

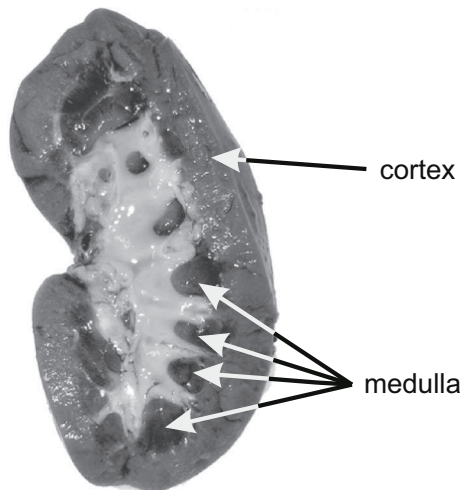


Fig. 1 Preparation of tissue samples for isolation of mitochondria. The kidney was cut in longitudinal direction, and tissue from selected regions was taken for mitochondria isolation. To get sufficient amount of medulla, few renal pyramids from each kidney were excised and pooled

180 mM KCl, 4 mM EDTA and 1 % of bovine serum albumin, pH 7.4) and homogenized by TissueRuptor homogenizer (Qiagen, Hilden, Germany). Homogenate was centrifuged for 10 min at 1000g and 4 °C. Supernatant was recovered; pellet was resuspended in 10 ml of IB and homogenized again. After centrifugation (10 min, 1000g, 4 °C), supernatant was recovered again. Both supernatants were pooled and centrifuged (15 min, 5000g, 4 °C). Then, pellet containing mitochondria was resuspended in IB without albumin (180 mM KCl, 4 mM EDTA, pH 7.4) and centrifuged (15 min, 5000g, 4 °C). Pellet containing mitochondria was resuspended in IB without albumin. An aliquot of suspension was taken for cytochrome c activity and outer membrane integrity assay by Cytocox1 kit (Sigma, Steinheim, Germany) and for morphology checking using transmission electron microscopy. The rest of suspension was centrifuged, pellet was solubilized in buffer (7 M urea, 2 M thiourea, 4 % CHAPS, 2 % ampholytes pH 3–10, 120 mM DTT) and used for two-dimensional electrophoresis. Total protein concentration was measured with Bradford assay.

Separation of proteins

Two-dimensional polyacrylamide gel electrophoresis (2DE) of each sample was performed in triplicate. Solution containing 200 µg of protein was mixed with rehydration buffer (7 M urea, 2 M thiourea, 4 % CHAPS, 2 % ampholytes pH 3–10, 120 mM DTT, traces of bromophenol blue) and rehydrated onto 11 cm IPG strip with non-linear pH gradient 3–10 (Bio-Rad, Hercules, USA). Isoelectric focusing was performed using Protean IEF device (Bio-Rad, Hercules, USA). After reaching 45 kVh,

proteins in strips were reduced (112 mM Tris-base, 6 M urea, 30 % v/v glycerol, 4 % w/v SDS, 130 mM DTT, 0.002 % bromophenol blue) and alkylated (112 mM Tris-base, 6 M urea, 30 % v/v glycerol, 4 % w/v SDS, 135 mM IAA, 0.002 % bromophenol blue). Separation in second dimension was performed on Criterion TGX polyacrylamide gels (Bio-Rad, Hercules, USA). Gels were stained with SimplyBlue Safe stain (Invitrogen, Carlsbad, USA) and images were acquired at 16-bit grayscale resolution.

Mass spectrometric protein identification

Acetonitrile (ACN), ammonium bicarbonate, trifluoroacetic acid, and alpha-cyano-4-hydroxycinnamic acid (CHCA) were purchased from Sigma (Steinheim, Germany). Sequencing grade trypsin was purchased from Roche (Basel, Switzerland).

For identification of selected protein spots, in gel tryptic digestion followed by MALDI-TOF/TOF mass spectrometry was used [20]. Protein spots were excised from gel slab, reduced with DTT, and alkylated with IAA. Then, gel pieces were rehydrated with buffer containing trypsin and incubated overnight at 37 °C. After digestion, proteolytic peptides were subsequently extracted with 50 % ACN/25 mM ammonium bicarbonate, 5 % formic acid, and 50 % ACN/H₂O. The three extracts were pooled, and 10 mM DTT solution in 50 mM ammonium bicarbonate was added. The mixture was then dried by SpeedVac. Tryptic peptides were redissolved in 5 % formic acid and desalted using ZipTip µC18 tips (Millipore, Bedford, USA) according to manufacturer's instructions. Proteolytic peptides were mixed with CHCA matrix and spotted onto MALDI target. All peptide mass fingerprint (PMF) and MS/MS spectra were acquired with a 4800 MALDI TOF/TOF Analyzer (Applied Biosystems, Framingham, USA). MS peaks with an S/N above 15 were listed, and the 10 strongest precursors with an S/N above 50 among the MS peaks were automatically selected for MS/MS acquisition.

Western blotting

Western blotting analysis was performed using Bio-Rad V3 workflow. Proteins were separated on Criterion TGX Stainfree gel (Bio-Rad, Hercules, USA), and transferred onto a PVDF membrane (Trans-Blot Turbo Midi PVDF Transfer Pack, Bio-Rad) by semidry transfer (25 V, 2.5 A, 7 min). The membranes were blocked in TBS (0.15 M NaCl, 20 mM TRIS-HCl, pH 7.5) with 0.1 % (v/v) Tween-20 and 5 % (w/v) non-fat dry milk and incubated overnight with primary antibody. Antibodies against ACADM (Abcam, ab23675, 1:750), GABT (Abcam, ab 81432, 1:1000), PCKGM (Abcam, ab70359, 1:1000), ODO2 (LSBio LS-C145464, 1:1000), QCR1 (Biorbyt, orb 2479, 1:500), and VDAC2

(Abcam, ab100956, 1:1000) were used for detection of corresponding proteins. The membranes were then incubated for 1.5 h with secondary antibody (Abcam ab99697, 1:5000). For analysis of mitochondrial fraction purity, antibodies Organelle detection WB cocktail (Abcam, ab133989, dilution 1:1000) and goat anti-mouse IgG(H+L)-HRP conjugate (Bio-Rad, 1:5000) were used. Detection was performed with Opti-4CN kit (Bio-Rad) and images were acquired using ChemiDoc MP imager (Bio-Rad).

Statistic evaluation, data handling

Computer-aided analysis of gel images was carried out using PDQuest 8.0.1 software (Bio-Rad). Detected spots were checked manually and streaks and artifacts were removed. Intensity of each spot was normalized per total density of gel image and intensities of each spot in triplicate were averaged. Using Wilcoxon signed-rank test, intensities of each spot were tested whether they significantly differ between kidney cortex and medulla mitochondrial fractions. To examine quantitative expression, ratio of spot intensity in medulla to cortex (KM/KC) was calculated for each animal. Spots with more than twofold change in expression (median of KM/KC ratio <0.5 or >2) and statistically significant difference ($p < 0.05$) between kidney cortex and medulla mitochondrial fraction were selected for identification.

Mass spectrometric data were processed with GPS Explorer software (Applied Biosystems, Framingham, MA, USA). Mass spectra were matched against “mammalia (mammals)” subset of the Uniprot protein database using Mascot 2.1.0 search algorithm (Matrix Science, London, UK). The general parameters for PMF search were considered to allow maximum two missed cleavages, ± 50 ppm of peptide mass tolerance, variable methionine oxidation, and fixed cysteine carbamidomethylation. MOWSE scores greater than 61 were considered significant for PMF. Fragment mass tolerance of ± 0.25 Da was used for the MS/MS ion search. Individual MS/MS ions scores >33 indicated identity or extensive homology for MS/MS ion search.

Intensities of bands acquired by Western blotting were normalized to total protein and ratio of band intensity in medulla to cortex (KM/KC) was calculated for each animal. Results of Western blotting were expressed as a median of KM/KC values.

Results

Mitochondria fractions from kidney cortex and medulla of all six pigs were processed. Calculated outer membrane integrity was $91 \pm 9\%$ in mitochondrial fractions from cortex and $98 \pm 2\%$ in mitochondrial fractions from medulla

(mean \pm SD). Cytochrome c oxidase activity in cortical fraction was 0.61 ± 0.16 and 1.09 ± 0.28 IU/mg of protein (mean \pm SD). Activity of cytochrome c oxidase activity in cortical fraction is close to activity in mitochondria of cultured renal epithelial cells [21]. Yield of mitochondrial fraction expressed as ratio of total protein in mitochondrial fraction to wet weight of tissue from kidney cortex was $(0.75 \pm 0.06)\%$ and $(0.35 \pm 0.09)\%$ from kidney medulla. Typical morphology of mitochondria obtained from kidney cortex and medulla is shown in Fig. 2a, b. Purity of mitochondrial fractions was examined by immunoblotting with antibody cocktail that detected proteins of nucleus, cytoplasm, mitochondria, and cytoplasmic membrane (Fig. 2c). In mitochondrial fractions of both kidney cortex and medulla, intensity of cytoplasm and nucleus marker decreased in comparison to corresponding whole tissue. The marker of cytoplasmic membrane was not detected due to incompatibility of the antibody with corresponding porcine protein.

Representative gel image of mitochondrial fraction of cortex and medulla is shown in Fig. 3. Total 635 spots were detected on polyacrylamide gels. A set of 343 spots, present in more than 90% of gels of kidney cortex or medulla fraction was arbitrarily considered representative. From this set, 161 protein spots with statistically significant difference ($p < 0.05$) between kidney cortex and medulla mitochondrial fraction and more than twofold change in expression were taken for mass spectrometric identification and 81 of them were successfully identified by mass spectrometry. Due to unavailability of complete porcine proteome database, mass spectra were matched against “mammalia (mammals)” subset of Uniprot [22]. Subcellular localization of identified proteins was searched in database Uniprot or literature and 41 spots that contained proteins with subcellular localization in mitochondria are shown in Table 1. The rest of protein spots contained proteins localized in endoplasmic reticulum, cytoplasm, peroxisomes, and cytoskeleton probably due to their co-isolation with mitochondria or association with mitochondrial membrane [23]. There were several spots that contained more than one protein due to their close molecular weights and isoelectric points and, therefore, quantity of proteins in these spots cannot be determined. Further information about identified mitochondrial proteins can be found in Supplemental Table 1. For confirmation of proteomic analysis, quantity of selected proteins was analyzed by Western blotting (Fig. 4). Their expression was in good agreement with proteomic results.

Discussion

Proteomic analysis of porcine kidney mitochondria based on 2DE was used as explorative method and significant differences in proteome composition between cortical and

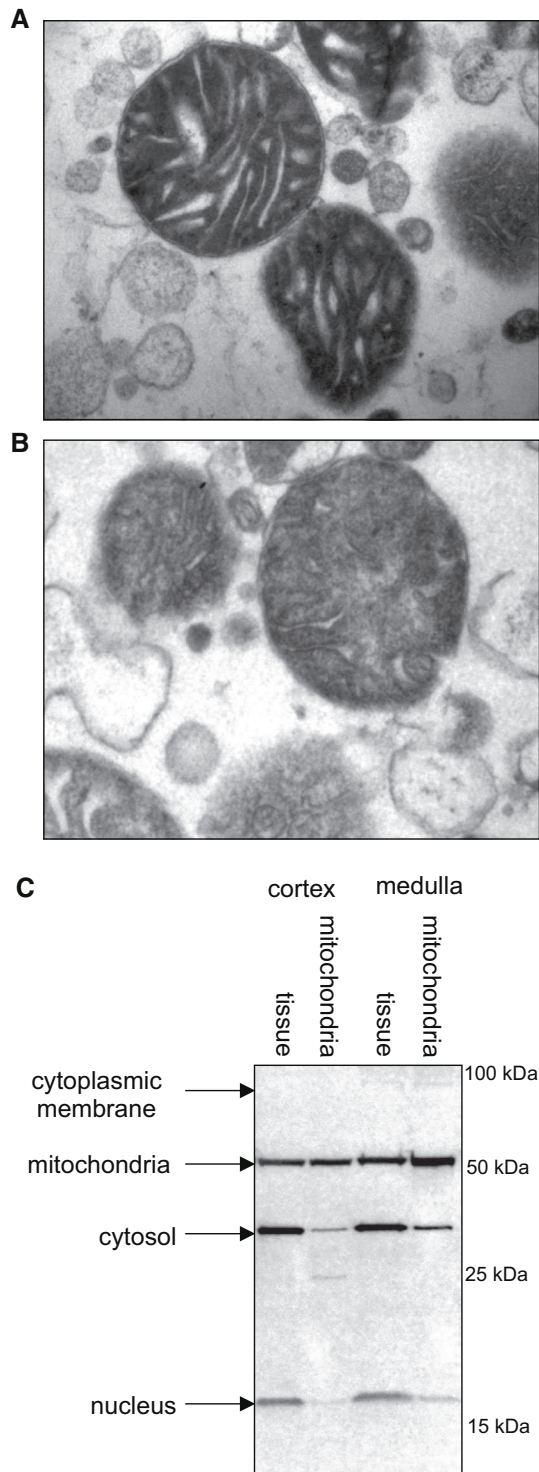


Fig. 2 Quality control of mitochondrial fractions. Morphology of isolated mitochondria was examined by transmission electron microscopy. **a** Transmission electron micrograph of mitochondria isolated from porcine renal cortex. **b** Transmission electron micrograph of mitochondria isolated from porcine renal medulla. **c** Western blotting analysis of whole tissue proteins and corresponding mitochondrial fractions of renal cortex and medulla. Decrease of cytosolic and nuclear markers was observed in mitochondrial fractions of both renal cortex and medulla; marker of cytoplasmic membrane was not detected

medullar mitochondria were found. Proteins with different abundance between mitochondrial fractions of kidney cortex and medulla (KM) were employed in fatty acid beta oxidation, amino acid metabolism, gluconeogenesis, TCA cycle, electron transport system, metabolite transport, and proteosynthesis. These data could provide an important foundation for the future proteomic studies in renal pathologic conditions such as AKI and sepsis performed in clinically relevant large animal models.

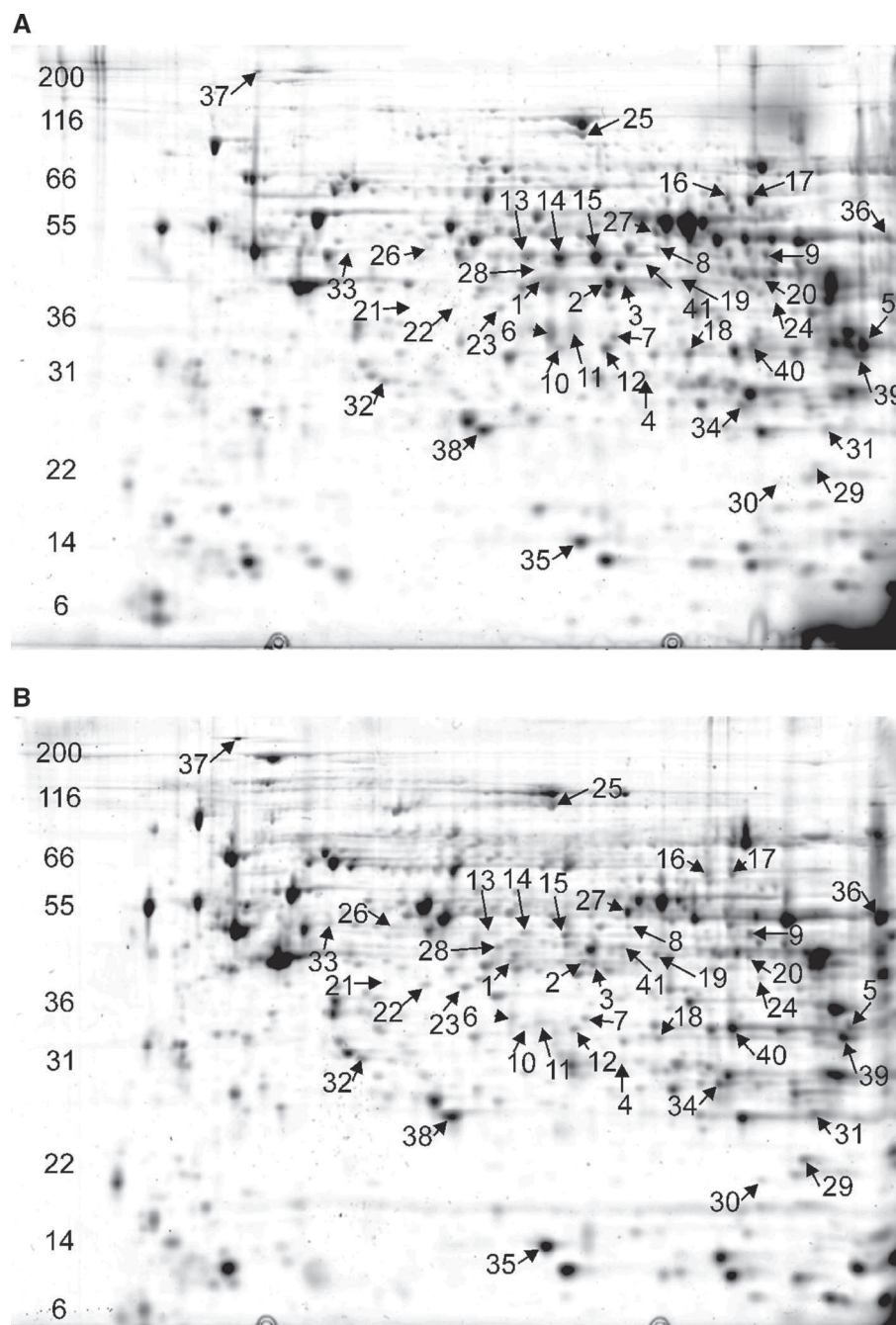
Organized distribution of nephrons in renal tissue results in the formation of regions with different biochemical and metabolic properties. In the renal cortex, glomeruli maintain filtration of blood plasma, and proximal tubules are sites of reabsorption of glucose, amino acids, water, and electrolytes. Distal tubules play a critical role in sodium, potassium, and divalent cation homeostasis. Structures of nephron in the renal medulla are the loop of Henle and the collecting tubule. The most important process in renal medulla is concentration of urine by osmotic processes. Cells of the renal medulla are exposed to a hypertonic and hypoxic environment.

Proteins more abundant in mitochondria of kidney cortex

In mitochondrial beta oxidation, fatty acids are converted to acetyl-CoA by sequential removal of two-carbon units in series of oxidative reactions [24]. It was demonstrated that fatty acids are important energy source for active transport process of sodium tubular reabsorption [27]. Our results agree with predominant presence of mitochondrial medium-chain specific acyl-CoA dehydrogenase (ACADM) in human kidney cortex [10] and higher activity of hydroxyacyl-coenzyme A dehydrogenase (HCDH) in cortical parts of rat nephron [25]. Beta oxidation is advantageous for tissues that are well supplied with oxygen, where more ATP per carbon can be produced [26]. It is preferred in parts of nephron that are located in renal cortex. On the other hand, relying on beta oxidation suggests sensitivity of renal cortex to hypoxia, when beta oxidation is downregulated [28].

The kidney is an important organ in amino acid metabolism. Amino acids are easily filtered by glomerulus, reabsorbed by proximal tubule, and further utilized for synthesis, conversion, energy production or ammonia excretion [35]. Most of amino acid metabolism pathways span across the cytoplasmic and mitochondrial locations. Amino acid metabolism enzymes probable 4-hydroxy-2-oxoglutarate aldolase (HOGA1), alanine-glyoxylate aminotransferase 2 (AGT2), 4-aminobutyrate aminotransferase (GABT), fumarylacetoacetate hydrolase domain-containing protein 2A (FAH2A), and glycine amidinotransferase (GATM) were found by us with higher

Fig. 3 Representative 2DE gel images of mitochondrial fractions. Separation of proteins was done by 2DE in molecular weight range 6–200 kDa (molecular weight is indicated by numbers in the left part of the image) and pI range 3–10 (gradient rises from left to right side of the image). Spot numbers of identified proteins correspond with numbers in Table 1. **(a)** 2DE gel image of kidney cortical mitochondrial fraction. **(b)** 2DE gel image of mitochondrial fraction of renal medulla



abundance in pig KC mitochondria. This is consistent with previous foundations. Hydroxyproline metabolism enzymes HOGA1 and AGT2 were previously detected with high activity in rat renal cortex [30]. Hydroxyproline metabolism important for processing of diet-derived hydroxyproline takes place in mitochondria of hepatocytes and renal proximal tubule cells oxalate [29]. Renal hydroxyproline metabolism may be also an important source of oxalate. It was found that in renal cortical tubules, significant amount of gamma aminobutyrate is

created from glutamate [31]. Then, GABT may contribute to utilization of gamma aminobutyrate in TCA cycle [32]. GATM is highly expressed in kidney and liver. In kidney, GATM is employed in creatine synthesis, which in mammals starts in the cortex [34]. In pig KC, mitochondrial pathways of amino acid metabolism serve for both synthetic and catabolic purposes. Abundance of amino acid metabolism enzyme in pig KC mitochondria matches the previously found role of proximal tubule in amino acid metabolism.

Table 1 Proteins identified in spots that showed higher expression in cortical mitochondrial fraction (spots 1–18) and medullar mitochondrial fractions (spots 19–41)

Spot no. ^a	Metabolic process	Protein name	Uniprot entry ^b	KM/KC ratio (IQR) ^c	<i>p</i> value ^d
1	Beta oxidation	Medium-chain specific acyl-CoA dehydrogenase	ACADM_PIG	0.20 (0.18–0.31)	0.028
2	Beta oxidation	Medium-chain specific acyl-CoA dehydrogenase	ACADM_PIG	0.31 (0.21–0.43)	0.028
3	Beta oxidation	Medium-chain specific acyl-CoA dehydrogenase	ACADM_PIG	0.49 (0.32–0.58)	0.028
4	Beta oxidation	Long-chain specific acyl-CoA dehydrogenase	ACADL_PIG		
	Beta oxidation	Enoyl-CoA hydratase domain-containing protein 2, mitochondrial	ECHD2_BOVIN	0.07 (0.02–0.29)	0.028
5	Beta oxidation	Hydroxyacyl-coenzyme A dehydrogenase	HCDH_MOUSE	0.44 (0.40–0.60)	0.028
6	Amino acid metabolism	Probable 4-hydroxy-2-oxoglutarate aldolase	HOGA1_BOVIN	0.18 (0.16–0.21)	0.028
7	Amino acid metabolism	Probable 4-hydroxy-2-oxoglutarate aldolase	HOGA1_BOVIN	0.45 (0.43–0.53)	0.028
8	Amino acid metabolism	Alanine-glyoxylate aminotransferase 2	AGT2_BOVIN	0.15 (0.08–0.19)	0.028
9	Amino acid metabolism	4-aminobutyrate aminotransferase	GABT_PIG	0.44 (0.31–0.58)	0.028
10	Amino acid metabolism	Fumarylacetoacetate hydrolase domain-containing protein 2A	FAH2A_HUMAN	0.38 (0.09–0.45)	0.028
11	Amino acid metabolism	Fumarylacetoacetate hydrolase domain-containing protein 2A	FAH2A_HUMAN	0.40 (0.35–0.43)	0.028
12	Amino acid metabolism	Fumarylacetoacetate hydrolase domain-containing protein 2A	FAH2A_HUMAN	0.39 (0.35–0.42)	0.028
13	Amino acid metabolism	Glycine amidinotransferase	GATM_PIG	0.23 (0.12–0.27)	0.028
14	Amino acid metabolism	Glycine amidinotransferase	GATM_PIG	0.10 (0.07–0.18)	0.028
15	Amino acid metabolism	Glycine amidinotransferase	GATM_PIG	0.19 (0.12–0.20)	0.028
16	Saccharides metabolism	Phosphoenolpyruvate carboxykinase [GTP], mitochondrial	PCKGM_HUMAN	0.36 (0.19–0.71)	0.028
17	Saccharides metabolism	Phosphoenolpyruvate carboxykinase [GTP], mitochondrial	PCKGM_HUMAN	0.19 (0.16–0.39)	0.028
18	Peptidase	Serine beta-lactamase-like protein LACTB, mitochondrial	LACTB_HUMAN	0.30 (0.18–0.40)	0.028
19	Sulfur metabolism	Thiosulfate sulfurtransferase	THTR_CRIGR		
	TCA cycle	Pyruvate dehydrogenase E1 component subunit alpha, somatic form, mitochondrial	ODPA_PIG	2.31 (1.64–4.40)	0.028
20	TCA cycle	Citrate synthase	CISY_MOUSE	5.61 (4.46–6.65)	0.028
21	Acyl-coenzyme metabolism	Acyl-coenzyme A thioesterase 2	ACOT2_HUMAN		
	TCA cycle	Isocitrate dehydrogenase [NAD] subunit alpha	IDH3A_HUMAN	4.77 (3.03–5.89)	0.028
22	TCA cycle	Isocitrate dehydrogenase [NAD] subunit alpha	IDH3A_HUMAN	2.99 (2.83–3.15)	0.028
23	TCA cycle	Isocitrate dehydrogenase [NAD] subunit alpha	IDH3A_MESAU	3.11 (2.85–3.60)	0.028
24	TCA cycle	Isocitrate dehydrogenase [NAD] subunit beta	IDH3B_RAT	2.08 (1.86–2.74)	0.028
25	TCA cycle	2-oxoglutarate dehydrogenase	ODO1_MACFA	2.14 (1.98–2.74)	0.028
26	TCA cycle	Dihydrolipoyllysine-residue succinyltransferase component of 2-oxoglutarate dehydrogenase complex	ODO2_PIG	2.16 (1.92–2.27)	0.028
27	TCA cycle	Dihydrolipoyl dehydrogenase	DLDH_CANFA	2.44 (1.96–3.16)	0.028
28	TCA cycle	Ornithine aminotransferase	OAT_BOVIN	2.77 (2.22–3.70)	0.028
29	ETS subunit	NADH dehydrogenase [ubiquinone] 1 alpha subcomplex subunit 8	NDUA8_MOUSE	3.47 (2.80–5.43)	0.028
30	ETS subunit	NADH dehydrogenase [ubiquinone] 1 beta subcomplex subunit 7	NDUB7_BOVIN	2.21 (1.77–2.95)	0.028

Table 1 continued

Spot no. ^a	Metabolic process	Protein name	Uniprot entry ^b	KM/KC ratio (IQR) ^c	<i>p</i> value ^d
31	ETS subunit	NADH dehydrogenase [ubiquinone] 1 beta subcomplex subunit 10	NDUBA_BOVIN	2.31 (2.06–2.56)	0.028
32	ETS subunit	NADH dehydrogenase [ubiquinone] iron-sulfur protein 3	NDUS3_BOVIN	2.48 (1.85–2.80)	0.028
	Chaperone	Prohibitin	PHB_HUMAN		
33	ETS subunit	Cytochrome b-c1 complex subunit 1	QCR1_HUMAN	3.55 (1.59–5.56)	0.028
34	ETS subunit	Cytochrome b-c1 complex subunit Rieske	UCRI_RAT	2.46 (1.81–3.29)	0.028
35	ETS subunit	Cytochrome c oxidase subunit 5B	COX5B_PIG	2.15 (1.81–2.23)	0.028
36	ETS subunit	ATP synthase subunit alpha	ATPA_BOVIN	8.89 (4.01–12.62)	0.028
37	ETS subunit	ATP synthase subunit beta	ATPB_RAT	3.12 (2.06–4.10)	0.028
38	ETS subunit	ATP synthase subunit d	ATP5H_HUMAN	2.03 (1.84–2.26)	0.028
	Nonmitochondrial	Inactive rhomboid protein 1	RHDF1_BOVIN		
39	ATP transport	Voltage-dependent anion-selective channel protein 1	VDAC1_HUMAN	2.57 (2.02–4.09)	0.028
40	ATP transport	Voltage-dependent anion-selective channel protein 2	VDAC2_HUMAN	2.69 (2.49–3.28)	0.028
41	Proteosynthesis	Elongation factor Tu	EFTU_MESAU	2.46 (1.85–2.91)	0.028

^a Spot numbers that refer to Fig. 3, ^b Uniprot entry name of identified protein, ^c KM/KC, median of spot intensity ratios and inter-quartile range (IQR), ^d *p* value of Wilcoxon signed-rank test

Renal gluconeogenesis is important in glucose level regulation, compensation of impaired hepatic glucose release, and contribution to the excessive glucose release in diabetes [26]. Mitochondrial phosphoenolpyruvate carboxykinase (PCKGM) that catalyzes the formation of phosphoenolpyruvate in gluconeogenesis was found strongly expressed in kidney [38] and its activity is induced by lactate [36]. Thus, higher amount of PCKGM in pig KC mitochondria may contribute to gluconeogenesis of pig renal cortex, possibly by utilization of lactate produced by the erythrocytes [38].

Proteins more abundant in kidney medullar mitochondria

Pyruvate dehydrogenase subunit E1 α (ODPA), alpha- and beta-subunits of isocitrate dehydrogenase (IDH3A and IDH3B), 2-oxoglutarate dehydrogenase subunits (ODO1 and ODO2), and dihydrolipoyl dehydrogenase (DLDH) are employed in TCA cycle. It was previously demonstrated in rat and rabbit nephrons that activities of isocitrate dehydrogenase and pyruvate dehydrogenase are higher in medullary structures of nephrons [39].

In TCA cycle, acetyl-CoA moieties produced by glycolysis and pyruvate decarboxylation are converted by series of reactions to carbon dioxide and reduced coenzymes NADH and FADH₂. When the oxygen availability is limited, regeneration of reduced coenzymes by electron transport system (ETS) is limited and TCA cycle shows

different way of operation [40]. Conversion of α -ketoglutarate to succinate by 2-oxoglutarate dehydrogenase is important for generation of ATP via substrate-level phosphorylation under hypoxic conditions [40]. Increased expression of pyruvate dehydrogenase and activity of 2-oxoglutarate dehydrogenase were found in liver mitochondria as a result of response to hypoxia [41]. Increased amount of ODPA and 2-oxoglutarate dehydrogenase subunits may suggest adaptation of renal medullar mitochondria to low oxygen environment. Ornithine aminotransferase (OAT) plays a key role in converting of ornithine to glutamate, which is further supplied to the TCA cycle for energy production. Our results correspond to OAT profile in rat kidney, where the highest concentration of OAT was found in the outer stripe of renal medulla [42].

Spots containing several subunits of electron transport system (ETS) complexes showed higher intensity in KM mitochondrial fraction. ETS performs transfer of electrons from reduced coenzymes and creates proton gradient between mitochondrial matrix and the intermembrane space. Five ETS complexes are composed of multiple subunits and anchored to inner mitochondrial membrane. Proteins NADH dehydrogenase subunit 8 of alpha-subcomplex (NDUA8), subunits 7 (NDUB7) and 10 (NDUBA) found in our experiment with higher intensity in KM mitochondrial fraction were described as supernumerary subunits of ETS complex I. Their predicted functions are activity regulation, assembling, and stabilization of complex I [43, 44]. Previous studies have found the importance



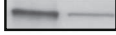
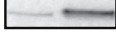
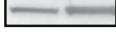

protein	Western blot	KM/KC (IQR)
ACADM		0.33 (0.25-0.38)
GABT		0.31 (0.21-0.48)
PCKGM		0.39 (0.36-0.44)
ODO2		1.96 (1.90-2.13)
QCR1		1.80 (1.68-2.05)
VDAC2		1.94 (1.85-2.06)

Fig. 4 Validation of proteomic results by Western blotting. Expression of selected proteins was analyzed by Western blotting in KC and KM mitochondrial fractions. Protein name, protein band in KC (*left band*) and KM (*right band*) mitochondrial fractions, and KM/KC ratio (interquartile range) determined by Western blotting are shown

of Rieske protein (UCRI) and Cytochrome c oxidase subunit 5B (COX5B) in response to hypoxia. UCRI is one of the catalytic subunits of complex III. Protein UCRI was found to be important for production of ROS in hypoxia [45] which is required for stabilization of hypoxia-induced factor HIF-1 α [45]. COX5B is a subunit of complex IV and this subunit was found to be expressed in cells as a result of their adaptation to low oxygen environment [46]. Therefore, we hypothesize that increased abundance of these ETS complex subunits in medullar mitochondria can be interpreted as adaptation of medullar mitochondrial to low oxygen environment and maintaining activity of ETS in relatively hypoxic renal medulla.

Voltage-dependent anion-selective channel proteins 1 and 2 (VDAC1 and VDAC2) form pores located on mitochondrial outer membrane responsible for transport of small molecules (e.g. nucleotides and metabolites) and regulation of ATP transport outside mitochondrion [47]. It was shown in kidney cell line that diminished VDAC1 expression caused slow proliferation, reduced ATP synthesis rates, ATP and ADP content [48]. Thus, higher amounts of VDAC may contribute to support exchange of metabolites and ATP in pig KM mitochondria. Elongation factor thermo unstable (EFTU) is one of factors required for the synthesis of proteins encoded by the mitochondrial DNA [49]. Overexpression of elongation factors can partially suppress the defect in assembly of ETS complexes [50] and enhanced expression of EFTU in pig KM mitochondria may be, therefore, important for maintaining levels of ETS subunits coded by mitochondrial DNA.

Proteomic analysis of mitochondrial fractions isolated from tissues is widely used for investigation of mitochondrial proteome in various physiological and pathological states, but limitations of this attempt should be considered. Limitations of 2DE in mitochondrial proteomics are limited dynamic range of detection, limited resolution of

extremely basic proteins, and underrepresentation of membrane proteins on 2DE gels. Another limitation of our work arises from tissue separation. Renal cortex and medulla have been excised from kidney and used without their further separation. This is the simplest way to reduce the sample complexity. For more detailed information about heterogeneity of renal mitochondria, it would be necessary to isolate individual nephron segments under microscopic control.

Taken together, proteins of beta oxidation, amino acid metabolism, and gluconeogenesis were predominant in mitochondria of kidney cortex. In renal cortex, the proximal tubule exhibits high amount of mitochondria and relative high oxygen availability in the cortex suggests preference of highly effective oxygen-dependent processes such as beta oxidation. Protein spots more abundant in kidney medullar mitochondrial fraction contained TCA cycle enzymes and ETS proteins, proteins maintaining metabolite transport and mitochondrial translation. In renal medulla, less oxygen is available in comparison with the cortex, and proteome of KM mitochondria shows their possible adaptation to hypoxic environment. Some proteins of TCA cycle and ETS system showed the pattern previously seen in hypoxic model systems and porin proteins may support nucleotide exchange between medullar mitochondria and cytoplasm. In conclusion, different and physiologically relevant composition of renal cortex versus renal medulla mitochondrial proteome was described in this study. This heterogeneity in the kidney compartments might dictate their different responses and susceptibility to various acute and chronic pathologic stimuli. We believe that our study has helped to establish a picture of the mitochondrial proteomic appearance of porcine kidney. The knowledge of a healthy renal mitochondrial proteome should help to identify and interpret novel pathways implicated in various renal diseases associated with mitochondrial dysfunction.

Acknowledgments This work was supported by the Research Project No. MSM0021620819 “Replacement of and Support to Some Vital Organs”, by the Charles University Research Fund (project number P36) by the project ED2.1.00/03.0076 by the European Regional Development Fund, and the Specific Student Research Project no. 260175/2015 of the Charles University in Prague.

Conflict of interest All the authors have declared no competing interest.

References

- Balaban RS, Mandel LJ, Soltoff SP, Storey JM. Coupling of active ion transport and aerobic respiratory rate in isolated renal tubules. *Proc Natl Acad Sci U S A*. 1980;77(1):447–51.
- Guder WG, Ross BD. Enzyme distribution along the nephron. *Kidney Int*. 1984;26(2):101–11.

3. Hall AM, Unwin RJ. The not so 'mighty chondrion': emergence of renal diseases due to mitochondrial dysfunction. *Nephron Physiol.* 2007;105(1):p1–10.
4. Brooks C, Wei Q, Cho SG, Dong Z. Regulation of mitochondrial dynamics in acute kidney injury in cell culture and rodent models. *J Clin Investig.* 2009;119(5):1275–85.
5. Funk JA, Schnellmann RG. Persistent disruption of mitochondrial homeostasis after acute kidney injury. *Am J Physiol Renal Physiol.* 2012;302(7):F853–64.
6. Dare AJ, Phillips AR, Hickey AJ, Mittal A, Loveday B, Thompson N, et al. A systematic review of experimental treatments for mitochondrial dysfunction in sepsis and multiple organ dysfunction syndrome. *Free Radic Biol Med.* 2009;47(11):1517–25.
7. Parikh SM. Therapeutic targeting of the mitochondrial dysfunction in septic acute kidney injury. *Current opinion in critical care.* 2013;19(6):554–9.
8. Thongboonkerd V. Current status of renal and urinary proteomics: ready for routine clinical application? *Nephrol Dial Transplant.* 2010;25(1):11–6.
9. Arthur JM, Thongboonkerd V, Scherzer JA, Cai J, Pierce WM, Klein JB. Differential expression of proteins in renal cortex and medulla: a proteomic approach. *Kidney Int.* 2002;62(4):1314–21.
10. Xu B, Yoshida Y, Zhang Y, Yaoita E, Osawa T, Yamamoto T. Two-dimensional electrophoretic profiling of normal human kidney: differential protein expression in glomerulus, cortex and medulla. *J Electrophor.* 2005;49(1):5–13.
11. Fountoulakis M, Berndt P, Langen H, Suter L. The rat liver mitochondrial proteins. *Electrophoresis.* 2002;23(2):311–28.
12. Bugger H, Chen D, Riehle C, Soto J, Theobald HA, Hu XX, et al. Tissue-specific remodeling of the mitochondrial proteome in type 1 diabetic akita mice. *Diabetes.* 2009;58(9):1986–97.
13. Freund DM, Prenni JE, Curthoys NP. Response of the mitochondrial proteome of rat renal proximal convoluted tubules to chronic metabolic acidosis. *Am J Physiol Renal Physiol.* 2013;304(2):F145–55.
14. Chaiyarit S, Thongboonkerd V. Changes in mitochondrial proteome of renal tubular cells induced by calcium oxalate monohydrate crystal adhesion and internalization are related to mitochondrial dysfunction. *J Proteome Res.* 2012
15. Goldfarb RD, Dellinger RP, Parrillo JE. Porcine models of severe sepsis: emphasis on porcine peritonitis. *Shock.* 2005;24(Suppl 1):75–81.
16. Doi K, Leelahavanichkul A, Yuen PS, Star RA. Animal models of sepsis and sepsis-induced kidney injury. *J clin investig.* 2009;119(11):2868–78.
17. Baumert H, Faure JP, Zhang K, Petit I, Goujon JM, Duthel D, et al. Evidence for a mitochondrial impact of trimetazidine during cold ischemia and reperfusion. *Pharmacology.* 2004;71(1):25–37.
18. Bendixen E. Animal models for translational proteomics. *Proteomics Clin Appl.* 2014;8(10):637–9.
19. de Cavanagh EM, Piotrkowski B, Basso N, Stella I, Insera F, Ferder L, et al. Enalapril and losartan attenuate mitochondrial dysfunction in aged rats. *FASEB j: off publ Fed Am Soc Exp Biol.* 2003;17(9):1096–8.
20. Mares J, Richtrova P, Hricinova A, Tuma Z, Moravec J, Lysak D, et al. Proteomic profiling of blood-dialyzer interactome reveals involvement of lectin complement pathway in hemodialysis-induced inflammatory response. *Proteomics Clin Appl.* 2010;4(10–11):829–38.
21. Kiyomiya K, Matsushita N, Matsuo S, Kurebe M. Cephaloridine-induced inhibition of cytochrome c oxidase activity in the mitochondria of cultured renal epithelial cells (LLC-PK(1)) as a possible mechanism of its nephrotoxicity. *Toxicol Appl Pharmacol.* 2000;167(2):151–6.
22. Verma N, Rettenmeier AW, Schmitz-Spanke S. Recent advances in the use of *Sus scrofa* (pig) as a model system for proteomic studies. *Proteomics.* 2011;11(4):776–93.
23. Lebieczinska M, Szabadkai G, Jones AW, Duszynski J, Wieckowski MR. Interactions between the endoplasmic reticulum, mitochondria, plasma membrane and other subcellular organelles. *Int J Biochem Cell Biol.* 2009;41(10):1805–16.
24. Eaton S, Bartlett K, Pourfarzam M. Mammalian mitochondrial beta-oxidation. *Biochem J.* 1996;320(Pt 2):345–57.
25. Lehir M, Dubach UC. Peroxisomal and mitochondrial beta-oxidation in the rat-kidney: distribution of fatty acyl-coenzyme a oxidase and 3-hydroxyacyl-coenzyme-a dehydrogenase-activities along the nephron. *J Histochem Cytochem.* 1982;30(5):441–4.
26. Gerich JE, Meyer C, Woerle HJ, Stumvoll M. Renal gluconeogenesis: its importance in human glucose homeostasis. *Diabetes Care.* 2001;24(2):382–91.
27. Yasuda M, Fujita T, Higashio T, Okahara T, Abe Y, Yamamoto K. Effects of 4-pentenoic acid and furosemide on renal functions and renal uptake of individual free fatty acids. *Pflug Arch.* 1980;385(2):111–6.
28. Huss JM, Levy FH, Kelly DP. Hypoxia inhibits the peroxisome proliferator-activated receptor alpha/retinoid X receptor gene regulatory pathway in cardiac myocytes: a mechanism for O₂-dependent modulation of mitochondrial fatty acid oxidation. *J Biol Chem.* 2001;276(29):27605–12.
29. Knight J, Jiang J, Assimios DG, Holmes RP. Hydroxyproline ingestion and urinary oxalate and glycolate excretion. *Kidney Int.* 2006;70(11):1929–34.
30. Lowry M, Hall DE, Brosnan JT. Hydroxyproline metabolism by the rat kidney: distribution of renal enzymes of hydroxyproline catabolism and renal conversion of hydroxyproline to glycine and serine. *Metab, Clin Exp.* 1985;34(10):955–61.
31. Burgmeier N, Zawislak R, Defeudis FV, Bollack C, Helwig JJ. Glutamic acid decarboxylase in tubules and glomeruli isolated from rat kidney cortex. *Eur J Biochem.* 1985;151(2):361–4.
32. Tillakaratne NJ, Medina-Kauwe L, Gibson KM. Gamma-aminobutyric acid (GABA) metabolism in mammalian neural and nonneural tissues. *Comp Biochem Physiol A Physiol.* 1995;112(2):247–63.
33. Pircher H, Straganz GD, Eehalt D, Morrow G, Tanguay RM, Jansen-Durr P. Identification of human fumarylacetoacetate hydrolase domain-containing protein 1 (FAHD1) as a novel mitochondrial acylpyruvase. *J Biol Chem.* 2011;286(42):36500–8.
34. Wyss M, Kaddurah-Daouk R. Creatine and creatinine metabolism. *Physiol Rev.* 2000;80(3):1107–213.
35. van de Poll MC, Soeters PB, Deutz NE, Fearon KC, Dejong CH. Renal metabolism of amino acids: its role in interorgan amino acid exchange. *Am J Clin Nutr.* 2004;79(2):185–97.
36. Monteil C, Fillastre JP, Morin JP. Expression and subcellular distribution of phosphoenolpyruvate carboxykinase in primary cultures of rabbit kidney proximal tubule cells: comparative study with renal and hepatic PEPCK in vivo. *Biochim Biophys Acta.* 1995;1243(3):437–45.
37. Watford M, Hod Y, Chiao YB, Utter MF, Hanson RW. The unique role of the kidney in gluconeogenesis in the chicken. The significance of a cytosolic form of phosphoenolpyruvate carboxykinase. *J Biol Chem.* 1981;256(19):10023–7.
38. Modaresi S, Brechtel K, Christ B, Jungermann K. Human mitochondrial phosphoenolpyruvate carboxykinase 2 gene. Structure, chromosomal localization and tissue-specific expression. *Biochem J.* 1998;333(Pt 2):359–66.
39. Schmidt U, Guder WG. Sites of enzyme activity along the nephron. *Kidney Int.* 1976;9(3):233–42.

40. Chinopoulos C. Which way does the citric acid cycle turn during hypoxia? The critical role of alpha-ketoglutarate dehydrogenase complex. *J Neurosci Res.* 2013;91(8):1030–43.
41. Dukhande VV, Sharma GC, Lai JC, Farahani R. Chronic hypoxia-induced alterations of key enzymes of glucose oxidative metabolism in developing mouse liver are mTOR dependent. *Mol Cell Biochem.* 2011;357(1–2):189–97.
42. Levillain O, Hus-Citharel A, Garvi S, Peyrol S, Reymond I, Mutin M, et al. Ornithine metabolism in male and female rat kidney: mitochondrial expression of ornithine aminotransferase and arginase II. *Am J Physiol Renal Physiol.* 2004;286(4):F727–38.
43. Hirst J. Why does mitochondrial complex I have so many subunits? *Biochem J.* 2011;437(2):e1–3.
44. Hirst J, Carroll J, Fearnley IM, Shannon RJ, Walker JE. The nuclear encoded subunits of complex I from bovine heart mitochondria. *Biochim Biophys Acta.* 2003;1604(3):135–50.
45. Guzy RD, Hoyos B, Robin E, Chen H, Liu LP, Mansfield KD, et al. Mitochondrial complex III is required for hypoxia-induced ROS production and cellular oxygen sensing. *Cell Metab.* 2005;1(6):401–8.
46. Trueblood CE, Wright RM, Poyton RO. Differential regulation of the two genes encoding *Saccharomyces cerevisiae* cytochrome c oxidase subunit V by heme and the HAP2 and REO1 genes. *Mol Cell Biol.* 1988;8(10):4537–40.
47. Rostovtseva T, Colombini M. ATP flux is controlled by a voltage-gated channel from the mitochondrial outer membrane. *J Biol Chem.* 1996;271(45):28006–8.
48. Abu-Hamad S, Sivan S, Shoshan-Barmatz V. The expression level of the voltage-dependent anion channel controls life and death of the cell. *Proc Natl Acad Sci U S A.* 2006;103(15):5787–92.
49. Worriax VL, Burkhardt W, Spremulli LL. Cloning, sequence analysis and expression of mammalian mitochondrial protein synthesis elongation factor Tu. *Biochim Biophys Acta.* 1995;1264(3):347–56.
50. Sasarman F, Antonicka H, Shoubridge EA. The A3243G tRNA^{Leu}(UUR) MELAS mutation causes amino acid misincorporation and a combined respiratory chain assembly defect partially suppressed by overexpression of EFTu and EFG2. *Hum Mol Genet.* 2008;17(23):3697–707.



Altered plasma proteome during an early phase of peritonitis-induced sepsis

Visith THONGBOONKERD*, Wararat CHIANGJONG*, Jan MARES†, Jiri MORAVEC†, Zdenek TUMA†, Thomas KARVUNIDIS†, Supachok SINCHAIKUL‡, Shui-Tein CHEN‡§, Karel OPATRŇY JR†¹ and Martin MATEJOVIC†

*Medical Proteomics Unit, Office for Research and Development, Faculty of Medicine Siriraj Hospital, Mahidol University, Bangkok 10700, Thailand, †Proteomics Laboratory, Department of Internal Medicine I and Intensive Care Unit, Charles University School of Medicine in Plzeň, 304 60 Plzeň, Czech Republic, ‡Institute of Biological Chemistry and Genomic Research Center, Academia Sinica, Taipei, Taiwan, and §Institute of Biochemical Sciences, College of Life Science, National Taiwan University, Taipei, Taiwan

A B S T R A C T

Sepsis is a systemic response to infection commonly found in critically ill patients and is associated with multi-organ failure and high mortality rate. Its pathophysiology and molecular mechanisms are complicated and remain poorly understood. In the present study, we performed a proteomics investigation to characterize early host responses to sepsis as determined by an altered plasma proteome in a porcine model of peritonitis-induced sepsis, which simulated several clinical characteristics of human sepsis syndrome. Haemodynamics, oxygen exchange, inflammatory responses, oxidative and nitrosative stress, and other laboratory parameters were closely monitored. Plasma samples were obtained from seven pigs before and 12 h after the induction of sepsis, and plasma proteins were resolved with two-dimensional gel electrophoresis ($n = 7$ gels/group; before being compared with during sepsis). The resolved proteins were stained with the SYPRO Ruby fluorescence dye and subjected to quantitative and comparative analyses. From approx. 1500 protein spots visualized in each gel, levels of 36 protein spots were significantly altered in the plasma of animals with sepsis (sepsis/basal ratios or degrees of change ranged from 0.07 to 21.24). Q-TOF (quadrupole–time-of-flight) MS and MS/MS (tandem MS) identified 30 protein forms representing 22 unique proteins whose plasma levels were increased, whereas six forms of five unique proteins were significantly decreased during sepsis. The proteomic results could be related to the clinical features of this animal model, as most of these altered proteins have important roles in inflammatory responses and some of them play roles in oxidative and nitrosative stress. In conclusion, these findings may lead to a better understanding of the pathophysiology and molecular mechanisms underlying the sepsis syndrome.

Key words: host response, infection, plasma, proteomics, sepsis, septicaemia.

Abbreviations: 2-D, two-dimensional; ACN, acetonitrile; BP, blood pressure; CO, cardiac output; CVP, central venous pressure; DO_2 , oxygen delivery; DTT, dithiothreitol; FiO_2 , fraction of inspired oxygen; IEF, isoelectric focusing; IL, interleukin; LPS, lipopolysaccharide; Q-TOF, quadrupole–time-of-flight; MS/MS, tandem MS; NCBI, National Center for Biotechnology Information; NO_x , nitrate/nitrite; PAOP, pulmonary artery occlusion pressure; P_{CO_2} , partial pressure of carbon dioxide; PEEP, positive end-expiratory pressure; P_{O_2} , partial pressure of oxygen; SVR, systemic vascular resistance; TBARS, thiobarbituric acid-reacting substances; TFA, trifluoroacetic acid; $TNF-\alpha$, tumour necrosis factor- α ; $\dot{V}O_2$, oxygen consumption.

¹ Deceased

Correspondence: Dr Visith Thongboonkerd (email thongboonkerd@dr.com or vthongbo@yahoo.com) or Dr Martin Matejovic (email matejovic@fnplzen.cz).

INTRODUCTION

Sepsis is defined as a systemic inflammatory response syndrome due to presumed or confirmed infection [1,2]. It is associated with multi-organ failure, which in turn serves as a marker for the high mortality rate of sepsis [2,3]. Even with treatments with the currently available regimens of antibiotics, fluid resuscitation, vasoactive compounds, corticosteroids etc. [4–6], the morbidity and mortality rates remain considerably high. Several attempts have been made to define new therapeutic targets, for example IL-12 (interleukin-12) [7], HMG (high-mobility group) box-1 isoforms [8], trypsin [9] and several others [10]; however, the molecular mechanisms underlying sepsis remain poorly understood. Searching for biomolecules that are involved in the pathophysiology of sepsis would be a significant advance and would facilitate defining new therapeutic targets for better treatment outcomes.

Over the last decade, proteomics has been emerging and used for the high-throughput analysis of proteins. It has been extensively applied to several subdisciplines of biomedical research, particularly for clinical applications, with the ultimate goals to understand normal physiology better, to explore the pathogenic mechanisms of diseases, and to search for novel biomarkers and therapeutic targets for improving treatment outcome [11–13]. In the present study, we applied a gel-based proteomics approach to characterize early responses to sepsis, as determined by changes in the plasma proteome during an early phase of sepsis. A porcine model of peritonitis-induced sepsis, which displays several clinical characteristics resembling those of sepsis syndrome in humans, was employed in our present study. Peritonitis-induced sepsis was initiated by intraperitoneal injection of autologous faeces with careful monitoring of haemodynamics, oxygen exchange, inflammatory responses, oxidative and nitrosative stress, and other laboratory parameters. The plasma proteome at 12 h after the induction of sepsis was compared with the basal plasma proteome (before sepsis induction) using 2-D (two-dimensional) gel electrophoresis. Differential analysis revealed significant differences in levels of 36 protein spots, which were subsequently identified by Q-TOF (quadrupole-time-of-flight) MS and/or MS/MS (tandem MS). Potential roles of these altered proteins induced by sepsis are discussed.

MATERIALS AND METHODS

Ethics

The present study was performed according to the National Institutes of Health Guidelines on the Use of Laboratory Animals, and the study protocol was

approved by the Ethical Committee at Charles University School of Medicine in Plzeň.

Experimental set up and the induction of sepsis

A total of seven pigs were included in the present study and all of them were closely monitored. After an induction of anaesthesia with intravenous atropine (0.5 mg), 2% (v/v) propofol (1–2 mg/kg of body weight) and ketamine (2 mg/kg of body weight), all of the animals were mechanically ventilated with an F_{iO_2} (fraction of inspired oxygen) of 0.4, PEEP (positive end-expiratory pressure) of 5–10 cmH₂O, and a tidal volume of 10 ml/kg of body weight. The respiratory rate was adjusted to maintain an arterial P_{CO_2} (partial pressure of carbon dioxide) between 4.0 and 5.0 kPa. Anaesthesia was maintained with continuous intravenous thiopental (10 mg · kg⁻¹ of body weight · h⁻¹) and fentanyl (10–15 µg · kg⁻¹ of body weight · h⁻¹) during surgery and then maintained with continuous intravenous thiopental (5 mg · kg⁻¹ of body weight · h⁻¹) and fentanyl (5 µg · kg⁻¹ of body weight · h⁻¹) thereafter until the end of the study. Muscle paralysis was achieved with pancuronium (0.2 mg · kg⁻¹ of body weight · h⁻¹). The intravenous fluid was Plasma Lyte[®] solution (Baxter Healthcare) with a rate of 15 ml · kg⁻¹ of body weight · h⁻¹ during surgery and then of 7 ml · kg⁻¹ of body weight · h⁻¹ as a maintenance fluid. Arterial blood glucose levels were maintained at 4.5–7.0 mmol/l using a 20% (w/v) glucose infusion.

A central venous catheter was inserted through the left jugular vein for administration of all of the drugs and fluids. A balloon-tipped thermodilution pulmonary artery catheter was placed via the right jugular vein. A femoral arterial catheter was placed for BP (blood pressure) monitoring and blood sampling. Two tubes were placed through the abdominal wall for the induction of peritonitis and ascites drainage. A cystostomy catheter for urine collection was placed percutaneously under ultrasound guidance.

After all measurements and sample collection at baseline, sepsis was initiated by the induction of peritonitis by inoculating 0.5 g of autologous faeces/kg of body weight suspended in 200 ml of saline into the abdominal cavity through the drainage tubes. A second set of measurements and sample collection were obtained 12 h after the induction of sepsis. In addition to the Plasma Lyte[®] solution, 6% (w/v) hydroxyethyl starch 130 kDa/0.4 (Voluven[®] 6%; Fresenius Kabi) at a rate of 10 ml · kg⁻¹ of body weight · h⁻¹ was infused to maintain a cardiac filling pressure ≥ 12 mmHg [the rate was decreased to 7 ml · kg⁻¹ of body weight · h⁻¹ if the CVP (central venous pressure) or PAOP (pulmonary artery occlusion pressure) ≥ 18 mmHg]. When the last set of data had been obtained, the animals were killed by KCl injection under deep anaesthesia.

Monitoring of haemodynamics, oxygen kinetics, inflammatory responses, oxidative and nitrosative stress, and other laboratory parameters

Measurements for monitoring systemic haemodynamics included CO (cardiac output), SVR (systemic vascular resistance), intrathoracic blood volume and filling pressures of both ventricles (CVP and PAOP for right and left ventricles respectively). Arterial and mixed venous blood samples were analysed for pH, P_{O_2} (partial pressure of oxygen), P_{CO_2} and haemoglobin oxygen saturation. Systemic DO_2 (oxygen delivery) and systemic $\dot{V}O_2$ (oxygen consumption) were derived from the appropriate blood gases and flow measurements [14,15]. Arterial blood samples were obtained for the determination of TNF- α (tumour necrosis factor- α) and IL-6 by immunoassay [14,15]. Oxidative and nitrosative stress was evaluated by measuring concentrations of arterial TBARS (thiobarbituric acid-reacting substances) by spectrophotometry, and arterial NO $_x$ (nitrate/nitrite) by colorimetric assay [14,15]. To correct for dilutional effects resulting from volume resuscitation, the levels of NO $_x$, TBARS, IL-6 and TNF- α were normalized to plasma protein content [14,15].

2-D Gel electrophoresis

Plasma samples were diluted 1:5 with deionized water, and protein concentrations in individual samples were measured using the Bradford method [16]. Protein solutions (each with 200 μ g of total protein) were then premixed with a rehydration buffer containing 7 mol/l urea, 2 mol/l thiourea, 2% (w/v) CHAPS, 120 mmol/l DTT (dithiothreitol), 40 mmol/l Tris base, 2% ampholytes (pH 3–10) and a trace of Bromophenol Blue to make the final volume of 150 μ l/sample. The mixtures were rehydrated on to ImmobilineTM DryStrips (7 cm long IPG strips; linear pH gradient of 3–10 and of 4–7; GE Healthcare) at room temperature (25 °C) for 10–15 h. The first-dimensional separation or IEF (isoelectric focusing) was performed in the Ettan IPGphor II IEF System (GE Healthcare) at 20 °C, using a stepwise mode to reach 9083 Vh. After completion of the IEF, the strips were first equilibrated for 15 min in an equilibration buffer containing 6 mol/l urea, 130 mmol/l DTT, 112 mmol/l Tris base, 4% (w/v) SDS, 30% (v/v) glycerol and 0.002% Bromophenol Blue, and then in another similar buffer, which replaced DTT with 135 mmol/l iodoacetamide, for a further 15 min. The second-dimensional separation was performed on a 12% (w/v) polyacrylamide gel using a SE260 mini-vertical electrophoresis unit (GE Healthcare) at 150 V for approx. 2 h. Separated proteins were visualized with SYPRO Ruby fluorescence staining (Invitrogen/Molecular Probes). Gel images were taken using a Typhoon laser scanner (GE Healthcare).

Matching and analysis of protein spots

Image Master 2D Platinum (GE Healthcare) software was used for matching and analysis of protein spots in 2-D gels. Parameters used for spot detection were (i) minimal area = 10 pixels; (ii) smooth factor = 2.0; and (iii) saliency = 2.0. A reference gel was created from an artificial gel combining all of the spots presenting in different gels into one image. The reference gel was then used for matching the corresponding protein spots between gels. Background subtraction was performed and the intensity volume of each spot was normalized with the total intensity volume (summation of the intensity volumes obtained from all spots within the same 2-D gel). Significant differences in intensity levels of protein spots were defined as changes with all of the followings: (i) sepsis/control ratios \geq 2-fold or \leq 0.5-fold; (ii) $P < 0.05$; and (iii) consistent presence (or absence) in all gels within the group.

In-gel tryptic digestion

The protein spots whose intensity levels significantly differed between groups were excised from the 2-D gels, washed twice with 200 μ l of 50% (v/v) ACN (acetonitrile)/25 mmol/l NH_4HCO_3 buffer (pH 8.0) at room temperature for 15 min, and then washed once with 200 μ l of 100% ACN. After washing, the solvent was removed, and the gel pieces were dried using a SpeedVac concentrator (Savant) and rehydrated with 10 μ l of 1% (w/v) trypsin (Promega) in 25 mmol/l NH_4HCO_3 (pH 8.0). After rehydration, the gel pieces were crushed with a siliconized blue stick and incubated at 37 °C for at least 16 h. Peptides were subsequently extracted twice with 50 μ l of 50% (v/v) ACN/5% (v/v) TFA (trifluoroacetic acid); the extracted solutions were then combined and dried with a SpeedVac concentrator. The peptide pellets were resuspended with 10 μ l of 0.1% TFA and purified using ZipTip_{C18} (Millipore). The peptide solution was drawn up and down in the ZipTip_{C18} ten times and then washed with 10 μ l of 0.1% formic acid by drawing up and expelling the washing solution for three times. The peptides were finally eluted with 5 μ l of 75% (v/v) ACN/0.1% formic acid.

Protein identification by MALDI (matrix-assisted laser-desorption ionization)–Q-TOF MS and MS/MS analyses

The proteolytic samples were premixed 1:1 with the matrix solution [5 mg/ml CHCA (α -cyano-4-hydroxycinnamic acid) in 50% (v/v) ACN, 0.1% (v/v) TFA and 2% (w/v) ammonium citrate] and spotted on to the 96-well sample stage. The samples were analysed using a Q-TOF UltimaTM mass spectrometer (Micromass), which was fully automated with a pre-defined probe motion pattern and the peak intensity threshold for switching over from MS survey scanning to MS/MS, and from one MS/MS to another. Within each sample well,

parent ions that met the pre-defined criteria (any peak within the m/z 800–3000 range with an intensity above 10 counts \pm include/exclude list) were selected for collision-induced dissociation MS/MS using argon as the collision gas and a mass dependent ± 5 V rolling collision energy until the end of the probe pattern was reached. The low-mass and high-mass resolution of the quadrupole were both set at ten to give a precursor selection window of approx. 4 Da wide. Manual acquisition and optimization for individual samples or peaks was also possible.

The instrument was externally calibrated to a < 5 p.p.m. accuracy over the mass range of m/z 800–3000 using sodium iodide and PEG [poly(ethylene glycol)] 200, 600, 1000 and 2000 mixtures and adjusted further with Glu-fibrinopeptide B as the near-point lock mass calibrant during data processing. At a laser firing rate of 10 Hz, individual spectra from a 5 s integration period acquired for each of the MS survey and MS/MS performed were combined, smoothed, de-isotoped (fast option) and centroided using the ProteinLynx™ GlobalSERVER 2.0 data processing software (Micromass). This entailed the identification of the monoisotopic carbon-12 peaks for MS data and deconvolution of multiply charged spectra to their singly charged equivalents for MS/MS data. MaxEnt 3™, a maximum-entropy-based technique, has been designed for this purpose and is an integral part of ProteinLynx™ GlobalSERVER 2.0 [17]. The combined MS and MS/MS ion meta data were searched in concert against the NCBI (National Center for Biotechnology Information) mammalian protein database using the ProteinLynx™ GlobalSERVER 2.0 workflow. The search algorithm employed a Hidden Markov Model that incorporates empirically determined fragmentation characteristics to increase the efficacy of the search. Additionally, the MS and MS/MS data were extracted and outputted as the searchable .txt and .pkl files respectively, for independent searches using the MASCOT search engine (<http://www.matrixscience.com>), assuming that peptides were monoisotopic. Fixed modification was carbamidomethylation at cysteine residues, whereas variable modification was oxidation at methionine residues. Only one missed trypsin cleavage was allowed, and peptide mass tolerances of 100 and 50 p.p.m. were allowed for the peptide mass fingerprinting and MS/MS ion search respectively.

Pathway analysis

Pathway analysis was performed using the Pathway Tools software version 12.5 (<http://bioinformatics.ai.sri.com/ptools/>). This bioinformatic tool is a comprehensive symbolic systems biology software that supports several applications in bioinformatics and systems biology [18,19]. Biological processes, molecular functions, subcellular localizations and MetaCyc pathways of the altered proteins were obtained by querying the protein or gene ID to the Pathway databases [18].

Table 1 Haemodynamic, metabolic and inflammatory changes at baseline and at 12 h after sepsis induction

Values are medians (interquartile range). * $P < 0.05$ compared with baseline. MAP, mean arterial pressure.

Parameter	At baseline	At 12 h after sepsis induction
CO (ml · kg ⁻¹ of body weight · min ⁻¹)	79 (63–85)	118 (101–141)*
SVR (dyne · s · cm ⁻⁵)	2774 (2718–2887)	1411 (1234–1809)*
MAP (mmHg)	103 (90–107)	93 (79–97)
CVP (mmHg)	11 (9–13)	13 (11–16)*
PAOP (mmHg)	10 (9–13)	14 (11–16)*
DO ₂ (ml · min ⁻¹ · kg ⁻¹ of body weight)	9 (8–11)	15 (14–18)*
$\dot{V}O_2$ (ml · min ⁻¹ · kg ⁻¹ of body weight)	5 (4–6)	6 (5–6)
Arterial pH	7.49 (7.48–7.52)	7.44 (7.43–7.48)*
IL-6 (nmol/g of protein)	2 (1–3)	28 (8–30)*
TNF- α (nmol/g of protein)	1.4 (1.3–1.5)	5 (4.7–9.6)*
NOx (μ mol/g of protein)	0.7 (0.6–0.9)	1.5 (1.2–1.5)*
TBARS (nmol/g of protein)	19 (16–22)	40 (36–60)*

Statistical analysis

All values are shown as means \pm S.E.M., unless otherwise stated. Comparisons between groups (basal control compared with 12 h after the induction of sepsis) were performed using either a paired Student's t test or Wilcoxon signed rank test. P values < 0.05 were considered statistically significant.

RESULTS

Clinical data

Haemodynamic and oxygen exchange parameters, inflammatory responses, oxidative and nitrosative stress, and other laboratory parameters are shown in Table 1. All animals developed normotensive hyperdynamic circulation with reduced SVR. Adequate fluid resuscitation was ensured by monitoring cardiac filling pressures (both CVP and PAOP were monitored for right and left ventricles respectively), which were significantly increased over time. The increased CO resulted in a significant rise in systemic DO₂, whereas systemic $\dot{V}O_2$ remained unchanged. The peritonitis-induced sepsis caused a significant fall in arterial pH and a marked increase in plasma levels of TNF- α and IL-6. Overproduction of NO in this model was documented by a significant increase in arterial NOx levels. These changes were accompanied by a remarkable increase in TBARS levels, providing the evidence for oxidative stress.

Proteomic data

We initially resolved the plasma proteome using the broad-range IPG strips (with a linear pH gradient of

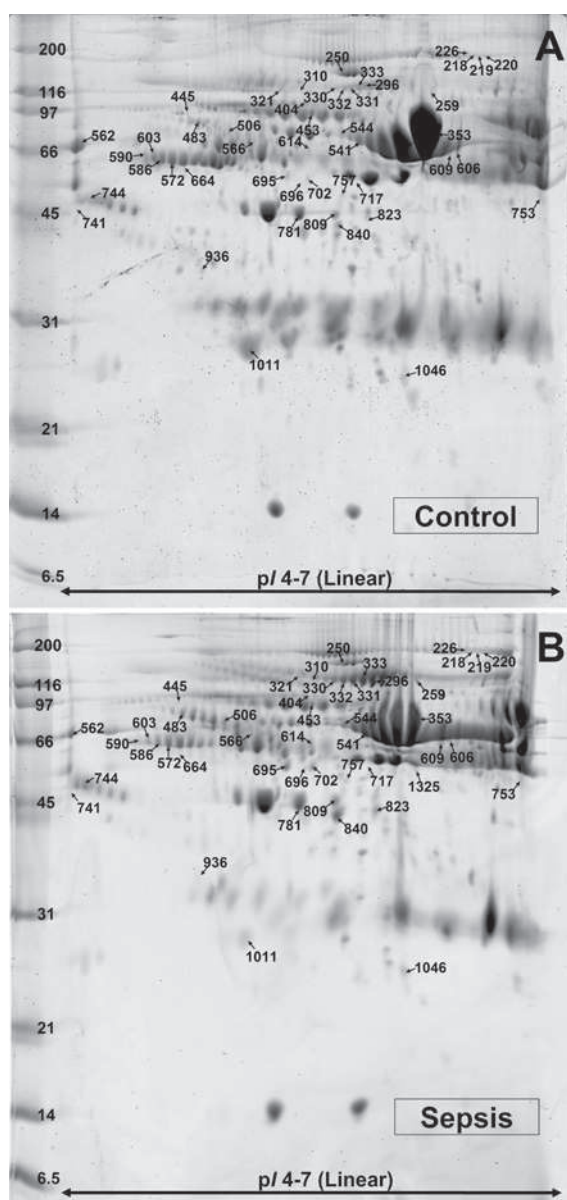


Figure 1 Proteome map of the altered plasma proteome during the early phase of sepsis in a porcine model

Gel images are derived from scans of representative gels from one animal in each group: (A) Control, and (B) Sepsis. Bands in the ladder at the left-hand side of each gel are molecular-mass markers. The significantly up- or down-regulated protein spots are marked with arrows and numbers, which correspond with those indicated in Table 2.

3–10) and observed that most of the porcine plasma proteins were resolved at a pH range of 4–7 (results not shown). We therefore used the narrow-range IPG strips (with a linear pH gradient of 4–7) for the differential proteomics study. Approx. 1500 protein spots were visualized in each 2-D gel (Figure 1). There were seven gels derived from basal plasma samples of seven animals, and another seven gels derived from these animals but at 12 h

after the induction of sepsis. Quantitative intensity analysis and statistics revealed significant differences in levels of 36 protein spots during sepsis (Figure 1 and Table 2). These differentially expressed protein spots included 30 spots with increased levels and six spots with decreased levels. All of these altered proteins were then successfully identified by Q-TOF MS and/or MS/MS analyses. Some of the altered proteins (e.g. albumin, haptoglobin and inter- α -trypsin inhibitor family heavy chain-related protein) were identified as multiple isoforms of the same proteins, most probably due to post-translational modifications. As a consequence, a total of 22 unique proteins were identified from the 30 up-regulated spots, whereas five unique proteins were identified from the six down-regulated spots. Identities, quantitative data, degrees of changes and other related information of all of the altered proteins are summarized in Table 2. Functional analysis using the Pathway Tools software revealed their biological processes, molecular functions, subcellular localizations and involved metabolic pathways, which are summarized in Supplementary Table S1 (see <http://www.ClinSci.org/cs/116/cs1160721add.htm>).

DISCUSSION

The pathophysiology of sepsis is considerably complex and understanding it could lead to identification of novel therapeutic targets with better treatment outcome. In the present study, we applied a proteomics approach to characterize changes in the plasma proteome during an early phase of sepsis in a porcine model of peritonitis-induced sepsis. Clinical features of this model simulated to a very large extent the clinical presentations of early sepsis syndrome in humans, including normotensive hyperdynamic circulation with reduced SVR, development of metabolic acidosis and increased plasma levels of inflammatory mediators (i.e. TNF- α and IL-6), accompanying nitrosative and oxidative stress.

The present study is the first to report the application of proteomics to the study of altered plasma proteome in a large animal model of sepsis, as previously available, but limited, findings had only been obtained from rodent models [20]. These small animal models are often criticized for their limited clinical relevance. Indeed, many emerging strategies, which have been found effective in these models, fail to show any benefit in large animal or human studies. This might be even more important in the context of proteomic analysis, as there are marked differences between species. The fundamental differences include different regulation of inflammation, cardiovascular response to endotoxin or bacteria etc. Rodents differ markedly from humans with respect to their tissue antioxidative capacity and susceptibility to oxidative stress [21–24]. In the present study, differential proteomics analysis revealed altered plasma levels of

Table 2 Plasma proteins whose levels were significantly altered during sepsis

Values for the intensity are means \pm S.E.M. *% Cov = % sequence coverage [(number of the matched residues/total number of residues in the entire sequence) \times 100 %]; †DIV/O = divided by zero. NA, not applicable; Ref. MW, reference molecular mass; Ref *p*, reference *p*.

(A) Proteins whose plasma levels were significantly increased during sepsis

Protein name	Spot no.	NCBI ID	Identified by	Identification scores (MS, MS/MS)	%Cov* (MS, MS/MS)	No. of matched peptides (MS, MS/MS)	Ref. <i>p</i>	Ref. MW (kDa)	Intensity		Ratio (sepsis/control)	<i>P</i> values
									Control (basal)	Sepsis (12 h)		
Albumin	606	gi:164318	MS, MS/MS	130, 129	35, 6	15, 3	5.92	71.35	0.0040 \pm 0.0040	0.0199 \pm 0.0056	4.98	0.040
Albumin	717	gi:833798	MS	130, NA	29, NA	15, NA	5.92	71.36	0.0031 \pm 0.0031	0.0230 \pm 0.0033	7.42	0.001
Albumin	753	gi:833798	MS	75, NA	29, NA	11, NA	5.92	71.36	0.0155 \pm 0.0070	0.0698 \pm 0.0198	4.50	0.024
α_1 -Anti-chymotrypsin I	566	gi:9968809	MS/MS	NA, 130	NA, 11	NA, 2	5.22	24.78	0.0195 \pm 0.0078	0.0765 \pm 0.0154	3.92	0.006
CD14 antigen	702	gi:85816356	MS	67, NA	27, NA	6, NA	5.83	40.37	0.0256 \pm 0.0060	0.0874 \pm 0.0138	3.41	0.001
Cytochrome P450, family 3, subfamily A, polypeptide 41A	696	gi:170295838	MS	73, NA	16, NA	8, NA	7.08	58.32	0.0066 \pm 0.0047	0.0583 \pm 0.0177	8.83	0.015
Haptoglobin	695	gi:47522826	MS	72, NA	25, NA	8, NA	6.51	39.03	0.0668 \pm 0.0127	0.1338 \pm 0.0249	2.00	0.033
Haptoglobin	809	gi:47522826	MS, MS/MS	90, 88	31, 4	10, 1	6.51	39.03	0.0750 \pm 0.0327	0.2290 \pm 0.0301	3.05	0.005
Haptoglobin	823	gi:47522826	MS	92, NA	34, NA	9, NA	6.51	39.03	0.0066 \pm 0.0066	0.1402 \pm 0.0132	21.24	< 0.001
Haptoglobin	840	gi:47522826	MS/MS	NA, 51	NA, 5	NA, 1	6.51	39.03	0.1287 \pm 0.0362	0.3341 \pm 0.0615	2.60	0.014
Heavy chain immunoglobulin variable region	506	gi:1277045	MS	72, NA	43, NA	4, NA	9.36	10.07	0.0211 \pm 0.0069	0.0782 \pm 0.0194	3.71	0.017
Haemopexin	609	gi:47522736	MS/MS	NA, 64	NA, 3	NA, 1	6.59	52.07	0.0031 \pm 0.0031	0.0299 \pm 0.0079	9.65	0.008
Hypothetical protein LOC23078 isoform a	220	gi:57863271	MS	80, NA	13, NA	18, NA	7.01	215.72	0.0234 \pm 0.0034	0.0536 \pm 0.0106	2.29	0.019
Hypothetical protein LOC330361	296	gi:70608163	MS	80, NA	29, NA	12, NA	5.41	88.19	0.0678 \pm 0.0133	0.2229 \pm 0.0462	3.29	0.007
Inter- α -trypsin inhibitor family heavy chain-related protein	333	gi:48374067	MS	51, NA	18, NA	12, NA	6.42	102.25	0.1030 \pm 0.0150	0.2764 \pm 0.0513	2.68	0.007
Inter- α -trypsin inhibitor family heavy chain-related protein	331	gi:48374067	MS, MS/MS	189, 101	35, 5	26, 3	6.42	102.25	0.1039 \pm 0.0119	0.2631 \pm 0.0382	2.53	0.002
Inter- α -trypsin inhibitor family heavy chain-related protein	332	gi:48374067	MS	84, NA	19, NA	14, NA	6.42	102.25	0.0854 \pm 0.0137	0.1757 \pm 0.0225	2.06	0.005
mCG140308, isoform CRA_b	664	gi:148688748	MS	92, NA	39, NA	8, NA	9.17	23.88	0.0081 \pm 0.0041	0.0438 \pm 0.0136	5.41	0.028
Microfilament and actin filament cross-linker protein isoform 3	218	gi:114555665	MS	76, NA	7, NA	31, NA	5.28	850.70	0.0432 \pm 0.0072	0.1048 \pm 0.0207	2.43	0.016

Microfilament and actin filament cross-linker protein isoform 4	219	gi:114555661	MS	68, NA	7, NA	32, NA	5.27	855.07	0.0268 ± 0.0036	0.0731 ± 0.0163	2.73	0.017
N-ethylmaleimide-sensitive fusion protein	321	gi:123241269	MS	63, NA	30, NA	6, NA	6.84	29.00	0.0201 ± 0.0104	0.0652 ± 0.0161	3.24	0.036
Pyruvate carboxylase	226	gi:28200301	MS	74, NA	16, NA	14, NA	6.32	130.47	0.0405 ± 0.0062	0.1205 ± 0.0266	2.98	0.013
Signal transducer and activator of transcription 1	1325	gi:118151390	MS	76, NA	20, NA	10, NA	6.10	83.48	0.0000 ± 0.0000	0.0315 ± 0.0140	DIV/0†	0.044
Similar to CG3493-PA isoform 2	483	gi:109116930	MS	67, NA	23, NA	15, NA	6.12	105.05	0.0472 ± 0.0099	0.1044 ± 0.0179	2.21	0.016
Similar to cytosolic purine 5'-nucleotidase (5-nucleotidase cytosolic II) isoform 8	936	gi:73998435	MS	77, NA	16, NA	8, NA	5.88	66.25	0.0147 ± 0.0071	0.0441 ± 0.0076	3.00	0.015
Similar to plectin 1 isoform 1	1046	gi:73974726	MS	77, NA	7, NA	24, NA	5.72	534.57	0.0457 ± 0.0231	0.1201 ± 0.0192	2.63	0.029
Similar to synaptic vesicle membrane protein VAT-1 homologue	614	gi:73957362	MS	74, NA	27, NA	11, NA	6.15	58.11	0.0308 ± 0.0080	0.0865 ± 0.0085	2.81	< 0.001
Similar to tweety homologue 3	310	gi:149755366	MS	74, NA	28, NA	9, NA	6.06	49.90	0.0231 ± 0.0084	0.0584 ± 0.0111	2.53	0.026
Transformation/transcription domain-associated protein isoform 2	744	gi:109065980	MS	85, NA	10, NA	24, NA	8.45	438.01	0.1672 ± 0.0330	0.3384 ± 0.0312	2.02	0.003
Viteliform macular dystrophy 2-like 3 isoform 1	259	gi:114645801	MS	86, NA	34, NA	9, NA	8.82	46.85	0.0432 ± 0.0104	0.0951 ± 0.0181	2.20	0.029

(B) Proteins whose plasma levels were significantly decreased during sepsis

Protein name	Spot no.	NCBI ID	Identified by	Identification scores (MS, MS/MS)	%Cov* (MS, MS/MS)	No. of matched peptides (MS, MS/MS)	Ref. pI	Ref. MW (kDa)	Intensity		Ratio (sepsis/control)	P values
									Control (basal)	Sepsis (12 h)		
Albumin	562	gi:164318	MS, MS/MS	158, 238	39, 9	17, 5	5.92	71.35	0.6597 ± 0.1326	0.2727 ± 0.1053	0.41	0.041
α ₂ -HS-glycoprotein precursor (fetuin-A)	603	gi:231467	MS	75, NA	31, NA	7, NA	5.50	39.20	0.2557 ± 0.0158	0.1022 ± 0.0213	0.40	< 0.001
Apolipoprotein A-I precursor (Apo-AI)	1011	gi:461519	MS	81, NA	35, NA	9, NA	5.48	30.31	1.4983 ± 0.1397	0.4730 ± 0.0481	0.32	< 0.001
Immunoglobulin heavy chain variable region	445	gi:91979054	MS	66, NA	59, NA	5, NA	8.73	10.80	0.0253 ± 0.0036	0.0118 ± 0.0023	0.47	0.008
Serum albumin precursor	741	gi:76363596	MS	73, NA	24, NA	11, NA	5.89	70.49	0.0576 ± 0.0177	0.0038 ± 0.0038	0.07	0.011
Vitronectin	590	gi:1754491	MS	92, NA	25, NA	8, NA	5.48	44.61	0.1714 ± 0.0427	0.0461 ± 0.0100	0.27	0.014

36 protein forms representing 27 unique proteins in our porcine sepsis model. The roles of some of these altered proteins are highlighted below.

CD14 is a receptor for bacterial LPS (lipopolysaccharide) that co-ordinates with TLR4 (Toll-like receptor 4) and MD-2 (myeloid differentiation-2) to mediate the innate immune response to bacterial LPS [25,26]. Activation of this upstream signalling pathway leads to the activation of the downstream factor NF- κ B (nuclear factor κ B), secretion of several inflammatory cytokines and, ultimately, inflammatory responses. Some bacterial infections use CD14 to enhance its invasion into hosts [27]. Moreover, monocyte CD14 and soluble CD14 can be used as markers for predicting mortality in patients with severe community-acquired infection [28]. In the present study, we identified an increased level of plasma CD14 in our porcine model of early sepsis, consistent with the findings published by Brunialti et al. [29], who reported an increased serum level of CD14 in patients with sepsis. These results indicate that CD14 is an important upstream molecule in the inflammatory cascade of sepsis.

Haptoglobin is one of the acute-phase reaction proteins [30,31] that also binds to haemoglobin with a potent affinity and thus can prevent renal iron loss and oxidative damage mediated by free haemoglobin [32–34]. Hence it serves not only as an acute-phase reactant, but is also involved in oxidative stress pathways. Several lines of evidence have demonstrated the increased level of haptoglobin as a scavenger system in a number of models of oxidative stress [35–37]. Another protein involved in oxidative stress is haemopexin, which binds to haem and transports it to the liver for its breakdown and iron recovery. As haem is highly toxic to cells due to pro-inflammatory and oxidative effects, haemopexin thus serves as an anti-inflammatory molecule and an oxidative scavenger [35,38]. Our present results are consistent with the findings in previous studies by Kalenka et al. [39] and Ren et al. [20], who reported increased plasma haptoglobin levels in patients with sepsis and increased plasma haemopexin in a murine model of sepsis respectively. The increased levels of both haptoglobin and haemopexin identified in our present study thus strengthen the important roles of these two molecules in mediating inflammatory processes and oxidative stress during an early phase of sepsis.

There were several altered proteins whose roles in sepsis remain unclear. For example, microfilament and actin filament cross-linker protein isoforms 3 and 4 (microtubule-actin cross-linking factor 1, isoforms 3 and 4) and plectin 1, which are involved in cytoskeletal assembly [40–44]. These proteins interlink intermediate filaments with microtubules and microfilaments, and also anchor intermediate filaments to desmosomes or hemidesmosomes [43–46]. The precise roles of these altered proteins in sepsis are somewhat interesting and deserve further investigation.

It should be noted that there are some limitations in our present study. First, 2-D gel electrophoresis is generally not a very sensitive technique to detect all components in the proteome. Therefore several low-abundance proteins and their subtle changes could not be detected. This fact was reflected in our present study as we did not find some of the proteins whose roles in sepsis and inflammatory responses have been established, for example CRP (C-reactive protein), serum amyloid A, fibrinogen and HSPs (heat-shock proteins). Secondly, we evaluated changes in the plasma proteome at only a single time point. Assessing dynamic changes over time would probably yield even more important results compared with the 'before–after' approach. This could serve as a platform or the starting point for our subsequent studies (i.e. sepsis compared with septic shock).

In summary, in the present study we have identified a set of plasma proteins with significantly altered levels during the early phase of sepsis in a porcine model of peritonitis-induced sepsis using a proteomics approach. The proteomics results could be related to the clinical features of this animal model, as most of these altered proteins have important roles in inflammatory responses and some of them play roles in oxidative and nitrosative stress. Some findings are considerably novel and exploring their roles in association with the pathophysiology of sepsis may lead to the identification of new therapeutic targets for better treatment outcome in sepsis. Additionally, some altered proteins may serve as potential markers for early sepsis.

ACKNOWLEDGEMENTS

We are grateful to the Core Facilities for Proteomics and Structural Biology Research, Institute of Biological Chemistry, Academia Sinica, Taiwan.

FUNDING

This work was supported by the Ministry of Education, Czech Republic [research project MSM 0021620819 (to M.M.)]; by The Thailand Research Fund, Commission on Higher Education, Mahidol University (to V.T.); the National Research Council of Thailand (Siriraj Grant for Research and Development; to V.T.); and by the National Center for Genetic Engineering and Biotechnology (to V.T.).

REFERENCES

- 1 Bone, R. C., Balk, R. A., Cerra, F. B., Dellinger, R. P., Fein, A. M., Knaus, W. A., Schein, R. M. and Sibbald, W. J. (1992) Definitions for sepsis and organ failure and guidelines for the use of innovative therapies in sepsis. The ACCP/SCCM Consensus Conference Committee. American College of Chest Physicians/Society of Critical Care Medicine. *Chest* **101**, 1644–1655

- 2 O'Brien, Jr, J. M., Ali, N. A., Aberegg, S. K. and Abraham, E. (2007) Sepsis. *Am. J. Med.* **120**, 1012–1022
- 3 Marshall, J. C., Cook, D. J., Christou, N. V., Bernard, G. R., Sprung, C. L. and Sibbald, W. J. (1995) Multiple organ dysfunction score: a reliable descriptor of a complex clinical outcome. *Crit. Care Med.* **23**, 1638–1652
- 4 Mackenzie, I. and Lever, A. (2007) Management of sepsis. *Br. Med. J.* **335**, 929–932
- 5 Claessens, Y. E. and Dhainaut, J. F. (2007) Diagnosis and treatment of severe sepsis. *Crit. Care* **11** (Suppl. 5), S2
- 6 Dellinger, R. P., Levy, M. M., Carlet, J. M., Bion, J., Parker, M. M., Jaeschke, R., Reinhart, K., Angus, D. C., Brun-Buisson, C., Beale, R. et al. (2008) Surviving Sepsis Campaign: international guidelines for management of severe sepsis and septic shock. *Crit. Care Med.* **36**, 296–327
- 7 Neurath, M. F. (2007) New therapies for sepsis: focus on the interleukin (IL)12 family member IL27. *Ann. Rheum. Dis.* **66** (Suppl. 3), iii29–iii31
- 8 Parrish, W. and Ulloa, L. (2007) High-mobility group box-1 isoforms as potential therapeutic targets in sepsis. *Methods Mol. Biol.* **361**, 145–162
- 9 Zhou, L. W., Wang, Y. L., Yan, X. T. and He, X. H. (2008) Urinary trypsin inhibitor treatment ameliorates acute lung and liver injury resulting from sepsis in a rat model. *Saudi Med. J.* **29**, 368–373
- 10 Cohen, J. (2003) Recent developments in the identification of novel therapeutic targets for the treatment of patients with sepsis and septic shock. *Scand. J. Infect. Dis.* **35**, 690–696
- 11 Banks, R. E., Dunn, M. J., Hochstrasser, D. F., Sanchez, J. C., Blackstock, W., Pappin, D. J. and Selby, P. J. (2000) Proteomics: new perspectives, new biomedical opportunities. *Lancet* **356**, 1749–1756
- 12 Colantonio, D. A. and Chan, D. W. (2005) The clinical application of proteomics. *Clin. Chim. Acta* **357**, 151–158
- 13 Tao, F. and Lazarev, A. (2007) Clinical proteomics: opportunities for diagnostics, pharmaceuticals and the clinical laboratory. *Expert Rev. Proteomics* **4**, 9–11
- 14 Matejovic, M., Krouzceky, A., Martinkova, V., Rokyta, Jr, R., Radej, J., Kralova, H., Treska, V., Radermacher, P. and Novak, I. (2005) Effects of tempol, a free radical scavenger, on long-term hyperdynamic porcine bacteremia. *Crit. Care Med.* **33**, 1057–1063
- 15 Matejovic, M., Krouzceky, A., Rokyta, Jr, R., Radej, J., Kralova, H., Treska, V., Radermacher, P. and Novak, I. (2007) Effects of combining inducible nitric oxide synthase inhibitor and radical scavenger during porcine bacteremia. *Shock* **27**, 61–68
- 16 Bradford, M. M. (1976) A rapid and sensitive method for the quantitation of microgram quantities of protein utilizing the principle of protein-dye binding. *Anal. Biochem.* **72**, 248–254
- 17 O'Malley, R. (2002) Life's (more than) a BLAST. *The Biochemist* **24**, 21–23
- 18 Karp, P. D. (2001) Pathway databases: a case study in computational symbolic theories. *Science* **293**, 2040–2044
- 19 Karp, P. D., Paley, S. and Romero, P. (2002) The Pathway Tools software. *Bioinformatics* **18** (Suppl. 1), S225–S232
- 20 Ren, Y., Wang, J., Xia, J., Jiang, C., Zhao, K., Li, R., Xu, N., Xu, Y. and Liu, S. (2007) The alterations of mouse plasma proteins during septic development. *J. Proteome Res.* **6**, 2812–2821
- 21 Reade, M. C. and Young, J. D. (2003) Of mice and men (and rats): implications of species and stimulus differences for the interpretation of studies of nitric oxide in sepsis. *Br. J. Anaesth.* **90**, 115–118
- 22 Godin, D. V. and Garnett, M. E. (1992) Species-related variations in tissue antioxidant status I. Differences in antioxidant enzyme profiles. *Comp. Biochem. Physiol. B* **103**, 737–742
- 23 Godin, D. V. and Garnett, M. E. (1992) Species-related variations in tissue antioxidant status II. Differences in susceptibility to oxidative challenge. *Comp. Biochem. Physiol. B* **103**, 743–748
- 24 Bauer, M. and Reinhart, K. (2006) From mice and MOF: rodent models, immune modulation, and outcome in the critically ill. *Crit. Care Med.* **34**, 921–923
- 25 Panaro, M. A., Cianciulli, A., Gagliardi, N., Mitolo, C. I., Acquafredda, A., Cavallo, P. and Mitolo, V. (2008) CD14 major role during lipopolysaccharide-induced inflammation in chick embryo cardiomyocytes. *FEMS Immunol. Med. Microbiol.* **53**, 35–45
- 26 Frantz, S., Ertl, G. and Bauersachs, J. (2007) Toll-like receptors in cardiovascular disease. *Nat. Clin. Pract. Cardiovasc. Med.* **4**, 444–454
- 27 Dessing, M. C., Knapp, S., Florquin, S., de Vos, A. F. and van der, P. T. (2007) CD14 facilitates invasive respiratory tract infection by *Streptococcus pneumoniae*. *Am. J. Respir. Crit. Care Med.* **175**, 604–611
- 28 Aalto, H., Takala, A., Kautiainen, H., Siitonen, S. and Repo, H. (2007) Monocyte CD14 and soluble CD14 in predicting mortality of patients with severe community acquired infection. *Scand. J. Infect. Dis.* **39**, 596–603
- 29 Brunialti, M. K., Martins, P. S., Barbosa de Carvalho, H., Machado, F. R., Barbosa, L. M. and Salomao, R. (2006) TLR2, TLR4, CD14, CD11B, and CD11C expressions on monocytes surface and cytokine production in patients with sepsis, severe sepsis, and septic shock. *Shock* **25**, 351–357
- 30 O'Riordain, M. G., Ross, J. A., Fearon, K. C., Maingay, J., Farouk, M., Garden, O. J. and Carter, D. C. (1995) Insulin and counterregulatory hormones influence acute-phase protein production in human hepatocytes. *Am. J. Physiol.* **269**, E323–E330
- 31 Conner, J. G., Eckersall, P. D., Wiseman, A., Bain, R. K. and Douglas, T. A. (1989) Acute phase response in calves following infection with *Pasteurella haemolytica*, *Ostertagia ostertagi* and endotoxin administration. *Res. Vet. Sci.* **47**, 203–207
- 32 Fagoonee, S., Gburek, J., Hirsch, E., Marro, S., Moestrup, S. K., Laurberg, J. M., Christensen, E. I., Silengo, L., Altruda, F. and Tolosano, E. (2005) Plasma protein haptoglobin modulates renal iron loading. *Am. J. Pathol.* **166**, 973–983
- 33 Lim, Y. K., Jenner, A., Ali, A. B., Wang, Y., Hsu, S. I., Chong, S. M., Baumman, H., Halliwell, B. and Lim, S. K. (2000) Haptoglobin reduces renal oxidative DNA and tissue damage during phenylhydrazine-induced hemolysis. *Kidney Int.* **58**, 1033–1044
- 34 Bowman, B. H. and Kurosky, A. (1982) Haptoglobin: the evolutionary product of duplication, unequal crossing over, and point mutation. *Adv. Hum. Genet.* **12**, 189–261
- 35 Van Campenhout, A., Van Campenhout, C., Lagrou, A. R., Abrams, P., Moorkens, G., Van Gaal, L. and Keenoy, B. (2006) Impact of diabetes mellitus on the relationships between iron-, inflammatory- and oxidative stress status. *Diabetes Metab. Res. Rev.* **22**, 444–454
- 36 Salvatore, A., Cigliano, L., Bucci, E. M., Corpillo, D., Velasco, S., Carlucci, A., Pedone, C. and Abrescia, P. (2007) Haptoglobin binding to apolipoprotein A-I prevents damage from hydroxyl radicals on its stimulatory activity of the enzyme lecithin-cholesterol acyl-transferase. *Biochemistry* **46**, 11158–11168
- 37 Faye, A., Ramey, G., Foretz, M. and Vaulont, S. (2007) Haptoglobin is degraded by iron in C57BL/6 mice: a possible link with endoplasmic reticulum stress. *Blood Cells Mol. Dis.* **39**, 229–237
- 38 Hvidberg, V., Maniecki, M. B., Jacobsen, C., Hojrup, P., Moller, H. J. and Moestrup, S. K. (2005) Identification of the receptor scavenging hemopexin-heme complexes. *Blood* **106**, 2572–2579
- 39 Kalenka, A., Feldmann, Jr, R. E., Otero, K., Maurer, M. H., Waschke, K. F. and Fiedler, F. (2006) Changes in the serum proteome of patients with sepsis and septic shock. *Anesth. Analg.* **103**, 1522–1526
- 40 Sun, D., Leung, C. L. and Liem, R. K. (2001) Characterization of the microtubule binding domain of microtubule actin crosslinking factor (MACF): identification of a novel group of microtubule associated proteins. *J. Cell Sci.* **114**, 161–172
- 41 Lin, C. M., Chen, H. J., Leung, C. L., Parry, D. A. and Liem, R. K. (2005) Microtubule actin crosslinking factor 1b: a novel plakin that localizes to the Golgi complex. *J. Cell Sci.* **118**, 3727–3738

- 42 Head, B. P., Patel, H. H., Roth, D. M., Murray, F., Swaney, J. S., Niesman, I. R., Farquhar, M. G. and Insel, P. A. (2006) Microtubules and actin microfilaments regulate lipid raft/caveolae localization of adenylyl cyclase signaling components. *J. Biol. Chem.* **281**, 26391–26399
- 43 Abrahamsberg, C., Fuchs, P., Osmanagic-Myers, S., Fischer, I., Propst, F., Elbe-Burger, A. and Wiche, G. (2005) Targeted ablation of plectin isoform 1 uncovers role of cytolinker proteins in leukocyte recruitment. *Proc. Natl. Acad. Sci. U.S.A.* **102**, 18449–18454
- 44 Sevcik, J., Urbanikova, L., Kost'an, J., Janda, L. and Wiche, G. (2004) Actin-binding domain of mouse plectin: crystal structure and binding to vimentin. *Eur. J. Biochem.* **271**, 1873–1884
- 45 Tilney, L. G., Connelly, P. S., Vranich, K. A., Shaw, M. K. and Guild, G. M. (2000) Regulation of actin filament cross-linking and bundle shape in *Drosophila* bristles. *J. Cell Biol.* **148**, 87–100
- 46 Selden, S. C. and Pollard, T. D. (1986) Interaction of actin filaments with microtubules is mediated by microtubule-associated proteins and regulated by phosphorylation. *Ann. N.Y. Acad. Sci.* **466**, 803–812

Received 17 September 2008/30 October 2008; accepted 13 November 2008
Published as Immediate Publication 13 November 2008, doi:10.1042/CS20080478

Altered plasma proteome during an early phase of peritonitis-induced sepsis

Visith THONGBOONKERD*, Wararat CHIANGJONG*, Jan MAREŠ†, Jiri MORAVEC†, Zdenek TUMA†, Thomas KARVUNIDIS†, Supachok SINCHAIKUL‡, Shui-Tein CHEN‡§, Karel OPATRŇY JR†¹ and Martin MATEJOVIC†

*Medical Proteomics Unit, Office for Research and Development, Faculty of Medicine Siriraj Hospital, Mahidol University, Bangkok 10700, Thailand, †Proteomics Laboratory, Department of Internal Medicine I and Intensive Care Unit, Charles University School of Medicine in Plzeň, 304 60 Plzeň, Czech Republic, ‡Institute of Biological Chemistry and Genomic Research Center, Academia Sinica, Taipei, Taiwan, and §Institute of Biochemical Sciences, College of Life Science, National Taiwan University, Taipei, Taiwan

Table S1 Functional analysis of the altered plasma proteins using the Pathway Tools (see [18,19] in the main text)

*A large multiprotein complex that possesses histone acetyltransferase activity and is involved in regulation of transcription. I κ B, inhibitor of NF- κ B; JAK, Janus kinase; STAT, signal transducer and activator of transcription; NA, not available by the Pathway Tools.

Protein name	Biological process(es)	Molecular function(s)	Cellular component(s)	MetaCyc Pathway
Albumin	Transport and water homeostasis	Transporter activity and lipid binding	Extracellular space	NA
α_1 -Anti-chymotrypsin I	Acute-phase response	Endopeptidase inhibitor activity	NA	NA
α_2 -HS-glycoprotein precursor (fetuin-A)	Ossification and regulation of bone mineralization	Cysteine protease inhibitor activity	Extracellular space and soluble fraction	NA
Apolipoprotein A-I precursor (Apo-AI)	Lipid transport, blood circulation and cholesterol metabolic process	Structural molecule activity, lipid transporter activity, high-density lipoprotein binding and lipid binding	NA	NA
CD14 antigen	Phagocytosis, apoptosis, inflammatory response, immune response and cell-surface-receptor-linked signal transduction	Peptidoglycan receptor activity	Plasma membrane	NA
Cytochrome P450, family 3, subfamily A, polypeptide 41A	Multiple	Mono-oxygenase activity	Endoplasmic reticulum, microsome and membrane	Oxidative ethanol degradation II (MEOS) and nicotine degradation II and III
Haptoglobin	Proteolysis, defence response and acute-phase response	Haemoglobin binding	NA	NA
Haemopexin	Transport, cellular iron homeostasis and haem transport	Binding and haem transporter activity	Extracellular space	NA
Hypothetical protein LOC23078 isoform a	NA	NA	NA	NA
Hypothetical protein LOC330361	NA	NA	NA	NA
Immunoglobulin heavy chain variable region	NA	NA	NA	NA

¹ Deceased

Correspondence: Dr Visith Thongboonkerd (email thongboonkerd@dr.com or vtthongbo@yahoo.com) or Dr Martin Matejovic (email matejovic@fnplzen.cz).

Table S1 cont.

Protein name	Biological process(es)	Molecular function(s)	Cellular component(s)	MetaCyc Pathway
Inter- α -trypsin inhibitor family heavy chain-related protein	Transport	Endopeptidase inhibitor activity, transporter activity and binding	NA	NA
mCGI40308, isoform CRA_b	NA	NA	NA	NA
Microfilament and actin filament cross-linker protein isoform 3	NA	NA	NA	NA
N-ethylmaleimide-sensitive fusion protein	Proteolysis and intracellular protein transport	Nucleotide binding, ATP-dependent peptidase activity, ATP binding and protein transporter activity	Endoplasmic reticulum and Golgi apparatus	Hydrolases
Pyruvate carboxylase	Gluconeogenesis, biotin metabolic process and lipid biosynthetic process	Pyruvate carboxylase activity, ATP binding, biotin binding, ligase activity and manganese ion binding	Mitochondria	Aspartate biosynthesis II
Signal transducer and activator of transcription 1	Regulation of transcription (DNA-dependent), transcription from RNA polymerase II promoter, caspase activation, signal transduction, intracellular signalling cascade, I κ B kinase/NF- κ B cascade, JAK/STAT cascade, tyrosine phosphorylation of STAT protein, JAK-induced STAT protein dimerization, STAT protein nuclear translocation, response to other organisms and regulation of cell cycle	DNA binding, transcription factor activity, signal transducer activity, haematopoietin/interferon-class (D200-domain) cytokine receptor signal transducer activity and translation regulator activity	Nucleus and cytoplasm	NA
Similar to CG3493-PA isoform 2	NA	NA	NA	NA
Similar to cytosolic purine 5'-nucleotidase (5-nucleotidase cytosolic II) isoform 8	NA	5'-Nucleotidase activity and hydrolase activity	Cytosol	Phosphoric monoester hydrolase
Similar to plectin 1 isoform 1	Cytoskeletal anchoring at plasma membrane	Actin binding, structural constituent of cytoskeleton and structural constituent of muscle	Cytoskeleton, kinesis complex, intermediate filament and plasma membrane	NA
Similar to synaptic vesicle membrane protein VAT-1 homologue	Cell growth	DNA binding, NADPH:quinone reductase activity, alcohol dehydrogenase activity (zinc-dependent), zinc ion binding and oxidoreductase activity	Nucleus, synaptic vesicle, integral to membrane and synapse	NA
Similar to tweety homologue 3	Iron transport	Iron ion transmembrane and membrane transporter activity	Integral to membrane	NA
Transformation/transcription domain-associated protein isoform 2	Signal transduction	Inositol or phosphatidylinositol kinase activity and copper ion binding	PCAF complex*	NA
Vitelliform macular dystrophy 2-like 3 isoform 1	Visual perception	NA	Membrane fraction and integral to membrane	NA
Vitronectin	Immune response and cell adhesion	Heparin binding	Extracellular space	NA

Received 17 September 2008/30 October 2008; accepted 13 November 2008
 Published as Immediate Publication 13 November 2008, doi:10.1042/CS20080478

SHOCK, Vol. xx, No. x, pp. 1–13, 2016

RENAL PROTEOMIC RESPONSES TO SEVERE SEPSIS AND SURGICAL TRAUMA: DYNAMIC ANALYSIS OF PORCINE TISSUE BIOPSIES

Martin Matejovic,^{*†} Zdenek Tuma,[†] Jiri Moravec,[†] Lenka Valesova,^{*†}
Roman Sykora,^{*} Jiri Chvojka,^{*†} Jan Benes,^{†‡} and Jan Mares^{*†}

AQ1

AQ2

^{*1st} Medical Department, Faculty of Medicine in Pilsen, Charles University in Prague, Plzen, Czech Republic; [†]Experimental Intensive Care Unit and Proteomic Laboratory, Biomedical Centre, Faculty of Medicine in Plzen, Charles University in Prague, Plzen, Czech Republic; and [‡]Department of Anesthesia and Intensive Care Medicine, Faculty of Medicine in Pilsen, Charles University in Prague, Teaching Hospital Plzen, Plzen, Czech Republic

Received 11 Dec 2015; first review completed 10 Feb 2016; accepted in final form 15 Mar 2016

ABSTRACT—Although the burden of septic acute kidney injury continues to increase, the molecular pathogenesis remains largely obscure. The aim of this exploratory study was a discovery-driven analysis of dynamic kidney tissue protein expression changes applied for the first time in a classic large mammal model of sepsis. To achieve this goal, analyses of protein expression alterations were performed in serial samples of kidney cortical biopsies (before, 12 and 22 h of sepsis) in mechanically ventilated pigs challenged with continuous infusion of *Pseudomonas aeruginosa* and compared with sham-operated control data. Global protein expression was analyzed using two-dimensional gel electrophoresis and mass spectrometry-based proteomics. Normodynamic sepsis was associated with 43% reduction in glomerular filtration. The exposure to surgical stress per se altered the renal protein expression profile, while sepsis induced distinct and highly dynamic proteome evolution shifting the balance toward cellular distress phenotype. We identified 20 proteins whose expression changes discriminated effects of sepsis from those induced by surgery. The data implicate endoplasmic reticulum stress, oxidative stress, mitochondrial energy metabolism, immune/inflammatory signaling, and tubular transport as major activated pathways. Thus, by coupling the power of sequential tissue proteomics with whole-animal physiological studies, our study helped to establish a first global overview of critical renal proteomic events occurring during surgical trauma and early sepsis in a porcine model. The study supports the notion that multiple potentially subtle and even transient changes in several proteins which are members of key functional interrelated systems appear to play a role in septic acute kidney injury.

KEYWORDS—Acute kidney injury, animal models, sepsis, surgery, tissue proteomics

INTRODUCTION

The burden of sepsis and acute kidney injury (AKI) has been steadily increasing in critically ill patients and both conditions portend an ominous outcome (1). Sepsis is the dominant cause of AKI, accounting for nearly 50% of episodes of acute renal failure (2). When occurring together, the associated mortality is significantly higher as compared with non-septic AKI or sepsis alone (2). In addition to different baseline demographics and acuity of illness, there is emerging evidence that pathogenesis of septic AKI also involves distinct mechanisms as compared with non-septic causes of AKI (3). Although understanding its pathophysiology is expected to have a marked impact on the development of new effective treatment strategies, underlying molecular mechanisms of renal dysfunction in sepsis are still largely unknown. Accordingly, investigating these mechanisms is one of the priorities within the field of AKI research (4).

There are two fundamental problems inherently associated with studies of renal responses to sepsis. First, difficult access to the renal tissue and the associated ethical issues make the human research into cellular and molecular biology in critically ill patients almost unfeasible. Moreover, investigation of human tissue samples might be compromised by several factors including disease state, tissue heterogeneity, genetic variability, and the patient's comorbidities and treatment history. Second, the process of AKI in sepsis involves a complex of multiple dynamically interacting factors and it is clear that renal dysfunction, similar to dysfunction of other organs in sepsis, is not caused by a single mechanism. Taken together, limited ability to study the renal molecular mechanisms in humans and the complexity of pathomechanisms involved in sepsis underscore the need for complex, dynamic, and clinically relevant animal trials employing novel molecular technologies. Proteomics represents such a powerful post-genomic biotechnology apt for simultaneous examination of large sets of proteins or the entire proteome. Applying dynamic tissue proteomics to clinically relevant models of sepsis rather than evaluating individual proteins one by one is therefore of utmost importance to reveal putative drug targets, therapeutic proteins, and disease biomarkers (5, 6).

To the best of our knowledge, no studies have so far used proteomic tools to analyze changes in kidney protein expression during the evolution of sepsis. Therefore, as a first step to delineate complex interacting pathways involved in the renal

AQ3 Address reprint requests to Martin Matejovic, MD, PhD, 1st Medical Department, Charles University Medical School and Teaching Hospital, alej Svobody 80, 304 60 Plzen, Czech Republic. E-mail: matejovic@fnplzen.cz

This study was supported by the National Sustainability Program I (NPU I) No. LO1503 provided by the Ministry of Education Youth and Sports of the Czech Republic, by the project No. CZ.1.07/2.3.00/30.0061 cofinanced by the European Social Fund and the state budget of the Czech Republic and by the Charles University Research Fund (project number P36).

AQ4 The authors report no conflicts of interest.
DOI: 10.1097/SHK.0000000000000613
Copyright © 2016 by the Shock Society

molecular responses to sepsis, we used a discovery-based proteomic approach to identify molecules modified in a clinically relevant model of sepsis. To achieve this goal, dynamic analyses of protein expression were performed in serial samples of kidney tissue biopsies from pigs challenged with continuous infusion of *Pseudomonas aeruginosa* and compared with sham-operated control data. This model replicates many of the biological features intrinsic to human septic shock and integration of standard day-to-day care resuscitative makes it an appealing sepsis model in studies of kidney injury. Quite recently, the pig has also been introduced as one of the most promising animal models from a proteomic and translational perspective (7).

METHODS

All experiments were performed in adherence to the National Institutes of Health Guidelines on the Use of Laboratory Animals and their protocols were approved by the University Animal Care Committee. Seventeen domestic pigs of either sex with a median body weight of 35 [32–40] kg were used. Of these, five sham operated, time-, age-, and weight-matched animals served as a control group.

Anesthesia and surgical preparation

Anesthesia was induced with intravenous propofol (1–2 mg/kg) and ketamine (2 mg/kg). Animals were intubated and mechanically ventilated with tidal volumes 8 mL/kg, positive end-expiratory pressure 0.6 kPa, and FiO_2 0.4. Respiratory rate was adjusted to maintain normocapnia (arterial carbon dioxide tension 4.0–5.0 kPa). During surgical procedure continuous infusions of fentanyl (10–15 $\mu\text{g}/\text{kg}/\text{h}$), thiopental (10 mg/kg/h) and pancuronium (4–6 mg/h) were administered. After surgical preparation the infusion of thiopental and fentanyl was decreased to 5 mg/kg/h and 5 $\mu\text{g}/\text{kg}/\text{h}$, respectively, and maintained until the end of the experiment. Ringerfudin (B. Braun, Germany) was used for fluid replacement at a dose of 15 mL/kg during the surgery and reduced to 7 mL/kg thereafter. Normoglycemia (arterial blood glucose level 4.5–7 mmol/L) was maintained throughout the whole experiment using 20% glucose infusion as needed.

Before surgical procedure a fiber-optic arterial catheter was inserted into the femoral artery for continuous blood pressure measurement, intermittent double-indicator transpulmonary dilution (COLD Z-021, PULSION Medical Systems GmbH, Germany) and blood sampling. Central venous and pulmonary artery catheters were introduced via jugular veins. Afterward, a midline laparotomy was performed and a precalibrated ultrasound flowprobe (Transonic Systems, Ithaca, NY) was placed around the left renal artery and a double-lumen catheter was inserted into the left renal vein for renal venous pressure measurements. Peritoneal drainage was inserted before abdominal wall closure and epicycstostomy was performed under ultrasound control. A curved linear incision was made caudal to the last rib and left kidney was manually exposed without entering the abdominal cavity. The flank approach allowed for visually controlled repeated kidney biopsies. The incision was closed using a sterile moistened compress. A recovery period of 6 h was provided before the baseline measurement.

Sepsis protocol

The study consisted of two arms; sepsis induced by intravenous live bacteria infusion (sepsis, $n = 12$), and sham-operated control group (control, $n = 5$). In the sepsis group, a continuous central venous infusion of live *Pseudomonas aeruginosa* (strain O1 isolated from a patient with suppurative otitis, 1×10^9 colony-forming units/mL determined serial dilution and colony counts) was commenced after baseline data acquisition and maintained until the end of the study. The infusion rate was titrated to clinical goal of moderate pulmonary hypertension (MPAP 35–40 mm Hg). To avoid any variations in virulence, all pigs were challenged with bacteria from the same bacterial strain. In addition to crystalloid solution, 6% hydroxyethyl starch 130 kD/0.4 (Voluven 6%, Fresenius Kabi Deutschland GmbH, Bad Homburg, Germany) was infused to maintain normovolemia in a goal-directed fashion guided by filling pressures response and intrathoracic blood volume (ITBV) measurement. Continuous i.v. noradrenaline was administered whenever mean arterial pressure (MAP) fell below 65 mm Hg and titrated to maintain MAP above 70 mm Hg. When the last

set of data had been obtained, the animals were euthanized by potassium chloride injection under deep anesthesia and section was performed.

Measurements and calculations

At each time-point (baseline, 12, and 22 h after induction of sepsis), the measurement of hemodynamics included cardiac output (CO), systemic vascular resistance (SVR), ITBV, filling pressures of both ventricles (CVP, PAOP), renal artery blood flow (Qren), and renal vein pressure (RVP). Renal vascular resistance was calculated according to the formula: $\text{RVR} = [\text{MAP (mm Hg)} - \text{RVP (mm Hg)}] / \text{Qren (L/min)}$. Arterial and mixed venous blood samples were analyzed for pH, pO_2 , pCO_2 , and for hemoglobin oxygen saturation. Arterial blood samples were also analyzed for plasma tumor necrosis factor alpha (TNF- α) and interleukin 6 (IL-6). Urinary (2-h urine collections before each timepoint) and blood creatinine levels were analyzed to enable calculation of creatinine clearance as a marker of glomerular filtration. Kidney biopsies were taken before (time-point 1), 12 (time-point 2), and 22 (time-point 4) h after initiation of bacterial infusion. Samples were flash frozen in liquid nitrogen and kept at -80°C until analysis.

Tissue processing, protein extraction, tryptic digestion

Whole tissue extract of swine kidney cortical biopsy was used for analysis. Samples (18.9 ± 7.3 mg) were ground under liquid nitrogen with a mortar and a pestle, followed by addition of 20 μL solubilizing buffer per mg sample. After that, samples were incubated in ice bath for 30 min (shook every 10 min), then centrifuged and decanted, yielding on average a total of $1,010 \pm 431$ μg protein ($5.1 \pm 2.5\%$ initial sample) as quantified using Bradford assay.

Two-dimensional electrophoresis

Urea, CHAPS, Tris base, thiourea, sodium dodecylsulphate (SDS), dithiothreitol (DTT), iod acetamide (IAA), and bromophenol blue used during the preparation were purchased from Sigma (Sigma-Aldrich, Steinheim, Germany); immobilized pH gradient (IPG) buffer (ZOOM carrier Ampholytes 3–10) was purchased from Invitrogen (Invitrogen Corporation, Carlsbad, CA). Equally, 200 μg proteins in both eluate and plasma samples were mixed with rehydration buffer (7 M urea, 4% CHAPS, 40 mM Tris base, 2 M Thiourea, 2% IPG buffer pH 3–10, 120 mM DTT, and a trace of bromophenol blue) to obtain the final volume of 140 μL . Samples were then rehydrated in IPG strips (7.7-cm-long, pH 3–10 nonlinear; Invitrogen), and focused in a MiniProtean cell (Bio-Rad). IPG strips were rehydrated passively for 1 h and actively for 10 h at 30 V, followed by a stepwise isoelectric focusing (IEF) as follows: 200 V until 400 Vh were reached, 450 V for another 500 Vh, 750 V for another 900 Vh, and finally 2,000 V for the other 10,000 Vh. After IEF, the IPG strips were equilibrated in equilibration buffer 1 (112 mM Tris-base, 6 M urea, 30% v/v glycerol, 4% w/v SDS, 130 mM DTT, and a trace of bromophenol blue) for 30 min, and subsequently alkylated in buffer 2 (112 mM Tris-base, 6 M urea, 30% v/v glycerol, 4% w/v SDS, 135 mM IAA, and a trace of bromophenol blue) for 30 min. Each equilibrated IPG strip was placed on the top of a 13% polyacrylamide gel (9×7 cm), and covered with 0.5% agarose. The second-dimension separation was performed with 65 mA per gel at 20°C until the bromophenol blue dye front reached the bottom of the gel. At the end of each run, the 2D gels were stained with Simply Blue (Invitrogen), and scanned with an Epson Perfection 4990 Photo scanner.

In-gel tryptic digestion

Acetonitrile (ACN), ammonium bicarbonate, DTT, IAA, trifluoroacetic acid (TFA), formic acid, and α -cyano-4-hydroxycinnamic acid (CHCA) were purchased from Sigma. Spots detected in all patients were excised manually. SimplyBlue stain was removed by washing with 50 mM ammonium bicarbonate, and ACN. Proteins in gel were reduced with 10 mM DTT/50 mM ammonium bicarbonate at 56°C for 45 min, and alkylated with 55 mM IAA/50 mM ammonium bicarbonate (for 30 min, in the dark at room temperature). Gel plugs were washed with 50 mM ammonium bicarbonate and ACN, and dried by SpeedVac. Dried gel particles were rehydrated with digestion buffer containing 12.5 ng/ μL sequencing grade trypsin (Roche) in 50 mM ammonium bicarbonate at 4°C . After 45 min, the remaining solution was removed, and replaced by 0.1 M ammonium bicarbonate. Tryptic digestion was performed overnight (37°C). After digestion, proteolytic peptides were subsequently extracted with 25 mM ammonium bicarbonate, ACN, and 5% formic acid. The three extracts were pooled, and 10 mM DTT solution in 50 mM ammonium bicarbonate was added. The mixture was then dried by SpeedVac, and resulting tryptic peptides were dissolved in 5% formic acid solution and desalted using ZipTip $\mu\text{C}18$ (Millipore, Bedford, MA).

Matrix-assisted laser desorption/ionization time-of-flight (TOF) tandem mass spectrometry and protein identification

Proteolytic peptides were mixed with CHCA matrix solution (5 mg/mL CHCA in 0.1% TFA/50% ACN 1:1, v/v) in 1:1 ratio, and 0.8 μ L of this mixture was spotted onto matrix-assisted laser desorption/ionization (MALDI) target. All mass spectra were acquired at a reflectron mode with a 4,800 MALDI TOF/TOF Analyzer (Applied Biosystems, Framingham, MA). A total of 2,000 and 3,000 laser shots were acquired, and averaged to MS and MS/MS spectra, respectively. The MS/MS analyses were performed using collision energy of 1 kV and collision gas pressure of 1.3×10^{-6} Torr. MS peaks with an S/N above 15 were listed, and the 15 strongest precursors with an S/N above 50 among the MS peaks were automatically selected for MS/MS acquisition. A mass filter was used to exclude autolytic peptides of trypsin.

Resulting data were analyzed with GPS Explorer 3.6 (Applied Biosystems) software. Proteins were identified by searching against human subset of the Swissprot protein database (release 54.6; Dec. 4, 2007) using MASCOT 2.1.0 search algorithm (Matrix Science, London, UK). The general parameters for peptide mass fingerprinting (PMF) search were considered to allow maximum one missed cleavage, ± 50 ppm of peptide mass tolerance, variable methionine oxidation, and fixed cysteine carbamidomethylation. Probability-based MOWSE scores were estimated by comparison of search results against estimated random match population, and were reported as $-10 \log_{10}(P)$ where P is the absolute probability. MOWSE scores greater than 55 were considered significant ($P < 0.05$) for PMF. A peptide charge state of +1 and fragment mass tolerance of ± 0.25 Da were used for the MS/MS ion search. Individual MS/MS ions scores > 28 indicated identity or extensive homology ($P < 0.05$) for MS/MS ion search.

Statistical analysis, data handling—All values shown are median and interquartile range. The calculations were done using SigmaStat software version 3.5 (Systat Software Inc, Erkrath, Germany). After exclusion of normality using the Kolmogorov–Smirnov test, time-dependent changes within each group were tested using the Friedman ANOVA on ranks and, subsequently, the Dunn test for multiple comparisons with the Bonferroni correction. Differences between the groups were analyzed using the Mann–Whitney rank sum test. A $P < 0.05$ was regarded as statistically significant. Computer-aided analysis of 2-DE gel images was carried out using PDQuest 2D software version 8.1 (Bio-Rad). Unless there was too little protein obtained from the biopsy, a synthetic image was constructed out of the triplicated gels processed from each sample, using only spots constantly present in at least two replicates. The protein quantity was determined relative to integrated spot density excluding saturated spots. With respect to the large numbers of detected protein spots, an exploratory data analysis was performed first (using t test) and only spots showing significantly altered intensities were selected for identification. To facilitate handling and comprehension of large, high-dimensional and collinear datasets together with isolating meaningful structures within them, hierarchical

clustering was applied using Ward method as a linkage rule and Euclidean distance as a dissimilarity measure. In the subset of identified proteins, interactions between temporal and group effects were then evaluated by means of mixed model ANOVA involving both repeated measures and between-subject factors.

RESULTS

Characterization of sepsis model

The systemic hemodynamic, inflammatory, and acid–base responses to the bacteremia are summarized in Table 1. There was no change over time in any of these parameters in the control animals. All animals challenged with i.v. infusion of PSAE developed normodynamic circulation with gradually increased cardiac output and significantly reduced systemic vascular resistance. Adequate fluid resuscitation was ensured by maintaining ITBV and monitoring cardiac filling pressures which significantly increased over time. The development of sepsis resulted in a significant fall of arterial pH. All animals received noradrenaline infusion to maintain MAP ≥ 70 mm Hg. The median dose of noradrenaline was 0.94 μ g/kg/min. While neither TNF- α nor IL-6 plasma levels changed in the control group over time, both cytokines progressively increased in animals challenged with i.v. PSEA.

Renal response to sepsis

Compared with the baseline, renal blood flow decreased in septic animals by the end of the experiment (Table 2). Reduced renal perfusion was associated with 43% decline in creatinine clearance and with tendency of renal vascular resistance to increase (Table 2). There was no change over time in any of these parameters in the control group.

Kidney tissue proteomics

Proteins spots on gels obtained from both sham-operated pigs and pigs challenged with sepsis were scanned and a computer-aided analysis of the images was carried out using

TABLE 1. Systemic hemodynamics, inflammation and acid–base data

Group	Baseline	12 h	22 h
CO (mL/kg/min)	Control 100 (78;110) Sepsis 96 (82;109)	90 (85;107) 105 (81;138)	86 (73;91) 115 (96;161)
SVR (dyne-s/cm ⁵)	Control 2,277 (2,081;2,511) Sepsis 2,553 (2,142;2,729)	2,113 (1,784;2,355) 1,357 (1,130;1,643)*	2,101 (1,797;2,366) 1,135 (867;1,682)*,†
MAP (mm Hg)	Control 104 (95;109) Sepsis 113 (107;123)	91 (84;106) 81 (76;89)*	93 (80;99) 80 (76;88)*
CVP (mm Hg)	Control 14 (12;16) Sepsis 12 (10;14)	15 (12;15) 17 (15;18)*	15 (13;15) 18 (16;20)*
PAOP (mm Hg)	Control 14 (11;16) Sepsis 13 (11;13)	15 (12;18) 19 (17;21)*	16 (15;16) 19 (17;20)*
ITBV (mL/kg)	Control 28 (25;32) Sepsis 29 (22;30)	27 (25;34) 25 (21;29)	25 (23;28) 24 (21;25)
Arterial (pH)	Control 7.57 (7.55;7.59) Sepsis 7.56 (7.55;7.63)	7.55 (7.52;7.56) 7.47 (7.44;7.51)*	7.50 (7.45;7.51) 7.44 (7.35;7.48)*
TNF- α (pg/g of protein)	Control 2.2 (1.4;2.6) Sepsis 2.3 (1.4;3.2)	1.4 (1.4;1.6) 5.9 (4.7;14.7)*,†	1.5 (1.4;1.6) 64.9 (18.0;155.0)*,†
IL-6 (pg/g of protein)	Control 114 (54;225) Sepsis 94 (58;109)	143 (90;166) 143 (133;166)	107 (101;181) 432 (279;596)*,†

*Significant difference versus baseline ($P < 0.05$).

†Significant difference versus control group ($P < 0.05$).

CO indicates cardiac output; CVP, central venous pressure; IL-6, interleukin 6; ITBV, intrathoracic blood volume; MAP, mean arterial pressure; PAOP, pulmonary artery occlusion pressure; SVR, systemic vascular resistance; TNF- α , tumor necrosis factor α .

TABLE 2. Renal effects of sepsis

	Group	Baseline	12 h	22 h
RBF (mL/kg/min)	Control	4.0 (3.6;4.4)	3.7 (2.7;4.5)	3.3 (2.7;4.4)
	Sepsis	6.0 (4.9;8.4)*	4.9 (2.9;6.4)	3.0 (1.3;4.8)*
RVR (dyne·s/cm ⁵)	Control	689 (535;922)	689 (535;922)	678 (533;826)
	Sepsis	471 (334;618)	415 (283;919)	777 (355;1741)
Creat. clearance (mL/s)	Control	1.2 (0.7;2.3)	1.1 (0.9;1.2)	1.2 (0.9;1.8)
	Sepsis	1.4 (0.8;2.5)	1.2 (0.9;1.7)	0.8 (0.2;1.1)*

*Significant difference versus baseline ($P < 0.05$).

Creat. clearance indicates creatinine clearance; RVR, renal vascular resistance.

PDQuest 2D software. Where possible, corresponding spots were matched across time-points, individuals, and groups. Relative protein quantity was assessed as spot intensity ratios based on the matching. On average, 679 ± 150 spots were thus detected on each 2D gel.

Time-dependent changes in renal proteome in the control and sepsis groups—Proteomic analysis of sham-operated animals was performed as an internal control for potential anesthesia/surgery-induced changes in renal proteome. The resolution of sample protein extracts by 2DE revealed a total of 1,269 unique protein spots. Of these, 62 were significantly altered at some point during the 22-h observational period. Compared with baseline, 13 protein spots were significantly and consistently overexpressed (up-regulated), 15 were strictly down-regulated, and 34 showed undulated behavior (up at some point and down at other). Eleven of these altered proteins were then successfully identified by MALDI-TOF-TOF MS analyses. Identities, quantitative data, degrees of changes, and other related information of all of the altered proteins are summarized in Table 3.

In renal biopsies obtained from the sepsis animals, a total of 1,388 spots were detected while 17 unique proteins were identified out of the 41 up-regulated spots, whereas 12 unique proteins were identified out of the 65 consistently down-regulated spots. In addition, 14 initially up-regulated proteins normalized by the end of the experiment, while 8 proteins normalized in the group of transiently down-regulated proteins. Identities, quantitative data, degrees of changes, and other related information of all of the altered proteins are summarized in Table 3. To examine the protein dynamics in a multivariate fashion (i.e. as one correlated set), hierarchical clustering was applied as an exploratory tool. Figure 1 shows a heatmap of the significantly varying proteins from both groups arranged with respect to their quantitative changes. Thus, considered in its full complexity, the data were naturally clustered into septic and sham-operated groups, confirming its potential to discriminate the two conditions.

Sepsis versus control: differentially expressed proteins—Next, we focused on proteins which were differentially expressed between septic and control animals during the course of the experiment. In Figure 2, a representative 2-DE gel displays a proteome map of renal cortex during sepsis. To separate changes caused by study procedures from the proper impact of sepsis, a combined analysis including both dependent and independent predictors (i.e. septic and sham-operated animals at all time points) was performed by means of General linear model ANOVA. Proteins qualified for the analysis if they

showed a statistically significant variation during exploratory phase (t test) at either group or time-point. In this way, we were able to distinguish 20 proteins changing exclusively due to sepsis or showing a different behavior in sepsis and sham-operated groups (Table 4). These proteins were unambiguously identified by mass spectrometry as stress response and protein repair chaperones (heat shock protein HSP 90- α ; heat shock protein HSP 90- β ; heat shock cognate 71 kDa protein) (Fig. 3A); proteins involved in endoplasmic reticulum (ER) stress (78 kDa glucose-regulated protein; calreticulin) (Fig. 3B), free radical scavengers/oxidative stress proteins (peroxiredoxin-6) (Fig. 3C); proteins involved in cellular energetics and ATP levels (ATP synthase subunit α) (Fig. 4), mitochondrial; glutamate dehydrogenase 1, mitochondrial; delta-1-pyrroline-5-carboxylate dehydrogenase, mitochondrial; enoyl-CoA hydratase, mitochondrial; glutamate dehydrogenase 1, mitochondrial; dihydrolipoyl dehydrogenase, mitochondrial; α -enolase); transporters (chloride intracellular channel protein 4; Na(+)/H(+) exchange regulatory cofactor NHE-RF3 (Fig. 5)); proteins involved in inflammatory regulation and signal transduction (annexin-4; mitogen-activated protein kinase 3); proteins of hemostasis (WD repeat-containing protein 1); and cytoskeleton (spectrin α chain, nonerythrocytic 1; collagen α -1(VI) chain; laminin subunit γ -1).

DISCUSSION

In the present exploratory study, we introduce the first dynamic proteomic investigation of kidney biopsies in a clinically relevant large animal model of sepsis. We aimed to provide an insight into the molecular signatures underlying the renal dysfunction in sepsis and to integrate these findings into the overall disease context. For this purpose, analysis of renal tissue remains necessary and the experimental animal model allowed us to study serial changes in renal tissue proteins over time, and to relate these changes to traditional parameters of renal physiology. The results suggest that exposure to surgical stress per se alters the renal protein expression profile in pigs, while sepsis induces a highly dynamic proteome transformation shifting the balance toward cellular distress phenotype. The data implicate endoplasmic reticulum (ER) stress, oxidative stress, mitochondrial energy metabolism, tubular transport, and immune/inflammatory signaling as major activated pathways. The study supports the notion that a single protein does not appear to be the dominant cause of AKI in

TABLE 3. (continued)

Spot no	Name	Gene	TP1x2 sepsis			TP2x4 sepsis			TP1x4 sepsis			TP1x2 sham			TP2x4 sham			TP1x4 sham			sepsis trend	sham trend
			Mean	SD	P	Mean	SD	P	mean	SD	P	mean	SD	P	mean	SD	P	mean	SD	P		
18	Chloride intracellular channel protein 4	CLIC4	0,997	0,375	0,641	0,900	0,303	0,211	0,820	0,262	0,038	0,861	0,576	0,566	2,585	2,498	0,054	1,483	0,723	0,264	↓	
19	Collagen alpha-1 (VI) chain	COL6A1	1,454	0,936	0,049	0,894	0,358	0,139	1,095	0,324	0,483	1,197	0,901	0,649	1,393	0,402	0,133	1,449	0,809	0,690	+/-	
20	Coactosin-like protein	COTL1	3,742	10,694	0,037	11,588	18,631	0,166	5,754	9,736	0,953	1,637	1,977	0,877	2,953	3,294	0,306	9,865	19,742	0,370	+/-	
21	Dihydrolipoyl dehydrogenase, mitochondrial	DLD	1,077	0,356	0,760	1,151	0,307	0,050	1,173	0,389	0,397	1,090	0,650	0,740	1,004	0,642	0,305	0,830	0,212	0,166	+/-	
22	Elongation factor 1-alpha 1	EEF1A1	5,998	18,986	0,099	11,566	24,631	0,546	0,507	0,590	0,018	12,931	19,289	0,791	22,845	49,005	0,295	36,843	49,493	0,446	↓	
23	Enoyl-CoA hydratase, mitochondrial	ECHS1	0,964	0,487	0,135	0,894	0,414	0,328	0,921	0,820	0,050	1,126	0,905	0,685	1,642	1,035	0,318	1,305	0,302	0,125	↓	
24	Enoyl-CoA hydratase, mitochondrial	ECHS1	1,094	0,350	0,644	0,850	0,251	0,054	0,923	0,377	0,296	1,275	0,509	0,185	1,036	0,338	0,746	1,237	0,408	0,050		↑
25	Alpha-enolase	ENO1	1,153	0,207	0,046	1,061	0,301	0,658	1,179	0,380	0,225	2,006	2,081	0,329	0,688	0,722	0,548	1,159	0,202	0,479	+/-	
26	Fibrinogen alpha chain	FGA	1,659	2,391	0,479	6,475	9,994	0,219	2,210	1,482	0,044	3,803	7,229	0,957	17,745	38,383	0,770	1,856	3,067	0,761	↑	
27	Fibrinogen alpha chain	FGA	6,086	15,456	0,469	13,074	18,546	0,416	6,090	5,443	0,014	1,479	2,478	0,446	16,532	33,305	0,407	5,939	11,606	0,552	↑	
28	Fibrinogen beta chain	FGB	2,155	2,181	0,196	15,185	43,771	0,054	5,007	6,741	0,015	0,936	0,692	0,908	8,310	15,138	0,929	1,609	1,417	0,972	↑	
29	Glyceraldehyde-3-phosphate dehydrogenase	GAPDH	7,956	13,542	0,045	8,211	16,271	0,569	18,199	27,630	0,257	1,965	1,872	0,339	6,286	8,865	0,454	2,443	0,386	0,020	+/-	
30	Glutamate dehydrogenase 1, mitochondrial	GLUD1	1,400	0,745	0,074	1,151	0,438	0,812	1,502	0,805	0,024	1,110	0,217	0,036	1,268	0,519	0,182	0,864	0,270	0,263	↑	+/-
31	Glycerol-3-phosphate dehydrogenase 1-like protein	GPD1L	4,686	12,519	0,251	14,665	22,263	0,028	12,296	31,205	0,032	0,846	0,354	0,464	1,125	0,594	0,196	1,109	0,718	0,788	↑	
32	Glutathione peroxidase 1 Thioredoxin-dependent peroxide reductase, mitochondrial	GPX1 PRDX3	9,758	16,207	0,020	0,481	0,602	0,003	0,902	0,867	0,244	0,965	0,221	0,617	0,872	0,538	0,571	0,768	0,468	0,560	+/-	
33	Glutathione S-transferase omega-1	GSTO1	2,147	5,383	0,010	4,545	8,496	0,055	8,462	17,478	0,542	0,959	0,664	0,733	1,399	1,521	0,780	1,127	1,454	0,662	+/-	
34	Heterogeneous nuclear ribonucleoproteins C1/C2	HNRPC	0,520	0,566	0,006	4,100	8,654	0,913	0,523	0,602	0,008	1,770	2,938	0,596	0,773	0,617	0,230	0,461	0,424	0,148	↓	
	Tumor protein p53-inducible protein 13	TP53I13																				
	Adenylyltransferase and sulfurtransferase	MOCS3																				
35	78 kDa glucose-regulated protein	HSPA5	1,323	0,451	0,059	1,131	0,222	0,060	1,465	0,517	0,018	2,028	0,331	0,457	0,968	0,517	0,650	0,786	0,172	0,046	↑	
36	Heat shock protein HSP 90-alpha	HSP90AA1	2,914	1,861	0,025	0,882	0,487	0,582	2,280	1,569	0,023	0,561	0,099	0,078	2,359	0,011	0,098	1,554	0,430	0,074	↑	
37	Heat shock protein HSP 90-alpha	HSP90AA1	1,798	1,294	0,040	1,053	0,560	0,307	1,339	0,629	0,104	0,795	0,382	0,320	1,709	0,522	0,154	1,492	1,183	0,689	+/-	

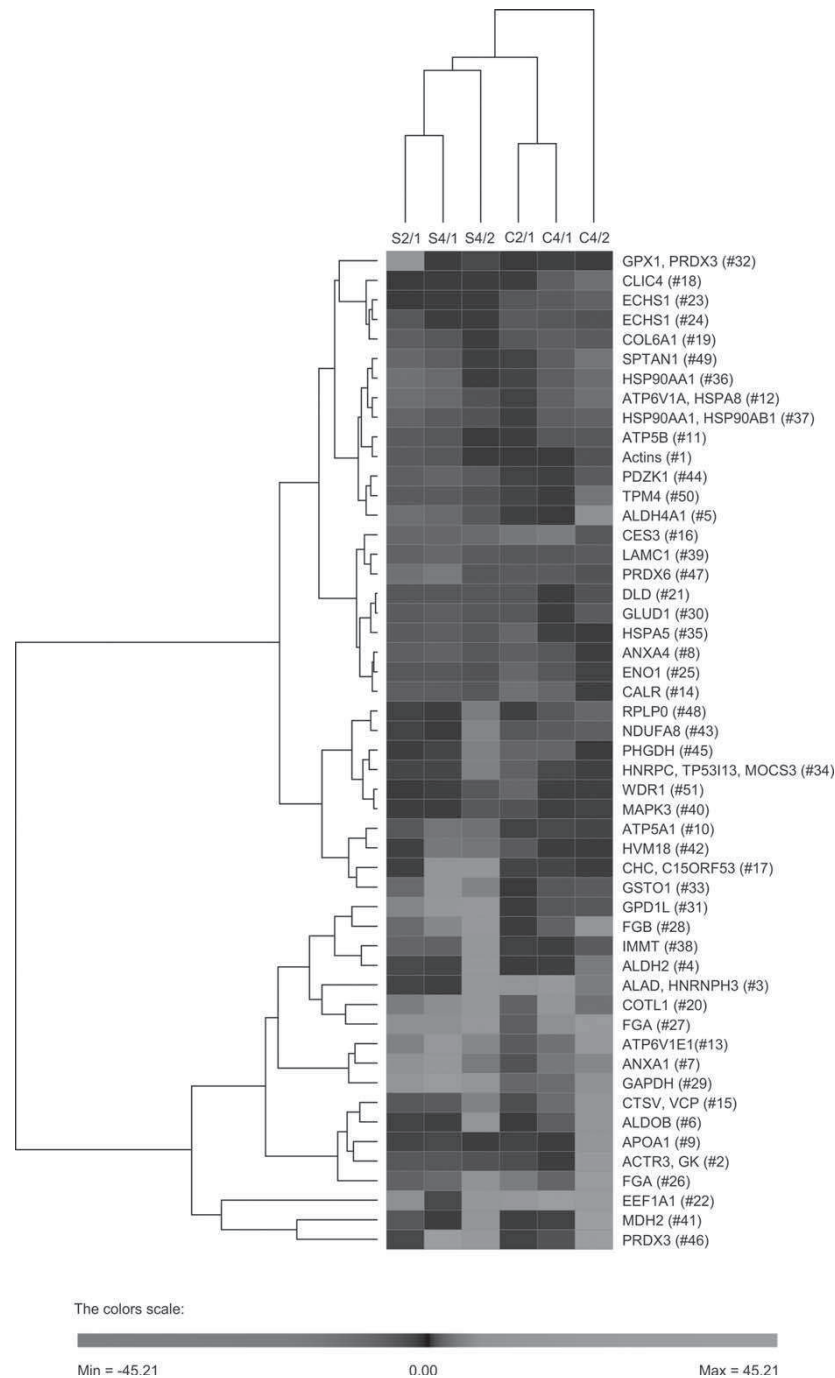


FIG. 1. Proteins undergoing significant changes during the study. Time evolution of protein expression for proteins showing significant variation at any group or time-point is given as a heat map. Tree graph at the top shows natural clustering of groups and time-points while the tree at the left shows natural clustering of proteins. Protein down-regulation is pictured red and up-regulation green.

sepsis. Instead, potentially subtle and even transient changes in several proteins that are members of key functional interrelated systems appear to occur in septic AKI.

Tremendous progress has been achieved in the understanding of fundamental mechanisms of septic AKI. However, the translation of these advances into clinically effective therapies

of AKI has been disappointing. Although basic clinical research using rodents will remain a key step in discovering further mechanistic insights and identifying new treatment targets, recent genomic data suggest substantial mouse-to-human incompatibilities in inflammatory models such as endotoxemia, trauma, and burns (8). Thus, targets identified in

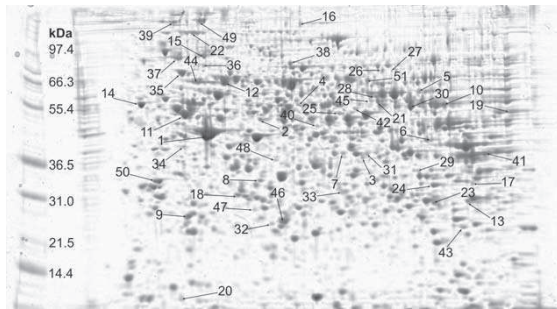


FIG. 2. A kidney proteome map from time-point 2, septic group. Pictured is a representative two-dimensional gel electrophoresis scanned image. Proteins listed in Table 3 are marked with arrows. Molecular weight ladder is pictured, pH range 3–10.

rodent models might not necessarily be germane to human physiology. To bridge the gap between preclinical and clinical studies, high-quality preclinical translational research simulating the complexity of AKI patients is required. In this context, the genetic and physiological proximity of pigs and humans make this species an excellent biomodel for translational research (7). It is therefore highly relevant not only to characterize differential expression of porcine renal proteins induced by the diseases itself (sepsis in this case), but also to provide information about the way surgical insult affects kidney proteome. The latter could serve as a useful reference for further experiments since sham-operated animals are often used as a control.

Indeed, our data revealed that sepsis-specific changes in renal proteome may be influenced to some extent by

non-disease-associated changes in protein expression occurring as a consequence of surgery and/or anesthesia. Interestingly, these local proteomic alterations corresponding to an acute phase response developed despite undetectable changes in systemic plasma cytokine levels and renal hemodynamics. The design of this study does not allow us to unequivocally determine the clinical significance of these changes (i.e. adaptive versus maladaptive response). Nevertheless, it seems that kidneys might be subject to a considerable local surgery-triggered stress which might not be fully compensated for, particularly in a high-risk population (e.g. preexisting kidney disease), resulting in postoperative AKI.

Kidneys from septic pigs showed different trajectories for proteins involved in inflammatory, metabolic, and cellular stress responses. This clearly implies that changes in renal proteome induced by surgical stress did not mask sepsis-induced proteomic signature, thus imparting validity and usefulness to these results. The vast majority of up-regulated pathways clustered into three broad functional categories—protein repair chaperones, ER and oxidative stress response, all playing a role in the pathogenesis of AKI as a central element of the network of “danger response” (9–11). Induction of the ER stress proteins GRP78 and calreticulin may be particularly relevant to the pathophysiology of septic AKI as the persistent and overwhelming ER stress is closely linked to the altered mitochondrial function, inflammation, oxidative stress, and cell death (11). Indeed, accumulating evidence suggests that severe ER stress contributes significantly to the progression of various pathological conditions including sepsis and kidney diseases (11, 12). Another interesting finding is the progressive up-regulation of peroxiredoxin-6, an important regulator of cellular redox balance and a marker of oxidative stress, and heat shock proteins with their

TABLE 4. Identified proteins showing statistically different behavior between septic and sham-operated groups throughout the experiment

	Group effect		Time effect		Time × group effect	
	F	P	F	P	F	P
AL4A1	0,7625	0,408004	0,3552	0,706416	4,2331	0,033452
ANXA4	10,1571	0,007144	0,7994	0,460330	3,5506	0,043319
ATPA	0,00344	0,955503	0,81426	0,470302	8,08581	0,008144
CLIC4	4,2655	0,057927	2,0701	0,145059	5,8167	0,007715
CO6A1	0,38379	0,545531	0,50446	0,609215	6,08864	0,006375
DHE3	3,20975	0,096497	0,84961	0,439114	3,46975	0,046167
DLDH	3,2569	0,092674	0,5171	0,601806	3,5956	0,040751
EF1A1	8,82568	0,010830	0,75313	0,480888	3,99196	0,030768
ECHM	6,1748	0,026220	0,2324	0,794138	3,6162	0,040088
ENOA	1,77390	0,209839	5,31788	0,013062	4,53077	0,022501
HS90A	4,70838	0,052788	2,21054	0,133412	4,42680	0,024226
HS90A/B	1,81035	0,199854	0,36441	0,697854	3,47702	0,044797
HSP7C	9,20281	0,008936	2,16781	0,133253	4,86919	0,015320
IMMT	0,8732	0,368490	1,3526	0,277578	4,2486	0,026325
LAMC1	9,06635	0,010842	0,38435	0,685008	4,93070	0,016072
MK03	0,1951	0,665989	2,6190	0,091995	4,3414	0,023614
NHRF3	7,3212	0,017062	5,3745	0,010582	17,1121	0,000014
PRDX6	5,07319	0,065228	7,07502	0,009338	4,44945	0,035838
SPTA2	7,14698	0,018179	0,12820	0,880187	5,89743	0,007288
THTR	8,2685	0,012219	2,3546	0,113455	4,5835	0,018967
WDR1	3,44975	0,086056	2,26957	0,123457	4,93435	0,015253

Listed are proteins exerting a different behavior between groups when all time points are taken into account. General linear models were set up for all proteins undergoing a significant change at any time point or group (Table 3). Proteins showing significance (<0.05) either with respect to group effect or higher order time × group effect were considered as affected by sepsis.

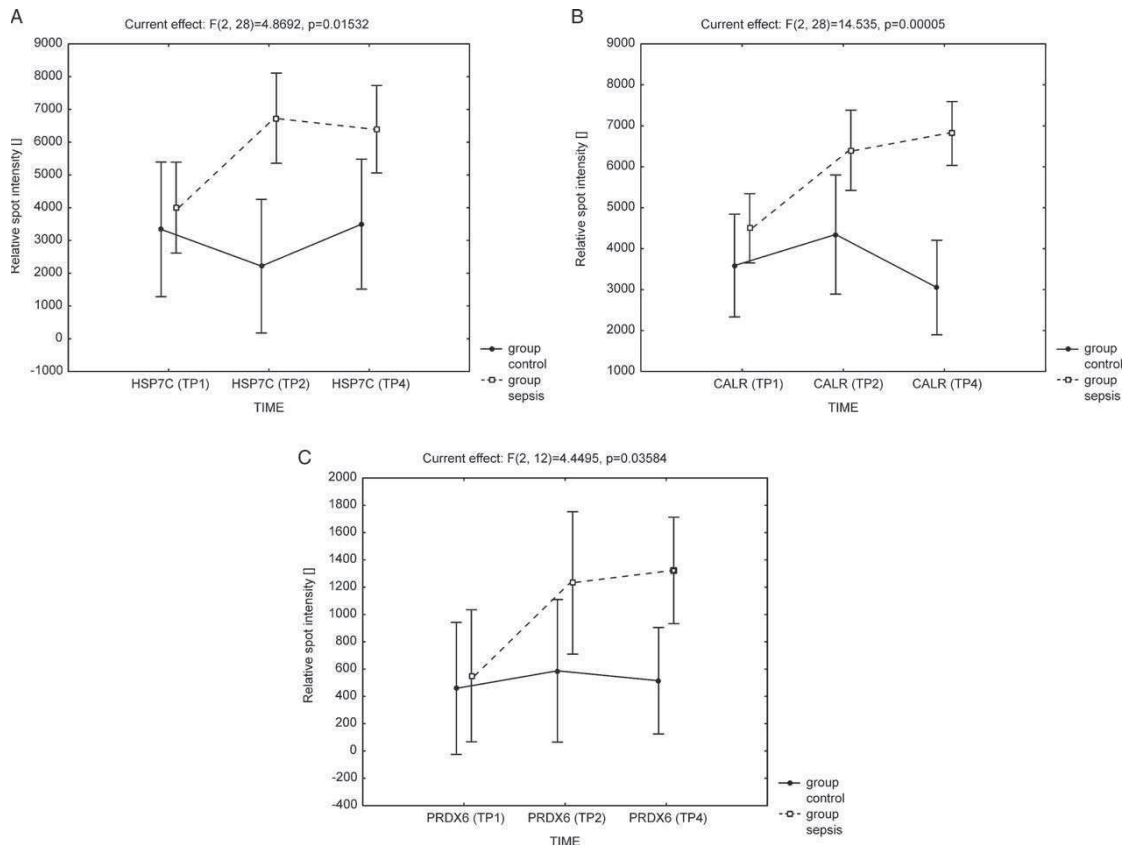


FIG. 3. Time course and group differences for heat shock cognate 71 kDa protein (A), calreticulin (B), and peroxiredoxin-6 (C). General linear model ANOVA.

multiple functions ranging from stress response to intracellular trafficking and cell regeneration (13). In addition to these well-established functions, recent data indicate that both peroxiredoxins and heat shock proteins may also act as endogenous damage-associated molecular pattern molecules (DAMPS) (14, 15). Both endothelial and tubular cells have been shown to serve

as sensitive sensors of DAMPS (16). Therefore, it is tempting to hypothesize that early renal DAMPS production (within 12 h in our study) preceding the development of regional hemodynamic and functional alterations allows for rapid amplification and propagation of local inflammatory signal, thus contributing to early microvascular and tubular injury.

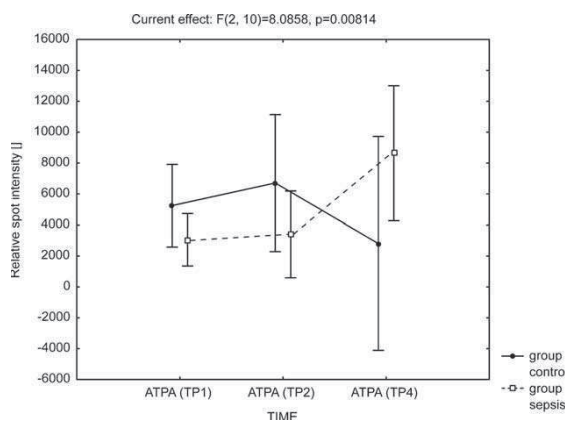


FIG. 4. Time course and group differences for ATP synthase subunit alpha. General linear model ANOVA.

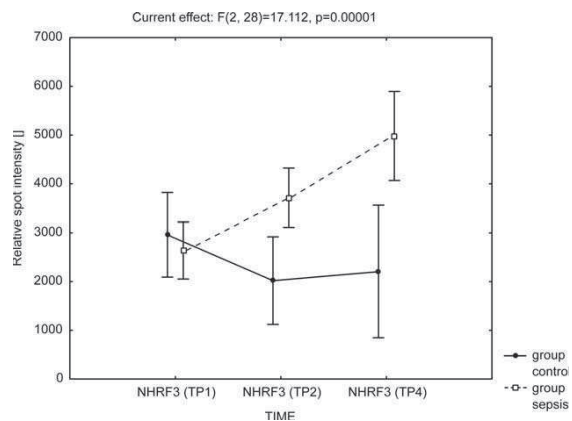


FIG. 5. Time course and group differences for Na⁽⁺⁾/H⁽⁺⁾ exchange regulatory cofactor NHE-RF3. General linear model ANOVA.

Investigation into the underlying cellular mechanisms of AKI increasingly point toward a predominant role of mitochondria (10, 17). It is therefore not surprising that almost 30% of identified unique proteins which changed their abundance exclusively in the sepsis group are involved in cellular energy metabolism. Of these, mitochondrial ATP-synthase subunit alfa should be regarded as an important finding since this enzyme is a key determinant of cellular energy state and mitochondrial respiratory function. In keeping with recent reports (18, 19), our finding of gradually up-regulated mitochondrial ATP-synthase subunit alfa provides further argument against bioenergetic failure or cellular metabolic downregulation, at least at the early phase of porcine sepsis-induced AKI.

Another potentially relevant finding coming from this proteomic analysis which may direct future research in septic AKI is the increased expression of Na(+)/H(+) exchange regulatory cofactor (NHE-RF3), inasmuch as this enzyme is critical to the regulation of cell surface expression and the activity of several membrane transporters and receptors in the renal tubular system, including Na+/H+ exchanger-3 (NHE3) (20). HNE3, which is inhibited by a family of NHE-RF proteins (21), has recently been shown to be substantially reduced in various forms of AKI, including endotoxemia (22–25). Suppression of HNE3 expression is associated with reduced reabsorption of filtered load and increased distal chloride delivery (26). The net consequence is activated tubuloglomerular feedback and reduced glomerular filtration (26). The latter may contribute to a form of “renal hibernation” that acts to protect injured tubules from further injury by reducing the filtered load and thereby the reabsorptive workload (27). Hence, the inhibitory effects of up-regulated NHE-RF3 could be viewed as an early adaptive rather than pathological event in the course of AKI. Over-expression of NHE-RF3 that occurred early in our study, i.e. before the reduction of renal blood flow and the fall in glomerular filtration, may fit into this hypothesis. However, the lack of detailed mechanistic molecular studies that would clearly document the link between up-regulated NHE-RF3, reduced activity of HNE3 and tubuloglomerular cross-talk prevent us from making any firm conclusions.

In this model, the renal proteomic responses to sepsis during the first 22 h could be interpreted as a transition period in the development of AKI. Of note, the design of the present study does not allow one to ultimately determine a causative link between this proteomic stress phenotype and AKI or to clarify its relative contribution to septic AKI. Admittedly, several changes in protein expression found in our study have been shown in different animal models as well as in different target organs (28, 29). Alternatively, different insults result in stereotypic and nonspecific downstream pathways which represent a secondary phenomenon. Such an explanation is also supported, for example, by Grigoryev et al (30) who found striking similarity in transcription patterns of inflammatory genes in kidney and lung tissue in a murine model of ischemic AKI.

Understanding the methodological limitations of our experimental approach is essential for any translational research. Studies using lysates of the entire kidney biopsy might be

confounded by tissue heterogeneity. Indeed, renal tissue is a highly complex structure comprising more than 20 different cell types, the proportion of which may differ among biopsies. Under the circumstances, renal proteome profile is a consequence of changes in intrinsic renal tissue constituted by diverse cellular types and, to a variable degree, by infiltrating inflammatory cells. Moreover, renal tissue injury is not uniform throughout the kidney during AKI, zones of inflammatory, hypoxic nephrons might coexist with clusters of relatively preserved nephrons (27). Further studies using subproteomic fractionation and advanced technologies such as multidimensional LC MS/MS are needed to capture less abundant proteins and posttranslational modifications. Furthermore, we studied young, otherwise healthy animals. Several risk factors like aging, hypertension, diabetes and chronic kidney disease are known to significantly increase the susceptibility to AKI in sepsis. Understanding the differences in renal danger response in the presence of pre-existing comorbidities in comparison to healthy kidneys would be highly informative. Validation of the discovered candidate molecules would be desirable before further mechanistic studies are undertaken.

In summary, our study combines the power of proteomics with a classic larger mammal model of sepsis. By coupling this approach with whole-animal physiological studies and small-molecule screening, our study helps to establish the first picture of the proteomic phenotype of surgical trauma- and sepsis-induced porcine renal proteome responses. Tangibly, the data revealed early septic kidney as a shifting landscape of biologic functions to multiple ongoing stress-related and defense functions. Investigating the contribution of these changes to altered cellular functions underlying renal dysfunction in sepsis is now a major challenge. From a methodological point of view, our approach represents a proof of principle highlighting that serial tissue samples collected at different time-points are readily amenable for in-depth molecular analyses and provide a foundation for the future translational studies of dynamic molecular changes in renal diseases such as sepsis.

REFERENCES

1. Hoste EA, Bagshaw SM, Bellomo R, Cely CM, Colman R, Cruz DN, Edipidis K, Forni LG, Gomersall CD, Govil D, et al.: Epidemiology of acute kidney injury in critically ill patients: the multinational AKI-EPI study. *Intensive Care Med* 41(8):1411–1423, 2015.
2. Matejovic M, Chvojka J, Radej J, Ledvinova L, Karvunidis T, Krouzicky A, Novak I: Sepsis and acute kidney injury are bi-directional. *Contrib Nephrol* 174:78–88, 2011.
3. Alobaidi R, Basu RK, Goldstein SL, Bagshaw SM: Sepsis-associated acute kidney injury. *Semin Nephrol* 35(1):2–11, 2015.
4. Bonventre JV, Basile D, Liu KD, McKay D, Molitoris BA, Nath KA, Nickolas TL, Okusa MD, Palevsky PM, Schnellmann R, et al.: Kidney Research National Dialogue (KRND). AKI: a path forward. *Clin J Am Soc Nephrol* 8(9):1606–1608, 2013.
5. Sedor JR: Tissue proteomics: a new investigative tool for renal biopsy analysis. *Kidney Int* 75(9):876–879, 2009.
6. Charonis A, Luider T, Baumann M, Schanstra JP: Is the time ripe for kidney tissue proteomics? *Proteomics Clin Appl* 5(5–6):215–221, 2011.
7. Bendixen E: Animal models for translational proteomics. *Proteomics Clin Appl* 8(10):637–639, 2014.
8. Seok J, Warren HS, Cuenca AG, Mindrinos MN, Baker HV, Xu W, Richards DR, McDonald-Smith GP, Gao H, Hennessy L, et al.: Inflammation and host response to injury, large scale collaborative research program: genomic responses in mouse models poorly mimic human inflammatory diseases. *Proc Natl Acad Sci U S A* 110(9):3507–3512, 2013.

9. Aksu U, Demirci C, Ince C: The pathogenesis of acute kidney injury and the toxic triangle of oxygen, reactive oxygen species and nitric oxide. *Contrib Nephrol* 174:119–128, 2011.
10. Gomez H, Ince C, De Backer D, Pickkers P, Payen D, Hotchkiss J, Kellum JA: A unified theory of sepsis-induced acute kidney injury: inflammation, micro-circulatory dysfunction, bioenergetics, and the tubular cell adaptation to injury. *Shock* 41:3–11, 2014.
11. Inagi R, Ishimoto Y, Nangaku M: Proteostasis in endoplasmic reticulum—new mechanisms in kidney disease. *Nat Rev Nephrol* 10(7):369–378, 2014.
12. Khan MM, Yang WL, Wang P: Endoplasmic reticulum stress in sepsis. *Shock* 44(4):294–304, 2015.
13. Fisher AB: Peroxiredoxin 6: a bifunctional enzyme with glutathione peroxidase and phospholipase A₂ activities. *Antioxid Redox Signal* 15(3):831–844, 2011.
14. Riddell JR, Wang XY, Minderman H, Gollnick SO: Peroxiredoxin 1 stimulates secretion of proinflammatory cytokines by binding to TLR4. *J Immunol* 184(2):1022–1030, 2010.
15. Tsan MF, Gao B: Heat shock proteins and immune system. *J Leukoc Biol* 85(6):905–910, 2009.
16. Molitoris BA: Therapeutic translation in acute kidney injury: the epithelial/endothelial axis. *J Clin Invest* 124:2355–2363, 2014.
17. Parikh SM, Yang Y, He L, Tang C, Zhan M, Dong Z: Mitochondrial function and disturbances in the septic kidney. *Semin Nephrol* 35(1):108–119, 2015.
18. Porta F, Takala J, Weikert C, Bracht H, Kolarova A, Lauterburg BH, Borotto E, Jakob SM: Effects of prolonged endotoxemia on liver, skeletal muscle and kidney mitochondrial function. *Crit Care* 10(4):R118, 2006.
19. May CN, Ishikawa K, Wan L, Williams J, Wellard RM, Pell GS, Jackson GD, Bellomo R: Renal bioenergetics during early gram-negative mammalian sepsis and angiotensin II infusion. *Intensive Care Med* 38(5):886–893, 2012.
20. Anzai N, Jutabha P, Kanai Y, Endou H: Integrated physiology of proximal tubular organic anion transport. *Curr Opin Nephrol Hypertens* 14:472–479, 2005.
21. Shenolikar S, Weinman EJ: NHERF: targeting and trafficking membrane proteins. *Am J Physiol Renal Physiol* 280(3):F389–F395, 2001.
22. Girardi AC, Di Sole F: Deciphering the mechanisms of the Na⁺/H⁺ exchanger-3 regulation in organ dysfunction. *Am J Physiol Cell Physiol* 302(11):C1569–C1587, 2012.
23. Di Sole F, Hu MC, Zhang J, Babich V, Bobulescu IA, Shi M, McLeroy P, Rogers TE, Moe OW: The reduction of Na/H exchanger-3 protein and transcript expression in acute ischemia-reperfusion injury is mediated by extractable tissue factor(s). *Kidney Int* 80(8):822–831, 2011.
24. Schmidt C, Höcherl K, Schweda F, Kurtz A, Bucher M: Regulation of renal sodium transporters during severe inflammation. *J Am Soc Nephrol* 18(4):1072–1083, 2007.
25. Schmidt C, Höcherl K, Schweda F, Bucher M: Proinflammatory cytokines cause down-regulation of renal chloride entry pathways during sepsis. *Crit Care Med* 35:2110–2119, 2007.
26. Morrell ED, Kellum JA, Hallows KR, Pastor-Soler NM: Epithelial transport during septic acute kidney injury. *Nephrol Dial Transplant* 29(7):1312–1319, 2014.
27. Matejovic M, Ince C, Chawla LS, Blantz R, Molitoris BA, Rosner MH, Okusa MD, Kellum JA, Ronco C, ADQI XIII Work Group. Renal hemodynamics in AKI: in search of new treatment targets. *J Am Soc Nephrol* 27(1):49–58, 2016.
28. Cieniewski-Bernard C, Mulder P, Henry JP, Drobecq H, Dubois E, Pottiez G, Thuillez C, Amouyel P, Richard V, Pinet F: Proteomic analysis of left ventricular remodeling in an experimental model of heart failure. *J Proteome Res* 7(11):5004–5016, 2008.
29. Gianazza E, Eberini I, Sensi C, Barile M, Vergani L, Vanoni MA: Energy matters: mitochondrial proteomics for biomedicine. *Proteomics* 11(4):657–674, 2011.
30. Grigoryev DN, Liu M, Hassoun HT, Cheadle C, Barnes KC, Rabb H: The local and systemic inflammatory transcriptome after acute kidney injury. *J Am Soc Nephrol* 19(3):547–558, 2008.

SHK

Manuscript No. 15-00546

SHOCK

Dear Author,

During the preparation of your manuscript for typesetting, some queries have arisen. These are listed below. Please check your typeset proof carefully and mark any corrections in the margin as neatly as possible or compile them as a separate list. This form should then be returned with your marked proof/list of corrections to the Production Editor.

QUERIES: to be answered by AUTHOR

QUERY NO.	QUERY DETAILS	RESPONSE
<AQ1>	Please confirm whether surnames/family names (red) have been identified correctly in the author byline.	
<AQ2>	Please check the affiliation for correctness.	
<AQ3>	Please check the correspondence address for correctness.	
<AQ4>	Please check the conflicts of interest statement for correctness.	
<AQ5>	Please provide city of B. Braun, PULSION Medical Systems GmbH, Bio-Rad, Roche.	

Proteomic Analysis of Proteins Bound to Adsorption Units of Extracorporeal Liver Support System under Clinical Conditions

Jan Mares,^{*,†} Visith Thongboonkerd,[‡] Zdenek Tuma,[§] Jiri Moravec,[§] Thomas Karvunidis,[†] and Martin Matejovic[†]

Department of Internal Medicine I, Charles University Medical School and Teaching Hospital, Plzen, Czech Republic, Medical Proteomics Unit, Office for Research and Development, Faculty of Medicine Siriraj Hospital, Mahidol University, Bangkok, Thailand, and Proteomic Laboratory, Charles University Medical School, Plzen, Czech Republic

Received November 7, 2008

Fractionated Plasma Separation, Adsorption and Dialysis (Prometheus) has a well-documented capacity to remove protein-bound organic toxins in patients with liver failure. However, the compositions of adsorbed proteins remain unknown. Elution of both adsorbers constituting Prometheus system was performed following a 6-h session in a patient with acute on chronic liver failure. Sodium dodecylsulphate was employed to elute proteins from the neutral adsorber (P1), while acetic acid was applied to the cationic one (P2). Eluted proteins were resolved by two-dimensional gel electrophoresis (2-DE) and identified by mass spectrometry (MS). Totally, 4113 and 8280 mg of proteins were obtained from P1 and P2 eluates, 2-DE yielded 148 and 163 protein fractions in P1 and P2, respectively. MS identified 18 unique proteins in P1, and 30 unique proteins in P2 sample. Proteins with the highest selective adsorption (as determined by eluate to plasma ratio) included transthyretin (37), trypsin-2 (29), prothrombin (23), hyaluronan-binding protein 2 (13) and plasma retinol-binding protein (8.7), all of which adsorbed to P2. We identified a large number of proteins removed by extracorporeal liver support system. A selective adsorption was demonstrated in a subset of proteins depending on the type of adsorber and proteins' characteristics.

Keywords: Liver failure • adsorption • proteome • elimination • Prometheus

Introduction

Temporary replacement of liver function by means of Fractionated Plasma Separation, Adsorption and Dialysis (Prometheus) is a novel technology available for patients with acute and chronic liver failure.^{1,2} There is a considerable pool of patients who may benefit from extracorporeal liver support if it proves effective and safe. In the near future, treatment of patients with liver metastases (colorectal cancer, etc.), exploiting new techniques of liver resection, could depend on the possibility of bridging the patient over the period necessary for transplant procurement or liver regeneration. Improving outcomes of liver transplants and new approaches to stimulation of liver regeneration (growth factors administration, stem cells technology, etc.) are promising definitive solutions in such cases. In some patients with toxic liver damage (e.g., alcoholic), spontaneous recovery may be awaited.

The system's capacity for removal of both water-soluble and albumin-bound toxins generated and retained in liver failure

(bilirubin, ammonium, phenols, cholic acids, etc.) has been well-established.^{3,4} However, we have very limited information about the elimination of other compounds. Available data show that plasma levels of high-abundance proteins (i.e., albumin, fibrinogen, and IgG) remain virtually unchanged during the procedure.⁵ Significant clearance of peptides and proteins (e.g., β_2 -microglobulin) by adsorption has been demonstrated to occur during hemodialysis.^{6–8} By virtue of its design, Prometheus is much more prone to adsorb proteins, especially due to its adsorbing capacity for hydrophobic molecules and owing to the beads' microarchitecture (with vast surface exposed to plasma).

Liver failure is associated with impaired proteosynthesis, accumulation, and dysregulation of signaling peptides and cytokines. Therefore, it seems crucial to ascertain proteins removed by the method before we investigate it in large clinical trials or even adopt in routine practice. We can speculate that removing proteins, especially those with high biological activities, can either improve or further deteriorate the vulnerable equilibrium in patients with liver failure. This issue has been addressed by several groups of investigators. Rifai et al.⁵ did not find changes in plasma levels of interleukin-6 (IL-6), tumor necrosis factor- α (TNF- α), and coagulation factors II and V during Prometheus procedure. However, Stadlbauer et al.⁹ observed differential concentrations of IL-6, IL-8, IL-10 and

* To whom correspondence should be addressed. Jan Mares, MD, Department of Internal Medicine I Charles University Medical School and Teaching Hospital, Alej Svobody 80, 301 60 Plzen, Czech Republic. Phone: 00420-37-7103650. Fax: 00420-37-7103506. E-mail: mares@fnplzen.cz.

[†] Department of Internal Medicine I, Charles University Medical School and Teaching Hospital.

[‡] Mahidol University.

[§] Proteomic Laboratory, Charles University Medical School.

TNF- α between the inlet and outlet of the system and showed that their clearance was probably outweighed by rapid production.

As the system has a high affinity to both hydrophilic and hydrophobic molecules, and the plasma-filter used to separate plasma from blood cells has a molecular weight (MW) cutoff of 300 kDa,¹⁰ there is a wide range of plasma proteins susceptible to adsorption and removal. A selection of target molecules for analysis seems to be quite difficult under these circumstances. It is therefore disputable whether we can derive system's characteristics (in terms of substance clearance) from plasma concentrations of selected proteins measured with specific immunoassays. However, recent advancement in the postgenomic biotechnologies, particularly proteomics that can simultaneously examine a large number of proteins with a wide variety of physicochemical properties, may overcome this limitation.

The aim of this study was to develop a technique allowing analysis of proteins adsorbed to the Prometheus system, to validate it by accomplishing proteomic identification of proteins released by the elution, and to provide a pilot characteristic of the proteins adsorbed to the Prometheus adsorption units.

Methods

Patient and Treatment. A 37 year-old man who suffered acute on chronic liver failure due to alcohol abuse was treated with a 6-h session of Fractionated Plasma Separation, Adsorption and Dialysis (Prometheus; Fresenius Medical Care, Homburg, Germany) under citrate anticoagulation. Before the procedure, a plasma sample was drawn for blood tests and proteomic analysis. At the end of the procedure, the system was flushed with 500 mL of replacement solution (Plasmalyte, Baxter, Deerfield, IL) and disconnected from the patient. The study protocol has been approved by the local ethics committee.

The Prometheus circuit included two adsorber cartridges, each of which had a filling volume of 90 mL. These cartridges contained adsorbing beads (styrenedivinyl benzene copolymer), one composed of neutral resin (Prometh 1), whereas the other one had anion exchanger properties (Prometh 2). Both units were emptied and flushed three times with 500 mL of PBS (pH 7.4). The protein concentration in the last flush was assessed with Bradford's dye-binding assay (Bio-Rad Protein Assay, Bio-Rad Laboratories; Hercules, CA).

Protein Elution and Sample Preparation. To elute the adsorbed proteins, Prometh 1 was filled with 90 mL of 10% SDS (SDS for electrophoresis, Sigma, Steinheim, Germany) and Prometh 2 was filled with 90 mL of 40% acetic acid (p.a., Sigma). After 30-min incubation at 24 °C, both capsules were drained. The eluates are henceforth referred to as P1 (from Prometh 1) and P2 (from Prometh 2). The eluates (10 mL) were precipitated with 40 mL of acetone (Sigma), incubated at -20 °C for 30 min and spinned down (4500g, 30 min, 4 °C). The protein pellets were washed once with 8 mL of a mixture of acetone-methanol-water-acetic acid (80:10:9.9:0.1), centrifuged as above, air-dried, and dissolved in 2 mL of lysis buffer (7 M urea, 4% CHAPS, 40 mM Tris base, 2 M Thiourea, 2% IPG buffer pH 3-10, and 120 mM DTT). To minimize salt contamination, P1 and P2 eluates were dialyzed against ultrahigh quality water using a semipermeable membrane with a MW cutoff at 7 kDa (Serva-Electrophoresis; Heidelberg, Germany) using five exchanges. P1 and P2 samples were then concentrated in a SpeedVac and proteins were resuspended in the lysis

buffer (same as above). Blood sample (4 mL) was processed by centrifugation only (10 min, 4 °C, 4000g) to separate plasma (supernatant).

Two-Dimensional Electrophoresis (2-DE). All reagents were supplied by Sigma; IPG buffer (ZOOM carrier Ampholytes 3-10) was purchased from Invitrogen (Invitrogen Corporation, Carlsbad, CA). P1, P2, and plasma samples (all in triplicate) were diluted with rehydration buffer (7 M urea, 4% CHAPS, 40 mM Tris base, 2 M Thiourea, 2% IPG buffer pH 3-10, 120 mM DTT, and a trace of bromophenol blue) to the final protein concentration of 200 μ g in 140 μ L. Samples were applied on IPG strips (7.7 cm, pH 3-10 nonlinear; Invitrogen) and focused in a MiniProtean cell (Bio-Rad). Isoelectric focusing (IEF) was performed as follows: IPG strips were rehydrated passively for 1 h and actively for 10 h at 30 V followed by stepwise of 200-750 V until 10 000 Vh was reached. After IEF, the IPG strips were equilibrated in equilibration buffer I (112 mM Tris-base, 6 M urea, 30% (v/v) glycerol, 4% (w/v) SDS, 130 mM DTT, and a trace of bromophenol blue) for 30 min, and subsequently alkylated in buffer II (112 mM Tris-base, 6 M urea, 30% (v/v) glycerol, 4% (w/v) SDS, 135 mM IAA, and a trace of bromophenol blue) for 30 min. Each equilibrated IPG strip was placed on top of a 13% polyacrylamide gel (9 \times 7 cm) and covered with 0.5% agarose. The second-dimension separation was carried out at 65 mA/gel at 20 °C until the bromophenol blue dye front reached the bottom of the gel. At the end of each run, the 2-D gels were stained with Simply Blue (Invitrogen) and scanned using an Epson Perfection 4990 Photo scanner.

2-D Spot Pattern Analysis. Computer-aided analysis of 2-D gel images was carried out using PDQuest 2-D software version 8.1 (Bio-Rad). A synthetic image was constructed from all triplicate gels processed from each sample, using only spots constantly present in all three gels. The protein quantity was determined relative to integrated spot density. Quantitative differences were considered significant when showing at least 2-fold intensity variation. The statistical analysis was carried out using SigmaPlot/SigmaStat data analysis software (Version 12.0, SPSS, Inc., Chicago, IL). Mann-Whitney rank sum test was used to compare continuous variables, Spearman rank order correlation coefficients were calculated to estimate association between different variables.

In-Gel Tryptic Digestion. Visualized protein spots were excised manually and washed with water and water/acetonitrile (ACN). SimplyBlue stain was removed by washing with 50 mM NH_4HCO_3 and ACN. Proteins in gel were reduced with 10 mM DTT/50 mM NH_4HCO_3 (45 min, 56 °C) and alkylated with 55 mM IAA/50 mM NH_4HCO_3 (30 min, in the dark at room temperature). Gel spots were washed with 50 mM NH_4HCO_3 and ACN and dried in SpeedVac. Dried gel particles were rehydrated with digestion buffer containing 12.5 ng/ μ L sequencing grade trypsin (Roche, Basel, Switzerland) in 50 mM NH_4HCO_3 at 4 °C. After 45 min, the remaining solution was removed and replaced by 0.1 M NH_4HCO_3 . Tryptic digestion was performed overnight at 37 °C.

After digestion, proteolytic peptides were subsequently extracted with 25 mM NH_4HCO_3 , ACN, and 5% formic acid. The three extracts were pooled and 10 mM DTT solution in 50 mM NH_4HCO_3 was added. The mixture was then dried in SpeedVac, and the resulting tryptic peptides were dissolved in 5% formic acid solution and desalted using ZipTip μ C18 (Millipore; Bedford, MA) following manufacturer's instructions.

Mass Spectrometry (MS). The resulting proteolytic peptides were mixed with α -cyano-4-hydroxycinnamic acid (CHCA)

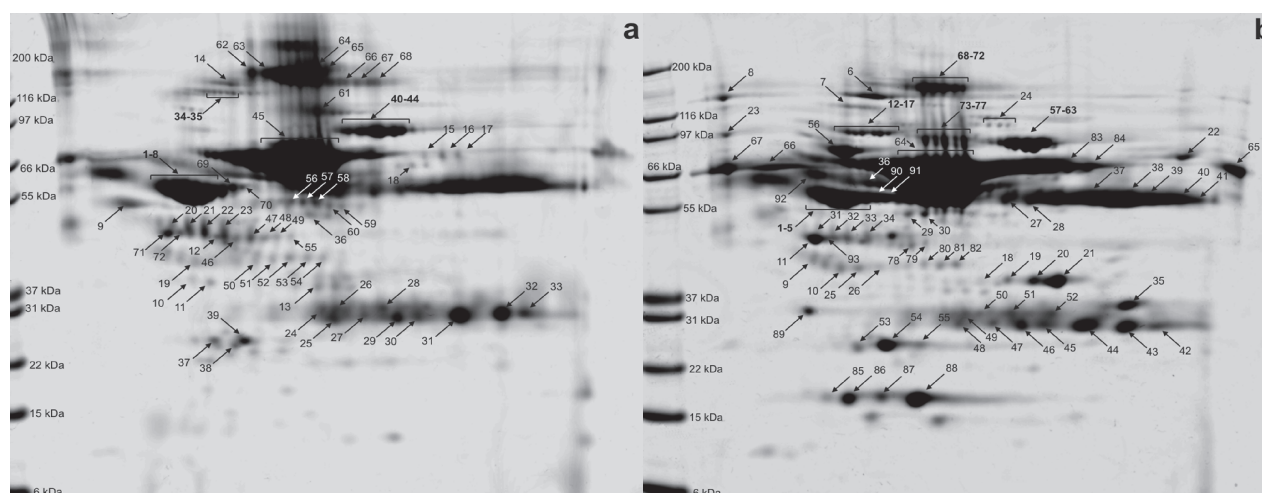


Figure 1. Representative 2-D gel images of Prometh 1 eluate (P1) (a) and Prometh 2 eluate (P2) (b). Spots labeled with numbers were successfully identified by MALDI-TOF/TOF analyses (see Tables 1 and 2). MALDI TOF/TOF = matrix assisted laser desorption and ionization time-of-flight tandem mass spectrometry.

matrix solution (5 mg/mL CHCA in 0.1% TFA/50% ACN 1:1 (v/v)) in 1:1 ratio and 0.8 μ L of this mixture was spotted onto MALDI target plate. All mass spectra were acquired using a reflectron mode of 4800 MALDI TOF/TOF Analyzer (Applied Biosystems; Framingham, MA). A total of 2000 and 3000 laser shots were acquired and averaged to MS and MS/MS spectra, respectively. The MS/MS analyses were performed using collision energy of 1 kV and a collision gas pressure of 1.3×10^{-6} Torr. MS peaks with an S/N above 15 were listed and the 15 strongest precursors with an S/N above 50 among the MS peaks were automatically selected for MS/MS acquisition. A mass filter was used to exclude autolytic peptides of trypsin.

Resulting data were analyzed with GPS Explorer 3.6 (Applied Biosystems) software. The proteins were identified by searching against human subset of the Swiss-Prot protein database (release 54.6; Dec. 4, 2007) using the MASCOT 2.1.0 search algorithm (Matrix Science; London, U.K.). The general parameters for peptide mass fingerprinting (PMF) were as follows: a maximum of one missed cleavage, a peptide mass tolerance of ± 50 ppm, variable oxidation of methionine residue, and fixed carbamidomethylation of cysteine residue. A peptide charge state of +1 and fragment mass tolerance of ± 0.25 Da were used for the MS/MS ion search. Probability-based MOWSE scores were estimated by comparison of search results against estimated random match population and were reported as $-10 \times \log_{10}(p)$ where p is the absolute probability.¹¹ MOWSE scores greater than 55 were considered as significant hits ($p < 0.05$) for PMF. Individual MS/MS ions scores >28 indicated identity or extensive homology ($p < 0.05$) for MS/MS ion search.

Results

The baseline plasma levels were as follows: bilirubin 475 μ mol/L, aspartate aminotransferase (AST) 3.7 μ kat/L, alanine aminotransferase (ALT) 0.5 μ kat/L, ammonium 47 μ mol/L, and plasma prothrombin ratio 2.6. The final flush of Prometh 1 and Prometh 2 cartridges with PBS yielded 81 mg (0.17 mg/mL) and 177 mg (0.36 mg/mL) of the washed proteins, whereas the eluates using SDS (P1) and acetic acid (P2) contained 4113 mg (47.2 mg/mL) and 8280 mg (97.2 mg/mL), respectively.

Representative 2-D gel images of proteins derived from P1 and P2 are shown in Figure 1, panels a and b. Using 200 μ g of

total protein and Simply Blue stain, there were 148 protein spots detected in all 3 replicate gels of P1 and 163 protein spots detected in all triplicate gels of P2. In both eluates, protein spots were distributed from MW of 12–194 kDa and their pI (isoelectric points) ranged from 3.5 to 9.0 (Figure 2, panels a and b). However, the majority (95%) of protein spots and their intensities were found mainly in the interval of MW of 30–150 kDa and pI of 4.8–8.6. Spot patterns in both eluates differed significantly from each other (in 64 spots intensity levels significantly differed between the two groups; $p < 0.05$). Concurrently, intensity levels of 38 spots in P1 and 45 spots in P2 significantly differed ($p < 0.05$) from those of plasma protein spots.

To evaluate potential selectivity of Prometheus system in protein adsorption, we compared spot distribution and intensity levels of P1 and P2 with the pattern of basal plasma proteins collected from the same patient. In gels from P1, 33 spots had E/P (intensity level in eluate per intensity level in plasma) > 2.0 , whereas other 53 spots had E/P < 0.5 . In P2 gels, 32 spots had E/P > 2.0 , whereas 71 spots had E/P < 0.5 .

Concerning MW and pI , P1 proteins with E/P > 2.0 had greater MW as compared to the P1 proteins with E/P < 0.5 (74 ± 11 vs 52 ± 8 kDa; $p < 0.05$), whereas pI values between these two subgroups of P1 were comparable (Figure 3, panels a and b). In contrast, P2 proteins with E/P > 2.0 had significantly less pI values compared to P2 proteins with E/P < 0.5 (4.8 ± 0.09 vs 5.4 ± 0.12 ; $p < 0.01$), whereas MW values between these two subgroups of P2 were comparable (Figure 3, panels a and b). Spearman correlation tests were performed and the results showed that there were significant correlations between MW and E/P values of P1 ($r = 0.2$; $p = 0.01$) and between pI and E/P values of P2 ($r = -0.32$; $p = 0.002$) (Figure 4). These data implicate that Prometh 1 preferably removed high-MW proteins, whereas Prometh 2 preferentially removed acidic proteins.

Spots that reached a relative intensity of 1000 ppm (of the total quantity of all valid spots) or greater were subjected to in-gel tryptic digestion and MS identification. Out of 109 spots excised from P1 gels, 72 were successfully identified providing 18 unique proteins (Table 1), while 113 spots were cut from P2 gels giving 93 positive identifications of 30 unique proteins (Table 2). The identification was verified by comparison of

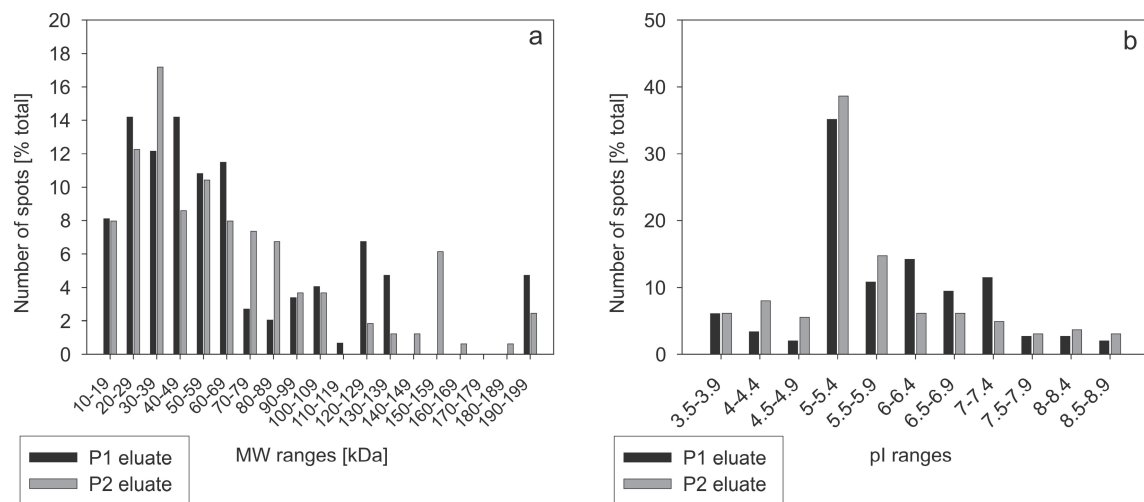


Figure 2. Molecular weight (a) and pI (b) distributions in Prometh 1 eluate (P1) and Prometh 2 eluate (P2). Percentage per category of total spot number is given. MW = molecular weight.

measured and theoretical *pI* and MW, and the confirmed spots are marked with an asterisk in Tables 1 and 2. By comparing the measured and theoretical values, 36 spots identified from P1 and 41 from P2 had difference in *pI* (ΔpI) > 1 or difference in MW (ΔMW) > 10%. These differences were most likely due to fragmentation or multimerization of these identified proteins.

Relative intensities of high-abundance proteins (i.e., transferrin, haptoglobin, alpha-1-antitrypsin, immunoglobulin light and heavy chains) in both eluates were comparable to those in plasma (E/P ratios were in between the range of 0.5–2.0), except for albumin which had a borderline E/P = 0.48 in P1 and E/P = 2.7 in P2. However, a greater degree of differences were detected in several low-abundance proteins, which had average E/P ranging from 0.16 (spot nos. 29, 30 in Figure 5a,d) for fibrinogen gamma to 37.0 (spot nos. 85–88 in Figure 5b,e) in case of transthyretin.

Discussion

There are a limited number of previous proteomic studies analyzing compositions of proteins adsorbed to artificial surface of devices exposed to human plasma. These studies mostly examined the proteins bound to hemodialysers during renal replacement therapy,^{12,13} whereas the analysis of molecules removed in this way during liver support therapy is lacking. To the best of our knowledge, this is the first study analyzing compositions of a large number of proteins eliminated by adsorption inside an extracorporeal liver support system during therapy in a patient with liver failure. For protein elution, we adjusted the algorithm described in a paper published by Ishikawa et al.¹³ As there are two adsorbers with different properties in the Prometheus system, one neutral (Prometh 1) and the other with anion exchanging property (Prometh 2), it seemed relevant to employ two elution solvents. With respect to their characteristics, we eluted P1 with 10% SDS and P2 with 40% acetic acid. The amount of total protein obtained from both adsorbers in our present study was in accordance with the amount of protein loss from this treatment as reported previously.³ Prior to the elution, we carefully washed the plasma remnants out of the cartridges. There were huge differences in the protein concentrations of plasma remnants compared to the eluates (several orders of magnitude) obtained from both cartridges. In addition, there were significant differences in the

proteome profiles and spot intensity levels of the eluate proteins (P1 and P2) compared to those of plasma proteins. Therefore, the data reported in our study were specific for the adsorbed proteins.

The membrane used in the Prometheus system to separate plasma had a sieving coefficient of 0.9 for proteins with MW 40 kDa and of 0.1 for 300-kDa proteins. We could therefore expect to see free filtration of proteins up to the size of albumin, while only a small proportion of plasma fibrinogen and virtually no IgM could be exposed and adsorbed to Prometh 1 and 2.¹⁰ Our proteomic data were consistent with this assumption as we found a majority of proteins had MW below 100 kDa even though some proteins with MW up to 200 kDa were also detectable. For instance, only a few faint protein spots were identified as fibrinogen. Furthermore, we also expected to observe both selective and unselective protein binding during the contact of plasma and adsorbers' surface. To assess this issue, we compared spot intensity distributions between P1 and P2 mutually, and between both eluates and plasma. In this way, we demonstrated substantial differences, which however could be attributed not only to preferential adsorption, but also to diverse elution methods.

We anticipated that selective adsorption should be explained in part by physical properties of the adsorbers and the bound proteins, mainly by their charges (should be dramatic in P2, as Prometh 2 had positively charged sites) and by their molecular sizes (should be obvious in P1, because of the excess of small molecules due to filtration threshold). To evaluate these possibilities, we tested correlations between E/P ratios of intensity levels and *pI*, as well as MW. We confirmed the preferential adsorption of acidic (negatively charged) proteins to the Prometh 2 cartridge. However, it was rather surprising that larger molecules were surplus in P1. This unexpected finding was hard to explain by means of the available data. However, we could speculate that the proposed effect of filter cutoff was not dramatic as gradient gels allowed separation of molecules up to 200 kDa (still had a sieving coefficient of 0.2). At the same time, neutral resin contained in Prometh 1 adsorber probably had an affinity for hydrophobic proteins, which generally had a limited detectability by 2-DE.

With the use of MS analysis, we were able to identify in eluates several high- and low-abundance plasma proteins. All

Table 1. Proteins Identified in Prometh 1 Eluate (P1)^a

spot no.	protein name	Swiss-Prot entry	PMF score/ sequence coverage	MS/MS peptide no./ total ion score	E/P
1*	Alpha-1-antitrypsin	P01009	182/44%	NA	2.12
2*	Alpha-1-antitrypsin	P01009	179/42%	10/745	1.66
3*	Alpha-1-antitrypsin	P01009	128/25%	11/992	1.68
4*	Alpha-1-antitrypsin	P01009	128/25%	10/700	1.84
5*	Alpha-1-antitrypsin	P01009	112/34%	7/543	1.45
6*	Alpha-1-antitrypsin	P01009	242/58%	11/1178	1.67
7*	Alpha-1-antitrypsin	P01009	105/26%	8/669	1.20
8*	Alpha-1-antitrypsin	P01009	136/36%	11/618	1.34
9	Alpha-1-antitrypsin	P01009	NA	1/37	0.66
10*	AMBP protein	P02760	NA	2/39	0.92
11*	AMBP protein	P02760	NA	2/46	0.97
12*	Apolipoprotein A-IV	P06727	NA	3/44	1.17
13*	Apolipoprotein E	P02649	65/35%	7/130	1.92
14*	Ceruloplasmin	P00450	NA	4/61	0.82
15*	Complement C3 beta chain	P01024	65/19%	4/50	0.44
16*	Complement C3 beta chain	P01024	82/18%	5/141	1.10
17*	Complement C3 beta chain	P02768	NA	4/128	0.82
18	Complement factor B	P00751	NA	2/37	0.98
19	Complement factor B	P00751	NA	3/112	1.51
20*	Haptoglobin	P00738	NA	3/62	0.21
21*	Haptoglobin	P00738	NA	5/195	0.79
22*	Haptoglobin	P00738	61/16%	4/222	0.63
23*	Haptoglobin	P00738	NA	3/53	1.34
24	Ig kappa chain C region	P01834	NA	2/165	3.12
25	Ig kappa chain C region	P01834	NA	3/95	1.63
	Ig lambda chain C regions	P01842	NA	2/45	
26	Ig kappa chain C region	P01834	NA	3/235	0.32
	Ig lambda chain C regions	P01842	NA	2/145	
27	Ig kappa chain C region	P01834	NA	2/66	1.32
28	Ig kappa chain C region	P01834	57/48%	3/256	4.07
29	Ig kappa chain C region	P01834	NA	3/131	3.51
30	Ig kappa chain C region	P01834	NA	3/86	1.57
	Ig lambda chain C regions	P01842	NA	2/48	
31	Ig kappa chain C region	P01834	NA	3/93	0.20
32	Ig kappa chain C region	P01834	NA	3/112	2.33
33	Ig lambda chain C regions	P01842	NA	3/110	0.36
34*	Interalpha-trypsin inhibitor heavy chain H4	Q14624	108/19%	6/121	0.46
35*	Interalpha-trypsin inhibitor heavy chain H4	Q14624	NA	1/49	0.84
36*	Pigment epithelium-derived factor	P36955	NA	3/170	2.22
37*	Plasma retinol-binding protein	P02753	NA	5/219	0.82
38*	Plasma retinol-binding protein	P02753	NA	3/108	0.55
39*	Plasma retinol-binding protein	P02753	NA	2/55	6.50
40*	Serotransferrin	P02787	125/24%	11/395	0.34
41*	Serotransferrin	P02787	167/25%	11/546	1.14
42*	Serotransferrin	P02787	186/27%	12/442	0.71
43*	Serotransferrin	P02787	93/14%	8/455	2.07
44*	Serotransferrin	P02787	138/26%	8/456	0.25
45*	Serum albumin	P02768	116/44%	5/132	0.48
46	Serum albumin	P02768	118/30%	7/156	0.54
47	Serum albumin	P02768	NA	4/123	2.19
48	Serum albumin	P02768	81/18%	8/382	0.61
49	Serum albumin	P02768	105/26%	4/94	0.82
50	Serum albumin	P02768	NA	4/68	1.07
51	Serum albumin	P02768	92/18%	NA	0.65
52	Serum albumin	P02768	61/11%	3/140	1.19
53	Serum albumin	P02768	76/19%	5/205	4.77
54	Serum albumin	P02768	NA	3/117	1.84
55	Serum albumin	P02768	NA	4/125	2.07
56	Serum albumin	P02768	69/13%	4/169	2.18
57	Serum albumin	P02768	NA	7/141	0.95
58	Serum albumin	P02768	NA	7/215	0.88
59	Serum albumin	P02768	NA	3/137	1.36
60	Serum albumin	P02768	NA	6/180	0.87
61	Serum albumin	P02768	75/20%	6/139	0.57
62	Serum albumin	P02768	70/20%	4/85	0.87
63	Serum albumin	P02768	NA	3/62	1.95
64	Serum albumin	P02768	162/44%	6/136	2.49
65	Serum albumin	P02768	155/46%	NA	2.80
66	Serum albumin	P02768	149/49%	5/112	5.93
	Ig gamma-1 chain C region	P01857	NA	1/28	
67	Serum albumin	P02768	NA	5/128	5.61
	Ig gamma-1 chain C region	P01857	NA	2/82	
68	Serum albumin	P02768	159/44%	5/168	21.43
	Ig gamma-1 chain C region	P01857	NA	3/207	
69*	Vitamin D-binding protein	P02774	70/34%	5/288	1.13
70*	Vitamin D-binding protein	P02774	69/39%	5/271	1.57
71*	Zinc-alpha-2-glycoprotein	P25311	93/46%	3/69	3.71
72*	Zinc-alpha-2-glycoprotein	P25311	100/36%	3/101	1.45

^a PMF, peptide mass fingerprinting; MS/MS, tandem mass spectrometry; NA, not applicable (identification by MS or MS/MS was not done or was unsuccessful); E/P, eluate-to-plasma ratio of relative spot intensity. (*) Spots whose measured MW and pI were in agreement with their theoretical values.

Table 2. Proteins Identified in Prometh 2 Eluate (P2)^a

spot no.	protein name	Swiss-Prot entry	PMF score/ sequence coverage	MS/MS peptide no./ total ion score	E/P
1*	Alpha-1-antitrypsin	P01009	193/50%	10/641	1.53
2*	Alpha-1-antitrypsin	P01009	260/61%	12/1099	1.24
3*	Alpha-1-antitrypsin	P01009	239/59%	11/1074	1.33
4*	Alpha-1-antitrypsin	P01009	266/59%	12/1097	0.98
5*	Alpha-1-antitrypsin	P01009	200/55%	10/773	1.20
6*	Ceruloplasmin	P00450	114/16%	14/585	1.03
7*	Ceruloplasmin	P00450	96/19%	12/231	0.55
8	Ceruloplasmin	P00450	156/31%	8/112	1.57
9*	Clusterin	P10909	NA	3/66	2.72
10*	Clusterin	P10909	NA	2/64	2.93
11*	Complement C3	P01024	94/16%	10/143	3.47
12*	Complement C4-A (alpha chain)	P0C0L4	NA	10/497	2.07
13*	Complement C4-A (alpha chain)	P0C0L4	62/9%	12/588	1.52
14*	Complement C4-A (alpha chain)	P0C0L4	66/6%	6/219	2.43
15*	Complement C4-A (alpha chain)	P0C0L4	66/8%	9/240	1.90
16*	Complement C4-A (alpha chain)	P0C0L4	79/13%	13/525	3.21
17*	Complement C4-A (alpha chain)	P0C0L4	69/11%	10/526	1.39
18*	Complement C4-A (gamma chain)	P0C0L4	NA	4/116	3.06
19*	Complement C4-A (gamma chain)	P0C0L4	NA	5/102	6.19
20*	Complement C4-A (gamma chain)	P0C0L4	NA	7/187	8.23
21*	Complement C4-A (gamma chain)	P0C0L4	NA	9/275	2.88
22	Complement C4-A	P0C0L4	122/15%	12/364	1.28
23	Complement C4-A	P0C0L5	NA	9/180	0.33
24*	Complement factor B	P0C0L5	NA	1/45	0.34
25	Complement factor B	P00751	NA	4/118	3.42
26	Complement factor B	P00751	NA	3/80	1.43
27*	Fibrinogen beta chain	P02675	NA	3/81	0.36
28*	Fibrinogen beta chain	P02675	NA	2/60	0.39
29*	Fibrinogen gamma chain	P02679	94/47%	3/37	0.16
30*	Fibrinogen gamma chain	P02679	104/49%	7/145	0.20
31*	Haptoglobin	P00738	NA	7/70	0.63
32*	Haptoglobin	P00738	56/29%	9/166	1.10
33*	Haptoglobin	P00738	NA	2/43	0.63
34*	Haptoglobin	P00738	NA	2/41	0.52
35*	Hyaluronan-binding protein 2	Q14520	NA	8/460	13.7
36	Ig alpha-1 chain C region	P01876	83/32%	9/548	0.35
37	Ig gamma-1 chain C region	P01857	NA	4/325	0.37
	Ig gamma-2 chain C region	P01859	NA	3/89	
38	Ig gamma-1 chain C region	P01857	NA	5/384	0.51
	Ig gamma-2 chain C region	P01859	NA	5/143	
39	Ig gamma-1 chain C region	P01857	NA	5/364	0.78
	Ig gamma-2 chain C region	P01859	NA	4/81	
40	Ig gamma-1 chain C region	P01857	104/54%	7/498	0.84
	Ig gamma-2 chain C region	P01859	NA	4/100	
41	Ig gamma-1 chain C region	P01857	84/42%	8/513	1.36
	Ig gamma-2 chain C region	P01859	NA	5/173	
42	Ig kappa chain C region	P01834	NA	3/175	1.26
43	Ig kappa chain C region	P01834	NA	3/172	0.81
44	Ig kappa chain C region	P01834	NA	3/162	1.20
45	Ig kappa chain C region	P01834	NA	3/246	2.43
46	Ig kappa chain C region	P01834	NA	3/305	1.24
47	Ig kappa chain C region	P01834	NA	3/231	5.48
48	Ig kappa chain C region	P01834	66/88%	3/277	4.45
49	Ig lambda chain C regions	P01842	NA	1/32	1.97
50	Ig lambda chain C regions	P01842	NA	3/68	0.72
51	Ig lambda chain C regions	P01842	NA	3/178	1.16
52	Ig lambda chain C regions	P01842	NA	3/227	0.45
53*	Plasma retinol-binding protein	P02753	62/37%	7/96	10.57
54*	Plasma retinol-binding protein	P02753	NA	5/63	4.70
55*	Plasma retinol-binding protein	P02753	57/48%	6/370	7.78
56*	Prothrombin	P00734	217/47%	14/630	22.9
57*	Serotransferrin	P02787	73/12%	6/242	1.80
58*	Serotransferrin	P02787	251/42%	15/620	1.74
59*	Serotransferrin	P02787	210/43	13/508	1.62
60*	Serotransferrin	P02787	218/37%	14/641	1.41
61*	Serotransferrin	P02787	180/33%	14/798	1.28
62*	Serotransferrin	P02787	201/46%	15/856	2.25
63*	Serotransferrin	P02787	113/28%	12/359	1.95
64*	Serum albumin	P02768	169/48%	12/710	2.74
65	Serum albumin	P02768	NA	1/33	3.27
66	Serum albumin	P02768	NA	5/95	1.24
67	Serum albumin	P02768	292/57%	15/679	436.97
68	Serum albumin	P02768	56/28%	5/287	0.90
69	Serum albumin	P02768	149/39%	13/792	5.78
70	Serum albumin	P02768	76/17%	8/169	1.09
71	Serum albumin	P02768	94/31%	13/521	1.35
72	Serum albumin	P02768	124/36%	14/651	1.70
73	Serum albumin	P02768	212/49%	14/853	10.07
74	Serum albumin	P02768	178/43	10/182	10.86
75	Serum albumin	P02768	234/55	14/404	9.61
76	Serum albumin	P02768	173/42	8/49	9.50

Table 2. Continued

spot no.	protein name	Swiss-Prot entry	PMF score/ sequence coverage	MS/MS peptide no./ total ion score	E/P
77	Serum albumin	P02768	80/17	8/191	14.75
78	Serum albumin	P02768	NA	8/196	1.01
79	Serum albumin	P02768	NA	11/433	1.58
80	Serum albumin	P02768	NA	11/533	1.78
81	Serum albumin	P02768	NA	11/638	1.99
82	Serum albumin	P02768	NA	4/65	0.87
83	Serum albumin	P02768	NA	4/70	1.40
84	Serum albumin	P02768	NA	2/74	0.77
85*	Transthyretin	P02766n	68/50%	6/229	73.24
86*	Transthyretin	P02766	120/69%	8/538	33.39
87*	Transthyretin	P02766	110/54%	8/440	198.35
88*	Transthyretin	P02766	134/73%	9/821	13.65
89*	Trypsin-2	P07478	NA	5/258	28.68
90*	Vitamin D-binding protein	P02774	57/30%	6/192	1.69
91*	Vitamin D-binding protein	P02774	65/31%	9/480	2.20
92*	Vitronectin	P04004	NA	4/277	3.48
93*	Zinc-alpha-2-glycoprotein	P25311	86/43%	NA	0.41

^a PMF, peptide mass fingerprinting; MS/MS, tandem mass spectrometry; NA, not applicable (identification by MS or MS/MS was not done or was unsuccessful); E/P, eluate-to-plasma ratio of relative spot intensity. (*) Spots whose measured MW and pI were in agreement with their theoretical values.

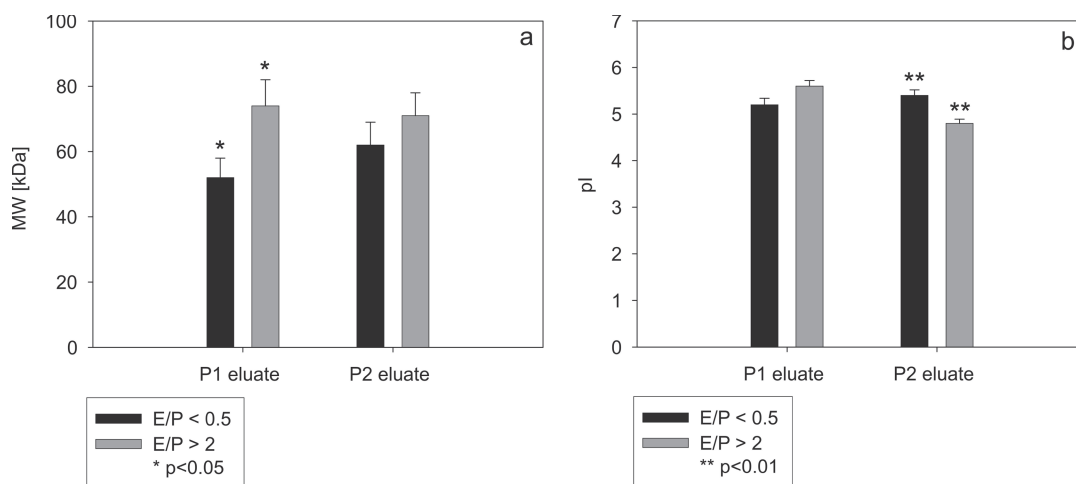


Figure 3. Molecular weight and pI differences between spots with eluate-to-plasma ratio greater than 2 and lower than 0.5. Data are given as means and standard errors, separately for Prometh 1 eluate (P1) and Prometh 2 eluate (P2). Statistical significance tested with rank sum test. MW = molecular weight, E/P = eluate-to-plasma ratio of spot intensity.

the identified proteins have been previously detected in human plasma and some of them have been also reported to bind to artificial materials in previously published articles (e.g., apolipoprotein A-IV and transthyretin in a study by Bonomini et al.;¹² complement C4, immunoglobulin light and heavy chains, and vitamin D-binding protein in a study by Kim, et al.;¹⁴ and albumin, transferrin, and alpha-1-antitrypsin in both of these two studies^{12,14}).

Positively identified proteins were then matched to corresponding spots found in gels derived from plasma samples to assess if there was any selectivity in adsorption of individual proteins. Taking into account that 2-DE allows only estimation of protein quantities and considering that reduced E/P ratio might be due to imperfect elution of some proteins, it could be delusive to draw a conclusion about adsorption profile of proteins with mild enhancement or even gross decrement of spot intensity. Very low eluate quantity of fibrinogen is almost certainly due to its large molecule, which should be hardly filtered from blood (sieving coefficient less than 0.1) and therefore did not get into contact with adsorbers. On the other hand, P2 eluate enrichment with albumin (bearing negative charge) is in accordance with anion-exchanging properties of Prometh 2 adsorber and the drop of serum albumin reported by Evenepoel et al.³

In case of proteins with substantially high E/P ratios, an assumption of preferential adsorption is probably well-justified. The highest clearance was demonstrated in transthyretin (synonym prealbumin) (spot nos. 85–88 in Figure 5b,e; average E/P = 37, MW 16 kDa, pI 5.5), which is a tetrameric protein synthesized in liver and involved in transporting thyroid hormones. It is known to form complexes with retinol-binding protein whose E/P ratio was elevated as well (spot nos. 53–55, Figure 5b,e; average E/P = 8.7, MW 23 kDa, pI 5.8). Other proteins with strikingly high E/P ratios included anionic trypsin (spot no. 89, Figure 5b,e; E/P = 29, MW 26 kDa, pI 4.8), prothrombin (spot no. 56, Figure 5a,d; E/P = 23, MW 70 kDa, pI 5.6), and hyaluronan-binding protein 2 (HABP) light chain (spot no. 35, Figure 5c,f; E/P = 13, MW 27 kDa, pI 7.7). These three proteins belong to serine endopeptidase family (Peptidase S1), suggesting a possible affinity of P2 adsorber for this group of enzymes.

Since this is a single-patient study, it would be misleading to draw conclusions about clinical impact (beneficial or detrimental) of any specific protein's removal. Nevertheless, in several proteins, we can speculate about potential consequences of their elimination. Transthyretin serves as a reliable nutrition marker (both for protein and energy metabolism), and its level decreases during inflammation and liver dysfunction.¹⁵

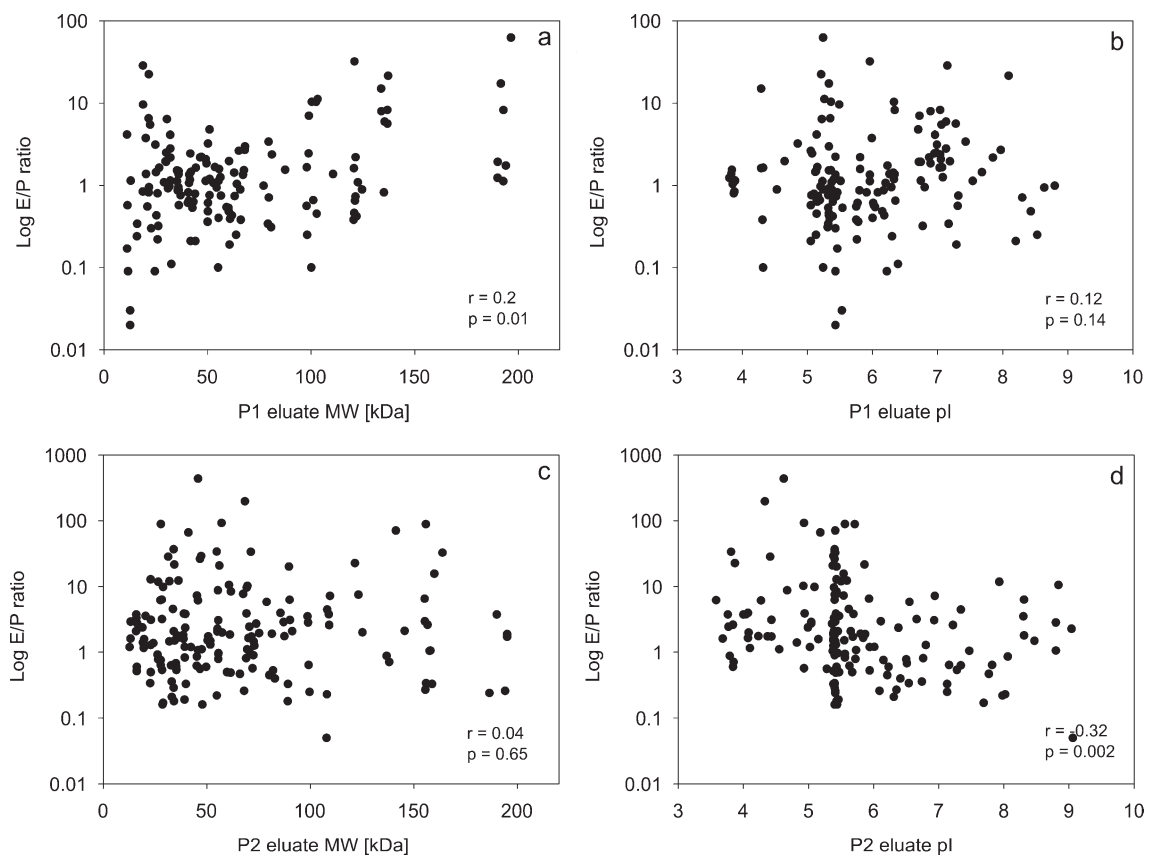


Figure 4. Scatter plot graphs of eluate-to-plasma ratio in relation to molecular weight (a and c) and pI (b and d) in Prometh 1 eluate (P1) (a and b) and Prometh 2 eluate (P2) (c and d). Correlation coefficients (r) were determined with Spearman rank order correlation (p = level of statistical significance). Logarithmic scale was used on Y-axis. E/P = eluate-to-plasma ratio of spot intensity, MW = molecular weight.

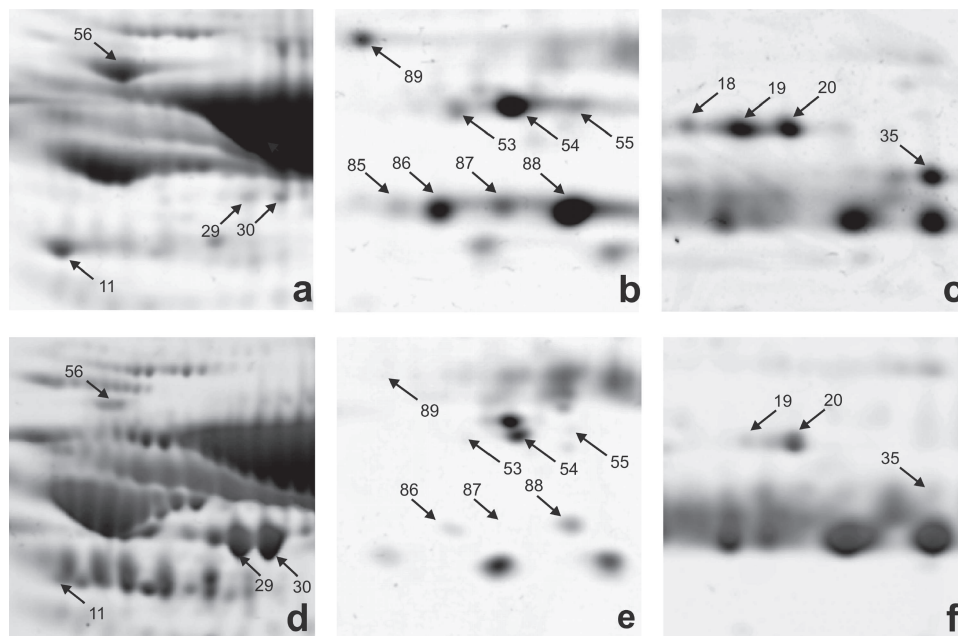


Figure 5. Illustration of marked differences in E/P relative quantities in low-abundance proteins in Prometh 2 eluate (P2) (a–c) compared to the plasma (d–f). E/P = eluate-to-plasma ratio of spot intensity.

Although its diagnostic value in liver failure is markedly limited, the depletion of prealbumin/retinol-binding protein complex might have clinical implication due to impaired thyroxine and retinol transport. Similarly, prothrombin deprivation may

further aggravate coagulation disorder invariably present in patients with severe liver dysfunction.

Activated (two-chain) form of HABP has been detected in P2 as evidenced by protein's MW and amino acid sequence

covered by MS/MS. HAPB activation has been observed to occur upon liver injury, at least in animal model, thus, leading to cleavage of urokinase type plasminogen activator which in turn activates matrix metalloproteases and triggers extracellular matrix degradation.¹⁶ Therefore, it has been proposed that hepatic injury-specific activation of HAPB may act as an early factor in the cascade responsible for tissue remodeling following liver damage.¹⁶ Besides that, HAPB amino acid sequence is homologous to that of hepatocyte growth factor activator,¹⁷ and HAPB has been reported to exert antiangiogenic effect.¹⁸ Given these circumstances, it is conceivable that selective clearance of HAPB might have direct influence on liver regeneration.

In summary, we identified for the first time a large number of proteins eliminated by adsorption to the Prometheus extracorporeal liver support system. There were also some degrees of selectivity of proteins preferentially bound to two Prometheus adsorption units; Prometh 1 preferentially adsorbed high-MW proteins, whereas Prometh 2 preferentially adsorbed acidic proteins. Some of the proteins found in eluates could imply safety concerns; however, concluding on their clinical relevance is beyond the scope of this study. To address such challenge, a larger clinical trial would be necessary.

Abbreviations: ACN, acetonitrile; ALT, alanine aminotransferase; AST, aspartate aminotransferase; CHAPS, 3-[(3-cholamidopropyl)dimethylammonio]-1-propanesulfonate; CHCA, α -cyano-4-hydroxycinnamic acid; 2-DE, 2-dimensional electrophoresis; DTT, dithiothreitol; E/P, eluate-to-plasma ratio (spot intensity); IAA, iodoacetamide; IEF, isoelectric focusing; IPG, immobilized pH gradient; IL, interleukin; MALDI, matrix-assisted laser desorption/ionization; MW, molecular weight; MS, mass spectrometry; MS/MS, tandem mass spectrometry; PBS, phosphate buffered saline; PMF, peptide mass fingerprinting; SDS, sodium dodecyl sulfate; TFA, trifluoroacetic acid; TNF, tumor necrosis factor; TOF, time-of-flight.

Acknowledgment. The study was supported by Research Project No. MSM0021620819 "Replacement of and support to some vital organs" awarded by the Ministry of Education, Youth, and Physical Training of the Czech Republic.

Supporting Information Available: MS/MS spectra of transthyretin, plasma retinol-binding protein, hyaluronan-binding protein, trypsin 2, prothrombin, vitronectin and clusterin detected in eluates plasma 2D-gel scanned image together with spots' MW and pI distributions in plasma Hyaluronan-binding protein 2 light chain sequence coverage by MS/MS. This material is available free of charge via the Internet at <http://pubs.acs.org>.

References

(1) Falkenhagen, D.; Strobl, W.; Vogt, G.; Schrefl, A.; Linsberger, I.; Gerner, F. J.; Schoenhofen, M. Fractionated plasma separation and adsorption system: a novel system for blood purification to remove albumin bound substances. *Artif. Organs* **1999**, *23* (1), 81–6.

(2) Rifai, K.; Ernst, T.; Kretschmer, U.; Bahr, M. J.; Schneider, A.; Hafer, C.; Haller, H.; Manns, M. P.; Fliser, D. Prometheus--a new extracorporeal system for the treatment of liver failure. *J. Hepatol.* **2003**, *39* (6), 984–90.

(3) Evenepoel, P.; Laleman, W.; Wilmer, A.; Claes, K.; Maes, B.; Kuypers, D.; Bammens, B.; Nevens, F.; Vanrenterghem, Y. Detoxifying capacity and kinetics of prometheus--a new extracorporeal system for the treatment of liver failure. *Blood Purif.* **2005**, *23* (5), 349–58.

(4) Evenepoel, P.; Laleman, W.; Wilmer, A.; Claes, K.; Kuypers, D.; Bammens, B.; Nevens, F.; Vanrenterghem, Y. Prometheus versus molecular adsorbents recirculating system: comparison of efficiency in two different liver detoxification devices. *Artif. Organs* **2006**, *30* (4), 276–84.

(5) Rifai, K.; Ernst, T.; Kretschmer, U.; Haller, H.; Manns, M. P.; Fliser, D. Removal selectivity of Prometheus: a new extracorporeal liver support device. *World J. Gastroenterol.* **2006**, *12* (6), 940–4.

(6) Aoi, I. Clinical significance of protein adsorbable membranes--long-term clinical effects and analysis using a proteomic technique. *Nephrol., Dial., Transplant.* **2007**, *22* Suppl 5, v13–9.

(7) De Vriese, A. S.; Vanholder, R. C.; Pascual, M.; Lameire, N. H.; Colardyn, F. A. Can inflammatory cytokines be removed efficiently by continuous renal replacement therapies. *Intensive Care Med.* **1999**, *25* (9), 903–10.

(8) Moachon, N.; Boullange, C.; Fraud, S.; Vial, E.; Thomas, M.; Quash, G. Influence of the charge of low molecular weight proteins on their efficacy of filtration and/or adsorption on dialysis membranes with different intrinsic properties. *Biomaterials* **2002**, *23* (3), 651–8.

(9) Stadlbauer, V.; Krisper, P.; Aigner, R.; Haditsch, B.; Jung, A.; Lackner, C.; Stauber, R. E. Effect of extracorporeal liver support by MARS and Prometheus on serum cytokines in acute-on-chronic liver failure. *Crit. Care* **2006**, *10* (6), R169.

(10) Vienken, J.; Christmann, H. How can liver toxins be removed? Filtration and adsorption with the Prometheus system. *Ther. Apheresis Dial.* **2006**, *10* (2), 125–31.

(11) Perkins, D. N.; Pappin, D. J.; Creasy, D. M.; Cottrell, J. S. Probability-based protein identification by searching sequence databases using mass spectrometry data. *Electrophoresis* **1999**, *20* (18), 3551–67.

(12) Bonomini, M.; Pavone, B.; Sirolli, V.; Del Buono, F.; Di Cesare, M.; Del Boccio, P.; Amoroso, L.; Di Ilio, C.; Sacchetta, P.; Federici, G.; Urbani, A. Proteomics characterization of protein adsorption onto hemodialysis membranes. *J. Proteome Res.* **2006**, *5* (10), 2666–74.

(13) Ishikawa, I.; Chikazawa, Y.; Sato, K.; Nakagawa, M.; Imamura, H.; Hayama, S.; Yamaya, H.; Asaka, M.; Tomosugi, N.; Yokoyama, H.; Matsumoto, K. Proteomic analysis of serum, outflow dialysate and adsorbed protein onto dialysis membranes (polysulfone and pmma) during hemodialysis treatment using SELDI-TOF-MS. *Am. J. Nephrol.* **2006**, *26* (4), 372–80.

(14) Kim, J. K.; Scott, E. A.; Elbert, D. L. Proteomic analysis of protein adsorption: serum amyloid P adsorbs to materials and promotes leukocyte adhesion. *J. Biomed. Mater. Res., Part A* **2005**, *75* (1), 199–209.

(15) Smith, F. R.; Goodman, D. S. The effects of diseases of the liver, thyroid, and kidneys on the transport of vitamin A in human plasma. *J. Clin. Invest.* **1971**, *50* (11), 2426–36.

(16) Choi-Miura, N. H.; Otsuyama, K.; Sano, Y.; Saito, K.; Takahashi, K.; Tomita, M. Hepatic injury-specific conversion of mouse plasma hyaluronan binding protein to the active hetero-dimer form. *Biol. Pharm. Bull.* **2001**, *24* (8), 892–6.

(17) Choi-Miura, N. H. Novel human plasma proteins, IHRP (acute phase protein) and PHBP (serine protease), which bind to glycosaminoglycans. *Curr. Med. Chem. Cardiovasc. Hematol. Agents* **2004**, *2* (3), 239–48.

(18) Jeon, J. W.; Song, H. S.; Moon, E. J.; Park, S. Y.; Son, M. J.; Jung, S. Y.; Kim, J. T.; Nam, D. H.; Choi-Miura, N. H.; Kim, K. W.; Kim, Y. J. Anti-angiogenic action of plasma hyaluronan binding protein in human umbilical vein endothelial cells. *Int. J. Oncol.* **2006**, *29* (1), 209–15.

PR800966W

Specific adsorption of some complement activation proteins to polysulfone dialysis membranes during hemodialysis

Jan Mares¹, Visith Thongboonkerd², Zdenek Tuma³, Jiri Moravec³ and Martin Matejovic¹

¹Department of Internal Medicine I, Charles University Medical School and Teaching Hospital, Plzen, Czech Republic;

²Medical Proteomics Unit, Office for Research, and Development Faculty of Medicine Siriraj Hospital, Mahidol University, Bangkok, Thailand and ³Proteomic Laboratory, Charles University Medical School, Plzen, Czech Republic

Dialyser bioincompatibility is an important factor contributing to complications of hemodialysis with well known systemic consequences. Here we studied the local processes that occur on dialysis membranes by eluting proteins adsorbed to the polysulfone dialyser membranes of 5 patients after 3 consecutive routine maintenance hemodialysis sessions. At the end of each procedure, a plasma sample was also collected. These eluates and their accompanying plasma samples were separated by 2-dimensional gel electrophoresis, and all proteins that were present in all patients were analyzed by tandem mass spectrometry and a ratio of the relative spot intensity of the eluate to plasma ratio was calculated. Out of 153 proteins detected, 84 were found in all patients, 57 of which were successfully identified by mass spectrometry as 38 components of 23 unique proteins. In 10 spots the relative eluate intensity differed significantly from that in the plasma implying preferential adsorption. These proteins included ficolin-2, clusterin, complement C3c fragment and apolipoprotein A1. Our finding of a selective binding of ficolin-2 to polysulfone membranes suggests a possible role of the lectin complement pathway in blood-dialyser interactions.

Kidney International advance online publication, 29 April 2009; doi:10.1038/ki.2009.138

KEYWORDS: biocompatibility; complement; dialyser elution; ficolin; lectin pathway; proteome

Hemodialyser bioincompatibility has long been established as an important factor in various complications accompanying both chronic and acute hemodialysis (HD). Several aspects of biological response triggered by blood exposure to a dialyser, namely coagulation, complement level, and leukocyte activation, were recognized shortly after the introduction of the artificial dialysis membrane into clinical practice.^{1,2} In the past decades, we gathered comprehensive information covering metabolic consequences of these processes; that is, chronic micro-inflammation, enhanced oxidative stress, and pro-coagulant condition.³⁻⁶ Although difficult to link directly with increased mortality, bioincompatibility is held (at least partially) responsible for accelerated atherosclerosis, malnutrition, and thrombotic diathesis found in HD patients.⁷⁻⁹

Although we have ample data regarding systemic effects of the interaction between artificial material surface and blood, its molecular substrates remain obscure. Yet, understanding the mechanisms responsible for foreign pattern recognition and launching a subsequent reaction cascade could help us to develop better-tolerated materials, and to prevent the adverse sequelae. Most studies addressing this issue were accomplished under simplified laboratory conditions (by means of phantoms and pre-fractionated plasma),¹⁰⁻¹⁴ or targeted onto a predefined set of molecules.¹⁵⁻²² However, to investigate the subject in its full complexity and in an unbiased manner, the elution of dialysers used in regular HD and in the proteomic approach is crucial.

Therefore, the aim of our study was to verify the elution algorithm eligible for proteomic analysis, to landmark the eluate proteome, and to qualify the potential molecules involved in the blood-dialyser interaction. To the best of our knowledge, this is the first trial studying with proteomic method the full spectrum of proteins adsorbed by a hemodialyser in a clinical setting.

RESULTS

The protein concentrations of both eluate (acetic acid) (449 (98.9, 2487.3) mg/l) and washout (ethylenediaminetetraacetic acid in phosphate buffered saline, PBS/EDTA) (260.3 (156, 779.4) mg/l) were significantly higher ($P < 0.001$) than

Correspondence: Jan Mares, Department of Internal Medicine I, Charles University Teaching Hospital, Alej Svobody 80, 30460 Plzen, Czech Republic. E-mail: mares@fnplzen.cz

Received 16 December 2008; revised 11 February 2009; accepted 18 March 2009

in the final 10-ml flush (Plasmalyte) (24.4 (19.2, 27.6) mg/l). The difference in protein concentrations between eluate and washout was not statistically significant ($P=0.17$). Although the variation in protein content was relatively low in the flush (coefficient of variation, $CV=22\%$), it was considerably higher in the washout ($CV=152\%$) and in the eluate ($CV=154\%$). Nevertheless, protein concentrations were closely correlated in the latter two samples ($r=0.82$, $P<0.001$).

In total, 45 gels derived from 15 dialyser eluates and the corresponding plasma samples were analyzed. A representative two-dimensional (2D) gel-scanned image is shown in Figure 1 to demonstrate the typical eluate proteome map. There were 153 spots detected in at least one eluate sample, 84 of them were found in all 5 patients, and 44 were present in all procedures. Protein spots were distributed along the molecular weight (MW) range of 15–175 kDa and pI range of 3.4–8.9. However, 95% of the overall protein spot intensity was localized inside the interval of MW of 18–85 kDa and pI of 3.4–7.7. Besides that, samples of the PBS/EDTA washout from three dialysers were used to prepare another nine gels

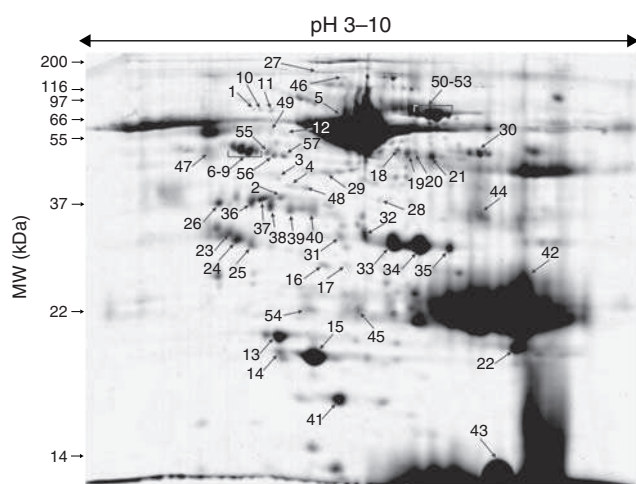


Figure 1 | Representative two-dimensional gel image of dialyser eluate. Spots labeled with numbers were successfully identified by tandem mass spectrometry analyses (see Table 1). MW, molecular weight.

and compared with corresponding plasma and eluate spot patterns. As all the spots detected in the washout were present in the acetic eluate as well, and the quantitative analysis of relative spot intensities did not show any significant differences between the washout and plasma, only acetic eluates were submitted for further analysis.

Spot distribution is shown in Figure 2. Spots detected in all patients ($n=84$) were excised from gels; 57 spots (those labeled with numbers in Figure 1) were successfully identified by mass spectrometry (MS) and tandem mass spectrometry (MS/MS) analyses as 38 components of 23 unique proteins (Table 1). Some of the identified spots contained multiple isoforms of one protein (most likely because of post-translational modifications), for example, ficolin-2 (spots no. 31–35) or clusterin (spots no. 23–25). The protein identifications were further verified by the comparison of measured pI and MW (estimated by the coordinates of the spots in gel) with their theoretical values (as predicted by the protein database). Confirmed identifications are marked with an asterisk in Table 1. Discrepant MWs were common particularly in albumin (spots no. 28, 29, 38–40) and in hemoglobin (spots no. 30, 42, 44) co-migrated with another protein.

In several protein spots (that is, complement C3, mannose-binding lectin-associated serine proteases (MASP) 1 and 2), the measured MWs were lower than the theoretical ones. This difference could be explained by the enzymatic cleavage of their inactive forms. Figure 3 illustrates peptide fragments and amino acid sequences of these proteins established with MS and MS/MS analyses, and indicates the presence of proteolytic cleavage products rather than full-length or native forms. Moreover, MW and pI measured in 2D gels corresponded better with the theoretical values of their respective fragments: C3 complement (spot no. 26; measured MW: 37 kDa, pI: 4.8) vs C3c α -chain fragment 2 (theoretical MW: 39.5 kDa, pI: 4.8); MASP-1 (spot no. 47; measured MW: 44 kDa, pI: 4.0) vs MASP-1 heavy chain (theoretical MW: 49 kDa, pI: 4.9); and MASP-2 (spot no. 48; measured MW: 39 kDa, pI: 5.5) vs MASP-2A (theoretical MW: 47.7 kDa, pI: 5.4).

The variability of eluate intensities of the corresponding spots among patients (CV inter-individual) ranged from 6 to

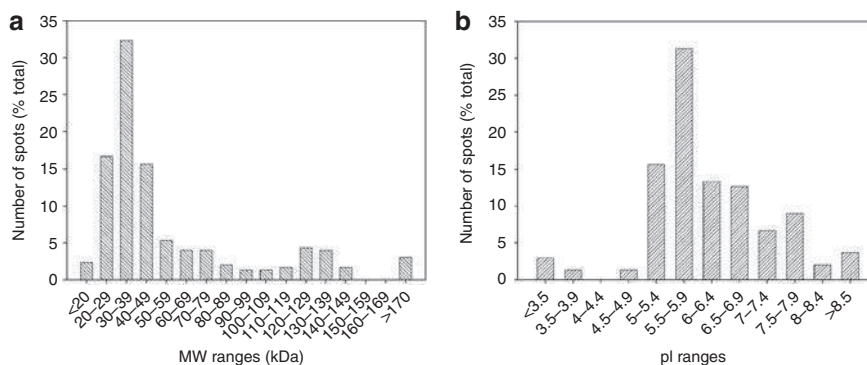


Figure 2 | Basic characteristics of proteins detected in dialyser eluate. (a) Molecular weight (MW) and (b) pI distributions of proteins in dialyser eluate. Percentage per category of total spot number is given.

Table 1 | Proteins identified in eluates from dialysers used in clinical hemodialysis

Spot no.	Protein name	Swissprot entry	PMF score/sequence coverage	MSMS peptide no./total ion score	CV inter-individual (%)	E/P ratio
1	78 kDa glucose-regulated protein ^a	P11021	107/29%	4/110	36	0.65
2	Actin, α -cardiac muscle 1 ^a	P68032	60/25%	NA	81	1.74
	Actin, cytoplasmic 1 ^a	P60709	174/51%	9/723		
3	Actin, cytoplasmic 1 ^a	P60709	64/45%	4/203	53	NM
4	Actin, cytoplasmic 1 ^a	P60709	NA	1/56	26	1.19
5	Albumin ^a	P02768	260/69%	10/833	6	0.83
6	α -1-Antitrypsin ^a	P01009	162/52%	4/413	13	0.93
7	α -1-Antitrypsin ^a	P01009	194/54%	6/542		
8	α -1-Antitrypsin ^a	P01009	226/52%	6/425		
9	α -1-Antitrypsin ^a	P01009	140/43%	4/238		
10	α -1B-glycoprotein	P04217	113/33%	5/273	25	0.82
11	α -1B-glycoprotein	P04217	180/41%	8/261	17	0.92
12	Antithrombin-III	P01008	NA	1/52	25	NM
13	Apolipoprotein A-I ^a	P02647	77/22%	6/234	45	0.73
14	Apolipoprotein A-I ^a	P02647	121/50%	5/327	18	2.06 [#]
15	Apolipoprotein A-I ^a	P02647	NA	1/37	38	29.89 [#]
	Peroxiredoxin-2 ^a	P32119	132/41%	7/426		
16	Apolipoprotein E ^a	P02649	240/71%	9/962	176	11.44
17	Apolipoprotein E ^a	P02649	113/41%	5/133		
18	β -2-Glycoprotein 1	P02749	95/48%	5/292	66	0.70
	Ig α -1 chain C	P01876	NA	4/72		
19	β -2-Glycoprotein 1	P02749	83/47%	6/401	52	0.27 [#]
	Ig α -2 chain C	P01877	NA	4/221		
20	β -2-Glycoprotein 1	P02749	59/20%	3/132	22	0.24 [#]
	Ig α -2 chain C	P01877	NA	1/31		
21	β -2-Glycoprotein 1	P02749	NA	1/44	49	0.52
22	Carbonic anhydrase 1 ^a	P00915	NA	4/279	69	NM
	Flavin reductase	P30043	NA	1/48		
23	Clusterin ^a	P10909	71/34%	2/112	90	9.08 [#]
24	Clusterin ^a	P10909	NA	3/61		
25	Clusterin ^a	P10909	NA	1/76		
	Apolipoprotein E ^a	P02649	132/29%	6/135		
26	Complement C3	P01024	66/13%	8/452	55	3.20 [#]
27	Complement factor H ^a	P08603	103/18%	6/394	79	NM
28	Complement factor H-related protein 1	Q03591	NA	2/109	152	NM
	Albumin	P02768	95/25%	5/186		
29	Fibrinogen γ -chain ^a	P02679	94/47%	3/37	88	0.52
	Albumin	P02768	118/22	2/84		
30	Fibrinogen β -chain ^a	P02675	NA	3/81	31	0.275
	Hemoglobin subunit- α	P69905	NA	2/152		
	Hemoglobin subunit- β	P06727	NA	4/181		
31	Ficolin-2 ^a	Q15485	NA	2/49	60	26.12 ^{##}
32	Ficolin-2 ^a	Q15485	132/52%	6/554		
33	Ficolin-2 ^a	Q15485	93/44%	7/470		
34	Ficolin-2 ^a	Q15485	119/44%	NA		
35	Ficolin-2 ^a	Q15485	85/28%	5/419		
36	Haptoglobin	P00738	91/28	6/353	29	0.88
	Apolipoprotein A-IV ^a	P06727	45/17%	NA		
37	Haptoglobin ^a	P00738	NA	1/31	14	0.94
	Apolipoprotein A-IV ^a	P06727	206/44%	8/441		
38	Haptoglobin ^a	P00738	88/17%	3/112	41	1.41
	Albumin	P02768	159/34%	6/336		
39	Haptoglobin ^a	P00738	NA	4/217	41	1.37
	Albumin	P02768	177/41%	7/451		
40	Haptoglobin ^a	P00738	NA	5/60	46	0.91
	Albumin	P02768	122/37%	5/261		
41	Haptoglobin	P00738	NA	4/224	57	1.82
42	Hemoglobin subunit- α	P69905	59/58%	5/382	32	4.82 [#]
	Hemoglobin subunit- β	P06727	101/78%	2/82		
	Ig κ -chain C	P01834	NA	4/407		
43	Hemoglobin subunit- α ^a	P69905	NA	2/152	39	39.22 [#]
	Hemoglobin subunit- β ^a	P06727	NA	4/181		
44	Ig γ -1-chain C	P01857	74/41%	2/86	72	6.04
	Ig γ -2-chain C	P01859	89/34%	4/130		

Table 1 continues on following page

Table 1 | Continued

Spot no.	Protein name	Swissprot entry	PMF score/sequence coverage	MSMS peptide no./total ion score	CV inter-individual (%)	E/P ratio
	Hemoglobin subunit- α	P69905	NA	2/152		
	Hemoglobin subunit- β	P06727	NA	4/181		
	Complement factor H-related protein 1 ^a	Q03591	91/31%	5/300		
45	Ig κ -chain C region	P01834	56/75%	3/269	21	0.44 [#]
	Ig λ -chain C regions	P01842	NA	1/100		
46	Lysozyme C	P61626	NA	1/47	116	NM
	Proline-rich protein 4	Q16378	NA	1/30		
47	Mannan-binding lectin serine protease 1	P48740	81/21%	6/374	77	NM
48	Mannan-binding lectin serine protease 2	O00187	NA	2/70	17	NM
49	Plastin-2 ^a	P13796	70/27%	3/245	29	0.75
50	Serotransferrin ^a	P02787	NA	2/62	19	1.04
51	Serotransferrin ^a	P02787	65/13%	2/92		
52	Serotransferrin ^a	P02787	82/20%	NA		
53	Serotransferrin ^a	P02787	170/27%	8/561		
54	Serum amyloid P ^a	P02743	60/24%	4/134	19	1.10
55	Vimentin ^a	P08670	289/65%	10/726	16	1.04
56	Vitamin D-binding protein ^a	P02774	NA	4/339	28	1.13
	Vimentin ^a	P08670	193/46%	6/271		
57	Vitamin D-binding protein ^a	P02774	105/31%	8/536	91	1.46

CV, coefficient of variance; E/P, eluate-to-plasma ratio of relative spot intensities; MSMS, tandem mass spectrometry; MW, molecular weight; NA, not applicable (identification by mass spectrometry (MS) or tandem mass spectrometry (MS/MS) was not done or was unsuccessful); NM, not matched (eluate spot could not be matched with plasma unambiguously); PMF, peptide mass fingerprinting.

Mean E/P ratios (from five patients, three hemodialysis procedures each) are given for all proteins matched to plasma. Relative protein spot intensities were compared in eluates and plasma ([#] $P < 0.01$, ^{**} $P < 0.001$).

For proteins represented by multiple spots, cumulative intensities of all spots were used to calculate CV and E/P. Therefore, only one value is given for each variable covering all spots containing a specific protein.

^aSpots which measured MW and pl were in agreement with their theoretical values.

176% (Table 1), whereas the method variability (mean CV inter-gel) reached 27%. A comparative analysis of the eluate proteome to matched plasma profile of the respective patients revealed significant differences (with >two-fold changes in the eluate-to-plasma (E/P) ratio, $P < 0.01$) in levels of 10 proteins (Table 1). Relative intensities of high-abundant plasma proteins (albumin, transferrin, haptoglobin, α -1-antitrypsin) in eluates were similar to plasma (E/P = 0.5–2) (Table 1). Only fibrinogen β - and γ -chains were depleted in eluates (spot no. 30, E/P = 0.28 and spot no. 29, E/P = 0.52, respectively), whereas immunoglobulin light chains seemed enriched (spot no. 42, E/P = 4.8) (Table 1). Nevertheless, the latter spot was co-migrated with hemoglobin α - and β -chains, and the spot intensity varied profoundly among samples. In several low-abundant plasma proteins, pronounced differences in eluate and plasma intensities were detected ranging from E/P = 3.2 ($P = 0.007$) for complement C3 (spot no. 26; Figure 4) to E/P = 26.1 ($P < 0.001$) in the case of ficolin-2 (spots no. 31–35 cumulative intensity; Figure 4). Figure 5 shows quantitative data of plasma proteins, the levels of which were significantly higher in eluates than those in the plasma. Naturally, several intracellular proteins, for example, hemoglobin (spot no. 43) or peroxiredoxin (spot no. 15), reached an even higher E/P ratio (39 and 29, respectively), or were not matched to plasma at all (spot no. 22; carbonic anhydrase, flavin reductase). Therefore, hemoglobin was considered the major contaminant released from erythrocytes entrapped within the dialysers. To avoid an error in the assessment of

eluate protein quantities (and consequently E/P ratios), spots containing hemoglobin were excluded from the integrated spot density while calculating relative intensities.

DISCUSSION

Proteins adsorbed to the polysulfone dialysis membrane during clinical HD were investigated using proteomic tools in five patients treated with chronic HD. A stepwise elution of the dialysers was performed following routine procedures, thrice in each patient. Proteins thus obtained were separated by electrophoresis on two-dimensional polyacrylamide gels (2-DE), and their relative intensities were measured. The results were then compared with the corresponding plasma protein patterns. Prominent spots were excised and identified by MS.

To minimize the contamination of desorbed proteins, we adopted a sequential elution algorithm. As soon as the patient was disconnected, the dialyser was flushed with saline to remove the residual plasma and cells. Protein concentration in the final 10 ml of this flush was negligible (compared with plasma) and similar in all patients, suggesting simple kinetics of plasma washout. In the next step, we applied EDTA solution, which had been shown earlier to detach adhering leukocytes more effectively than PBS alone.²³ Finally, elution with acetic acid was performed, because it had been used successfully to solubilize adsorbed proteins while preserving them for proteomic analysis.²⁴ Protein denaturation and solubilization, necessary for 2D electrophoresis, can

a	1	11	21	31	41	51	
1	MGPTSGPSSL	LLLLTHLPLA	LGSPMYSIIT	PNILRLESEE	TMVLEAHDQA	GDVPVTVTVH	60
61	DFPGKLVLS	SEKTVLTPAT	NHMGVTFIT	PANREFKSEK	GRNKFVTVQA	TFGTQVVEKV	120
121	VLVLSQSGYL	FIQTDKTIYT	PGSTVLYRIF	TVNHKLLPVG	RTVMVNIENP	EGIPVKQDSL	180
181	SSQNQLGVLP	LSWDIPELVN	MGQWKIRAYY	ENSPQQVFST	EFEVKKEYVLP	SFEVIVEPTE	240
241	KFYIYNEKG	LEVITITAREL	YGKKEVGTA	VIFGIQDGEQ	RISLPESLKR	IPIEDGSGEV	300
301	VLSRKVLLDG	VQNPRAEDEL	GKSLYVSATV	ILHSGSDMVQ	AERSGPIVTV	SPYQIHFTKT	360
361	PKYFKPGMPF	DLMVFTNPD	GSPAYRVPVA	VQGEDTVQSL	TQGDGVAKLS	INTHPSQKPL	420
421	SITVRTKQKE	LSEAEQATRT	MQALPYSTVG	NSNNYLHLSV	LRTELRPGET	LNVNFLLRMD	480
481	RAHEAKIRYY	TYLIMNKGR	LKAGRQVREP	GQDLVVLPLS	ITDFIPISEF	LVAYYTLGA	540
541	SGQREVVADS	VWVDVKDSCV	GSLVVKSGQS	EDRQFPVPGQ	MTLKEIGDHG	ARVVLVAVDK	600
601	GVFVLNKNK	LTQSKIWDVV	EKADIGCTPG	SGKDYAGVFS	DAGLFTFTSS	QQQTAQRAEL	660
661	QCQPAPARR	RSVQLTEKRM	DKVGKYPKEL	RKCCEDGMRE	NPMRFSCQRR	TRFISLGEAC	720
721	KKVFLDCCN	ITELRRQHAR	ASHLGLARSN	LDEDIIAEEN	IVSRSEFPES	WLVNVEDLKE	780
781	PPKNGISTKL	MNIFLKDST	TWEILAVSMS	DKKGICVADP	FEVTVMQDFE	IDLRLPYSVV	840
841	RNEQVEIRAV	LYNYRQNEEL	KVRVELLHNP	AFCSLATTKR	RHQQTVTIPP	KSSLVSVYVI	900
901	VPLKTLGQEV	EVKAAVYHFF	ISDGVKSLK	VVPEGIRMNK	TVAVRTLDEP	RLGREGVQKE	960
961	DIPPADLSDQ	VPDTESETRI	LQGTTPVAQM	TEDAUDAERL	KHLIVTPSGC	GEQNMIGMTP	1020
1021	TVIAYHYLDE	TEQWEKFGLE	KRQGALELIK	KGYTQQLAFR	QSSAFAAFV	KRAPSTWLTA	1080
1081	YVVKVFLAV	NLIAIDSQVL	CGAVKWLILE	KQKPDGVFQE	DAPVIHQEMI	GGLRNNNEKD	1140
1141	MAITAFVLIS	LQEAKDICEE	QVNSLPGSIT	KAGDFLEANY	MNLQRSYTV	IAGYALAKMG	1200
1201	RLKGPLLNKF	LTTAKDKNRW	EDPGKQLYNV	EATSYALLAL	LQLKDFDEVP	PVVRWLNEQR	1260
1261	YVGGYVSTQ	ATFMVFQALA	QYQKADPDHQ	EINLNDVSLQ	PSRSSKITHR	IHWESASLLR	1320
1321	SEETKENE <u>GF</u>	TVTAEKGG <u>QG</u>	TL <u>SVVTM</u> YHA	KAKDQL <u>TCNK</u>	FDLKV <u>TIKPA</u>	PETE <u>KRPODA</u>	1380
1381	KNTMILE <u>ICT</u>	RYR <u>GDQDATM</u>	SILD <u>ISMMTG</u>	FAPD <u>DDLKQ</u>	LANG <u>VDRYIS</u>	KYEL <u>DKAFSD</u>	1440
1441	RNTLI <u>IYLDK</u>	VSH <u>EDDCLA</u>	FKV <u>HQYFNVE</u>	LIQ <u>PQAVKVI</u>	AYN <u>LEESCT</u>	RFY <u>HPEKEDG</u>	1500
1501	KLNL <u>CRDEL</u>	CR <u>CAEENC<u>FI</u></u>	QK <u>SDDKVTLE</u>	ER <u>LDKACE<u>PG</u></u>	VD <u>YVYKTR</u> <u>ILV</u>	KV <u>LSNDFDE</u>	1560
1561	YIM <u>AIEQTIK</u>	SG <u>SDEVQV<u>GQ</u></u>	QR <u>TIFISPIK</u>	RE <u>ALKLEE<u>KK</u></u>	HY <u>LMWGLSSD</u>	FW <u>GEKPNLSY</u>	1620
1621	IIG <u>KD</u> TVEH	WPE <u>ED</u> ECQDE	EN <u>KQCQ</u> DLG	AF <u>TESM</u> VVFG	CP <u>N</u>		

b	1	11	21	31	41	51		
1	MRWLLLLYYAL	CFSLSKASA						
			H	TVELNNMFGQ	IQSPGYPDSY	PSDSEVTWNI	TVPDGFRIKL	60
61	YFMHFNLESS	YLCEYDYVKV	ETED <u>QVLATF</u>	CG <u>RETTDTEQ</u>	TP <u>GQEVVLS</u>	GS <u>FMSITFRS</u>	120	
121	DF <u>SNEERFTG</u>	FD <u>AHYMAVDV</u>	DE <u>CKEREDEE</u>	LS <u>CDHYCHNY</u>	IG <u>GYCSCR</u> F	GY <u>ILHTDNRT</u>	180	
181	CR <u>VECDNLF</u>	TQ <u>RTGVITSP</u>	DF <u>FNYPKSS</u>	ECL <u>YTIELEE</u>	GF <u>MVNLQFED</u>	IF <u>DIQDHPEV</u>	240	
241	PC <u>PYDYIKIK</u>	VG <u>PKVLGFFC</u>	GE <u>KAPEFIST</u>	QSH <u>SVLILFH</u>	SD <u>NSAENRNG</u>	RL <u>SYRAAGNE</u>	300	
301	CP <u>ELQPPVHG</u>	KIE <u>PSQAKYF</u>	FK <u>DQVLVSCD</u>	TG <u>YKVLKDNV</u>	EM <u>DTFQIECL</u>	KD <u>GTWSNKIP</u>	360	
361	TC <u>KIVDCRAP</u>	GE <u>LEHGLITF</u>	STR <u>NNLTYYK</u>	SE <u>IKYSCQEP</u>	YK <u>MLNNTG</u>	IY <u>TCSAQGVW</u>	420	
421	MN <u>KVLRSLP</u>	TCL <u>PVCGLPK</u>	FS <u>RKLMAR</u>					
				I	NGRPAQKGT	PWIAMLSHLN	GQPFCCGSSL	480
481	GSSWIVTAAH	CLHQSLDFPKD	PTLRDSDLLS	PSDFKILGK	HWRLRSDENE	QHLGVKHTTL	540	
541	HPQYDNPTE	NDVALVELLE	SPVLNAFVMP	ICLPEGPQOE	GAMVIVSGWG	KQLQRFPEP	600	
601	LMEIEIPIVD	HSTCQKAYAP	LKKKVTRDMI	CAGEKEGGKD	ACAGDSGGPM	VTLNRERQGW	660	
661	YLVGTVSWG	DCGKKDRYGV	YSYIHHNKDW	IQRVTGVRN				

Figure 3 | Peptide fragments and sequence coverage of complement C3 and mannose-binding protein-associated serine protease-1 (MASP-1) identified in dialyser eluate. Complement C3 (a) and MASP-1 (b) amino acid sequences (in one-letter code). C3c α -chain fragment 2 (1321–1663) and MASP-1 heavy chain (20–448) are framed within a box. Peptides covered by peptide mass fingerprinting are highlighted in bold; sequences confirmed by tandem mass spectrometry are underscored.

be achieved by means of acidic, alkaline, chaotropic, or detergent agents. Ishikawa *et al.*²⁴ report, having tested acetic acid, bicarbonate, urea, and sodium dodecylsulfate (SDS) to find, acetic elution to be the most efficient. This observation has been confirmed by us; acetic acid has been shown to be superior to SDS in a preliminary sequential elution study.

In our experiment, recirculation with PBS/EDTA yielded a protein at a concentration an order of magnitude higher than the final portion of PBS flush. This protein gain can be explained by the release of proteins attached to the dialyser, considering the inert nature of PBS, probably because of convective forces and equilibrium shift between adsorption and desorption occurring in a protein-free medium. Moreover, the protein profile of the PBS/EDTA washout resembled that of acetic eluate. The following elution with acetic acid induced an additional discharge of more firmly bound proteins, which even slightly exceeded the first one. Taking into account the high variation of the protein content, the adsorption seems to be patient- and procedure-

dependent. The described advantage of acidic eluent over other solvents can be theoretically attributed to the surface negativity of polysulfone membrane (ζ -potential -5 mV), which would be suppressed by strong anions thus dissociating electrostatic bindings.

In eluates, the complete spectrum of MW and pI fractions detectable with the 2-DE technique was discovered, thus substantiating the use of proteomic rather than the targeted approach. Of the 153 protein spots, 84 were present in all patients constituting the typical proteome adsorbed to a hemodialyser during clinical HD. Among them, 23 unique proteins were identified with MS. Most of them were plasma proteins, both high (serum albumin, transferrin, α -1-antitrypsin, haptoglobin, immunoglobulin chains) and low abundant (MASP-1 and MASP-2, ficolin-2, clusterin, etc.). However, several proteins arose from the blood cells, mainly erythrocytes (hemoglobin α - and β -subunits, peroxidase, carbonic anhydrase).

The only available trial addressing a similar issue with proteomic technology was performed *ex vivo*, using minidialysers

composed of cellulose diacetate or ethylenevinyl alcohol, and blood treated with EDTA.¹³ Nine proteins, mostly high abundant, were identified in this model, all of which were also detected in our setting, except aspartyl-tRNA synthetase.

Yet, none of these proteins were clearly related to complement, coagulation, or leukocyte activation.

Mulzer and Brash²⁰ selected 16 plasma proteins, mainly those engaged in blood clotting and complement activa-

tion, and tested their presence in various dialyser eluates using specific immunoassays. All high-abundance proteins reported in this experiment were also identified by us, namely albumin, transferrin, immunoglobulin, fibrinogen, α -1-antitrypsin, apolipoproteins, and haptoglobin. Mulzer and Brash²⁰ found the adsorption of low-abundance proteins to be largely dependent on the dialyser type. Cuprophane, which is considered standard in terms of bioincompatibility, bound substantially various cleavage products of HMWK (high MW kininogen), antithrombin III, C3 (mainly C3c and C3d), fibronectin, and α 2-macroglobulin. Of these, the C3c fragment and antithrombin III stained as strong bands during immunoblot and were also confirmed in our study. The absence of HMWK, fibronectin, and α 2-macroglobulin fragments in our experiment may reflect different properties (biocompatibility) of polysulfone, as well as the lower sensitivity of MS detection (respective bands were assessed as moderate or weak by Mulzer and Brash²⁰).

Several lines of references indicate that many of the adsorbed proteins identified in this study are involved in blood-dialyser interaction. These included complement C3, ficolin-2, clusterin, MASP-1, MASP-2, complement factor H, and complement factor H-related protein 1, which participate in complement activation, as well as²⁵⁻³⁰ fibrinogen, antithrombin, and β -2-glycoprotein-1, which control blood coagulation,^{31,32} and serum amyloid P, which mediates leukocyte adhesion and activation.³³ To ascertain proteins undergoing selective adsorption, and hence possibly a specific interaction with the dialyser membrane, we calculated E/P ratios. Although 2-DE allows only estimation of protein quantities, and low E/P may be caused by imperfect elution, as well as by lack of affinity to the dialyser; it is reasonable to consider high E/P as evidence of preferential binding. In this manner, the relevance of ficolin-2 and clusterin has been emphasized.

Ficolin-2 (MW = 34 kDa, its synonyms include 1-ficolin and hucolin) is a lectin family member secreted in the plasma, and complexed with serine proteases, particularly MASP-1 and MASP-2. It acts as a soluble pattern recognition

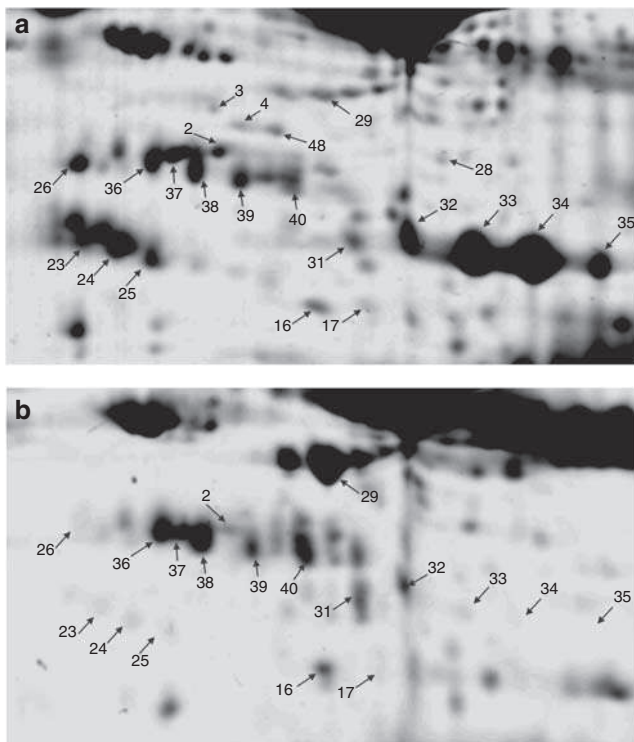


Figure 4 | Enlarged images of corresponding sections in gels derived from dialyser eluate and plasma. Significant differences in relative intensities of plasma proteins identified in (a) dialyser eluate compared with (b) plasma. The highest eluate-to-plasma ratio (E/P) of spot intensity was detected in ficolin-2 (spots no. 31–35), clusterin (spots no. 23–25), and complement C3c fragment (spot no. 26).

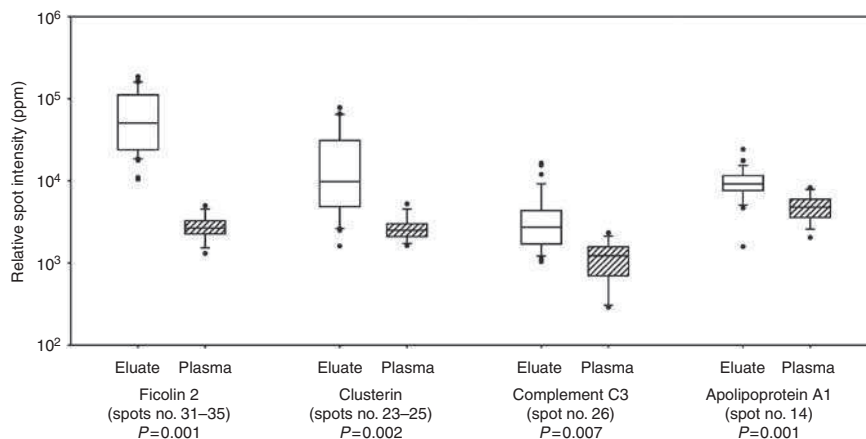


Figure 5 | Plasma proteins identified in dialyser eluate and reaching significantly different relative spot intensities in eluate vs plasma. Statistical significance was tested using Mann-Whitney rank sum test.

protein, which upon binding to polysaccharide bacterial wall promotes auto-cleavage of MASPs, and thus initiates the lectin complement pathway.³⁴ In addition, it has an opsonic activity,^{35,36} and both MASP proteases cleave prothrombin and trigger blood clotting.^{37,38} The role of the lectin pathway in biomaterial-induced inflammation has not been evaluated so far, and both alternative and classical pathways have been attributed major significance. According to the accepted models, the classical pathway accounts for the initiation of the process, whereas the alternative pathway (demonstrated by complement factor B conversion) is responsible for its amplification.³⁹ Nevertheless, it may be difficult to discern the classical from the lectin pathway, as most studies dealing with this issue determine complement activation according to C5a or C4a levels, and this part of the cascade is shared by both pathways. Namely, the activated MASP cleaves C4, which in turn activates C2 thus, giving rise to C3 convertase (C4b2a); C3b is central to all the three pathways. Substrate specificity of the ficolins has been addressed before, and includes various kinds of acetylated oligosaccharides;^{40,41} however, a possible capacity of polysulfone membrane to activate ficolin-2 and associated MASP should be confirmed directly.

Our data show excessive binding of ficolin-2 (spots no. 31–35; E/P = 26.1) in a clinical setting together with C3c fragment (spot no. 26; E/P = 3.2). C3c is a degradation product of activated C3b providing evidence of both C3 activation and subsequent C3b inactivation. Relative abundance of C3c in eluates from cuprophane dialysers was reported in early studies, whereas only minimal amounts of C3d were obtained.^{20,42} This is easily comprehensible as the latter fragment contains the thioester site covalently binding to the surface,⁴³ and its release is not probable under the described elution conditions. Moreover, we documented the concurrent presence of the activated forms of MASP-1 (spot no. 47) and MASP-2 (spot no. 48)⁴⁴ which infer a possible connection between ficolin adsorption and C3 activation. Therefore, it is conceivable that ficolin-2 adsorption and lectin pathway contribute to complement activation, as well as leukocyte adhesion and perhaps even blood coagulation.

Factor H adsorption to polyanionic surfaces recognized as 'self' and the subsequently enhanced degradation of C3b have been shown to play a role in tissue protection from improper complement-dependent lysis.^{29,30,45} Yet, complement factor H and its related protein-1 (key regulatory molecules of the alternative pathway) detected in our experiment showed low relative quantities, and were hardly matched with the plasma (complement factor H has MW > 130 kDa, and was located in a low-resolution area on 13% gels). Quite speculatively, adsorption of factor H and its related protein 1, evidenced in our study, could be, in part, responsible for the accelerated turnover of C3b (we showed the adsorption of its cleavage fragment C3c only; no intact C3b was observed).

Another candidate biocompatibility factor derived from our results is clusterin (complement cytolysis inhibitor, spots no. 23–25; E/P = 9.1), which is a plasma protein consisting of two non-identical subunits (each ~ 35 kDa). Clusterin has

been shown to interfere with the soluble membrane attack complex (C5b-9) formation, and to prevent (or limit) cytolysis in this manner.⁴⁶ Biological consequences of its adsorption are difficult to predict; we may hypothesize that enhanced clearance of clusterin by binding to the dialyser membrane could increase the burden brought about by complement activation due to lack of circulating clusterin (as observed in experiment).⁴⁷

In several other proteins, their role in the blood-dialyser interaction (while plausible) is difficult to define. The β -2-glycoprotein-1 is an important inhibitor of the contact phase system neutralizing negatively charged surfaces and suppressing the intrinsic blood coagulation pathway. Binding of the β -2-glycoprotein-1 to a dialyser might have a favorable effect on thrombogenicity, yet its eluate quantity was significantly decreased (E/P below 0.5). Nevertheless, its spots on the 2D gels overlapped with the immunoglobulin heavy chains fraction, which might have substantially corrupted the quantification. It has been proposed that actin and vimentin co-assemble under the guidance of fimbrin (L-plastin) at the cell adhesion sites of macrophages.⁴⁸ All these proteins were identified in the dialyser eluate; however, it is questionable whether their presence in the eluate predicates more than leukocyte lysis.

In summary, we report an elution technique allowing the preparation of proteins adsorbed to a dialyser during clinical HD. The proteins obtained were subjected to gel electrophoresis and subsequently to MS to show their applicability for proteomic profiling. To screen out proteins undergoing preferential adsorption, and hence presumably a specific interaction with the dialyser, we calculated the E/P ratios of relative spot intensities. The proteins concentrated significantly in the eluate were considered to be potentially engaged in the blood-dialyser interaction. These criteria were met, especially in ficolin-2 and clusterin, both of which play an important role in complement activation (ficolin-2 is also a potent opsonic agent). With respect to our data, we hypothesize that the lectin pathway could contribute to complement activation occurring on contact of human blood with the polysulfone hemodialyser.

MATERIALS AND METHODS

Patients and treatment

Patients were recruited at the Hemodialysis Center of the Charles University Teaching Hospital in Plzen, and the study protocol was approved by the Institutional Ethics Committee. Inclusion criteria were as follows: regular HD for more than 3 months, established 4-h dialysis thrice a week with F6 dialyser (polysulfone, 1.3 m², Fresenius Medical Care, Bad Homburg, Germany), native arterio-venous shunt allowing blood flow for 300 ml/min or more, and heparin anticoagulation with a total dose (bolus + continuous) 4000–6000 i.u. as per procedure. Patients meeting the following criteria were excluded from the study: current or past anti-coagulation treatment (oral or parenteral) other than during the dialysis session, history of thrombotic complication or known coagulation disorder, diabetes mellitus, active inflammation, malignancy, or liver disease. Within a 3-week screening period,

the heparin dose was maintained, and the proportion of the dialyser filled with coagulum was assessed visually at the end of every procedure. A semi-quantitative scale commonly used in the center was applied (1 = no visible clot; 2 = up to 50% capillaries in the dialyser filled with clot; 3 = more than 50% capillaries filled with clot; 4 = macroscopic coagulum in the lines, outside the dialyser; 5 = complete obstruction of the extracorporeal circuit), and only patients with a score of 1 or 2 were considered eligible.

Finally, five patients aged 58–82 years, treated with HD for 5–42 months were included in the study. In this group, hemodialysers were eluted on three consecutive procedures, following the protocol described below. All HD sessions were performed routinely; that is, blood flow (300 ml/min), dialysate flow (500 ml/min), and ultra-filtration rate (250–500 ml/h). At the end of the HD session, 4 ml of plasma was collected, and blood residuum left in the lines was retrieved using 250-ml rinse (Plasmalyte, Baxter, Deerfield, IL, USA). Thereafter, the patient was disconnected from the system and the dialyser was flushed immediately with another 1000 ml Plasmalyte solution. The final 10 ml of this flush was gathered from the dialyser outlet and stored at -80°C .

Elution protocol and sample preparation

The F6 dialyser has a declared priming volume of 78 ml. Initially, it was emptied and directly filled with 80 ml of 3 mM EDTA (EDTA/PBS, pH = 7.4), thereafter it was re-circulated with the peristaltic pump (flow rate: 80 ml/min) at 24°C for 30 min to detach and wash out adhering leukocytes. The dialyser was drained thereafter; the obtained fluid was centrifuged at 1200 g at 4°C for 10 min. The supernatant, denoted as washout, was separated from the sediment containing cells and stored at -80°C . The dialyser was immediately loaded with 80 ml of 40% acetic acid, re-circulated again with a flow rate of 80 ml/min at 24°C for 30 min, emptied, and the resulting eluate was centrifuged at 4000 g at 4°C for 10 min to remove cellular detritus, and stored at -80°C .

To minimize salt contamination, eluates were dialyzed against ultra-high quality water at 4°C (10 exchanges, 1.5l each) using a semi-permeable membrane with a molecular mass cutoff at 7 kDa (Serva-Electrophoresis, Heidelberg, Germany) for 5 days. Dialyzed samples were concentrated by vacuum evaporation (SpeedVac, Thermo Fisher Scientific, Waltham, MA, USA), and the proteins were dissolved in a lysis buffer (7 M urea, 4% 3-[(3-Cholamidopropyl)dimethylammonio]-1-propanesulfonate, 40 mM Tris base, 2 M Thiourea, 2% immobilized pH gradient, IPG, buffer pH 3–10, 120 mM dithiothreitol, DTT). Blood samples (4 ml) were processed by centrifugation only (at 4000 g and 4°C for 10 min) to separate plasma (supernatant). Protein concentrations in all samples were assessed using Bradford's dye-binding assay (Bio-Rad Protein Assay, Bio-Rad Laboratories, Hercules, CA, USA).

To assess the effectivity of the elution process, we performed additional studies evaluating a sequential elution with an SDS detergent. Two dialysers were eluted consecutively either with 40% acetic acid followed by 10% SDS or vice versa. The protein quantities obtained were 9.33 and 0.014 mg using the eluent sequence acetic acid–SDS, whereas 6.99 and 2.85 mg were eluted when the inverse order was used. However, in case of SDS subsequent to acetic elution, the protein concentration (0.21 $\mu\text{g}/\text{ml}$) was at the detection limit of the method.

Two-dimensional electrophoresis

Urea, CHAPS, Tris base, thiourea, SDS, DTT, IAA (iodoacetamide), and bromphenol blue used during the preparation were purchased from Sigma (Sigma-Aldrich, Steinheim, Germany); immobilized

IPG buffer (ZOOM carrier Ampholytes 3–10) was purchased from Invitrogen (Invitrogen Corporation, Carlsbad, CA, USA). Equally, 200- μg proteins in both the eluate and plasma samples were mixed with rehydration buffer (7 M urea, 4% CHAPS, 40 mM Tris base, 2 M Thiourea, 2% IPG buffer pH 3–10, 120 mM DTT, and a trace of bromophenol blue) to obtain the final volume of 140 μl . Samples were then rehydrated in IPG strips (7.7-cm length, pH 3–10 nonlinear; Invitrogen), and focused in a MiniProtean cell (Bio-Rad). IPG strips were rehydrated passively for 1 h and actively for 10 h at 30 V, followed by a stepwise isoelectric focusing (IEF) as follows: 200 V until 400 Vh were reached, 450 V for another 500 Vh, 750 V for another 900 Vh, and finally 2000 V for the other 10,000 Vh. After isoelectric focusing, the IPG strips were equilibrated in the equilibration buffer 1 (112 mM Tris-base, 6 M urea, 30% v/v glycerol, 4% w/v SDS, 130 mM DTT, and a trace of bromophenol blue) for 30 min, and subsequently alkylated in buffer 2 (112 mM Tris-base, 6 M urea, 30% v/v glycerol, 4% w/v SDS, 135 mM IAA, and a trace of bromophenol blue) for 30 min. Each equilibrated IPG strip was placed on the top of a 13% polyacrylamide gel (9×7 cm) and covered with 0.5% agarose. Second-dimension separation was performed with 65 mA per gel at 20°C until the bromophenol blue dye front reached the bottom of the gel. At the end of each run, the 2D gels were stained with Simply Blue (Invitrogen), and scanned with an Epson Perfection 4990 Photo scanner (Epson, Long Beach, CA, USA).

2-DE pattern analysis and statistics

Computer-aided analysis of 2-DE gel images was carried out using PDQuest 2D software version 8.1 (Bio-Rad). A synthetic image was constructed out of the triplicated gels processed from each sample, using only the spots constantly present in at least two gels. The protein quantity was determined relative to the integrated spot density. The intensity levels of the protein spots in the eluate samples were compared with those of the corresponding or matched spots of the plasma samples collected from the same patients, and expressed as E/P ratios. Quantitative differences were considered significant when showing at least a two-fold intensity variation. The statistical analysis was performed using the SigmaPlot/SigmaStat data analysis software (version 12.0, SPSS Inc., Chicago, IL, USA). The inter-gel variability was determined as the CV of relative spot intensities across triplicates. Moreover, the inter-individual variability (CV among patients) was assessed in identified spots. Mann–Whitney rank sum test was used to compare the continuous variables. Data are given as medians (ranges), differences were considered statistically significant if the *P*-values were below 0.01.

In-gel tryptic digestion

Acetonitrile (ACN), ammonium bicarbonate, DTT, IAA, TFA (trifluoroacetic acid), formic acid, and CHCA (α -cyano-4-hydroxycinnamic acid) were purchased from Sigma. Spots detected in all patients were excised manually. The SimplyBlue stain (Invitrogen Corporation, Carlsbad, CA, USA) was removed by washing with 50 mM ammonium bicarbonate and ACN. Proteins in the gel were reduced with 10 mM DTT/50 mM ammonium bicarbonate at 56°C for 45 min and alkylated with 55 mM IAA/50 mM ammonium bicarbonate (for 30 min, in the dark at room temperature). Gel plugs were washed with 50 mM ammonium bicarbonate and ACN and dried by SpeedVac. Dried gel particles were rehydrated with a digestion buffer containing 12.5 ng/ μl sequencing grade trypsin (Roche, Basel, Switzerland) in 50 mM ammonium bicarbonate at 4°C . After 45 min, the remaining solution was removed and replaced by 0.1 M ammonium bicarbonate.

Tryptic digestion was performed overnight (37°C). After digestion, proteolytic peptides were subsequently extracted with 25 mM ammonium bicarbonate, ACN, and 5% formic acid. The three extracts were pooled and 10 mM DTT solution in 50 mM ammonium bicarbonate was added. The mixture was then dried using SpeedVac and the resulting tryptic peptides were dissolved in 5% formic acid solution and desalted using ZipTip μ C18 (Millipore, Bedford, MA, USA).

MALDI (matrix-assisted laser desorption/ionization) TOF (time-of-flight) tandem MS and protein identification

Proteolytic peptides were mixed with CHCA matrix solution (5 mg/ml CHCA in 0.1% TFA/50% ACN 1:1, v/v) in a 1:1 ratio, and 0.8 μ l of this mixture was spotted onto the MALDI target. All mass spectra were acquired at a reflectron mode using a 4800 MALDI TOF/TOF Analyzer (Applied Biosystems, Framingham, MA, USA). A total of 2000 and 3000 laser shots were acquired and averaged to MS and MS/MS spectra, respectively. The MS/MS analyses were performed using collision energy of 1 kV and collision gas pressure of 1.3×10^{-6} Torr. MS peaks with a signal to noise above 15 were listed, and the 15 strongest precursors with a signal to noise above 50 among the MS peaks were automatically selected for MS/MS acquisition. A mass filter was used to exclude autolytic peptides of trypsin.

The resulting data were analyzed using the GPS Explorer 3.6 (Applied Biosystems) software. Proteins were identified by searching against the human subset of the Swissprot protein database (Swiss Institute of Bioinformatics, Basel, Switzerland) (release 54.6; 4 December 2007) using the MASCOT 2.1.0 search algorithm (Matrix Science, London, UK). The general parameters for the peptide mass fingerprinting search were considered to allow maximum one missed cleavage, ± 50 p.p.m. of peptide mass tolerance, variable methionine oxidation, and fixed cysteine carbamidomethylation. Probability-based Molecular Weight Search scores were estimated by comparison of the search results against the estimated random match population, and were reported as $-10\log_{10}(p)$ where p is the absolute probability. MOWSE scores > 55 were considered significant ($P < 0.05$) for peptide mass fingerprinting. A peptide charge state of $+1$ and fragment mass tolerance of ± 0.25 Da were used for the MS/MS ion search. Individual MS/MS ions scores > 28 indicated identity or extensive homology ($P < 0.05$) for the MS/MS ion search.

DISCLOSURE

All the authors declared no competing interests.

ACKNOWLEDGMENTS

The study was supported by Research Project No. MSM0021620819 'Replacement of, and support to some vital organs' awarded by the Ministry of Education of the Czech Republic. The authors specially thank Professor Christopher Bremer from the East Carolina University for language revision.

REFERENCES

- Lindner A, Charra B, Sherrard DJ et al. Accelerated atherosclerosis in prolonged maintenance hemodialysis. *N Engl J Med* 1974; **290**: 697–701.
- Cheung AK. Biocompatibility of hemodialysis membranes. *J Am Soc Nephrol* 1990; **1**: 150–161.
- Jofre R, Rodriguez-Benitez P, Lopez-Gomez JM et al. Inflammatory syndrome in patients on hemodialysis. *J Am Soc Nephrol* 2006; **17**: S274–S280.
- Himmelfarb J, Hakim RM. Oxidative stress in uremia. *Curr Opin Nephrol Hypertens* 2003; **12**: 593–598.
- Sagripanti A, Cupisti A, Baicchi U et al. Plasma parameters of the prothrombotic state in chronic uremia. *Nephron* 1993; **63**: 273–278.
- Deguchi N, Ohigashi T, Tazaki H et al. Haemodialysis and platelet activation. *Nephrol Dial Transplant* 1991; **6**(Suppl 2): 40–42.
- Kaysen GA. The microinflammatory state in uremia: causes and potential consequences. *J Am Soc Nephrol* 2001; **12**: 1549–1557.
- Horl WH. Hemodialysis membranes: interleukins, biocompatibility, and middle molecules. *J Am Soc Nephrol* 2002; **13**(Suppl 1): S62–S71.
- Locatelli F, Canaud B, Eckardt KU et al. Oxidative stress in end-stage renal disease: an emerging threat to patient outcome. *Nephrol Dial Transplant* 2003; **18**: 1272–1280.
- Clark WR, Macias WL, Molitoris BA et al. Plasma protein adsorption to highly permeable hemodialysis membranes. *Kidney Int* 1995; **48**: 481–488.
- Tsuchida K, Nakatani T, Sugimura K et al. Biological reactions resulting from endotoxin adsorbed on dialysis membrane: an in vitro study. *Artif Organs* 2004; **28**: 231–234.
- Liu TY, Lin WC, Huang LY et al. Hemocompatibility and anaphylatoxin formation of protein-immobilized polyacrylonitrile hemodialysis membrane. *Biomaterials* 2005; **26**: 1437–1444.
- Bonomini M, Pavone B, Siroli V et al. Proteomics characterization of protein adsorption onto hemodialysis membranes. *J Proteome Res* 2006; **5**: 2666–2674.
- Cornelius RM, Brash JL. Identification of proteins adsorbed to hemodialyzer membranes from heparinized plasma. *J Biomater Sci Polym Ed* 1993; **4**: 291–304.
- Neveceral P, Markert M, Wauters JP. Role of protein adsorption on haemodialysis-induced complement activation and neutrophil defects. *Nephrol Dial Transplant* 1995; **10**: 372–376.
- Matata DM, Courtney JM, Sundaram S et al. Determination of contact phase activation by the measurement of the activity of supernatant and membrane surface-adsorbed factor XII (FXII): its relevance as a useful parameter for the in vitro assessment of haemodialysis membranes. *J Biomed Mater Res* 1996; **31**: 63–70.
- Fujimori A, Naito H, Miyazaki T. Adsorption of complement, cytokines, and proteins by different dialysis membrane materials: evaluation by confocal laser scanning fluorescence microscopy. *Artif Organs* 1998; **22**: 1014–1017.
- Moachon N, Boullange C, Fraud S et al. Influence of the charge of low molecular weight proteins on their efficacy of filtration and/or adsorption on dialysis membranes with different intrinsic properties. *Biomaterials* 2002; **23**: 651–658.
- Francoise Gachon AM, Mallet J, Tridon A et al. Analysis of proteins eluted from hemodialysis membranes. *J Biomater Sci Polym Ed* 1991; **2**: 263–276.
- Mulzer SR, Brash JL. Identification of plasma proteins adsorbed to hemodialyzers during clinical use. *J Biomed Mater Res* 1989; **23**: 1483–1504.
- Cornelius RM, McClung WG, Barre P et al. Effects of reuse and bleach/formaldehyde reprocessing on polysulfone and polyamide hemodialyzers. *ASAIO J* 2002; **48**: 300–311.
- Cornelius RM, McClung WG, Richardson RM et al. Effects of heat/citric acid reprocessing on high-flux polysulfone dialyzers. *ASAIO J* 2002; **48**: 45–56.
- Grooteman MP, Nube MJ, Bos JC et al. Ex vivo elution of hemodialyzers. An additional criterion for the assessment of bioincompatibility. *Blood Purif* 1996; **14**: 421–430.
- Ishikawa I, Chikazawa Y, Sato K et al. Proteomic analysis of serum, outflow dialysate and adsorbed protein onto dialysis membranes (polysulfone and pmma) during hemodialysis treatment using SELDI-TOF-MS. *Am J Nephrol* 2006; **26**: 372–380.
- Matsushita M, Endo Y, Fujita T. Cutting edge: complement-activating complex of ficolin and mannose-binding lectin-associated serine protease. *J Immunol* 2000; **164**: 2281–2284.
- Ma YG, Cho MY, Zhao M et al. Human mannose-binding lectin and L-ficolin function as specific pattern recognition proteins in the lectin activation pathway of complement. *J Biol Chem* 2004; **279**: 25307–25312.
- Takahashi M, Iwaki D, Kanno K et al. Mannose-binding lectin (MBL)-associated serine protease (MASP)-1 contributes to activation of the lectin complement pathway. *J Immunol* 2008; **180**: 6132–6138.
- Wallis R, Dodds AW, Mitchell DA et al. Molecular interactions between MASP-2, C4, and C2 and their activation fragments leading to complement activation via the lectin pathway. *J Biol Chem* 2007; **282**: 7844–7851.
- Meri S, Pangburn MK. Regulation of alternative pathway complement activation by glycosaminoglycans: specificity of the polyanion binding site on factor H. *Biochem Biophys Res Commun* 1994; **198**: 52–59.
- Kuhn S, Zipfel PF. Mapping of the domains required for decay acceleration activity of the human factor H-like protein 1 and factor H. *Eur J Immunol* 1996; **26**: 2383–2387.

31. Schousboe I. beta 2-Glycoprotein I: a plasma inhibitor of the contact activation of the intrinsic blood coagulation pathway. *Blood* 1985; **66**: 1086–1091.
32. Hulstein JJ, Lenting PJ, de Laat B *et al.* beta2-Glycoprotein I inhibits von Willebrand factor dependent platelet adhesion and aggregation. *Blood* 2007; **110**: 1483–1491.
33. Kim JK, Scott EA, Elbert DL. Proteomic analysis of protein adsorption: serum amyloid P adsorbs to materials and promotes leukocyte adhesion. *J Biomed Mater Res A* 2005; **75**: 199–209.
34. Lynch NJ, Roscher S, Hartung T *et al.* L-ficolin specifically binds to lipoteichoic acid, a cell wall constituent of Gram-positive bacteria, and activates the lectin pathway of complement. *J Immunol* 2004; **172**: 1198–1202.
35. Aoyagi Y, Adderson EE, Min JG *et al.* Role of L-ficolin/mannose-binding lectin-associated serine protease complexes in the opsonophagocytosis of type III group B streptococci. *J Immunol* 2005; **174**: 418–425.
36. Matsushita M, Endo Y, Taira S *et al.* A novel human serum lectin with collagen- and fibrinogen-like domains that functions as an opsonin. *J Biol Chem* 1996; **271**: 2448–2454.
37. Krarup A, Gulla KC, Gal P *et al.* The action of MBL-associated serine protease 1 (MASP1) on factor XIII and fibrinogen. *Biochim Biophys Acta* 2008; **1784**: 1294–1300.
38. Krarup A, Wallis R, Presanis JS *et al.* Simultaneous activation of complement and coagulation by MBL-associated serine protease 2. *PLoS ONE* 2007; **2**: e623.
39. Nilsson B, Ekdahl KN, Mollnes TE *et al.* The role of complement in biomaterial-induced inflammation. *Mol Immunol* 2007; **44**: 82–94.
40. Krarup A, Thiel S, Hansen A *et al.* L-ficolin is a pattern recognition molecule specific for acetyl groups. *J Biol Chem* 2004; **279**: 47513–47519.
41. Krarup A, Mitchell DA, Sim RB. Recognition of acetylated oligosaccharides by human L-ficolin. *Immunol Lett* 2008; **118**: 152–156.
42. Cheung AK, Parker CJ, Janatova J. Analysis of the complement C3 fragments associated with hemodialysis membranes. *Kidney Int* 1989; **35**: 576–588.
43. Law SK, Dodds AW. The internal thioester and the covalent binding properties of the complement proteins C3 and C4. *Protein Sci* 1997; **6**: 263–274.
44. Thielens NM, Cseh S, Thiel S *et al.* Interaction properties of human mannan-binding lectin (MBL)-associated serine proteases-1 and -2, MBL-associated protein 19, and MBL. *J Immunol* 2001; **166**: 5068–5077.
45. Schmidt CQ, Herbert AP, Hocking HG *et al.* Translational mini-review series on complement factor H: structural and functional correlations for factor H. *Clin Exp Immunol* 2008; **151**: 14–24.
46. Choi NH, Mazda T, Tomita M. A serum protein SP40,40 modulates the formation of membrane attack complex of complement on erythrocytes. *Mol Immunol* 1989; **26**: 835–840.
47. Li DQ, Lundberg F, Ljungh A. Binding of vitronectin and clusterin by coagulase-negative staphylococci interfering with complement function. *J Mater Sci Mater Med* 2001; **12**: 979–982.
48. Correia I, Chu D, Chou YH *et al.* Integrating the actin and vimentin cytoskeletons. adhesion-dependent formation of fimbrin-vimentin complexes in macrophages. *J Cell Biol* 1999; **146**: 831–842.

RESEARCH ARTICLE

Proteomic profiling of blood-dialyzer interactome reveals involvement of lectin complement pathway in hemodialysis-induced inflammatory response

Jan Mares^{1,2}, Pavlina Richtrova¹, Alena Hricinova¹, Zdenek Tuma², Jiri Moravec², Daniel Lysak³ and Martin Matejovic¹

¹ Department of Internal Medicine I, Charles University Medical School and Teaching Hospital, Plzen, Czech Republic

² Proteomic Laboratory, Charles University Medical School, Plzen, Czech Republic

³ Department of Hematology, Charles University Medical School and Teaching Hospital, Plzen, Czech Republic

Purpose: Dialysis-induced inflammatory response including leukocyte and complement activation is considered a significant cofactor of chronic morbidity in long-term hemodialysis (HD) patients. The aim of this study was to provide better insight into its molecular background.

Experimental design: In 16 patients, basic biocompatibility markers, *i.e.* leukocyte counts and C5a levels, were monitored during HD on a polysulfone membrane. Proteins adsorbed to dialyzers were eluted and separated by 2-DE. Selected proteins were identified by MS; ficolin-2 plasma levels were assessed. Data are given as medians (quartile ranges).

Results: In total, 7.2 (34.7) mg proteins were retrieved from dialyzer eluates and were resolved into 217 protein spots. The proteins most enriched in eluates (and hence selectively adsorbed) were those involved in complement activation (C3c, ficolin-2, mannan-binding lectin serine proteases, properdin) and cell adhesion (actin, caldesmon, tropomyosin, vitronectin, vinculin). A significant decrease of plasma ficolin-2 (41% [4.7], $p < 0.001$) was evidenced during one HD session, associated with leukopenia ($r = 0.73$, $p = 0.001$) and C5a production ($r = -0.62$, $p = 0.01$) at 15 min.

Conclusions and clinical relevance: Ficolin-2 adsorption to polysulfone dialyzer initiates the lectin pathway of complement activation, mediates dialysis-induced leukopenia, and results in a significant depletion of ficolin-2, an essential component of innate immunity.

Received: April 21, 2010

Revised: July 26, 2010

Accepted: August 8, 2010

**Keywords:**

Complement / Hemodialysis / Lectin / Leukopenia / Polysulfone

1 Introduction

Over a million patients worldwide undergo regular hemodialysis (HD), most of them using polysulfone membranes [1].

Correspondence: Dr. Jan Mares, Department of Internal Medicine I, Charles University Teaching Hospital, Alej Svobody 80, 30460 Plzen Czech Republic

E-mail: mares@fnplzen.cz

Fax: +420-377-103-278

Abbreviations: *E/P*, eluate to plasma ratio of relative spot intensities; **HD**, hemodialysis; **IAA**, iodoacetamide; **MASP-1**, mannan-binding lectin serine protease 1; **MASP-2**, mannan-binding lectin serine protease 2; **MW**, molecular weight; **TAT**, thrombin-antithrombin

Although HD is a life-saving procedure in kidney failure, end-stage renal disease (ESRD) patients suffer from chronic inflammation and disturbed immune defense, and their yearly mortality approaches 20% [2]. In an “average” patient, more than 10 000 L of blood are exposed to 300 m² of artificial membrane for over 600 h every year. Therefore, it is not surprising that the immune response elicited by such contact is considered a major factor [3]. Yet, the grim statistics have not improved despite the introduction of so-called bio-compatible materials, among which polysulfone is the most common [4].

The dialyser-induced inflammatory reaction has been extensively characterized by changes in peripheral blood leukocyte counts and surface antigens, and complement activation markers [5, 6]. It has been demonstrated that both the alternative and the C4-dependent pathways are involved

in complement activation by hemodialyser [7, 8]. However, these observations are based on the systemic consequences while the local mechanisms responsible for the foreign pattern recognition and mediating subsequent processes remain unclear [6]. Closer examination of the molecular background might help us to prevent the sequelae of chronic inflammation seen in ESRD disease patients (*e.g.* by developing better-tolerated materials).

We have recently reported a novel method allowing to investigate the molecular substrates of blood–biomaterial interaction by means of proteomic technologies [9, 10]. In a pilot study, we performed a sequential elution of polysulfone dialyzers employed in clinical HD to show that profiling the protein–dialyzer interactome provides reproducible and useful information. Besides validating the method, we suggested possible role of the lectin pathway, implied by massive adsorption of ficolin-2, in polysulfone-induced complement activation.

The aim of this study was to study the molecular mechanisms of HD-associated inflammatory response in a representative group of patients.

2 Materials and methods

Methods described are similar to those used in our previous study [10] with slight modifications.

2.1 Patients and treatment

Patients were recruited at the Hemodialysis Center of Charles University Teaching Hospital in Plzen, and the study protocol had been approved by Institutional Ethics Committee. Inclusion criteria were as follows: regular HD for more than 3 months, established 4-h dialysis three times a week with F6 HPS dialyzer (polysulfone, 1.3 m², Fresenius Medical Care, Bad Homburg, Germany), native arterio-venous shunt allowing blood flow 250 mL/min or more, and heparin anticoagulation with total dose (bolus+continuous) 3000–6000 IU *per* procedure. Patients meeting the following criteria were excluded from the study: subjects examined during the protocol-optimization phase reported previously, in-shunt recirculation greater than 10%, hematocrit above 45%, current or past anticoagulation treatment (oral or parenteral) other than during dialysis session, history of thrombotic complication or known coagulation disorder, diabetes mellitus, active inflammation, malignancy, or liver disease.

Finally, 16 patients aged 65.5 (23.5) years, treated with HD for 14.5 (21) months were included into the study. In this group, blood samples were collected into EDTA tubes at the beginning, at 15 min and after 4 h of the study HD procedure. At all time points, samples were drawn both from the ports proximal (denoted as arterial) and distal to the filter (denoted as venous). Following the dialysis session, used hemodialyzers were eluted according to the protocol

described below. Elution at 15 min was tested in two patients; however, as it yielded little protein and complete resetting of the extracorporeal circuit was required, it was abandoned. All HD sessions were performed routinely: blood flow, 250 mL/min; dialysate flow, 500 mL/min; dialysate temperature, 36°C; ultrafiltration rate, 250–500 mL/h. At the end of the HD procedure, blood residuum left in the lines was retrieved by means of 250 mL rinse (PlasmalyteTM, Baxter, Deerfield, IL, USA). Then, the patient was disconnected from the system, and dialyzer flushed immediately with another 1000 mL Plasmalyte solution.

2.2 Elution protocol and sample preparation

The F6 dialyzer has a declared priming volume of 78 mL. First, it was emptied, and directly filled with 80 mL of 3 mM EDTA (EDTA/PBS, pH 7.4), then recirculated with the peristaltic pump (flow rate, 80 mL/min) at 24°C for 30 min to detach and wash out adhering leukocytes. The dialyzer was drained afterward; obtained fluid was centrifuged at 1200 × *g*/4°C for 20 min. The sediment containing cells was resuspended in 10% BSA in PBS and directly analyzed by flow cytometry. The dialyzer was immediately loaded with 80 mL of 40% acetic acid, recirculated again with a flow rate of 80 mL/min at 24°C for 30 min, emptied, and resulting eluate was centrifuged at 4000 × *g*/4°C for 10 min to remove cellular detritus, and stored at –80°C.

To minimize salt contamination, eluates were dialyzed against ultra high-quality water at 4°C (ten exchanges, 1.5 L each) using a semi-permeable membrane with a molecular mass cutoff at 7 kDa (Serva-Electrophoresis, Heidelberg, Germany) for 5 days. Dialyzed samples were dried down by vacuum evaporation (SpeedVac), and proteins were dissolved in a lysis buffer (7 M urea, 4% CHAPS, 40 mM Tris base, 2 M Thiourea, 2% IPG buffer, pH 3–10, 120 mM DTT). Blood samples for electrophoresis and immunoassays were processed by centrifugation only (at 1500 × *g* and 4°C for 10 min) to separate plasma (supernatant) and stored at –80°C. Samples for flow cytometry were kept at 5°C until analysis which followed within 1 h. Protein concentrations in samples were assessed using Bradford's dye-binding assay (Bio-Rad Protein Assay, Bio-Rad, Hercules, CA, USA).

2.3 2-DE

Urea, CHAPS, Tris base, thiourea, SDS, DTT, iodoacetamide (IAA), and bromphenol blue used during the preparation were purchased from Sigma-Aldrich (Steinheim, Germany); IPG buffer (ZOOM carrier Ampholytes 3–10) was purchased from Invitrogen (Carlsbad, CA, USA). Equally, 200 µg proteins in both eluate and plasma samples were mixed with rehydration buffer (7 M urea, 4% CHAPS, 40 mM Tris base, 2 M Thiourea, 2% IPG buffer pH 3–10, 120 mM DTT, and a trace amount of bromphenol blue) to

obtain the final volume of 185 μ L. Samples were then rehydrated in IPG strips (11 cm, pH range 3–10 nonlinear, Bio-Rad), and focused in a Protean IEF cell (Bio-Rad). IPG strips were rehydrated actively for 10 h at 50 V, followed by a stepwise IEF as follows: 250 V for 15 min, rapid ramp to 8000 V for 150 min, and finally 8000 V for the other 35 000 Vh. After focusing, the IPG strips were equilibrated in the equilibration buffer 1 (112 mM Tris-base, 6 M urea, 30% v/v glycerol, 4% w/v SDS, 130 mM DTT, and a trace of bromophenol blue) for 10 min, and subsequently alkylated in buffer 2 (112 mM Tris-base, 6 M urea, 30% v/v glycerol, 4% w/v SDS, 135 mM IAA, and a trace of bromophenol blue) for 10 min. Each equilibrated IPG strip was placed on the top of a 12.5% Criterion Tris-HCl gel (Bio-Rad) and covered with 0.5% agarose. Second-dimension separation was performed at 200 V until the bromophenol blue dye front reached the bottom of the gel. At the end of each run, the 2-D gels were stained with Simply Blue stain (Invitrogen), and scanned with an Epson Perfection 4990 Photo scanner (Epson, Long Beach, CA, USA) at 400 dpi resolution and in 16-bit greyscale.

2.4 2-DE pattern analysis and statistics

Computer-aided analysis of gel images was carried out using PDQuest 2-D software version 8.1 (Bio-Rad). A synthetic image was constructed out of the triplicated gels processed from each sample, using only spots constantly present in at least two gels. The protein quantity was determined relative to integrated spot density. For subsequent studies of characteristics in protein distribution, only spots detectable in at least 50% patients were considered eligible.

The statistical analysis was carried out by means of Statistica data analysis software (Version 8.0, Statsoft, Tulsa, OK, USA). PCA based on the correlation matrix of normalized spot intensities was applied on the proteomic data to reduce their dimensionality before picking spots for identification and designing the confirmatory studies. Due to relatively small sample size, data were assumed non-normally distributed. Therefore, Wilcoxon signed rank test was employed to compare dependent continuous variables, whereas Spearman rank order correlations were calculated to evaluate dependencies between variables. Multivariate analysis was performed using forward stepwise regression. If not stated otherwise, data are given as medians (inter-quartile ranges) to comply with nonparametric statistics. Differences were considered statistically significant if the *p*-values were below 0.01 for proteomic data and 0.05 for other data.

2.5 In-gel tryptic digestion

ACN, ammonium bicarbonate, DTT, IAA, TFA, formic acid, and CHCA were purchased from Sigma. First, selected spots were excised by EXQuest spot cutter (Bio-Rad). SimplyBlue

stain was removed by washing with 50 mM ammonium bicarbonate, and ACN. Proteins in gel were reduced with 10 mM DTT/50 mM ammonium bicarbonate at 56°C for 45 min, and alkylated with 55 mM IAA/50 mM ammonium bicarbonate (for 30 min, in the dark at room temperature). Gel plugs were washed with 50 mM ammonium bicarbonate and ACN, and dried by SpeedVac. Dried gel particles were rehydrated with digestion buffer containing 12.5 ng/ μ L sequencing grade trypsin (Roche) in 50 mM ammonium bicarbonate at 4°C. After 45 min, the remaining solution was removed, and replaced by 50 mM ammonium bicarbonate. Tryptic digestion was performed overnight (37°C). After digestion, proteolytic peptides were subsequently extracted with 50% ACN/25 mM ammonium bicarbonate, 5% formic acid, and 50% ACN/H₂O. The three extracts were pooled, and 10 mM DTT solution in 50 mM ammonium bicarbonate was added. The mixture was then dried by SpeedVac, and resulting tryptic peptides were dissolved in 5% formic acid solution and desalted using ZipTip μ C18 (Millipore, Bedford, MA, USA).

2.6 Protein identification by MALDI-TOF/TOF MS

Proteolytic peptides were mixed with CHCA matrix solution (5 mg/mL CHCA in 0.1% TFA/50% ACN 1:1, v/v) in 1:1 ratio, and 0.8 μ L of this mixture was spotted onto MALDI target. All mass spectra were acquired at a reflectron mode with a 4800 MALDI TOF/TOF Analyzer (Applied Biosystems, Framingham, MA, USA). A total of 2000 and 3000 laser shots were acquired, and averaged to MS and MS/MS spectra, respectively. The MS/MS analyses were performed using collision energy of 1 keV and collision gas pressure of 1.3 10⁻⁶ torr. MS peaks with an *S/N* above 15 were listed, and the ten strongest precursors with an *S/N* above 50 among the MS peaks were automatically selected for MS/MS acquisition. A mass filter was used to exclude autolytic peptides of trypsin and peaks of contaminant from polypropylene tubes [11].

Resulting data were analyzed with GPS ExplorerTM 3.6 (Applied Biosystems) software. Proteins were identified by searching against human subset of the Swiss-Prot protein database (release 54.6; December 4, 2007) using MASCOT 2.1.0 search algorithm (Matrix Science, London, UK). The general parameters for PMF search were considered to allow maximum two missed cleavages, \pm 50 ppm of peptide mass tolerance, variable methionine oxidation, and fixed cysteine carbamidomethylation. Probability-based MOWSE scores were estimated by comparison of search results against estimated random match population, and were reported as $-10 \log_{10}(p)$ where *p* is the absolute probability. MOWSE scores greater than 55 were considered significant (*p* < 0.05) for PMF. A peptide charge state of +1 and fragment mass tolerance of \pm 0.25 Da were used for the MS/MS ion search. Individual MS/MS ions scores > 28 indicated identity or extensive homology (*p* < 0.05) for MS/MS ion search.

2.7 Fluorescence-activated cell sorting (FACS)

Both whole blood and dialyzer elution samples were incubated with purified rabbit immunoglobulin for 10 min at room temperature to decrease nonspecific binding. Samples were then washed in PBS-BSA and incubated for 15 min at 4°C with FITC-, PE- or PE-Cy5-conjugated monoclonal antibodies against antigens CD15, CD63, CD14, CD62L, CD11b, CD66b, and CD45 (Exbio, Prague, Czech Republic; CD66b BioLegend, San Diego, CA, USA). Following the PBS-BSA washing, erythrocytes were lysed by adding NH₄Cl-based in-house lysing solution for 10 min at room temperature.

Stained cells were measured immediately on Coulter Epics XL flow cytometer (Beckman Coulter, Fullerton, CA, USA). The instrument was standardized daily for fluorescence and light scatter using calibrating fluorospheres (Beckman Coulter). Neutrophils and monocytes were identified in the CD45 *versus* side-scatter plot. Data of minimally 20 000 cells were gathered in list mode files and analyzed

using System II software. Antigen expression was defined as mean fluorescence intensity.

2.8 ELISA

Ficolin-2 concentrations were determined using human L-Ficolin kit (Hycult Biotech, Uden, the Netherlands) at all time points, both before and after the hemodialyzer, whereas mannan-binding lectin serine protease 2 (MASP-2) was measured using MASP-2 kit (Hycult Biotech) at all timepoints before the dialyzer only. C5a plasma levels were assessed with human C5a kit (DRG Instruments, Marburg, Germany) at all time points, in blood taken before the dialyzer only. Thrombin-antithrombin (TAT) plasma concentrations were quantified by Enzygnost TAT micro kit (Behring Diagnostics, Marburg, Germany) before and at the end of the HD procedure, in blood taken from the arterial line. All ELISA measurements were performed according to the manufacturer's directions.

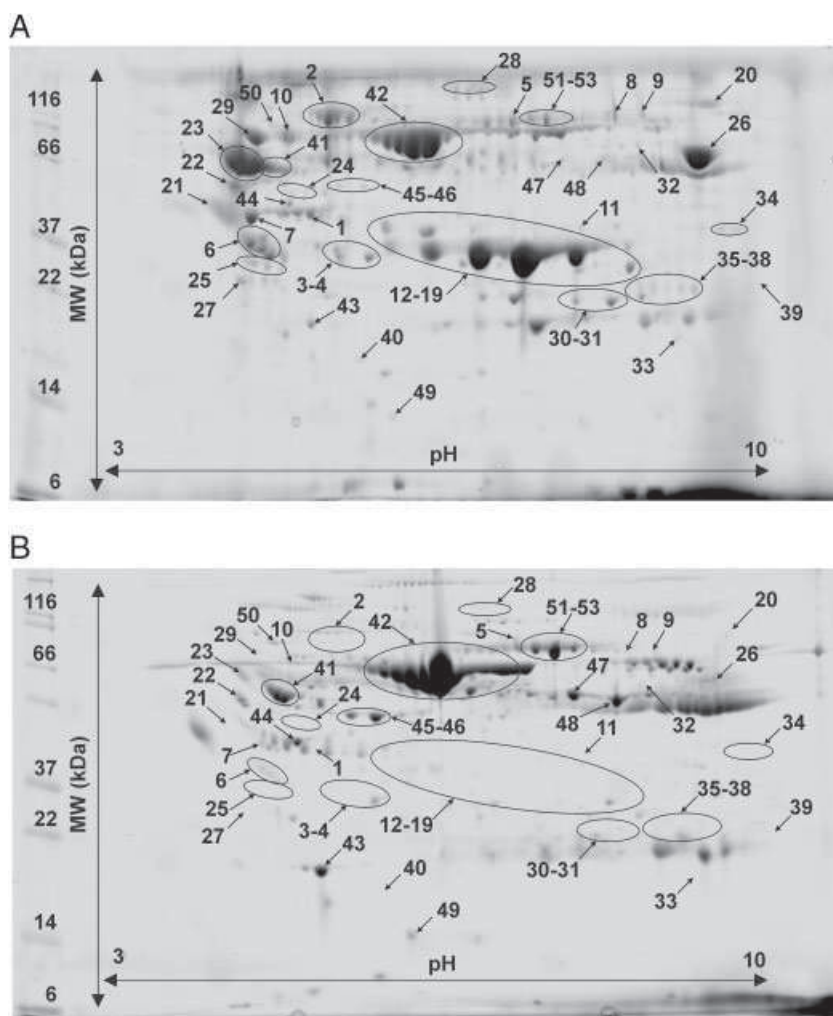


Figure 1. Representative gel images of eluate and plasma. Representative gel images of eluate (A) and plasma (B). Identified proteins are labeled with spot numbers (identifications in Table 1). MW, molecular weight.

3 Results

3.1 Proteomics of the hemodialyzer eluate

Dialyzer elution with acetic acid yielded a median of 7.2 mg proteins with relatively high variation (quartile range, 34.7 mg). Following 2-DE, 217 protein fractions (spots) were detected in hemodialyzer eluates. Of those, 164 spots were found in at least 50% patients and 42 spots were present constantly in all patients. In 112 spots, relative intensities differed significantly (with $p < 0.01$) between eluate and plasma – 46 spots prevailed in eluate, whereas 66 were predominant in plasma. Representative gel images are shown in Fig. 1.

To reduce data complexity and uncover specific patterns in protein distribution, the spot intensities derived from both eluate and plasma were submitted to PCA. Depending on the two major factors, protein fractions formed three separate clusters with diverse eluate to plasma ratios of relative spot intensities (E/P) (Fig. 2). The largest cluster (C) comprises spots with E/P less than one, whereas the other two reach average E/P several orders of magnitude higher. Meaning of this unsupervised classification was subsequently validated by MS identification of specific spots from each group and ensuing biological context analysis (Table 1).

The proteins' identity was further verified by a match between theoretical (calculated from gene-sequence data in Swiss-Prot database) and measured (as estimated by spot's coordinates in gel) molecular weight (MW) and pI . Where the observed MW showed lower than expected, fragmentation was suspected and checked by detailed analysis of

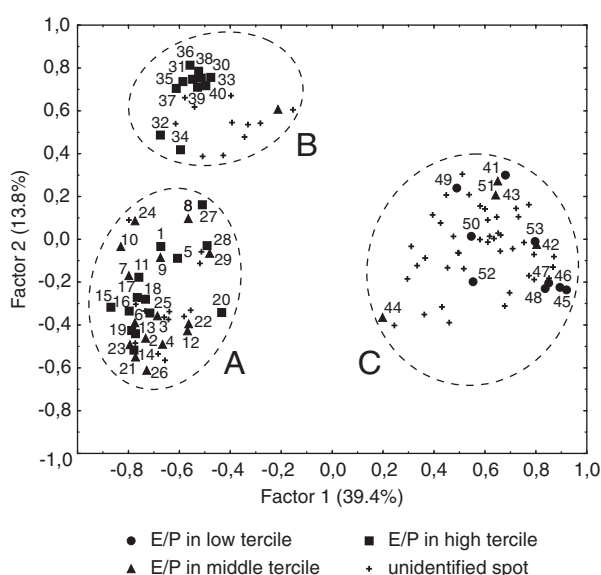


Figure 2. Exploratory data analysis of relative spot intensities. PCA – projection of individual protein spots onto the factor plane, three clusters are distinguished with different E/P : A 189.4 (73.9), B 498.1 (97.7), and C 0.5 (64.5); ANOVA $p < 0.001$.

identification spectra. In this way, we ascertained proteolytic activation of mannan-binding lectin serine protease 1 (MASP-1), MASP-2, and C3 complement as their proper cleavage products were detected by PMF and MS/MS.

Concurrent detection of caldesmon with albumin and transferrin in one spot is a clear example of contamination from adjacent high-volume spots. Yet in another case, proteins with rather disparate MW and pI were identified in one spot: MASP-1 light chain occurred in conjunction with antithrombin III and complement C3g fragment. Moreover, the actual MW of the spot estimated from its coordinates in gel is 84 kDa, *i.e.* corresponding to the sum of their weights (49, 28, and 5 kDa, respectively). Thus, the presence of a SDS-stable (*i.e.* covalently bound) complex formed by these three proteins was confirmed.

3.2 Systemic biocompatibility markers

A significant decrease in total leukocyte count was documented in systemic blood at 15 min which was diminished yet persistent at the end of HD (Fig. 3A). Similar trend was demonstrated for leukocyte subpopulations, namely granulocytes, monocytes, and lymphocytes (Supporting Information file). Leukocyte surface antigens were investigated on blood granulocytes and monocytes during HD and thereafter in dialyzer eluates. In this way, enhanced adhesivity (estimated by CD11b, CD14, and CD15 upregulation and CD62L downregulation) and degranulation (evaluated by CD63 and CD66b upregulation) were confirmed both in blood leaving the dialyzer at 15 min and in dialyzer eluates obtained immediately after dialysis (Supporting Information file).

The rate of complement activation during HD was assessed by measuring systemic concentration of C5a component (Fig. 3B). Plasma level of TAT complexes rose significantly from 4.6 (3.5) $\mu\text{g/L}$ to 16.6 (20.2) $\mu\text{g/L}$ ($p < 0.001$) during the 4-h dialysis session. The initial thrombocyte count was found to decrease slightly at 15 min in blood leaving the dialyzer (180 [70] $10^9/\text{L}$ versus 170 [76] $10^9/\text{L}$, $p = 0.04$); however, no significant drop in systemic blood could be documented, and the count recovered completely before 240 min.

3.3 Plasma ficolin-2 and MASP-2 dynamics and relationships to biocompatibility parameters

The extent of ficolin-2 extraction inside hemodialyzer was determined as a difference in serum concentrations between arterial and venous ports. It was found to be maximum at the beginning and steadily decreasing afterward, however, still significant at 15 min (Fig. 3C). Concurrently, a sustained decline in systemic ficolin-2 level was observed throughout the HD session, such that the procedure resulted in 41 (4.7) % decrement of serum ficolin-2. As much as

Table 1. Proteins identified in dialyzer eluates

Spot no. ^{a)}	Protein name	Acc. no	<i>E/P</i> ^{b)}	<i>p</i> ^{c)}	MW ^{d)}	<i>pI</i> ^{d)}	PMF ^{e)} pep/sco	MS/MS ^{e)} pep/sco
Cluster A^{f)}								
1	Actin β	P60709	366.3 (814.48)	<0.001	42	5.3	8/76	NA
	Actin γ	P63261			42	5.3	9/90	NA
2	Antithrombin 3	P01008	4.8 (12.97)	<0.001	49	6	14/69	6/523
	Mannan-binding lectin serine protease1 light chain	P48740			28	6	NA	1/78
	Complement C3g	P01024			5	4	NA	1/95
3–4	Apolipoprotein E	P02649	3.6 (6.68)	0.002	34	5.5	25/198	6/195
5	Caldesmon 1	Q05682	100.3 (245.26)	<0.001	93	5.6	NA	1/35
	Albumin	P02768			67	5.7		
	Transferrin	P02787			75	6.7		
6	Clusterin	P10909	6.0 (7.89)	<0.001	50	5.9	10/63	5/187
7	Complement C3c α 2	P01024	9.1 (128.34)	<0.001	24	6.9	29/99	9/555
8/9	Complement C3 β	P01024	3.6 (3.93)	<0.001	71	6.8	27/109	9/449
10	Complement C9	P02748	6.6 (6.94)	<0.001	61	5.4	NA	4/133
11	Complement factor H-related protein 1	Q03591	70.3 (80.92)	<0.001	36	7.1	NA	2/28
12–19	Ficolin 2	Q15485	119.7 (171.10)	<0.001	34	6.3	12/91	5/203
20	Lactotransferrin	P02788	161.6 (259.81)	<0.001	76	8.5	23/107	4/173
21–23	Mannan-binding lectin serine protease 1 heavy chain	P48740	3.2 (6.69)	<0.001	49	4.9	18/151	8/287
24	Mannan-binding lectin serine protease 2 chain A	O00187	10.6 (14.12)	<0.001	48	5.4	13/66	8/447
25	Microfibril-associated glycoprotein 4	P55083	41.1 (60.90)	<0.001	26	5.2	NA	3/73
26	Properdin	P27918	4.3 (12.29)	0.01	51	8.3	12/72	3/30
27	Tropomyosin 3	P06753	185.9 (570.28)	<0.001	33	4.7	13/77	4/76
	Tropomyosin 4	P67936			29	4.7	18/143	5/103
28	Vinculin	P67936	53.7 (159.26)	0.01	124	5.5	18/127	2/32
29	Vitronectin	P04004	8.0 (175.45)	0.004	54	5.6	8/6	NA
Cluster B								
30–31	Carbonic anhydrase 1	P00915	1568.2 (2482.90)	<0.001	29	6.6	10/77	3/43
32	Catalase	P04040	170.5 (221.33)	<0.001	60	7	NA	2/28
33	Flavin reductase	P30043	295.2 (288.90)	<0.001	22	7.3	NA	1/60
34	Glyceraldehyde-3-phosphate dehydrogenase	P04406	137.7 (206.87)	<0.001	36	8.6	NA	3/110
35–39	Hemoglobin α	P69905	849.0 (1999.73)	<0.001	15	8.7	NA	2/86
	Hemoglobin β	P68871			16	6.8	5/57	4/160
40	Peroxiredoxin 2	P32119	399.5 (503.07)	<0.001	22	5.7	5/92	2/30
Cluster C								
41	α 1-Antitrypsin	P01009	0.5 (0.24)	0.005	44	5.4	19/226	6/425
42	Albumin	P02768	0.6 (0.36)	<0.001	67	5.7	31/149	8/490
43	Apolipoprotein A1	P02647	0.7 (0.55)	0.01	28	5.3	11/88	4/180
44	Apolipoprotein A4	P06727	0.7 (0.37)	0.005	43	5.2	23/171	5/84
45–46	Fibrinogen β	P02675	0.1 (0.20)	<0.001	56	8.5	11/77	NA
47–48	Fibrinogen γ	P02679	0.1 (0.24)	<0.001	52	5.4	4/63	1/30
49	Haptoglobin	P00738	0.5 (0.34)	0.002	45	6.1	NA	3/47
50	Prothrombin	P00734	0.5 (0.54)	0.006	65	5.2	8/78	3/49
51–53	Transferrin	P02787	0.5 (0.23)	<0.001	75	6.7	26/170	8/561

a) Spot numbers correspond with labels in Fig. 2.

b) Data are given as median (quartile range).

c) Statistical significance of differences between eluate and plasma (*E/P*) relative spot intensities was confirmed with a signed rank test.

d) Theoretical value calculated from Swiss-Prot sequence data.

e) Peptide sequences and spectra of selected proteins are available as a Supporting Information file.

f) The division into clusters corresponds to Fig. 1B.

35% of the overall loss of ficolin-2 occurred during the first 15 min. This intradialytic loss of serum ficolin-2 did not correlate with either procedure settings (heparin dose and ultrafiltration rate) or predialysis laboratory parameters (blood picture, activated partial thromboplastin time, and serum calcium) but depended largely on the initial ficolin-2 level ($R = 0.74$, $p < 0.001$). The alterations in MASP-2 plasma concentration were much more discreet – at 15 min, only a trend to decrease was notable ($p = 0.07$) followed by a mild, though statistically significant, elevation at 240 min (Fig. 3D).

Leukocyte depletion in peripheral blood, both at 15 min and at the end of dialysis, was found to be clearly proportional to parallel ficolin-2 elimination ($r = 0.73$, $p = 0.001$; $r = 0.74$, $p = 0.001$, respectively). In a multivariate model, separate effects of ficolin-2 concentration decrease ($R^2 = 0.62$, $p = 0.01$) and C5a level elevation ($R^2 = 0.36$, $p = 0.01$) were shown to predict independently the changes in leukocyte count (all parameters at 15 min *versus* baseline). CD62L expression in peripheral blood at 15 min was related to ficolin-2 adsorption ($r = 0.76$, $p < 0.001$) and the down-regulation of CD62L on granulocytes retrieved from the dialyzer postdialysis was negatively correlated with ficolin-2 adsorption until 15 min ($r = -0.64$, $p = 0.01$) and during the complete procedure ($r = -0.61$, $p = 0.02$). Similarly in monocytes – both in peripheral blood leaving the dialyzer

($r = -0.66$, $p = 0.005$) and in the eluates ($r = -0.69$, $p = 0.004$), the decrement of CD62L expression was inversely proportional to ficolin-2 adsorption until 15 min.

Both initial and 15 min ficolin-2 levels correlated with C5a production expressed as ratio of concentrations at 15 min to baseline ($r = 0.68$, $p = 0.004$ and $r = 0.72$, $p = 0.002$, respectively). Moreover, the magnitude of ficolin-2 consumption during the first 15 min was associated with C5a generation ($r = 0.64$, $p = 0.01$). No correlation whatsoever was observed between TAT production or platelet counts and ficolin-2 levels or clearance at any timepoint.

4 Discussion

A recently introduced technique of sequential elution combined with gel-based proteomics [10] was employed to study proteins adsorbed to a polysulfone hemodialyzer during clinical HD. At the same time, basic markers of dialyzer incompatibility, namely leukocyte counts and surface antigen expression, thrombogenicity, and complement activation, were monitored. To the best of our knowledge, this is the first report describing blood-dialyzer interactome and connecting it to systemic biocompatibility.

PCA was used to discriminate meaningful structures among more than 4500 spot intensities generated during

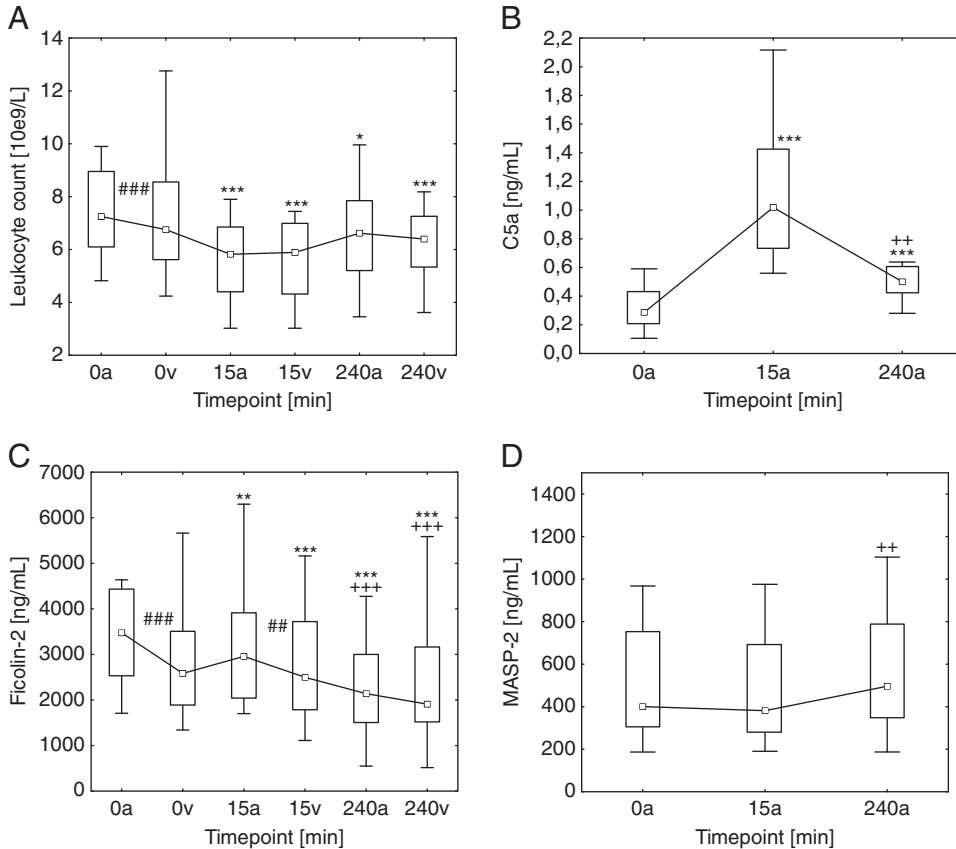


Figure 3. Systemic biocompatibility markers. Leukocyte counts (A), complement C5a (B), ficolin-2 (C), and MASP-2 (D) plasma levels were assessed before dialysis (0 min), at 15 min and at 4 h (240 min). Leukocyte counts and ficolin-2 concentrations were determined both at the dialyzer inlet (a) and at the outlet (v). Data are presented as box plots with medians, quartiles, and nonoutlier ranges, statistical significance confirmed with Wilcoxon signed rank test. 15 and 240 min *versus* 0 min: * $p < 0.05$, ** $p < 0.01$, *** $p < 0.001$; 240 min *versus* 15 min: + $p < 0.05$, ++ $p < 0.01$; pre *versus* post-dialyzer: # $p < 0.05$, ## $p < 0.01$, and ### $p < 0.001$.

Clinical Relevance

The number of patients receiving HD is still increasing yet their mortality stays extremely high (15–20% *per year*) mainly due to accelerated atherosclerosis and disturbed immune defense. Chronic inflammation elicited by contact of blood with the dialysis membrane is considered a significant factor despite the introduction of biocompatible materials, *e.g.* polysulfone. The systemic consequences of dialyzer-induced inflammation have been extensively scrutinized; however, its local triggers remain unclear. We have adopted a completely novel approach to biocompatibility and report the first representative picture of blood-dialyzer interactome

obtained in clinical context. Besides describing the molecular background of dialysis-associated inflammatory response, our study provides at least two messages with potential significance for clinical practice. First, we suggest lectin-mediated carbohydrate recognition pathway plays a central role in initiating the complement and leukocyte activation. This knowledge could help to develop better tolerated biodevices. Second, we show that extracorporeal procedures may result in unwanted and possibly harmful depletion of individual proteins. Proteomic tools seem appropriate to characterize adsorptive properties of new materials.

the analysis of eluate proteome. The first principal component clearly segregated the proteins with low *E/P*. Similar occurrence in plasma and eluate indicates this group as contamination, probably due to the imperfect wash-out of plasma residues. Indeed, most of the spots were later identified as abundant plasma proteins (cluster C). Along the second component, two clusters of proteins significantly accumulated in eluates were separated. Maximum eluate enrichment was apparent in ubiquitous intracellular enzymes (cluster B) which undoubtedly arose from lysis of entrapped blood cells. On the other hand, high *E/P* observed in plasma proteins from cluster A can be interpreted as an indicator of a specific adsorption to the dialyzer [9, 10].

Proteins classified into the same group display similar spot intensity patterns and thus could imply biologically relevant interactions which, however, need to be validated either experimentally or by analysis of references. In this way, several well-established physiological circuits can be distinguished within the cluster A. Co-occurrence of ficolin-2 and MASPs indicates involvement of the lectin pathway [12], whereas the vicinity of properdin probably reflects coupling to amplification loop of the alternative pathway [13], or, alternatively, properdin could operate as another pattern recognition molecule [14]. The course of complement activation can be further modulated by clusterin and FHR1.

Cytoskeleton elements, *i.e.* tropomyosins, actins, caldesmon, and vinculin, together with G3P constitute a morphological and functional complex [15] responsible for cell-substrate adhesion [16, 17]. Their clear separation from cluster B suggests they represent rather the process of adhesion *per se* than just residual cellular debris. Such concept is further supported by the association with vitronectin, a soluble mediator of cell adhesion [18]. Speculatively, lactotransferrin accumulation might also be related due to actin-dependent exocytosis of neutrophil-specific granules [19]. Other relationships can be hypothesized with regard to the literature – adsorption of MFAP-4

might reflect its reported affinity for both carbohydrates and collectins [20], whereas the role of antithrombin 3 as MASP inhibitor is favored by observed covalent binding with MASP-1 [21].

Parallel and abundant occurrence of key molecules involved in lectin pathway implies contribution of this mode of complement activation to dialyzer-induced inflammatory response. To test this assumption, we chose two proteins inherent to the lectin pathway and reaching high *E/P*, namely ficolin-2 and MASP-2. Sequential determination of their plasma levels showed a continuous removal of ficolin-2 during HD, resulting in its substantial depletion. With respect to the size of native ficolin-2 [22] (multimers with MW of 403 and 807 kDa), and taking into account its prevalence in eluate proteome, the major cause of this elimination seems to be adsorption to the dialyzer (ultrafiltrate is devoid of ficolin-2, gel image is available as a Supporting Information file). Any potential changes in MASP-2 levels were probably outbalanced by other sources of the protein (MBL and H-ficolin complexes) [23].

Our results demonstrate for the first time a loss of ficolin-2 occurring in patients treated with HD on a polysulfone membrane. Whether this depletion is only transient and the ficolin-2 level recovers completely or if these patients suffer from chronic ficolin-2 insufficiency cannot be concluded from this study. Still, it is pertinent to hypothesize about potential clinical impact of such condition. Ficolin-2 (L-ficolin) is a pattern recognition molecule which plays an important role in innate immunity, both cellular and humoral [24]. It has been shown to bind to a variety of surface antigen structures found in many Gram-positive and Gram-negative bacteria including significant pathogens, *e.g.* pneumococci, staphylococci, and *E. coli*, as well as yeasts [25–29]. Ficolin itself promotes opsonophagocytosis and in concert with MASP-2 activates complement.

Low levels of MBL, an earlier discovered member of the lectin family, have been linked to increased risk of infections

[30, 31] and similar data on ficolin-2 began to emerge recently [32]. Considering their different substrate specificities [33], isolated ficolin-2 deficiency might induce susceptibility to particular pathogens. As the amount of ficolin-2 removed during dialysis depended largely on its initial level, the process of adsorption seems to be governed by direct ficolin–polysulfone affinity. Therefore, we would expect even higher ficolin-2 consumption with larger dialyzer or prolonged exposure (continuous renal replacement therapy).

Apart from quantifying the loss of ficolin-2, the confirmatory studies were targeted to elucidate whether binding of ficolin–MASP complexes can be linked to any accepted markers of dialyzer incompatibility. The adsorption is specific for the lectin pathway, yet further downstream localized steps could significantly modify its impact on complement activation [13]. Therefore, in addition to providing direct evidence of ficolin-2 adsorption and MASP-2 activation by proteomic analysis, we documented, for the first time, its association with dialysis-induced leukopenia and C5a generation.

The principal finding derived from FACS analysis was the correlation of CD62L surface expression with ficolin-2 adsorption discovered in both granulocytes and monocytes. CD62L (L-selectin) is an important leukocyte homing receptor of lectin nature which is required to initiate leukocyte capture, rolling, and adhesive interactions [34, 35]. The cytoplasmic domain of L-selectin has been reported to be anchored to actin-tropomyosin cytoskeleton *via* vinculin [36, 37], and hence identification of the latter proteins in eluate supports the role of CD62L. Nevertheless, provided ficolin-2 mediates the interaction of leukocytes with dialysis membrane *via* L-selectin, we would expect to find an opposite correlation due to receptor shedding. An intriguing explanation could be that ficolin-2 might occupy putative lectin ligands on polysulfone membrane and thus prevent interaction with leukocyte L-selectin and its shedding. Such competition between ficolin-2 and L-selectin would anticipate an overlap of substrate specificity in these two lectins.

We can conclude that proteomic analysis of dialyzer eluates provides solid data to consider lectin pathway initiated by ficolin-2 adsorption a significant process involved in complement activation by polysulfone membrane. It has been demonstrated that plasma exposure to artificial material may cause unwanted elimination of individual proteins during extracorporeal procedures. The proteomic technique has been proved effective in identifying the proteins subject to specific adsorption.

The study was supported by Research Project No. MSM0021620819 “Replacement of, and support to some vital organs” awarded by the Ministry of Education of the Czech Republic.

The authors have declared no conflict of interest.

5 References

- [1] Grassmann, A., Gioberge, S., Moeller, S., Brown, G., End-stage renal disease: global demographics in 2005 and observed trends. *Artif. Organs* 2006, **30**, 895–897.
- [2] Goodkin, D. A., Bragg-Gresham, J. L., Koenig, K. G., Wolfe, R. A. *et al.*, Association of comorbid conditions and mortality in hemodialysis patients in Europe, Japan, and the United States: the Dialysis Outcomes and Practice Patterns Study (DOPPS). *J. Am. Soc. Nephrol.* 2003, **14**, 3270–3277.
- [3] Jofre, R., Rodriguez-Benitez, P., Lopez-Gomez, J. M., Perez-Garcia, R., Inflammatory syndrome in patients on hemodialysis. *J. Am. Soc. Nephrol.* 2006, **17**, S274–S280.
- [4] MacLeod, A., Daly, C., Khan, I., Vale, L. *et al.*, Comparison of cellulose, modified cellulose and synthetic membranes in the haemodialysis of patients with end-stage renal disease. *Cochrane Database Syst. Rev.* 2005, DOI: 10.1002/14651858.CD003234. pub2.
- [5] Hernandez, M. R., Galan, A. M., Cases, A., Lopez-Pedret, J. *et al.*, Biocompatibility of cellulosic and synthetic membranes assessed by leukocyte activation. *Am. J. Nephrol.* 2004, **24**, 235–241.
- [6] Nilsson, B., Ekdahl, K. N., Mollnes, T. E., Lambris, J. D., The role of complement in biomaterial-induced inflammation. *Mol. Immunol.* 2007, **44**, 82–94.
- [7] Lhotta, K., Wurzner, R., Kronenberg, F., Oppermann, M., Konig, P., Rapid activation of the complement system by cuprophane depends on complement component C4. *Kidney Int.* 1998, **53**, 1044–1051.
- [8] Craddock, P. R., Fehr, J., Dalmasso, A. P., Brigham, K. L., Jacob, H. S., Hemodialysis leukopenia. Pulmonary vascular leukostasis resulting from complement activation by dialyzer cellophane membranes. *J. Clin. Invest.* 1977, **59**, 879–888.
- [9] Mares, J., Thongboonkerd, V., Tuma, Z., Moravec, J. *et al.*, Proteomic analysis of proteins bound to adsorption units of extracorporeal liver support system under clinical conditions. *J. Proteome Res.* 2009, **8**, 1756–1764.
- [10] Mares, J., Thongboonkerd, V., Tuma, Z., Moravec, J., Matejovic, M., Specific adsorption of some complement activation proteins to polysulfone dialysis membranes during hemodialysis. *Kidney Int.* 2009, **76**, 404–413.
- [11] Sachon, E., Matheron, L., Clodic, G., Blasco, T., Bolbach, G., MALDI TOF-TOF characterization of a light stabilizer polymer contaminant from polypropylene or polyethylene plastic test tubes. *J. Mass Spectrom.* 2010, **45**, 43–50.
- [12] Matsushita, M., Fujita, T., Ficolins and the lectin complement pathway. *Immunol. Rev.* 2001, **180**, 78–85.
- [13] Harboe, M., Mollnes, T. E., The alternative complement pathway revisited. *J. Cell. Mol. Med.* 2008, **12**, 1074–1084.
- [14] Kemper, C., Hourcade, D. E., Properdin: new roles in pattern recognition and target clearance. *Mol. Immunol.* 2008, **45**, 4048–4056.
- [15] Xu, P., Crawford, M., Way, M., Godovac-Zimmermann, J. *et al.*, Subproteome analysis of the neutrophil cytoskeleton. *Proteomics* 2009, **9**, 2037–2049.

- [16] Asijee, G. M., Sturk, A., Bruin, T., Wilkinson, J. M., Ten Cate, J. W., Vinculin is a permanent component of the membrane skeleton and is incorporated into the (re)organising cytoskeleton upon platelet activation. *Eur. J. Biochem.* 1990, *189*, 131–136.
- [17] Wernimont, S. A., Cortesio, C. L., Simonson, W. T., Huttenlocher, A., Adhesions ring: a structural comparison between podosomes and the immune synapse. *Eur. J. Cell. Biol.* 2008, *87*, 507–515.
- [18] Jenney, C. R., Anderson, J. M., Adsorbed serum proteins responsible for surface dependent human macrophage behavior. *J. Biomed. Mater. Res.* 2000, *49*, 435–447.
- [19] Jog, N. R., Rane, M. J., Lominadze, G., Luerman, G. C. *et al.*, The actin cytoskeleton regulates exocytosis of all neutrophil granule subsets. *Am. J. Physiol. Cell. Physiol.* 2007, *292*, C1690–C1700.
- [20] Lausen, M., Lynch, N., Schlosser, A., Tornoe, I. *et al.*, Microfibril-associated protein 4 is present in lung washings and binds to the collagen region of lung surfactant protein D. *J. Biol. Chem.* 1999, *274*, 32234–32240.
- [21] Presanis, J. S., Hajela, K., Ambrus, G., Gal, P., Sim, R. B., Differential substrate and inhibitor profiles for human MASP-1 and MASP-2. *Mol. Immunol.* 2004, *40*, 921–929.
- [22] Hummelshoj, T., Thielens, N. M., Madsen, H. O., Arlaud, G. J. *et al.*, Molecular organization of human Ficolin-2. *Mol. Immunol.* 2007, *44*, 401–411.
- [23] Cseh, S., Vera, L., Matsushita, M., Fujita, T. *et al.*, Characterization of the interaction between L-ficolin/p35 and mannan-binding lectin-associated serine proteases-1 and -2. *J. Immunol.* 2002, *169*, 5735–5743.
- [24] Runza, V. L., Schwaeble, W., Mannel, D. N., Ficolins: novel pattern recognition molecules of the innate immune response. *Immunobiology* 2008, *213*, 297–306.
- [25] Aoyagi, Y., Adderson, E. E., Rubens, C. E., Bohnsack, J. F. *et al.*, L-Ficolin/mannose-binding lectin-associated serine protease complexes bind to group B streptococci primarily through N-acetylneuraminic acid of capsular polysaccharide and activate the complement pathway. *Infect. Immun.* 2008, *76*, 179–188.
- [26] Lynch, N. J., Roscher, S., Hartung, T., Morath, S. *et al.*, L-ficolin specifically binds to lipoteichoic acid, a cell wall constituent of Gram-positive bacteria, and activates the lectin pathway of complement. *J. Immunol.* 2004, *172*, 1198–1202.
- [27] Matsushita, M., Endo, Y., Taira, S., Sato, Y. *et al.*, A novel human serum lectin with collagen- and fibrinogen-like domains that functions as an opsonin. *J. Biol. Chem.* 1996, *271*, 2448–2454.
- [28] Lu, J., Le, Y., Ficolins and the fibrinogen-like domain. *Immunobiology* 1998, *199*, 190–199.
- [29] Ma, Y. G., Cho, M. Y., Zhao, M., Park, J. W. *et al.*, Human mannose-binding lectin and L-ficolin function as specific pattern recognition proteins in the lectin activation pathway of complement. *J. Biol. Chem.* 2004, *279*, 25307–25312.
- [30] Hoefflich, C., Unterwalder, N., Schuett, S., Schmolke, K. *et al.*, Clinical manifestation of mannose-binding lectin deficiency in adults independent of concomitant immunodeficiency. *Hum. Immunol.* 2009, *70*, 809–812.
- [31] Brouwer, N., Frakking, F. N., van de Wetering, M. D., van Houdt, M. *et al.*, Mannose-binding lectin (MBL) substitution: recovery of opsonic function *in vivo* lags behind MBL serum levels. *J. Immunol.* 2009, *183*, 3496–3504.
- [32] Cedzynski, M., Atkinson, A. P., St Swierzko, A., MacDonald, S. L. *et al.*, L-ficolin (ficolin-2) insufficiency is associated with combined allergic and infectious respiratory disease in children. *Mol. Immunol.* 2009, *47*, 415–419.
- [33] Krarup, A., Thiel, S., Hansen, A., Fujita, T., Jensenius, J. C., L-ficolin is a pattern recognition molecule specific for acetyl groups. *J. Biol. Chem.* 2004, *279*, 47513–47519.
- [34] Rabb, H., Agosti, S. J., Bittle, P. A., Fernandez, M. *et al.*, Alterations in soluble and leukocyte surface L-selectin (CD 62L) in hemodialysis patients. *J. Am. Soc. Nephrol.* 1995, *6*, 1445–1450.
- [35] Rosen, S. D., Ligands for L-selectin: homing, inflammation, and beyond. *Annu. Rev. Immunol.* 2004, *22*, 129–156.
- [36] Pavalko, F. M., Walker, D. M., Graham, L., Goheen, M. *et al.*, The cytoplasmic domain of L-selectin interacts with cytoskeletal proteins via alpha-actinin: receptor positioning in microvilli does not require interaction with alpha-actinin. *J. Cell. Biol.* 1995, *129*, 1155–1164.
- [37] Yuruker, B., Niggli, V., Alpha-actinin and vinculin in human neutrophils: reorganization during adhesion and relation to the actin network. *J. Cell Sci.* 1992, *101*, 403–414.

Proteomic approaches to the study of renal mitochondria

Zdenek Tuma^a, Jitka Kuncova^{a,b}, Jan Mares^{a,c}, Martina Grundmanova^{a,b}, Martin Matejovic^{a,c}

Background and Aims. Dysfunction of kidney mitochondria plays a critical role in the pathogenesis of a number of renal diseases. Proteomics represents an untargeted attempt to reveal the remodeling of mitochondrial proteins during disease. Combination of separation methods and mass spectrometry allows identification and quantitative analysis of mitochondrial proteins including protein complexes. The aim of this review is to summarize the methods and applications of proteomics to renal mitochondria.

Methods. Using keywords "mitochondria", "kidney", "proteomics", scientific databases (PubMed and Web of knowledge) were searched from 2000 to August 2015 for articles describing methods and applications of proteomics to analysis of mitochondrial proteins in kidney. Included were publications on mitochondrial proteins in kidneys of humans and animal model in health and disease.

Results and Conclusion. Proteomics of renal mitochondria has been/is mostly used in diabetes, hypertension, acidosis, nephrotoxicity and renal cancer. Integration of proteomics with other methods for examining protein activity is promising for insight into the role of renal mitochondria in pathological states. Several challenges were identified: selection of appropriate model organism, sensitivity of analytical methods and analysis of mitochondrial proteome in different renal zones/biopsies in the course of various kidney disorders.

Key words: renal mitochondria, proteomics, gel electrophoresis, liquid chromatography-mass spectrometry, diabetes, acidosis, nephrotoxicity, renal cancer

Received: October 12, 2015; Accepted with revision: March 3, 2016; Available online: March 17, 2016
<http://dx.doi.org/10.5507/bp.2016.012>

^aBiomedical Center, Faculty of Medicine in Pilsen, Charles University in Prague, Pilsen, Czech Republic

^bDepartment of Physiology, Faculty of Medicine in Pilsen, Charles University in Prague, Pilsen, Czech Republic

^cDepartment of Internal Medicine I, Faculty of Medicine in Pilsen, Charles University in Prague and Teaching Hospital, Pilsen, Czech Republic
Corresponding author: Zdenek Tuma, e-mail: Zdenek.Tuma@lfp.cuni.cz

INTRODUCTION

Mitochondria were recognized in the cell in the 19th century. In the first half of the 20th century, biochemical studies were carried out on mitochondrial enzymes and pathways. Electron transport mechanisms and oxidative phosphorylation were then intensively studied¹. Currently, mitochondria are known to be responsible for a variety of functions including regulation of intracellular calcium², generation of reactive oxygen species (ROS) (ref.³), production of nitric oxide⁴ and processes leading to cell death⁵.

Renal mitochondria are important as energy suppliers for active transport processes in nephrons⁶. Dysfunction of mitochondria caused by inherited mitochondrial cytopathies or acquired defects of proteins involved in mitochondrial metabolic pathways contributes to the pathophysiology of acute and chronic renal disorders⁷. Disruption of mitochondrial energetic metabolism⁷⁻⁹ and morphology^{10,11} is recognized as important contributors to tubular dysfunction in acute kidney injury (AKI). Increased production of ROS triggered by hypoxia in mitochondria during sepsis leads to kidney dysfunction and contributes to dysfunction of organs. ROS produced by mitochondria are important in the development of endothelial cell damage during focal segmental glomerulosclerosis (FSGS) (ref.¹²). Specific impairment of renal

mitochondrial metabolism has also been observed in cancer¹³, diabetes^{14,15} and as a consequence of toxic metabolite removal¹⁶. Emerging evidence also suggests that mitochondria represent a promising target for novel treatments¹⁷⁻¹⁹.

Proteomics was initially defined as an effort to identify and describe the complete set of proteins expressed in biological systems. Nowadays, proteomics include the study of protein-protein interactions, subcellular locations, expression levels, and posttranslational modifications of all proteins within cells and tissues. Hence, the proteomics of mitochondria is a powerful tool for understanding the mechanism of mitochondrial response to pathological conditions, evaluating the effects of drugs and for the development of new mitochondria-targeted therapies^{20,21}. Proteomic analysis of renal mitochondria represents a multi-step process that starts with selection of appropriate biological sample and optional reduction of complexity. The next step is a combination of separation methods and mass spectrometry for qualitative and quantitative analysis of proteins and their identification. Data on changes in expression of mitochondrial enzymes, posttranslational modifications, and subunit structure of protein complexes are acquired. The purpose of this review is to provide an update on the methodological progress and potential of the rapidly evolving mitochondrial proteomics approach to facilitate new discoveries in the field of renal pathology.

Sample preparation

For studies of renal mitochondrial proteome, tissue samples acquired from animal models or human tissues after resection are used. Renal biopsies are challenging due to small size and therefore limited amount of mitochondrial protein available. Cell cultures as an alternative to laboratory animals are useful for investigation of processes in specific renal cell types²².

Organized distribution of nephrons in renal tissue results in formation of regions with different biochemical and metabolic properties. Differences in the activity of mitochondrial enzymes along the nephron reflect the heterogeneity of the mitochondrial population in nephron segments²³. Therefore, separation of kidney regions (e.g. cortex and medulla) or individual nephron segments is an alternative for reducing sample complexity. Nephron segments dissected from kidney slices²⁴, proximal and distal tubules isolated from renal cortex by collagenase digestion and centrifugation on density gradient^{25,26}, or glomeruli isolated by standard sieving method²⁷ have been used for detailed study of metabolism. These separation methods may also be useful for proteomic studies on renal mitochondria. Using laser capture microdissection, selected cell populations from complex tissue sections can be acquired with high specificity. However, only a part of total cell protein is from mitochondria, and hence sensitive analytical techniques are necessary for using this procedure in the analysis of mitochondria from nephron segments.

Differential centrifugation is often used for separation of mitochondria from cells or tissue homogenates²⁸. Isolation of mitochondria is performed in two centrifugation steps – removing of nuclei, cell membranes and unbroken cells in the first centrifugation step and sedimentation of mitochondria in the second step. A pellet that contains the mitochondrial fraction of the cell can be used for proteomic analysis directly^{29,30} or after purification of mitochondria by centrifugation in density gradients^{31,32}. In purified mitochondria, proteins from other organelles (e.g. endoplasmic reticulum, peroxisomes and cytoskeleton) still may be present due to association of these organelles with mitochondria³³. Analysis of markers of subcellular compartments by Western blotting is used for determination of purity of isolated mitochondrial fractions. Further, subcellular localization of identified proteins can be checked in databases of mitochondrial proteins³⁴ or by systems that predict subcellular localization³⁵. Commercially available kits based on differential centrifugation can simplify and speed up the separation and could be an alternative approach when limited amounts of sample are available or for processing large numbers of samples³⁶.

Alternatives to differential centrifugation are separation of mitochondria using magnetic microbeads of free flow electrophoresis. Using free flow electrophoresis, high purity of mitochondria can be reached³⁷. Low yield and the necessity for specialized equipment are major drawbacks of free flow electrophoresis³⁶. Mitochondria can be isolated with enrichment and purity comparable to ultracentrifugation methods using magnetic microbeads³⁸.

Methods for analysis of mitochondrial proteome

The mammalian mitochondrial proteome comprises approximately 1500 proteins^{39,40}. Most of them are encoded by the nuclear genome and imported into mitochondria. Only 13 protein chains of electron transport system (ETS) subunits are encoded by the mitochondrial DNA.

Mitochondrial proteome contains proteins with a wide range of hydrophobicity. Membrane proteins form a significant part of mitochondrial proteins and are a challenge for separation methods used in proteomics. These proteins are attached to the membrane in hydrophobic regions (e.g. ETS complexes⁴¹⁻⁴⁴, electron transferring flavoprotein⁴⁵), or embedded in the membrane (e.g. pore forming proteins). Relatively soluble enzymes are present in mitochondrial matrix⁴⁶ and intermembrane space⁴⁷. A significant part of mitochondrial proteins is associated into homo- or heterooligomeric protein complexes whose subunit composition is important for their function³⁰. Analysis subunit composition and stoichiometry of mitochondrial protein complexes requires analysis under native conditions to prevent their dissociation. At present, there is no universal proteomic method that can cover all aspects of mitochondrial proteins. Proteomic workflows based on two-dimensional electrophoresis, blue native electrophoresis and gel-free chromatographic methods have been used for analysis of mitochondria. A short summary of methods used for the analysis of mitochondrial proteome is shown in Table 1.

Two-dimensional electrophoresis (2-DE) combines separation of proteins according to their net charge by isoelectric focus in the first step and by molecular weight on polyacrylamide gel in the second dimension. Proteins resolved as spots on gels are then visualized using visible or fluorescent stains and digital images of gels are acquired using a scanner or camera. With 2-DE, fast resolution of soluble proteins with the option of direct evaluation of their isoelectric points and molecular weights can be done. The use of 2-DE for mitochondrial proteomics is limited by resolution of proteins with extreme isoelectric point and molecular weight values, poor separation of hydrophobic membrane proteins, and limited detection of low abundance proteins^{48,49}. Two-dimensional fluorescence difference gel electrophoresis (2D-DIGE) is a variant of 2-DE that improves reproducibility⁵⁰. 2D-DIGE relies on labeling of samples with spectrally resolvable fluorescent cyanine dyes (Cy2, Cy3, and Cy5) and their simultaneous separation on a single polyacrylamide gel. Internal standard prepared by mixing equal amount of each sample is labeled by Cy2; dyes Cy3 and Cy5 are then used for labeling individual samples. Internal standard and two individual samples are mixed together, separated by 2DE, and gels are scanned with the excitation wavelength of each dye used. The use of internal standard in DIGE minimizes inter-gel variability and makes processing of gel images easier⁵⁰. Images are then imported to a specialized 2-DE image analysis software that allows spot detection, and quantification by calculation of the spot volumes⁵¹. Spots of interest are then excised and proteins are identified by combination of in gel digestion and mass spectrometry.

Table 1. Summarization of proteomic methods and their suitability for analysis of mitochondrial proteome.

Method	Principle	Advantages	Disadvantages
Two-dimensional electrophoresis (2DE)	Separation of proteins according to their net charge by isoelectric focusing followed by separation according their masses by polyacrylamide gel electrophoresis.	Widespread, robust, relatively simple method. Compatibility with subsequent analyses (e.g. immunochemic detection, mass spectrometry).	Difficult separation of hydrophobic, extremely acidic or basic proteins. Limited dynamic range. Low throughput, labor-intensiveness.
Two-dimensional fluorescence difference gel electrophoresis (DIGE)	Labeling of samples with fluorescent dyes and separation on one gel with internal standard by 2DE.	Improved reproducibility and less sample demand in comparison with 2DE.	Difficult separation of hydrophobic and extremely acidic or basic proteins. Labor-intensiveness
Blue native polyacrylamide gel electrophoresis (BN-PAGE)	Separation of protein extract on polyacrylamide gel in presence of Coomassie Brilliant Blue.	Analysis of subunit composition of protein complexes. Analysis of hydrophobic complexes. Maintaining activity of protein complexes during separation.	Low throughput and labor-intensiveness. Only protein complexes are detected.
Gel free methods (LC-MS)	Digestion of a complex protein sample, separation of proteolytic peptides by one- or multiple-step of liquid chromatography, on-line mass spectrometric analysis of eluted peptides.	In comparison with gel based methods, less sample requirement and better detection of hydrophobic proteins. Ability to analyze very complex samples by employing multidimensional chromatographic separation.	Incomplete sequence coverage of identified proteins. Low efficiency to detect posttranslationally modified peptides without enrichment.
Microarrays	Detection of proteins captured on surfaces with specific antibodies or surfaces optimized for capture of certain protein types.	High throughput. Analysis of specific molecules by selection of different array types (e.g. posttranslationally modified proteins).	Number of targets is limited by the selected array. Cross reactivity in complex protein mixtures.

Blue native polyacrylamide gel electrophoresis (BN-PAGE) was designed for separation of intact protein complexes. Hydrophobic proteins and complexes are solubilized with a nonionic detergent. Coomassie blue added to sample and cathode buffer binds to hydrophobic proteins and complexes and gives them a negative charge^{52,53}. In two dimensional setup, separation in second dimension in the presence of sodium dodecylsulfate under denaturing conditions allows resolution of subunits of individual complexes⁵⁴. These methods are utilized for investigation of respiratory complexes and their subunit composition in health and disease.

Methods utilizing a combination of high performance liquid chromatography with mass spectrometry (LC-MS) are used with increasing tendency in proteomics for qualitative and quantitative analyses of complex protein mixtures extracted from biological samples; they can be also used for identification of proteins in spots from gel electrophoreses. Protein mixture extracted from a biological sample is digested by proteolytic enzyme and resulting peptides are then separated by high performance liquid chromatography. Proteolytic digestion of complex samples results in huge number of proteolytic peptides and multidimensional fractionation of peptides based on combination of two or more chromatographic steps (e.g., reverse phase liquid chromatography, ion exchange chro-

matography) (ref.⁵⁵) offers increased separation capacity and higher resolution. Separated peptides are eluted from the column directly into the mass spectrometer. During the whole chromatographic run, masses of eluting peptides and their fragmentation spectra are recorded by the mass spectrometer. These data are then used for identification of proteins and for their quantification. For quantification of proteins, label free workflows or isotopic labeling are used⁵⁶. Strategies for label free quantification include two distinct groups: measurement based on measurement of area under the curve or signal intensity of precursor ion spectra, and spectral counting in which the number of fragment spectra identifying peptides from a given protein is used to assess relative protein abundance⁵⁷. Quantification by isotopic labeling is based on incorporating of isotopic compound either metabolically by incorporation of specific isotopes, or enzymatically or chemically using reagents that bound to peptides^{58,59}. Labeled samples are combined and subjected to analysis by liquid chromatography and mass spectrometry. Quantitative data are extracted from the intensities of characteristic ions in tandem mass spectra⁵⁹. Advantage of gel free attempts for analysis of mitochondrial proteome is improved detection of membrane proteins that are underrepresented in 2-DE analyses⁶⁰. Microscale techniques that comprise protein extraction, fractionation and pro-

teolytic digestion optimized for the microgram protein range would allow analysis of small samples of mitochondria from biopsies or nephron segments⁶¹.

Protein microarrays allow simultaneous detection of a set of proteins and offer the ability to study multiple samples in an effort to develop protein profile changes across multiple proteins^{62,63}. The ability of microarrays for screening of multiple proteins is advantageous for detection of protein expression changes, protein-protein interactions, and biomarker discovery and validation⁶⁴. Analysis of intact proteins by microarrays instead of proteolytic digests can be advantageous for preservation of specific motifs but conjugation of sample with the tag necessary for subsequent detection or signal amplification may denature, damage, or mask the epitope⁶⁵. Antibody cross-reactivity to non-target proteins can also decrease performance in antibody microarrays^{62,63}. The potential for utilization of protein microarrays in analysis of renal mitochondria could be in high throughput monitoring of selected pathways by analysis of multiple, predefined set of proteins. Arrays based on mass spectrometric detection of proteins bound to affinity surfaces (surface-enhanced laser desorption and ionization, SELDI) have been used for analysis of brain mitochondria^{66,67}. Chips with wide range of surfaces are available for SELDI. The use of chip surface optimized for binding of hydrophobic proteins could be potentially advantageous for analysis of mitochondrial membrane proteins.

CLINICAL AND RESEARCH APPLICATION OF RENAL MITOCHONDRIAL PROTEOMICS

Basic characterization of renal mitochondrial proteome

In renal tissue of various species including mouse, rat and human, mitochondrial proteins have been identified by proteomic methods⁶⁸⁻⁷⁰. Comparison of 2-DE maps of rat kidney cortex and medulla⁶⁸ or human kidney cortex, medulla and glomeruli⁷¹ showed alterations in spots containing mitochondrial proteins. However, this attempt is not suitable for detailed analysis of the mitochondrial proteome due to very low amount of mitochondrial proteins detected. The coverage of mitochondrial proteome is increased when mitochondria prepared by differential centrifugation are used for analysis instead of whole tissue. Analysis of mitochondrial fractions of porcine renal cortex and medulla showed that mitochondrial proteome of the cortex contained enzymes employed in oxygen dependent pathways and mitochondrial proteome in the medulla proteins important for adaptation to low oxygen availability⁷². Further datasets that contain proteins of renal mitochondria are available in experiments that investigated composition of mitochondrial proteome from mouse tissues by 2-DE (ref.⁷³) and rat organs by BN-PAGE (ref.³⁰) and LC-MS (ref.⁷⁴). High throughput proteome analysis done by LC-MS allowed characterization of multiple mitochondrial metabolic pathways⁷⁵. However, translation of animal data to humans is limited by differences in anatomy, metabolism and physiology. On

the other hand, several factors make the human research into renal cellular and molecular biology problematic. In particular, difficult access to the human renal tissue and several confounding factors including disease state, the patient's comorbidities and treatment history represent main impediments to the study of human renal mitochondrial proteome. Therefore, the use of clinically relevant animal models remains a cornerstone in the study renal mitochondrial pathology. In this context, pig is highly valuable model organism due to anatomic, physiological and biochemical similarities of porcine and human kidney⁷⁶.

Recent advances in mitochondrial studies: a focus on selected renal pathologies

In the following text, we summarize recent advances from various mitochondrial proteomic studies of the most common pathological states of the kidney. Short summary of utilization of these methods is also available in Table 2. Detailed analysis of all research applications of mitochondrial proteomics falls outside the scope of this work and the reader is referred to recent in-depth reviews^{21,77-80}.

Diabetes

All forms of diabetes are characterized by hyperglycemia, a relative or absolute lack of insulin action, pathway-selective insulin resistance, and the development of diabetes-specific pathology in the retina, renal glomerulus, and peripheral nerves. Oxidative stress is a key component in the development of diabetic nephropathy. Reactive oxygen species (ROS) are produced by cytosolic (such as glycolysis, specific defects in the polyol pathway, uncoupling of nitric oxide synthase, xanthine oxidase, and advanced glycation) and mitochondrial pathways (electron leakage at complex I and at the interface between coenzyme Q and complex III) (ref.⁸¹). Excess amounts of ROS modulate activation of protein kinase C, mitogen-activated protein kinases, and various cytokines and transcription factors which eventually cause increased expression of extracellular matrix genes with progression to fibrosis and end stage renal disease⁸². Impairment of renal mitochondria induced by oxidative stress is an important factor in diabetes; therefore mitochondria represent an important site due to their intensive oxidative metabolism and using proteomics, specific targets for therapy in mitochondria can be revealed.

Proteomic analysis showed upregulation of TCA cycle and fatty acid oxidation proteins by analysis cytosolic compartment of kidney cortex⁸³ and renal mitochondria⁸⁴ of diabetic mice. Increased level of mitochondrial fatty acid metabolism enzymes in renal cortex of diabetic animals supported the hypothesis that insulin resistance can be attributed to increases in intracellular fatty acid metabolites that disrupted insulin signaling⁸³.

Increased expression of mitochondrial 3-hydroxy-3-methylglutaryl-CoA synthase 2 (HMGCS2) was found using 2-DE analysis in kidney of diabetic mice. It was proposed that excess of ketogenic activity resulting from

Table 2. Applications of proteomic methods that were used in studies of the most common pathological states of the kidney.

Pathology	Method	Sample, organism	What was studied
Diabetes	2-DE	Kidney tissue, mouse ^{83,85} . Mitochondria, mouse ⁸⁶ . Mitochondria, rat ¹⁵ .	Changes of proteome during diabetes ⁸³ . Proteomic profile of kidney and identification of mitochondrial ketogenic enzyme ⁸⁵ . Posttranslational modification of mitochondrial proteome ^{86,15} .
	LC-MS	Mitochondria, mouse ⁸⁴ . Kidney tissue, rat ⁸⁷ .	Changes of protein expression during diabetes ⁸⁴ . Identification of potential therapy targets ⁸⁷ .
Hypertension	2-DE	Kidney tissue, rat ⁹³ .	Protein expression profile in a model of hypertension ⁹³ .
	LC-MS	Mitochondria, rat ⁹⁴ .	Mitochondrial metabolism in mitochondria in a model of hypertension ⁹⁴ .
Acidosis	2D-DIGE	Proximal tubules, rat ⁹⁵ .	Changes in protein expression during acidosis ⁹⁵ .
	LC-MS	Mitochondria, rat ²⁹ .	Response of the mitochondrial proteome of renal proximal convoluted tubules to chronic metabolic acidosis ²⁹ .
Acute kidney injury	Western blotting	Kidney tissue, mouse ^{17,96} .	Expression of mitochondrial protein after treatment of AKI by antioxidant ¹⁷ . Protective mechanism of mitochondrial sirtuin ⁹⁶ .
Nephrotoxicity	2-DE	Kidney tissue, rat ^{98,99} . Cell culture ^{101,102} . Mitochondria ²² .	Interaction of gentamicin ⁹⁸ and cyclosporine A ⁹⁹ with kidney. Effect of calcium oxalate monohydrate ^{101,22} and dihydrate ¹⁰² .
Renal cancer	2-DE	Tissue, human ¹⁰⁴ . Mitochondria, human ¹⁰⁵ . Cell culture, human ¹⁰⁸ .	Protein profiles of tissue and tumor ¹⁰⁴ . Mitochondrial proteomes of different tumors ¹⁰⁵ . Impact of cisplatin administration on protein expression levels ¹⁰⁸ .
	2D-DIGE	Tumor tissue, human ¹⁰⁷ .	Stage-related changes of proteins in tumors ¹⁰⁷ .
	BN-PAGE	Tumor tissue, human ¹⁰⁶ .	Composition of ETS complexes in tumors ¹⁰⁶ .

increased expression of HMGCS2 contributes to diabetic nephropathy and HMGCS2 may therefore represent a potential therapeutic target⁸⁵.

Proteomic analysis of cytosolic and mitochondrial fractions of diabetic mice kidney provided data about migration of mitochondrial proteins⁸⁶. Increased amount of prohibitin and cytochrome c was detected in cytosolic fraction of diabetic kidney. Mitochondrial prohibitin is involved in cell cycle function and its increased amount in cytoplasmic fraction was attributed to damage of mitochondrial membrane or impaired transport into mitochondrion. The leakage of cytochrome c into cytosol indicated alteration in permeability of mitochondrial membrane.

In diabetes, high blood glucose level results in post-translational modifications of proteins. Proteins modified by methylglyoxal (MGO) were found in renal mitochondria of diabetic rats and identified as enzymes of beta oxidation and subunits of ETS complex I and III. It was shown that activity of complex III was decreased due to its modification by MGO (ref.¹⁵).

Effect of triethylenetetramine (TETA) on mitochondria of diabetic kidney was studied by proteomics⁸⁷. TETA is a copper chelator that prevents or reverses diabetic copper overload and thereby suppress oxidative stress. Analysis of kidney of diabetic animals revealed that treatment by TETA restored decrease of mitochondrial chaperones involved in protein turnover and assembly,

and enzymes involved in oxidative phosphorylation and mitochondrial fatty acid metabolism expression caused by diabetes⁸⁷.

Hypertension

Essential hypertension is a heterogeneous disorder in which both genetics and environmental factors contribute to increased cardiovascular and renal morbidity and mortality⁸⁸. Changes in renal mitochondria in rat models of hypertension include alterations in respiratory functions⁸⁹ and oxidative stress^{90,91} and renal mitochondria represent possible therapeutic target⁹².

Protein expression profiles of the kidney in spontaneously hypertensive rats revealed decreased expression of NADPH dependent mitochondrial isocitrate dehydrogenase⁹³. Decreased defense against mitochondrial oxidative damage in hypertensive rats was suggested due to involvement of this protein in process of glutathione regeneration.

Using salt-sensitive rats as model organism for hypertension, effect of salt-induced hypertension on mitochondria of thick ascending limb of Henle's loop was tested by proteomics⁹⁴. Downregulation of proteins connected with energy metabolism predicted reduction of oxygen utilization in mitochondria in medullary thick ascending limb of Henle's loop of salt sensitive rats⁹⁴.

Acidosis

Metabolic acidosis is caused by overproduction of an acid or reduced recovery of bicarbonate. Adaptive response of renal proximal tubule includes rapid increase of ammoniogenesis and gluconeogenesis. In proximal tubules of acidotic rats, increased levels of mitochondrial proteins associated with catabolism of plasma glutamine were detected by proteomics using 2D-DIGE (ref.⁹⁵). These changes in protein expression levels contributed significantly to the adaptive response to metabolic acidosis and/or renal hypertrophy. In mitochondria of rat proximal convoluted tubules²⁹, abundance of proteins including mitochondrial enzymes involved in glutamine metabolism and acid-base balance was significantly altered in response to metabolic acidosis. During acidosis, increased acetylation of mitochondrial proteins was detected and it was hypothesized that acetylation may prevent protein degradation by blocking sites of ubiquitination.

Acute kidney injury

In experimental models of AKI, abnormal mitochondrial biogenesis, fission/fusion, and autophagy have been characterized and recovery of mitochondrial functions was found to be important for function of the kidney¹¹. Ischemia-reperfusion injury in AKI contributes to fragmentation of mitochondria and processes leading to cell death¹⁰. Although proteomic analysis of mitochondria or kidney tissue affected by AKI is not available to date, experimental data suggest that changes in mitochondrial proteins structure and activity could substantially contribute to the onset or progress of renal dysfunction associated with AKI (ref.¹⁷). Recent research showed that mitochondrial proteins could be an important target for therapy^{96,97}. Therefore, proteomic analysis of mitochondria on model systems during AKI could bring important information about mechanisms of mitochondrial damage and reveal potential therapeutic targets.

Detection of nephrotoxic compounds effect

Kidney plays an important role in elimination of xenobiotics, including drugs and toxic environmental agents. During concentration of urine, tubular structures of nephrons are exposed to relative high concentrations of xenobiotic compounds. Knowledge of putative interactions of xenobiotics, drugs or their metabolites with renal mitochondria could help to prevent potential damage to the kidney.

Proteomic analysis of renal cortex was performed to delineate the effects of gentamicin⁹⁸. Gentamicin belongs to aminoglycosides which are known to inhibit sodium and potassium ATPase activity. The analysis revealed that expression of mitochondrial proteins employed in gluconeogenesis and glycolysis, fatty acid utilization and TCA cycle was affected by gentamicin.

Effect of cyclosporine A (CsA) nephrotoxicity was studied on the kidney of normal and salt-depleted rat models by combined strategy employing proteomics and metabolomics⁹⁹. CsA is used after renal transplantation to prevent organ rejection. Mitochondrial proteins of oxidative phosphorylation and fatty acid β -oxidation were

upregulated in low-salt control rats compared to normal-fed animals. Upregulation of these proteins suggested increased energy demand, possibly for retaining normal osmolarity within the cells. In low salt animals, CsA treatment decreased the level of TCA cycle and ETS proteins. CsA more strongly affected the kidneys of rats fed with a low-salt diet due to their higher dependence on the energy production by mitochondrial respiration⁹⁹.

In hyperoxaluria, renal tubular epithelial cells are exposed to oxalate which lead to the activation of intracellular responses, including overproduction of free radicals and reactive oxygen species. Mitochondrial dysfunction is an important event favoring kidney stone formation¹⁰⁰. In renal tubular epithelial cells incubated with calcium oxalate monohydrate (COM) (ref.¹⁰¹) or calcium oxalate dihydrate (COD) (ref.¹⁰²), changes in expression of several mitochondrial proteins were detected. Proteomic analysis of mitochondria²² revealed that COM treatment affected enzymes of cell cycle regulation, carbohydrate, amino acid and energy metabolism. Increased level of oxidatively modified proteins indicated ROS overproduction in COM treated cells. Proteomic approach documented a complex effect of COM crystals on renal cells and showed that mitochondrial pathways of energy metabolism, ROS regulation and oxidative stress response were affected.

Renal cancer

In tumors, energy metabolism is shifted from oxidative phosphorylation to glycolysis. However, synthetic pathways in mitochondria are still important for cancer cells and mitochondria represent important targets for therapy¹⁰³. Increased expression of glycolytic proteins and downregulation of mitochondrial gluconeogenic enzymes that reflect the predominance of glycolysis followed by lactic acid fermentation in the presence of adequate oxygen (Warburg effect) in was detected in renal carcinoma tissue¹⁰⁴. Analysis of mitochondria isolated from renal oncocytoma and chromophobe cell carcinoma was performed by 2-DE (ref.¹⁰⁵). Differences in abundance of ETS subunits, proteins of glycolysis, beta oxidation and antioxidant proteins have been found.

Analyses by BN-PAGE can reveal alterations and abundance of ETS protein complexes in renal tumor tissues in comparison with healthy tissue or between tumor types. Using BN-PAGE, differences in patterns of ETS complexes in three types of renal tumors were examined¹⁰⁶. It was found that decreased amount of ETS complexes II, III IV and ATP synthase correlated with aggressiveness of renal cell carcinoma.

Recent evidence showed that mitochondrial proteome is changed during tumor progression¹⁰⁷. Samples of renal cell carcinoma of different stages have been analyzed by 2D-DIGE. Mitochondrial proteins of TCA cycle and ETS system were found to be downregulated according to Warburg hypothesis. Mitochondrial prohibitin and peroxiredoxin-3 showed stage-dependent changes in expression and may be used as potential markers of progression.

Compounds used for anticancer therapy may influence the mitochondrial proteins¹⁰⁸. Cisplatin is an important anticancer drug and its use is frequently limited by

various significant side effects including nephrotoxicity¹⁰⁹. Proteome analysis of renal cells incubated with cisplatin identified changes in several mitochondrial proteins. Upregulation of mitochondrial heat shock protein HSP70 may indicate a defense mechanism against apoptosis. Increase of glycolytic enzyme glyceraldehyde 3-phosphate dehydrogenase was attributed to compensatory effect on disturbed mitochondrial oxidative processes and decrease of mitochondrial superoxide dismutase to decreased activity of free radical defense mechanisms¹⁰⁸.

CONCLUSION AND RESEARCH PERSPECTIVES

Proteomic analyses of renal mitochondria holds great potential for providing information on remodeling of mitochondrial metabolic pathways, protein posttranslational modifications and composition of mitochondrial protein complexes during various renal pathological states. These data can be then used for investigating the pathophysiology of diseases associated with mitochondrial dysfunction and for revealing potential targets for therapy. Nevertheless, many challenges remain. We have developed the following research agenda in relation to the renal mitochondrial proteomics aimed to identify potential research questions to address the existing knowledge gaps.

- Complex structure of kidney tissue is an important factor for analysis of the renal mitochondrial proteome; therefore the important step is the reduction of sample complexity by isolation of renal cortex, medulla, nephron segments and isolation of mitochondria.
- Analysis of mitochondria in renal biopsies represents a significant challenge due to low amount of available protein. Optimization of methods for isolation of mitochondria in high purity and analytical methods for covering wide range of hydrophobicity, abundance and posttranslational modifications of mitochondrial proteome is important.
- Combination of proteomics with methods that reflect metabolic activity (e.g. metabolomics, high resolution respirometry) can provide more detailed understanding of renal mitochondrial physiology and pathology.
- There is a pressing need to better understand the nature, time course and magnitude of mitochondrial proteome changes in different renal zones in the course of various kidney disorders.
- Further proteomic studies are also required to better understand how multiple comorbidities (such as diabetes, heart failure) as well as aging alter the renal mitochondrial proteome, enhance the intrinsic susceptibility of mitochondrial system to insults and how they affect the effectiveness of novel therapies.
- Due to the inaccessibility of the kidney tissue under clinical conditions, future research will need better preclinical models of AKI and CKD that recapitulate the complex nature of human disease.

ABBREVIATIONS

ATP, Adenosine triphosphate; AKI, Acute kidney injury; BN-PAGE, Blue native polyacrylamide gel electrophoresis; CKD, Chronic kidney disease; COD, Calcium oxalate dihydrate; COM, Calcium oxalate monohydrate; CsA, Cyclosporin A; ETS, Electron transport system; HMGS2, 3-hydroxy-3-methylglutaryl-CoA synthase 2; HPLC, High performance liquid chromatography; IMM, Inner mitochondrial membrane; LC-MS, Liquid chromatography - mass spectrometry; MGO, Methylglyoxal; MPT, Mitochondrial permeability transition pore; MW, Molecular weight; OMM, Outer mitochondrial membrane; pI, Isoelectric point; ROS, Reactive oxygen species; SELDI, Surface-enhanced laser desorption and ionization; TCA, Tricarboxylic acid cycle; TETA, Triethylenetetramine; VDAC1, Voltage-dependent anion-selective channel 1; VDAC2, Voltage-dependent anion-selective channel 2; 2-DE, Two-dimensional electrophoresis; 2D-DIGE, Two-dimensional fluorescence difference gel electrophoresis.

Acknowledgment: This work was supported by the National Sustainability Program I (NPU I) Nr. LO1503 provided by the Ministry of Education Youth and Sports of the Czech Republic, the Charles University Research Fund (project number P36), and the Specific Student Research Project no. 260175/2015 of the Charles University in Prague.

Author contributions: ZT, JK, JM, MG, MM: literature search; ZT, JK, MM: manuscript writing, ZT, JK, JM, MG, MM: final approval.

Conflict of interest statement: The authors state that there are no conflicts of interest regarding the publication of this article.

REFERENCES

1. Ernster L, Schatz G. Mitochondria: a historical review. *The Journal of cell biology* 1981;91(3 Pt 2):227s-255s.
2. Dedkova EN, Blatter LA. Mitochondrial Ca²⁺ and the heart. *Cell calcium* 2008;44(1):77-91.
3. Murphy MP. How mitochondria produce reactive oxygen species. *The Biochemical journal* 2009;417(1):1-13.
4. Nisoli E, Carruba MO. Nitric oxide and mitochondrial biogenesis. *Journal of cell science* 2006;119(Pt 14):2855-62.
5. Kroemer G, Reed JC. Mitochondrial control of cell death. *Nature medicine* 2000;6(5):513-19.
6. Yasuda M, Fujita T, Higashio T, Okahara T, Abe Y, Yamamoto K. Effects of 4-pentenoic acid and furosemide on renal functions and renal uptake of individual free fatty acids. *Pflugers Archiv : European journal of physiology* 1980;385(2):111-6.
7. Che R, Yuan Y, Huang S, Zhang A. Mitochondrial dysfunction in the pathophysiology of renal diseases. *American journal of physiology. Renal physiology* 2014;306(4):F367-78.
8. Funk JA, Schnellmann RG. Persistent disruption of mitochondrial homeostasis after acute kidney injury. *American journal of physiology. Renal physiology* 2012;302(7):F853-64.
9. Gomez H, Ince C, De Backer D, Pickkers P, Payen D, Hotchkiss J, Kellum JA. A unified theory of sepsis-induced acute kidney injury: inflammation, microcirculatory dysfunction, bioenergetics, and the tubular cell adaptation to injury. *Shock* 2014;41(1):3-11.
10. Hall AM. Maintaining mitochondrial morphology in AKI: looks matter. *Journal of the American Society of Nephrology* 2013;24(8):1185-7.

11. Stallons LJ, Funk JA, Schnellmann RG. Mitochondrial Homeostasis in Acute Organ Failure. *Current pathobiology reports* 2013;1(3):169-77.
12. Daehn I, Casalena G, Zhang T, Shi S, Fenninger F, Barasch N, Yu L, D'Agati V, Schlondorff D, Kriz W, Haraldsson B, Bottinger EP. Endothelial mitochondrial oxidative stress determines podocyte depletion in segmental glomerulosclerosis. *The Journal of clinical investigation* 2014;124(4):1608-21.
13. Gogvadze V, Orrenius S, Zhivotovsky B. Mitochondria in cancer cells: what is so special about them? *Trends in cell biology* 2008;18(4):165-73.
14. Rolo AP, Palmeira CM. Diabetes and mitochondrial function: role of hyperglycemia and oxidative stress. *Toxicology and applied pharmacology* 2006;212(2):167-78.
15. Rosca MG, Mustata TG, Kinter MT, Ozdemir AM, Kern TS, Szweda LI, Brownlee M, Monnier VM, Weiss MF. Glycation of mitochondrial proteins from diabetic rat kidney is associated with excess superoxide formation. *American journal of physiology. Renal physiology* 2005;289(2):F420-30.
16. Izzedine H, Launay-Vacher V, Deray G. Antiviral drug-induced nephrotoxicity. *American journal of kidney diseases* 2005;45(5):804-17.
17. Patil NK, Parajuli N, MacMillan-Crow LA, Mayeux PR. Inactivation of renal mitochondrial respiratory complexes and manganese superoxide dismutase during sepsis: mitochondria-targeted antioxidant mitigates injury. *American journal of physiology. Renal physiology* 2014;306(7):F734-43.
18. Papazova DA, Friederich-Persson M, Joles JA, Verhaar MC. Renal transplantation induces mitochondrial uncoupling, increased kidney oxygen consumption, and decreased kidney oxygen tension. *American journal of physiology. Renal physiology* 2015;308(1):F22-8.
19. Saba H, Batinic-Haberle I, Munusamy S, Mitchell T, Lichti C, Megyesi J, MacMillan-Crow LA. Manganese porphyrin reduces renal injury and mitochondrial damage during ischemia/reperfusion. *Free radical biology & medicine* 2007;42(10):1571-8.
20. Jiang Y, Wang X. Comparative mitochondrial proteomics: perspective in human diseases. *Journal of hematology & oncology* 2012;5:11.
21. Peinado JR, Diaz-Ruiz A, Fruhbeck G, Malagon MM. Mitochondria in metabolic disease: getting clues from proteomic studies. *Proteomics* 2014;14(4-5):452-66.
22. Chaiyarit S, Thongboonkerd V. Changes in mitochondrial proteome of renal tubular cells induced by calcium oxalate monohydrate crystal adhesion and internalization are related to mitochondrial dysfunction. *Journal of proteome research* 2012;11(6):3269-80.
23. Guder WG, Ross BD. Enzyme distribution along the nephron. *Kidney international* 1984;26(2):101-11.
24. Klein KL, Wang MS, Torikai S, Davidson WD, Kurokawa K. Substrate oxidation by isolated single nephron segments of the rat. *Kidney international* 1981;20(1):29-35.
25. Doctor RB, Chen J, Peters LL, Lux SE, Mandel LJ. Distribution of epithelial ankyrin (Ank3) spliceforms in renal proximal and distal tubules. *The American journal of physiology* 1998;274(1 Pt 2):F129-38.
26. Walmsley SJ, Broeckling C, Hess A, Prenni J, Curthoys NP. Proteomic analysis of brush-border membrane vesicles isolated from purified proximal convoluted tubules. *American journal of physiology. Renal physiology* 2010;298(6):F1323-31.
27. Yoshida Y, Miyazaki K, Kamiie J, Sato M, Okuizumi S, Kenmochi A, Kamijo K, Nabetani T, Tsugita A, Xu B, Zhang Y, Yaoita E, Osawa T, Yamamoto T. Two-dimensional electrophoretic profiling of normal human kidney glomerulus proteome and construction of an extensible markup language (XML)-based database. *Proteomics* 2005;5(4):1083-96.
28. Graham JM. Isolation of mitochondria from tissues and cells by differential centrifugation. *Current protocols in cell biology* 2001;Chapter 3:Unit 3.3.
29. Freund DM, Prenni JE, Curthoys NP. Response of the mitochondrial proteome of rat renal proximal convoluted tubules to chronic metabolic acidosis. *American journal of physiology. Renal physiology* 2013;304(2):F145-55.
30. Reifschneider NH, Goto S, Nakamoto H, Takahashi R, Sugawa M, Dencher NA, Krause F. Defining the mitochondrial proteomes from five rat organs in a physiologically significant context using 2D blue-native/SDS-PAGE. *Journal of proteome research* 2006;5(5):1117-32.
31. Graham JM. Purification of a crude mitochondrial fraction by density-gradient centrifugation. *Current protocols in cell biology* 2001;Chapter 3:Unit 3.4.
32. Sims NR, Anderson MF. Isolation of mitochondria from rat brain using Percoll density gradient centrifugation. *Nat. Protoc.* 2008;3(7):1228-39.
33. Raturi A, Simmen T. Where the endoplasmic reticulum and the mitochondrion tie the knot: the mitochondria-associated membrane (MAM). *Biochimica et biophysica acta* 2013;1833(1):213-24.
34. Andreoli C, Prokisch H, Hortnagel K, Mueller JC, Munsterkotter M, Scharfe C, Meitinger T. MitoP2, an integrated database on mitochondrial proteins in yeast and man. *Nucleic Acids Res* 2004;32(Database issue):D459-62.
35. Gaston D, Tsaousis AD, Roger AJ. Predicting proteomes of mitochondria and related organelles from genomic and expressed sequence tag data. *Methods in enzymology* 2009;457:21-47.
36. Hartwig S, Feckler C, Lehr S, Wallbrecht K, Wolgast H, Muller-Wieland D, Kotzka J. A critical comparison between two classical and a kit-based method for mitochondria isolation. *Proteomics* 2009;9(11):3209-14.
37. Eubel H, Lee CP, Kuo J, Meyer EH, Taylor NL, Millar AH. Free-flow electrophoresis for purification of plant mitochondria by surface charge. *The Plant journal : for cell and molecular biology* 2007;52(3):583-94.
38. Hornig-Do HT, Gunther G, Bust M, Lehnartz P, Bosio A, Wiesner RJ. Isolation of functional pure mitochondria by superparamagnetic microbeads. *Analytical biochemistry* 2009;389(1):1-5.
39. Lopez MF, Kristal BS, Chernokalskaya E, Lazarev A, Shestopalov AI, Bogdanova A, Robinson M. High-throughput profiling of the mitochondrial proteome using affinity fractionation and automation. *Electrophoresis* 2000;21(16):3427-40.
40. Taylor SW, Fahy E, Zhang B, Glenn GM, Warnock DE, Wiley S, Murphy AN, Gaucher SP, Capaldi RA, Gibson BW, Ghosh SS. Characterization of the human heart mitochondrial proteome. *Nature biotechnology* 2003;21(3):281-6.
41. Cecchini G. Function and structure of complex II of the respiratory chain. *Annual review of biochemistry* 2003;72:77-109.
42. Hirst J. Why does mitochondrial complex I have so many subunits? *The Biochemical journal* 2011;437(2):e1-3.
43. Iwata S, Lee JW, Okada K, Lee JK, Iwata M, Rasmussen B, Link TA, Ramaswamy S, Jap BK. Complete structure of the 11-subunit bovine mitochondrial cytochrome bc1 complex. *Science* 1998;281(5373):64-71.
44. Wittig I, Schagger H. Structural organization of mitochondrial ATP synthase. *Biochimica et biophysica acta* 2008;1777(7-8):592-8.
45. Watmough NJ, Fierman FE. The electron transfer flavoprotein: ubiquinone oxidoreductases. *Biochimica et biophysica acta* 2010;1797(12):1910-6.
46. Rhee HW, Zou P, Udeshi ND, Martell JD, Mootha VK, Carr SA, Ting AY. Proteomic mapping of mitochondria in living cells via spatially restricted enzymatic tagging. *Science* 2013;339(6125):1328-31.
47. Vogtle FN, Burkhart JM, Rao S, Gerbeth C, Hinrichs J, Martinou JC, Chacinska A, Sickmann A, Zahedi RP, Meisinger C. Intermembrane space proteome of yeast mitochondria. *Molecular and cellular proteomics* 2012;11(12):1840-52.
48. Mathy G, Sluse FE. Mitochondrial comparative proteomics: strengths and pitfalls. *Biochimica et biophysica acta* 2008;1777(7-8):1072-7.
49. Silvestri E, Lombardi A, Glinni D, Senese R, Cioffi F, Lanni A, Goglia F, Moreno M, de Lange P. Mammalian Mitochondrial Proteome And Its Functions: Current Investigative Techniques And Future Perspectives On Ageing And Diabetes. *Journal of Integrated OMICS* 2011;1(1):17-27.
50. O'Connell K, Ohlendieck K. Proteomic DIGE analysis of the mitochondria-enriched fraction from aged rat skeletal muscle. *Proteomics* 2009;9(24):5509-24.
51. Chevalier F. Highlights on the capacities of "Gel-based" proteomics. *Proteome science* 2010;8(1):23-32.
52. Schagger H, von Jagow G. Blue native electrophoresis for isolation of membrane protein complexes in enzymatically active form. *Analytical biochemistry* 1991;199(2):223-31.
53. Wittig I, Schagger H. Features and applications of blue-native and clear-native electrophoresis. *Proteomics* 2008;8(19):3974-90.
54. Nijtmans LG, Henderson NS, Holt IJ. Blue Native electrophoresis to study mitochondrial and other protein complexes. *Methods* 2002;26(4):327-34.
55. Zhang X, Fang A, Riley CP, Wang M, Regnier FE, Buck C. Multi-dimensional liquid chromatography in proteomics--a review. *Analytica chimica acta* 2010;664(2):101-13.

56. Sjodin MO, Wetterhall M, Kultima K, Artemenko K. Comparative study of label and label-free techniques using shotgun proteomics for relative protein quantification. *Journal of chromatography B* 2013;928:83-92.
57. Neilson KA, Ali NA, Muralidharan S, Mirzaei M, Mariani M, Assadourian G, Lee A, van Sluyter SC, Haynes PA. Less label, more free: approaches in label-free quantitative mass spectrometry. *Proteomics* 2011;11(4):535-53.
58. Aggarwal K, Choe LH, Lee KH. Shotgun proteomics using the iTRAQ isobaric tags. *Briefings in Functional Genomics and Proteomics* 2006;5(2):112-20.
59. Zhou Y, Shan Y, Zhang L, Zhang Y. Recent advances in stable isotope labeling based techniques for proteome relative quantification. *Journal of chromatography A* 2014;1365:1-11.
60. Tan S, Tan HT, Chung MC. Membrane proteins and membrane proteomics. *Proteomics* 2008;8(19):3924-32.
61. Feist P, Hummon AB. Proteomic challenges: sample preparation techniques for microgram-quantity protein analysis from biological samples. *International journal of molecular sciences* 2015;16(2):3537-63.
62. Gahoi N, Ray S, Srivastava S. Array-based proteomic approaches to study signal transduction pathways: prospects, merits and challenges. *Proteomics* 2015;15(2-3):218-31.
63. Pratsch K, Wellhausen R, Seitz H. Advances in the quantification of protein microarrays. *Current Opinion in Chemical Biology* 2014;18:16-20.
64. Ramachandran N, Srivastava S, Labaer J. Applications of protein microarrays for biomarker discovery. *Proteomics. Clinical applications* 2008;2(10-11):1444-59.
65. Liotta LA, Espina V, Mehta AI, Calvert V, Rosenblatt K, Geho D, Munson PJ, Young L, Wulfkuehle J, Petricoin EF, 3rd. Protein microarrays: meeting analytical challenges for clinical applications. *Cancer cell* 2003;3(4):317-25.
66. Azzam S, Broadwater L, Li S, Freeman EJ, McDonough J, Gregory RB. A SELDI mass spectrometry study of experimental autoimmune encephalomyelitis: sample preparation, reproducibility, and differential protein expression patterns. *Proteome science* 2013;11(1):19.
67. Broadwater L, Pandit A, Clements R, Azzam S, Vadnal J, Sulak M, Yong VW, Freeman EJ, Gregory RB, McDonough J. Analysis of the mitochondrial proteome in multiple sclerosis cortex. *Biochimica et biophysica acta* 2011;1812(5):630-41.
68. Arthur JM, Thongboonkerd V, Scherzer JA, Cai J, Pierce WM, Klein JB. Differential expression of proteins in renal cortex and medulla: a proteomic approach. *Kidney international* 2002;62(4):1314-21.
69. Zhang Y, Yoshida Y, Xu B, Magdeldin S, Fujinaka H, Liu Z, Miyamoto M, Yaoita E, Yamamoto T. Comparison of human glomerulus proteomic profiles obtained from low quantities of samples by different mass spectrometry with the comprehensive database. *Proteome science* 2011;9(1):47.
70. Zhao Y, Denner L, Haidacher SJ, LeJeune WS, Tilton RG. Comprehensive analysis of the mouse renal cortex using two-dimensional HPLC - tandem mass spectrometry. *Proteome science* 2008;6(15):15.
71. Xu B, Yoshida Y, Zhang Y, Yaoita E, Osawa T, Yamamoto T. Two-dimensional electrophoretic profiling of normal human kidney: differential protein expression in glomerulus, cortex and medulla. *Journal of Electrophoresis* 2005;49(1):5-13.
72. Tuma Z, Kuncova J, Mares J, Matejovic M. Mitochondrial proteomes of porcine kidney cortex and medulla: foundation for translational proteomics. *Clinical and Experimental Nephrology* 2016;20(1):39-49. doi:10.1007/s10157-015-1135-x
73. Tschritz S, Lutzkendorf S, Bazant E, Becker S, Klose J, Schuelke M. Quantitative and qualitative 2D electrophoretic analysis of differentially expressed mitochondrial proteins from five mouse organs. *Proteomics* 2013;13(1):179-95.
74. Johnson DT, Harris RA, French S, Blair PV, You J, Bemis KG, Wang M, Balaban RS. Tissue heterogeneity of the mammalian mitochondrial proteome. *American journal of physiology. Cell physiology* 2007;292(2):C689-97.
75. Johnson DT, Harris RA, Blair PV, Balaban RS. Functional consequences of mitochondrial proteome heterogeneity. *American journal of physiology. Cell physiology* 2007;292(2):C698-707.
76. Giraud S, Favreau F, Chatauret N, Thuillier R, Maiga S, Hauet T. Contribution of large pig for renal ischemia-reperfusion and transplantation studies: the preclinical model. *Journal of biomedicine & biotechnology* 2011;2011:532127.
77. Amado FM, Barros A, Azevedo AL, Vitorino R, Ferreira R. An integrated perspective and functional impact of the mitochondrial acetylome. *Expert Review of Proteomics* 2014;11(3):383-94.
78. Gianazza E, Eberini I, Sensi C, Barile M, Vergani L, Vanoni MA. Energy matters: Mitochondrial proteomics for biomedicine. *Proteomics* 2011;11(4):657-74.
79. Gregersen N, Hansen J, Palmfeldt J. Mitochondrial proteomics—a tool for the study of metabolic disorders. *Journal of inherited metabolic disease* 2012;35(4):715-26.
80. Lau E, Huang D, Cao Q, Dincer TU, Black CM, Lin AJ, Lee JM, Wang D, Liem DA, Lam MP, Ping P. Spatial and temporal dynamics of the cardiac mitochondrial proteome. *Expert Review of Proteomics* 2015;12(2):133-46.
81. Forbes JM, Coughlan MT, Cooper ME. Oxidative stress as a major culprit in kidney disease in diabetes. *Diabetes* 2008;57(6):1446-54.
82. Kashiwara N, Haruna Y, Kondeti VK, Kanwar YS. Oxidative stress in diabetic nephropathy. *Current Medicinal Chemistry* 2010;17(34):4256-69.
83. Tilton RG, Haidacher SJ, LeJeune WS, Zhang XQ, Zhao YX, Kurosky A, Brasier AR, Denner L. Diabetes-induced changes in the renal cortical proteome assessed with two-dimensional gel electrophoresis and mass spectrometry. *Proteomics* 2007;7(10):1729-42.
84. Bugger H, Chen D, Riehle C, Soto J, Theobald HA, Hu XX, Ganesan B, Weimer BC, Abel ED. Tissue-specific remodeling of the mitochondrial proteome in type 1 diabetic akita mice. *Diabetes* 2009;58(9):1986-97.
85. Zhang D, Yang H, Kong X, Wang K, Mao X, Yan X, Wang Y, Liu S, Zhang X, Li J, Chen L, Wu J, Wei M, Yang J, Guan Y. Proteomics analysis reveals diabetic kidney as a ketogenic organ in type 2 diabetes. *American journal of physiology. Endocrinology and metabolism* 2011;300(2):E287-95.
86. Kartha GK, Moshal KS, Sen U, Joshua IG, Tyagi N, Steed MM, Tyagi SC. Renal mitochondrial damage and protein modification in type-2 diabetes. *Acta diabetologica* 2008;45(2):75-81.
87. Gong D, Chen X, Middleditch M, Huang L, Vazhoor Amarsingh G, Reddy S, Lu J, Zhang S, Ruggiero K, Phillips AR, Cooper GJ. Quantitative proteomic profiling identifies new renal targets of copper(II)-selective chelation in the reversal of diabetic nephropathy in rats. *Proteomics* 2009;9(18):4309-20.
88. Lee H, Abe Y, Lee I, Shrivastav S, Crusan AP, Huttemann M, Hopfer U, Felder RA, Asico LD, Armando I, Jose PA, Kopp JB. Increased mitochondrial activity in renal proximal tubule cells from young spontaneously hypertensive rats. *Kidney international* 2014;85(3):561-9.
89. Mujkosova J, Ulicna O, Waczulikova I, Vlkovicova J, Vancova O, Ferko M, Polak S, Ziegelhoffer A. Mitochondrial function in heart and kidney of spontaneously hypertensive rats: influence of captopril treatment. *Gen. Physiol. Biophys.* 2010;29(2):203-7.
90. Cowley AW, Jr., Abe M, Mori T, O'Connor PM, Ohsaki Y, Zheleznova NN. Reactive oxygen species as important determinants of medullary flow, sodium excretion, and hypertension. *American journal of physiology. Renal physiology* 2015;308(3):F179-97.
91. de Cavanagh EM, Toblli JE, Ferder L, Piotrkowski B, Stella I, Inserra F. Renal mitochondrial dysfunction in spontaneously hypertensive rats is attenuated by losartan but not by amlodipine. *American journal of physiology. Regulatory, integrative and comparative physiology* 2006;290(6):R1616-25.
92. Eirin A, Ebrahimi B, Zhang X, Zhu XY, Woollard JR, He Q, Textor SC, Lerman A, Lerman LO. Mitochondrial protection restores renal function in swine atherosclerotic renovascular disease. *Cardiovascular research* 2014;103(4):461-72.
93. Yu M, Wang XX, Du YX, Chen HJ, Guo XG, Xia L, Chen JZ. Comparative analysis of renal protein expression in spontaneously hypertensive rat. *Clinical and Experimental Hypertension* 2008;30(5):315-25.
94. Zheleznova NN, Yang C, Ryan RP, Halligan BD, Liang M, Greene AS, Cowley AW, Jr. Mitochondrial proteomic analysis reveals deficiencies in oxygen utilization in medullary thick ascending limb of Henle in the Dahl salt-sensitive rat. *Physiological genomics* 2012;44(17):829-42.
95. Curthoys NP, Taylor L, Hoffert JD, Knepper MA. Proteomic analysis of the adaptive response of rat renal proximal tubules to metabolic acidosis. *American journal of physiology. Renal physiology* 2007;292(1):F140-7.

96. Morigi M, Perico L, Rota C, Longaretti L, Conti S, Rottoli D, Novelli R, Remuzzi G, Benigni A. Sirtuin 3-dependent mitochondrial dynamic improvements protect against acute kidney injury. *J Clin Invest* 2015;125(2):715-26.
97. Ishimoto Y, Inagi R. Mitochondria: a therapeutic target in acute kidney injury. *Nephrology Dialysis Transplantation* 2015;Sep 1. [Epub ahead of print] doi:10.1093/ndt/gfv317
98. Charlwood J, Skehel JM, King N, Camilleri P, Lord P, Bugelski P, Atif U. Proteomic analysis of rat kidney cortex following treatment with gentamicin. *Journal of proteome research* 2002;1(1):73-82.
99. Klawitter J, Schmitz V, Brunner N, Crunk A, Corby K, Bendrick-Pearl J, Leibfritz D, Edelstein CL, Thurman JM, Christians U. Low-salt diet and cyclosporine nephrotoxicity: changes in kidney cell metabolism. *Journal of proteome research* 2012;11(11):5135-44.
100. Veena CK, Josephine A, Preetha SP, Rajesh NG, Varalakshmi P. Mitochondrial dysfunction in an animal model of hyperoxaluria: a prophylactic approach with fucoidan. *European journal of pharmacology* 2008;579(1-3):330-6.
101. Thongboonkerd V, Semangoen T, Sinchaikul S, Chen ST. Proteomic analysis of calcium oxalate monohydrate crystal-induced cytotoxicity in distal renal tubular cells. *Journal of proteome research* 2008;7(11):4689-4700.
102. Semangoen T, Sinchaikul S, Chen ST, Thongboonkerd V. Altered proteins in MDCK renal tubular cells in response to calcium oxalate dihydrate crystal adhesion: a proteomics approach. *Journal of proteome research* 2008;7(7):2889-96.
103. Ahn CS, Metallo CM. Mitochondria as biosynthetic factories for cancer proliferation. *Cancer Metabolism* 2015;3(1):1-9.
104. Unwin RD, Craven RA, Harnden P, Hanrahan S, Totty N, Knowles M, Eardley I, Selby PJ, Banks RE. Proteomic changes in renal cancer and co-ordinate demonstration of both the glycolytic and mitochondrial aspects of the Warburg effect. *Proteomics* 2003;3(8):1620-32.
105. Yusenko MV, Ruppert T, Kovacs G. Analysis of differentially expressed mitochondrial proteins in chromophobe renal cell carcinomas and renal oncocytomas by 2-D gel electrophoresis. *International journal of biological sciences* 2010;6(3):213-24.
106. Simonnet H, Alazard N, Pfeiffer K, Gallou C, Beroud C, Demont J, Bouvier R, Schagger H, Godinot C. Low mitochondrial respiratory chain content correlates with tumor aggressiveness in renal cell carcinoma. *Carcinogenesis* 2002;23(5):759-68.
107. Junker H, Venz S, Zimmermann U, Thiele A, Scharf C, Walther R. Stage-related alterations in renal cell carcinoma-comprehensive quantitative analysis by 2D-DIGE and protein network analysis. *PloS one* 2011;6(7):e21867.
108. Vasko R, Mueller GA, von Jaschke AK, Asif AR, Dihazi H. Impact of cisplatin administration on protein expression levels in renal cell carcinoma: a proteomic analysis. *European journal of pharmacology* 2011;670(1):50-7.
109. Ozkok A, Edelstein CL. Pathophysiology of cisplatin-induced acute kidney injury. *BioMed research international* 2014;2014:967826.

Research Article

Effects of the Czech Propolis on Sperm Mitochondrial Function

Miroslava Cedikova,^{1,2} Michaela Miklikova,^{1,2} Lenka Stachova,³
Martina Grundmanova,⁴ Zdenek Tuma,^{2,5} Vaclav Vetvicka,⁶ Nicolas Zech,⁷
Milena Kralickova,^{1,2} and Jitka Kuncova^{2,4}

¹ Department of Histology and Embryology, Faculty of Medicine in Pilsen, Charles University in Prague, 301 00 Pilsen, Czech Republic

² Biomedical Centre, Faculty of Medicine in Pilsen, Charles University in Prague, 301 00 Pilsen, Czech Republic

³ Institute of Pharmacology and Toxicology, Faculty of Medicine in Pilsen, Charles University in Prague, 301 00 Pilsen, Czech Republic

⁴ Department of Physiology, Faculty of Medicine in Pilsen, Charles University in Prague, 301 00 Pilsen, Czech Republic

⁵ 1st Internal Department, Faculty of Medicine and Teaching Hospital in Pilsen, Charles University in Prague, 301 00 Pilsen, Czech Republic

⁶ Department of Pathology, University of Louisville, Louisville, KY 40292, USA

⁷ IVF Centers Prof. Zech - Pilsen, 301 00 Pilsen, Czech Republic

Correspondence should be addressed to Jitka Kuncova; jitka.kuncova@lfp.cuni.cz

Received 11 April 2014; Revised 2 June 2014; Accepted 6 June 2014; Published 1 July 2014

Academic Editor: Shi-Biao Wu

Copyright © 2014 Miroslava Cedikova et al. This is an open access article distributed under the Creative Commons Attribution License, which permits unrestricted use, distribution, and reproduction in any medium, provided the original work is properly cited.

Propolis is a natural product that honeybees collect from various plants. It is known for its beneficial pharmacological effects. The aim of our study was to evaluate the impact of propolis on human sperm motility, mitochondrial respiratory activity, and membrane potential. Semen samples from 10 normozoospermic donors were processed according to the World Health Organization criteria. Propolis effects on the sperm motility and mitochondrial activity parameters were tested in the fresh ejaculate and purified spermatozoa. Propolis preserved progressive motility of spermatozoa in the native semen samples. Oxygen consumption determined in purified permeabilized spermatozoa by high-resolution respirometry in the presence of adenosine diphosphate and substrates of complex I and complex II (state OXPHOS_{I+II}) was significantly increased in the propolis-treated samples. Propolis also increased uncoupled respiration in the presence of rotenone (state ETS_{II}) and complex IV activity, but it did not influence state LEAK induced by oligomycin. Mitochondrial membrane potential was not affected by propolis. This study demonstrates that propolis maintains sperm motility in the native ejaculates and increases activities of mitochondrial respiratory complexes II and IV without affecting mitochondrial membrane potential. The data suggest that propolis improves the total mitochondrial respiratory efficiency in the human spermatozoa in vitro thereby having potential to improve sperm motility.

1. Introduction

Propolis (bee glue) is a natural product that honeybees (*Apis mellifera*) collect from various plants. It is used as building material (filling of cracks and gaps) or for protection against intruders (embalms killed invader insects) [1].

Propolis has been used as a remedy for thousands of years. The term is derived from Greek word *pro-* (meaning in front of) and *polis* (city, community). Its chemical composition depends on the place, time of collection, and plant sources

making it highly variable. To date, more than 300 compounds have been detected in various propolis extracts [2, 3]. It is composed mainly of resin (50%) and wax (30%). Other components are pollen (5%), essential and aromatic oils (10%), and minor compounds as flavonoids (quercetin, kaempferol, pinocembrin, apigenin, chrysin, etc.), beta-steroids, terpenes, minerals, and vitamins [1, 4–6]. Propolis is known in folk medicine for its pharmacological effects: antibacterial, antiviral, antifungal, antiparasitic, anti-inflammatory, chemopreventive, immunomodulatory, hepatoprotective, antioxidant,

and antitumor [1, 7]. As a result of these effects, over the past 30 years, propolis has been the subject of intense medical studies.

Infertility affects 10–15% of couples of reproductive age and plenty of unanswered questions remain concerning the physiological mechanisms underlying the successful fertility [8]. Male factor contributes to about 50% of cases of infertility and most of them are still idiopathic [9]. More than 90% of male infertility cases are due to low sperm count (oligozoospermia), poor sperm motility (asthenozoospermia), abnormal sperm morphology (teratozoospermia), or all three. The remaining cases of male infertility can be caused by a number of factors including anatomical problems, hormonal imbalances, and genetic defects.

Appropriate sperm motility is fundamental for reproductive success in mammals since the spermatozoa have to travel a relatively long distance through the female reproductive system by active flagellar motion. The energy for the sperm movement in the form of adenosine triphosphate (ATP) is supplied by two metabolic processes: glycolysis taking place in the cytoplasm or oxidative phosphorylation in the mitochondria found only in the sperm midpiece, where 72–80 helically arranged organelles can be detected. However, the relative contributions of both pathways to the sperm motility in different species are a matter of long-standing debate [10, 11]. Nevertheless, recent experimental data suggest that reduced efficiency of the mitochondrial respiratory activity may contribute to the reduced sperm motility. In asthenozoospermic patients, morphological and functional changes in sperm mitochondria have been described [12, 13].

Until now, the effects of propolis on the mitochondrial morphology and function have been studied particularly in the somatic cells. However, the results of these studies are far from uniform showing both stimulation and inhibition of various mitochondrial functions including oxygen consumption, apoptosis, and mitochondrial membrane potential [14–17]. The aim of our study was to assess the effect of ethanolic extract of propolis (EEP) on the human sperm motility, mitochondrial respiratory activity, and membrane potential to test the putative therapeutic potential of this natural product in the treatment of asthenozoospermia.

2. Methods

2.1. Ethanolic Extract of Propolis Preparation. Propolis was collected using plastic nets in region of West Bohemia (Horní Slavkov—50° 8'17.268" N, 12° 48'48.992" E) in September 2012. Propolis was frozen at –20°C and ground in a mill. The resulting powder (10 g) was mixed at room temperature with 70% ethanol (100 mL) for 24 h and then filtered. The filtrate was then made up to 100 mL with 70% ethanol [18]. The sample was kept in darkness at 4°C until analysis. For experiments with live cells, propolis was further diluted resulting in a final ethanol concentration below 1% which is not toxic to cells [19]. The final concentration of propolis chosen for further experiments was 0.01 mg/mL of the corresponding medium.

2.2. High Performance Liquid Chromatography Analysis (HPLC). Qualitative and quantitative chromatographic analyses of phenolics were performed on a HPLC system equipped with a binary pump (Waters 1525), Waters 717 plus Autosampler, and dual UV/VIS detector 2487. Separation was performed on a Symmetry C18 column, particle size 5 μm (150 mm × 4.6 mm), using a mobile phase of 0.08% acetic acid in methanol (A) and 0.1% acetic acid and 10% methanol in water (B). The gradient was 10–47% A (25 min), 47% A (25–40 min), 47–70% A (40–70 min), and 70–100% A (70–80 min) at a flow rate of mobile phase 0.5 mL/min. Injection volume was 10 μL, and column temperature was 30°C.

Spectrophotometric detection was conducted at 280 nm and 330 nm. Identification of polyphenolic compounds was achieved by comparison of retention times with those of commercial pure compounds. All standards were dissolved in dimethyl sulfoxide (Sigma-Aldrich; St. Louis, USA) to give 10 mmol/L standard solutions. Calibration standards were prepared by dilution of the standard solution in ethanol.

Quantitative analysis was carried out by external standard method. Calibration curves showed a linear response of $R^2 > 0.97$ over a concentration range of 5–100 μmol/L. Before the HPLC analysis, the EEP was filtered on teflon syringe microfilter Separon 0.45 μm. The propolis extract was diluted one hundred times for HPLC analysis.

Phenolic compounds were purchased from Sigma-Aldrich (St. Louis, USA) (apigenin, chrysin, genistein, kaempferol, luteolin, naringenin, pinocembrin, galangin and phenolic acids: caffeic, p-coumaric, t-ferulic, t-cinnamic, benzoic, and gallic acid and caffeic acid phenethyl ester). Vanillin was purchased from Merck (Darmstadt, Germany).

2.3. Sperm Sample Preparation. The study design was approved by the Local Ethics Committee of the University Hospital in Pilsen and a written informed consent was obtained from each of the 10 participants included in the study (mean age 24.2 years, SEM ± 2.8).

Ejaculates were collected after 3 days of sexual abstinence in IVF Center Prof. Zech, Pilsen. Semen samples were evaluated by an experienced employee. After liquefaction, they were analyzed according to the World Health Organization criteria 2010 [20]. We investigated semen volume and, under the microscope with phase-contrast optics at magnification ×200, concentration of spermatozoa, motility of spermatozoa and pathologies. Sperm motility was assessed at room temperature in Makler counting chamber. Two hundred spermatozoa per replicate were classified into three motility categories (progressive, nonprogressive, and immotile sperm cells). All samples were considered normozoospermic ejaculates (Table 1).

Fresh ejaculate (0.1 mL) was subjected to experiment with propolis. Propolis or ethanol only (1 μL) was added to 0.1 mL of fresh ejaculate (final concentration of propolis was 0.01 mg/mL) and sperm motility was evaluated after 60 minutes.

The remaining sample was prepared by gradient separation technique and used for experiment with polarographic oxygraph (Oroboros, Innsbruck, Austria) and sperm flow

TABLE 1: Main sperm parameters of the normozoospermic men (\pm SEM).

Parameters	Normozoospermic men ($n = 10$)
Volume (mL)	3.18 \pm 0.26
Concentration ($\times 10^6$ /mL)	81.22 \pm 13.97
Progressive motility (%)	62.5 \pm 4.4
Pathology morphology (%)	42.00 \pm 2.26
Concentration after separation ($\times 10^6$ /mL)	158.44 \pm 18.09
Progressive motility after separation (%)	86.43 \pm 2.10

cytometry evaluation. Sperm number after separation was also determined in the Makler counting chamber.

2.4. The Sperm Density Gradient Separation Technique. The sperm was separated and purified. This was performed using gradient solution media SpermGrad medium (SGm, Vitrolife, Sweden) and SpermRinse medium (SRm, Vitrolife, Sweden). SpermGrad medium was diluted to 90% (0.15 mL SGm : 1.35 mL SRm), 70% (0.09 mL SGm : 0.21 mL SRm) and 50% (0.15 mL SG : 0.15 mL SRm). Into a conical tube 1.5 mL 90%, 0.3 mL 70% and 0.3 mL of a 50% gradient media were layered. Full ejaculate was added and the sample was centrifuged for 20 minutes at 300 g. After removal of the supernatant, 8 mL SRm was added and then the sample was centrifuged 8 minutes at 300 g. After removal of supernatant, the sample was evaluated for the concentration and motility of spermatozoa and ready for injection into the oxygraph.

2.5. High-Resolution Respirometry. Oxygen consumption by purified spermatozoa was measured at 36°C in 2 mL glass chambers of oxygraph Oroboros (Oroboros, Innsbruck, Austria) connected to the computer with DatLab software for data acquisition and analysis (Oroboros, Innsbruck, Austria). The oxygen flux was calculated as a negative time derivative of the oxygen concentration. All values of oxygen fluxes were corrected for instrumental and chemical background measured in separate experiments performed in the same medium without human gametes.

The medium consisting of 0.5 mmol/L ethylene glycol tetraacetic acid, 3 mmol/L $MgCl_2 \cdot 6H_2O$, 60 mmol/L K-lactobionate, 20 mmol/L taurine, 10 mmol/L KH_2PO_4 , 20 mmol/L HEPES, 110 mmol/L sucrose, and 1 g/L albumin essentially fatty acid free [21] was stirred at 750 rpm and equilibrated for 60 min with air. After equilibration, oxygen concentration in the chamber corresponded to its concentration in the atmospheric air and solubility in the medium (0.92). The chambers were then closed and the samples of intact spermatozoa were injected into the chambers using Hamilton syringe. Into one of two chambers recording in parallel, propolis (0.01 mg/mL) was injected and the samples were further incubated at 36°C for 20 min. The spermatozoa cell membrane was permeabilized with digitonin (Sigma-Aldrich, St. Louis, USA; 5 μ g/mL) and combination of substrates, inhibitors, and uncouplers was

sequentially injected into the chambers to measure the respiration through different segments of the electron transport system (Figure 1). (1) Resting respiration with substrates providing electrons to complex I malate (2 mmol/L) and glutamate (10 mmol/L) was measured as a state S2 (non-phosphorylating LEAK state, L_N). (2) Active respiration was induced by 5 mmol/L adenosine diphosphate (ADP; state S3 or OXPHOS). (3) Oxygen consumption was further measured with pyruvate (5 mmol/L) and a substrate of electron transfer flavoprotein (ETF) palmitoyl carnitine (20 μ mol/L). (4) Integrity of the mitochondrial inner membrane was checked with cytochrome c (10 μ mol/L). (5) Mitochondrial respiration was then increased by succinate, complex II substrate (10 mmol/L). (6) State LEAK was induced again by inhibition of ATP-synthase oligomycin (2 μ g/mL). (7) Maximum capacity of the electron-transporting system (state S3u or ETS) was reached by titration of uncoupler trifluorocarbonylcyanide phenylhydrazide (FCCP; 0.05 μ mol/L titration steps). (8) After addition of a complex I inhibitor rotenone, the oxygen flux corresponded to maximum capacity of the electron-transporting system with the complex II only. (9) Then, antimycin A (2.5 μ mol/L), a complex III inhibitor was injected into the chambers to measure residual oxygen consumption (ROX). (10) N,N,N',N'-tetramethyl-p-phenylenediamine dihydrochloride (TMPD; 0.5 mmol/L) and ascorbate (2 mmol/L) were injected simultaneously for respirometric assay for cytochrome c oxidase (C IV) activity. In the results, oxygen fluxes recorded in the individual titration steps were corrected for residual oxygen consumption.

The dose-response relationship between the propolis concentration and sperm respiratory activity was tested in another set of experiments, where the final concentrations of propolis 0.001, 0.005, and 0.01 mg/mL were used. Higher dose of propolis was not tested as in experiments running in parallel, higher concentrations of propolis in the incubation medium (0.03 and 0.05 mg/mL) were toxic for mouse embryonic stem cells reducing their growth, survival, and proliferation (unpublished observation).

2.6. Permeability of Cell Membrane in Sperm. Sperm was treated with the impermeable fluorescent dye propidium iodide to check cell membrane permeability for substrates, inhibitors, and uncouplers after treatment by digitonin. Final concentration of propidium iodide was 1 μ g/mL.

2.7. Sperm Flow Cytometry Evaluation. Mitochondrial membrane potential ($\Delta\Psi_m$) was determined with MitoProbe JC-1 Assay Kit (Life Technologies). Each sperm sample was resuspended in 37°C warm phosphate-buffered saline (PBS) at approximately 1×10^6 cells/mL. Propolis (1 μ L) was added to test samples (100 μ L) to reach final concentration 0.01 mg/mL. Controls remained without intervention. Samples were incubated in propolis for 60 min and after that were washed with PBS. JC-1 (10 μ L of 200 μ mol/L) was added for 20 min incubation (37°C, 5% CO_2). Wash with PBS followed (5 min, 1500 rpm). Samples were resuspended in 500 μ L PBS and measured on BD FACS CANTO II cytometer (BD Biosciences, New Jersey, USA). Analysis was performed with BD FACS Diva software with 488 nm excitation using

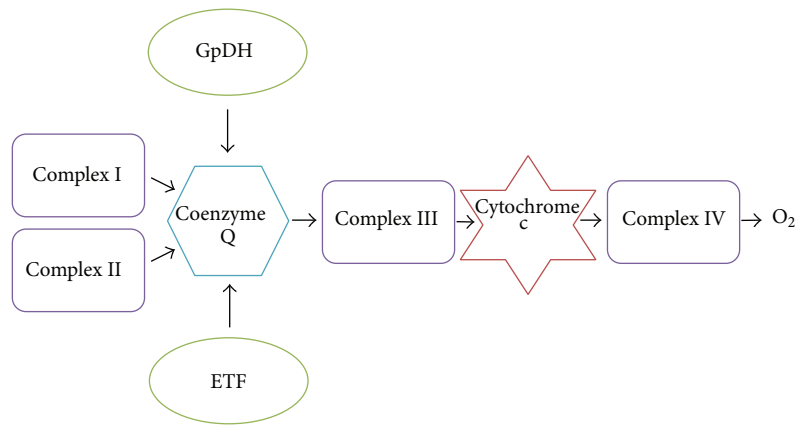


FIGURE 1: A scheme of an electrotransport convergent system. System is situated on the inner mitochondrial membrane. GpDH = glucose-6-phosphate dehydrogenase; complex I = NADH-Q reductase; complex II = succinate-Q oxidoreductase; complex III = cytochrome reductase; complex IV = cytochrome oxidase; ETF = electron-transporting flavoprotein; O₂ = oxygen.

emission filters appropriate for Alexa Fluor 488 dye and R-phycoerythrin.

2.8. Citrate Synthase Activity. Mitochondrial content in the samples aspirated from each oxygraph chamber was assayed by determination of the citrate synthase activity [22, 23]. The assay medium consisted of 0.1 mmol/L 5,5-dithio-bis-(2-nitrobenzoic) acid, 0.25% Triton-X, 0.5 mmol/L oxalacetate, 0.31 mmol/L acetyl coenzyme A, 5 μ mol/L EDTA, 5 mmol/L triethanolamine hydrochloride, and 0.1 mol/L Tris-HCl, pH 8.1 [22]. Two hundred microliters of the mixed and homogenized chamber content was added to 800 μ L of the medium. The enzyme activity was measured spectrophotometrically at 412 nm and 30°C over 200 s and expressed in mIU per 10⁷ cells.

2.9. Data Analysis and Statistics. Results are presented as mean \pm SEM. Statistical differences were analyzed using software package STATISTICA Cz, 8 (StatSoft Inc., Prague, Czech Republic). After testing for the normality of distribution and homogeneity of variances, comparisons were made using Student's *t*-test, Wilcoxon signed-rank test and analysis of variance (ANOVA) with post hoc tests corrected for multiple comparisons by Bonferroni's method. The results were considered significantly different when $P < 0.05$.

3. Results

3.1. HPLC Analysis. Analyzing the propolis by the HPLC, we were able to identify compounds as *t*-ferulic acid, *p*-coumaric acid, vanillin, caffeic acid, *t*-cinnamic acid, kaempferol, apigenin, and chrysin. Although we analyzed standards of gallic acid, benzoic acid, quercetin, naringenin, luteolin, genistein, pinocembrin, galangin, and caffeic acid phenethyl ester, they were not identified in our propolis sample. Chromatogram of ethanolic extract of the Czech propolis is presented in Figure 2. Detailed results with concentrations of observed substances are shown in Table 2.

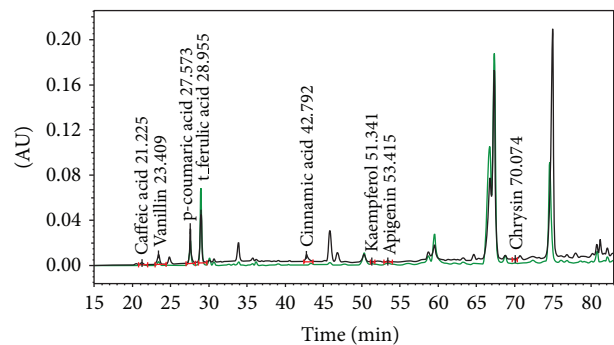


FIGURE 2: HPLC chromatogram of the Czech propolis extract and the identified compounds/retention time ($\lambda = 280$ nm—black line and $\lambda = 330$ nm—green line).

3.2. Semen Parameters and Effect of Propolis on Sperm Motility in Fresh Ejaculate. Ten healthy men were included in this study. The mean age was 24.2 years. The general sperm characteristic of the normozoospermic men after ejaculation is shown in Table 1. The effect of propolis on human sperm motility after incubation for 60 minutes is presented in Figure 3. Propolis preserved the progressive motility of spermatozoa in the native semen samples, since the percentage of the progressively motile spermatozoa after incubation with propolis remained nearly the same as in the fresh samples, whereas in the ejaculates without propolis, the progressive motility significantly declined with time ($P = 0.028$). Ethanol alone had no negative effect on sperm motility.

3.3. High Resolution Respirometry. Representative traces of the oxygen consumption in permeabilized spermatozoa with and without propolis 0.01 mg/mL are depicted in Figure 4. Oxygen consumption of intact spermatozoa (0.13 ± 0.01 nmol/(s·IU)) was significantly enhanced by propolis (0.27 ± 0.03 nmol/(s·IU); $P = 0.006$). After permeabilization with digitonin, state 2 determined in the presence of malate

TABLE 2: Analysis of the ethanolic extract of propolis by the HPLC.

Compound	Rt [min]	Concentration [mg/L of EEP]
Gallic acid	6.0	n.d
Caffeic acid	21.2	65 ± 11
Vanillin	23.4	65 ± 11
p-Coumaric acid	27.5	231 ± 10
t-Ferulic acid	28.9	514 ± 15
Benzoic acid	33.6	n.d
Quercetin	42.3	n.d
t-Cinnamic acid	42.7	29 ± 1
Naringenin	43.2	n.d.
Luteolin	44.7	n.d
Genistein	45.6	n.d
Kaempferol	51.3	101 ± 45
Apigenin	53.4	73 ± 8
Chrysin	70.0	36 ± 5
Pinocembrin	65.1	n.d.
Galangin	73.1	n.d.
CAPE	71.4	n.d.

(n.d. = nondetected; CAPE = caffeic acid phenethyl ester).

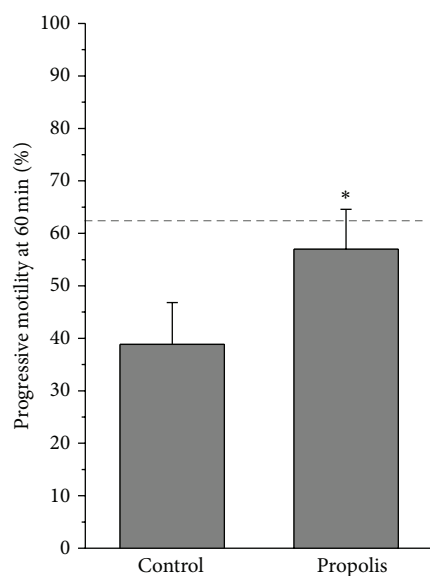


FIGURE 3: Effect of propolis on sperm motility. Columns represent progressive motility of spermatozoa in native ejaculates after 60 min incubation with propolis extract (mean ± SEM). Dashed line = progressive motility at time 0. * $P < 0.05$, compared to the respective control value.

and glutamate was 0.19 ± 0.04 nmol/(s-IU) in the control samples and it was significantly higher in the propolis-treated sperm samples (0.29 ± 0.05 nmol/(s-IU); $P = 0.014$). State 3, that is, oxygen consumption during oxidative phosphorylation, determined in the presence of ADP and substrates of the complex I, ETF, and complex II is depicted in Figure 5. Propolis significantly increased (by ~50%) S_{3I+II} oxygen flux ($P = 0.003$) suggesting increased activity of the complex II. Propolis did not influence state 4 induced by oligomycin that

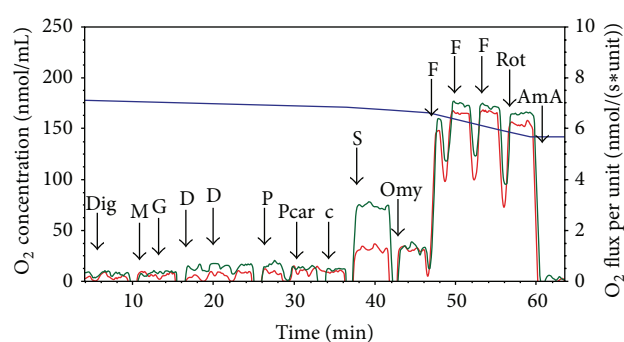


FIGURE 4: Substrate-uncoupler-inhibitor titration protocol in human spermatozoa. Substrate-uncoupler-inhibitor titration (SUIT) protocol with substrates for complex I, complex II, and electron-transferring flavoprotein (ETF) in human spermatozoa. Red line = oxygen flux expressed per IU citrate synthase activity in the control sample, green line = oxygen flux expressed per IU citrate synthase activity in the sample treated with propolis 0.01 mg/mL, and blue line = oxygen concentration in the oxygraph chamber. Dig = digitonin, M = malate, G = glutamate, D = ADP, P = pyruvate, Pcar = palmitoylcarnitine, c = cytochrome c, S = succinate, Omy = oligomycin, F = FCCP, Rot = rotenone, and AmA = antimycin A.

reached 0.81 ± 0.07 and 0.94 ± 0.09 nmol/(s-IU) in the control and propolis-treated spermatozoa, respectively. Maximum capacity of the electron-transporting system (state S3u) tested for both complexes I and II and in the presence of the complex I inhibitor rotenone was significantly higher after propolis administration (Figure 6). In measurements with TMPD + ascorbate, complex IV respiration was 12.16 ± 2.58 nmol O_2 /(s-IU) in the control samples and it was significantly enhanced by propolis to 15.4 ± 3.19 nmol O_2 /(s-IU). Absolute ethanol alone (medium for propolis, oligomycin, antimycin A, FCCP, and rotenone) in the volume up to $10 \mu\text{L}$ did not influence respirometric parameters measured with substrates of complexes I, II, and ETF in the presence of ADP.

Flux control ratios were calculated to estimate the relative efficiency of individual interventions and coupling state of the sperm mitochondria. The ratio $\text{OXPHOS}_{I+II}/\text{OXPHOS}_I$ was significantly higher in the propolis-treated samples (3.53 ± 0.42) compared to controls (2.8 ± 0.28) suggesting increased efficiency of coupled respiration when complex II was stimulated by succinate. The LEAK control ratio is the ratio of LEAK respiration and ETS capacity; it reached 0.25 ± 0.02 in the control samples and it significantly decreased after propolis to 0.21 ± 0.02 ($P = 0.024$).

The dose-response relationship tested in separate experiments is shown in Figure 7 for state S3 (OXPHOS), where glutamate, malate, pyruvate, succinate, and ADP were present in the medium, and for state S3u (ETS), where mitochondria were uncoupled by FCCP. Propolis dose-dependently increased oxygen consumption, although the extent of its effect was greater for state S3 than for state S3u.

3.4. Permeability of Cell Membrane in Sperm. Addition of $5 \mu\text{g/mL}$ of digitonin made the sperm cell membrane permeable to dye propidium iodide and for the substrates,

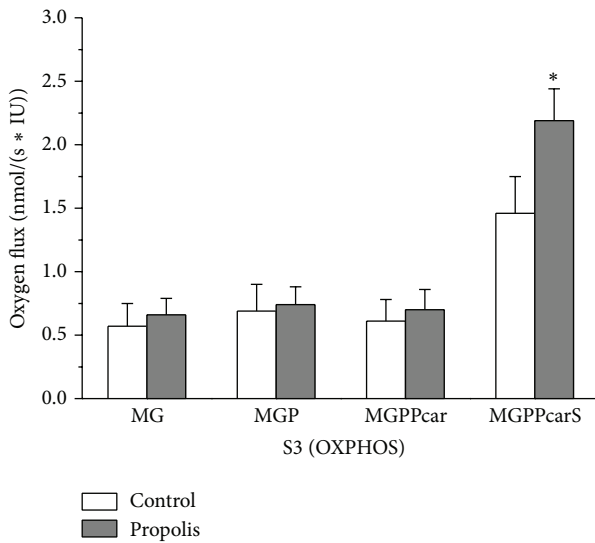


FIGURE 5: Oxygen consumption rates in the state S3 (OXPHOS) measured under control conditions and with propolis. Oxygen consumption rates in the state S3 (OXPHOS) measured under control conditions (control) and with propolis extract added (propolis) in the presence of ADP and substrates providing electrons to complex I, ETF, and complex II. M = malate, G = glutamate, P = pyruvate, Pcar = palmitoylcarnitine, and S = succinate. Oxygen fluxes were corrected for residual oxygen consumption and expressed per IU citrate synthase activity. * $P < 0.05$, compared to the respective control value.

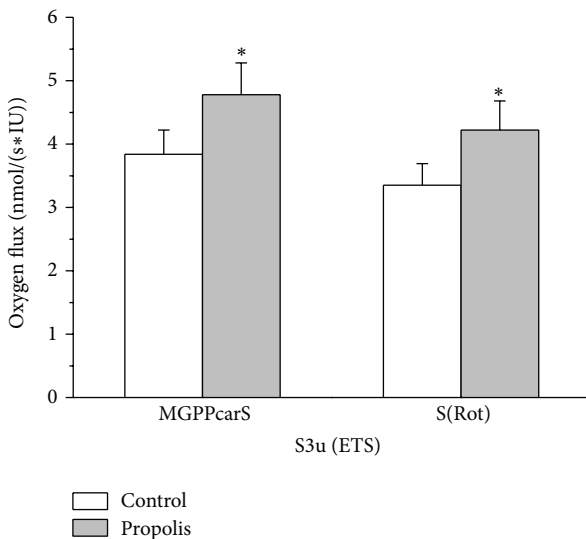


FIGURE 6: Oxygen consumption rates in the state S3u in permeabilized spermatozoa. Oxygen consumption rates in the state S3u (ETS) in permeabilized spermatozoa measured under control conditions (control) and with propolis extract added (propolis) in the presence of FCCP and substrates providing electrons to complex I, ETF, and complex II. M = malate, G = glutamate, P = pyruvate, Pcar = palmitoylcarnitine, S = succinate, and complex I inhibitor rotenone (Rot). Oxygen fluxes were corrected for residual oxygen consumption and expressed per IU citrate synthase activity. * $P < 0.05$, compared to the respective control value.

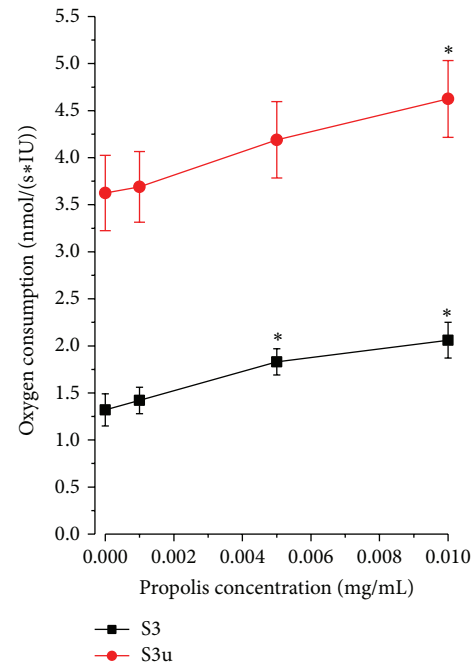


FIGURE 7: Dose response relationship between oxygen consumption and final propolis concentration. State S3 (OXPHOS) = oxygen consumption rate in permeabilized spermatozoa measured with malate, glutamate, pyruvate, succinate, and ADP. State S3u = oxygen consumption rate in permeabilized spermatozoa measured after sequential addition of malate, glutamate, ADP, pyruvate, succinate, and FCCP. Oxygen fluxes were corrected for residual oxygen consumption and expressed per IU citrate synthase activity. * $P < 0.05$, compared to the respective value without propolis.

inhibitors, and uncouplers required to determine high resolution respirometry (Figure 8).

3.5. Sperm Flow Cytometry Evaluation. Depolarization of the mitochondrial membrane is a sensitive indicator of mitochondrial damage. JC-1 is a membrane-permeable fluorescent probe aggregating in the mitochondrial matrix and then emitting red fluorescence, if $\Delta\Psi_m$ is high. In case of mitochondrial depolarization, the monomeric form of JC-1 cannot accumulate in the mitochondrial matrix and produce green fluorescence in the cytoplasm. In the spermatozoa, loss of $\Delta\Psi_m$ could serve as a marker of early apoptosis and sperm dysfunction [24]. In our experiments, incubation of the sperm samples with propolis (60 minutes) had no significant effect on $\Delta\Psi_m$ (Figure 9). In the control samples, the percentage of cells with high $\Delta\Psi_m$ was $98.43 \pm 1.07\%$ and it even slightly increased in the propolis-treated spermatozoa reaching $99.33 \pm 0.25\%$.

3.6. Citrate Synthase Activity. In the control samples, citrate synthase activity was 6.58 ± 0.84 mIU/ 10^7 cells and it was not significantly affected by propolis (6.08 ± 0.84 mIU/ 10^7 cells) and by the substances (substrates, inhibitors, media) added during the respirometric measurements, as tested in separate controls.

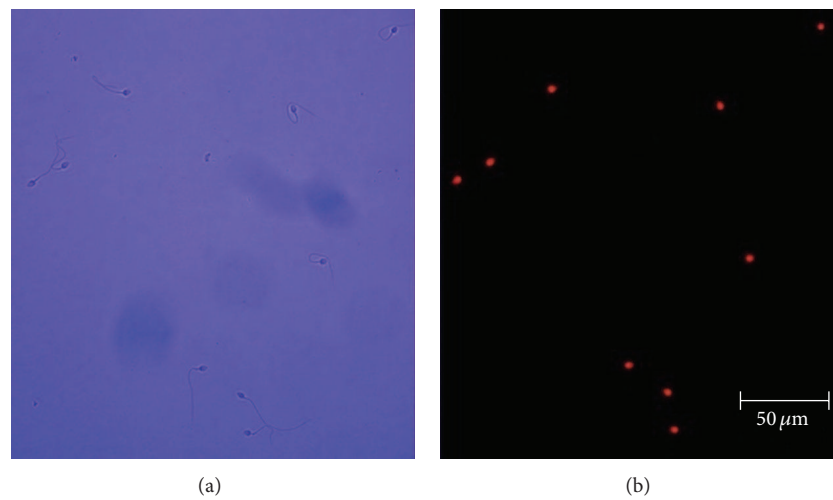


FIGURE 8: Effect of digitonin treatment on spermatozoa. (a) Micrograph of human spermatozoa and (b) fluorescent micrograph of the same optical field after treatment with the nonpermeable nuclear dye propidium iodide.

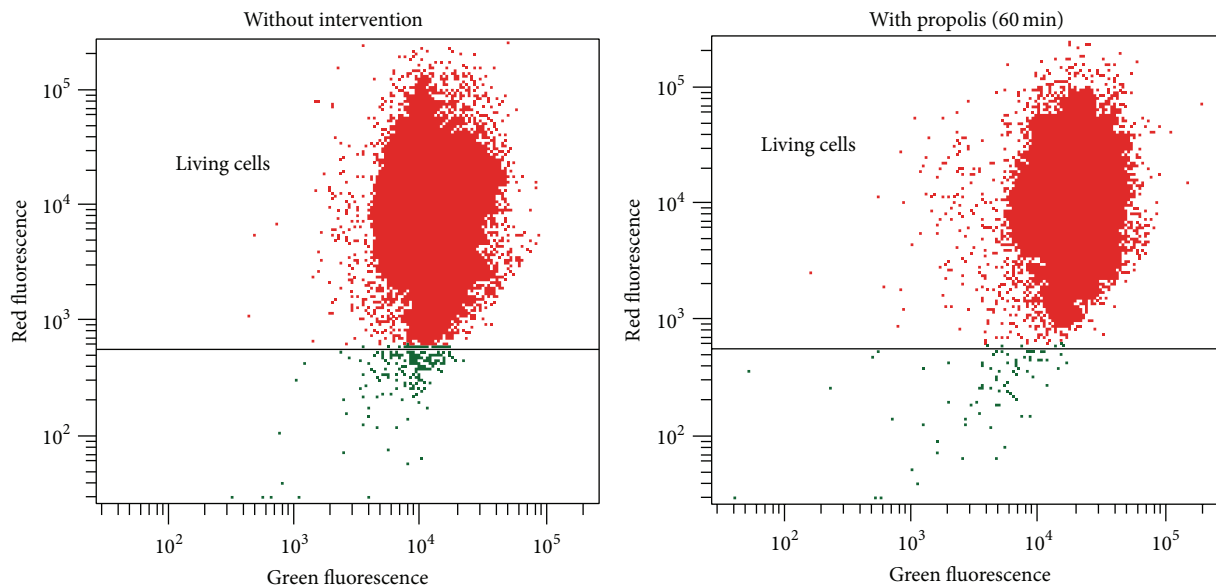


FIGURE 9: Typical double fluorescence dot plots of flow cytometry analysis. Mitochondrial membrane potential was determined with MitoProbe JC-1 Assay Kit (Life Technologies). R-phycoerythrin = red fluorescence, normal cells; Alexa Fluor 488 dye = green fluorescence, reduced mitochondrial membrane potential.

4. Discussion

This is the first study showing chemical composition of propolis collected in the Czech Republic. Bee glue has a very complex chemical composition that depends on a number of factors including diversity of plants and geographical location from which bees collect it. Although the region of collection of the tested sample of propolis is situated in the northern temperate zone where the “poplar” type propolis is a typical bee product [3], the tree structure within the mentioned locality is composed of coniferous trees (90%), birch (6%), alder (2%), beech (1%), and oak (1%) [25]. However, the tested sample contained chrysin,

the reference flavonoid in poplar propolis, and phenolic acids and other flavonoids typically found in bee glue extracts originating from similar geographical regions and reported to be responsible for various beneficial effects of propolis [26]. Among them, ferulic acid, coumaric acid, and kaempferol were present in the highest concentrations in the Czech propolis extract. Caffeic acid phenethyl ester, naringenin, and quercetin—substances frequently contained in the poplar propolis [2, 3] and widely tested for their anti-inflammatory, anticancer, and antioxidant activities in recent years [27]—have not been detected in the Czech propolis. The factors that could contribute to the above mentioned differences could include not only diversity of plant species growing around

the hive, but also season, illumination, altitude, collector type, and food availability [28]. It should be noted that the search for a single substance or a particular substance class that could be responsible for the beneficial actions of propolis has not been successful to date. Scientific studies demonstrated that biological activity of propolis could be almost identical (i.e., antimicrobial, antitumor, antioxidant, anti-inflammatory, etc.) in samples from different climatic zones and of completely different chemical composition [3]. Most probably, a combination of substances is essential for the biological activity of bee glue [29].

The present study describes the effects of propolis on the sperm motility, mitochondrial membrane potential, and mitochondrial respiratory activity assessed by high-resolution respirometry allowing determination of individual respiratory states in a sequential manner on the same sample, thus allowing complex evaluation of the mitochondrial function close to the situation *in vivo*. In addition, high sensitivity of the method enables determination of respirometric activity of individual mitochondrial complexes in a relatively small amount of cells [30]. In our experiments, we have used the purified spermatozoa that were subjected to membrane permeabilization by mild nonionic detergent digitonin, the dose of which was carefully titrated to permeabilize the cell membrane without damaging the mitochondrial function. To date, oxygen consumption by human sperm mitochondria has been determined mostly by traditional oxygraphy in the germ cells subjected to hypotonic swelling [13, 31–33]. However, in the spermatozoa of several mammalian species, hypotonic challenge could substantially influence the activity of various protein kinases (PK), including PKA, PKC, and protein-tyrosine kinase via osmosensitive K^+ and Cl^- channels in the process called regulatory volume decrease requiring energy supply [34].

The major finding of the present study is that propolis enhances the activity of mitochondrial respiratory complexes II and IV without affecting the coupling of the electron transport to ATP synthesis and/or mitochondrial membrane potential in permeabilized human spermatozoa *in vitro*. In the coupled state, propolis enhanced oxygen consumption with complex I and complex II substrates by ~50%. This increase was attributed to complex II, since the activity of complex I alone was not affected by propolis. In addition, the ratio P_{I+II}/P_I was significantly higher in the propolis-treated samples. Similarly, in the uncoupled state (S3u, E), oxygen consumption was significantly (by ~25%) higher after propolis, both in the presence of substrates of complexes I and II and after inhibition of complex I by rotenone. Activity of the complex IV was increased to the same extent (~27%).

The data available on the effects of propolis and its major compounds on mitochondrial respiration or activity of individual mitochondrial enzymes involved in the electron-transport convergent system are scarce. The most frequent finding is that this effect is negligible in normal somatic cells (cardiomyocytes, neurons, and hepatocytes), but becomes beneficial in the cells challenged by toxic stimuli where oxidative phosphorylation is compromised [16, 35, 36]. In contrast, in various types of tumor cells, propolis extract or its constituents inhibit oxidative phosphorylation and trigger

release of cytochrome c and subsequent apoptosis [15, 17]. In view of this, the action of propolis on the cellular respiration is not easily predictable and depends on the cell type.

Some studies suggested that propolis or its phenolic constituents might influence mitochondrial membrane potential via increased permeability of the inner mitochondrial membrane [14]. This issue was addressed in the experiments with MitoProbe JC-1 Assay Kit that clearly showed that in the human spermatozoa, mitochondrial membrane potential was not affected by propolis. In addition, oligomycin-induced respiratory state (LEAK) that reflects compensation for the proton leak, proton slip, electron slip, and cation cycling [30] was not affected by propolis. Thus, the decrease in the LEAK control ratio after propolis could be attributed to the increased efficiency of the electron transport through complex II. The putative molecular mechanism of complex II activation was suggested in study of Cimen et al. [37], where propolis constituent kaempferol increased deacetylation of succinate dehydrogenase thus increasing its activity.

To date, the effects of propolis or propolis compounds on the sperm characteristics have been rarely studied. The whole propolis extract was used in studies conducted by Yousef and collaborators on rats and rabbits that were treated with propolis for 10 to 12 weeks [38, 39]. Administration of propolis resulted in an increased sperm count and motility, plasma testosterone levels, and a decreased dead and abnormal sperm count. A single study documented positive effect of the propolis compound chrysin on the sperm motility, sperm concentration, and serum testosterone levels [40]. Ferulic acid was also reported to enhance sperm motility and viability [41]. All these findings were attributed to the activity of propolis as antioxidant and none of these studies dealt with the action of propolis or its constituents on mitochondrial energy production. Our study describes a novel beneficial effect of propolis on the sperm characteristics.

Recent experimental evidence suggests that oxidative phosphorylation in the human spermatozoa plays a crucial role in gaining energy for the sperm motility and indicates that asthenozoospermia might be related to the impaired mitochondrial functionality [42]. High-resolution respirometry could provide new data in search for substances that could positively affect human sperm motility and thus improve sperm fertilizing ability. In addition, detailed analysis of respiratory efficiency of individual mitochondrial enzymatic complexes under coupled and uncoupled conditions could provide better insight into pathophysiology of asthenozoospermia.

5. Conclusions

This study demonstrates, for the first time, that ethanolic extract of propolis increases activities of mitochondrial respiratory complexes II and IV without affecting mitochondrial membrane potential. The obtained data suggest that propolis improves the total mitochondrial respiratory efficiency in the human spermatozoa *in vitro* thereby having potential to improve the sperm motility.

Conflict of Interests

The authors declare that they have no conflict of interests regarding the publication of this paper.

Authors' Contribution

Miroslava Cedikova and Jitka Kuncova contributed equally to this work.

Acknowledgments

This work was supported by the Project ED2.1.00/03.0076 from European Regional Development Fund, the Charles University Research Fund (Project no. P36), the Specific Student Research Project no. 260048/2014 of the Charles University in Prague and by the Grant from Charles University Grant Agency no. 969212.

References

- [1] M. Viuda-Martos, Y. Ruiz-Navajas, J. Fernández-López, and J. A. Pérez-Álvarez, "Functional properties of honey, propolis, and royal jelly," *Journal of Food Science*, vol. 73, no. 9, pp. R117–R124, 2008.
- [2] V. Bankova, M. Popova, S. Bogdanov, and A. G. Sabatini, "Chemical composition of European propolis: expected and unexpected results," *Zeitschrift für Naturforschung C: A Journal of Biosciences*, vol. 57, no. 5–6, pp. 530–533, 2002.
- [3] V. Bankova, "Chemical diversity of propolis and the problem of standardization," *Journal of Ethnopharmacology*, vol. 100, no. 1–2, pp. 114–117, 2005.
- [4] A. Russo, R. Longo, and A. Vanella, "Antioxidant activity of propolis: role of caffeic acid phenethyl ester and galangin," *Fitoterapia*, vol. 73, supplement 1, pp. S21–S29, 2002.
- [5] A. M. Gómez-Caravaca, M. Gómez-Romero, D. Arráez-Román, A. Segura-Carretero, and A. Fernández-Gutiérrez, "Advances in the analysis of phenolic compounds in products derived from bees," *Journal of Pharmaceutical and Biomedical Analysis*, vol. 41, no. 4, pp. 1220–1234, 2006.
- [6] M. L. Khalil, "Biological activity of bee propolis in health and disease," *Asian Pacific Journal of Cancer Prevention*, vol. 7, no. 1, pp. 22–31, 2006.
- [7] A. H. Banskota, Y. Tezuka, and S. Kadota, "Recent progress in pharmacological research of propolis," *Phytotherapy Research*, vol. 15, no. 7, pp. 561–571, 2001.
- [8] M. Králícková, P. Síma, and Z. Rokyta, "Role of the leukemia-inhibitory factor gene mutations in infertile women: the embryo-endometrial cytokine cross talk during implantation—a delicate homeostatic equilibrium," *Folia Microbiologica*, vol. 50, no. 3, pp. 179–186, 2005.
- [9] J. C. St. John, D. Sakkas, and C. L. R. Barratt, "A role for mitochondrial DNA and sperm survival," *Journal of Andrology*, vol. 21, no. 2, pp. 189–199, 2000.
- [10] W. C. L. Ford, "Glycolysis and sperm motility: does a spoonful of sugar help the flagellum go round?" *Human Reproduction Update*, vol. 12, no. 3, pp. 269–274, 2006.
- [11] R. M. Turner, "Moving to the beat: a review of mammalian sperm motility regulation," *Reproduction, Fertility and Development*, vol. 18, no. 1–2, pp. 25–38, 2006.
- [12] V. Y. Rawe, R. Hermes, F. N. Nodar, G. Fiszbajn, and H. E. Chemes, "Results of intracytoplasmic sperm injection in two infertile patients with abnormal organization of sperm mitochondrial sheaths and severe asthenoteratozoospermia," *Fertility and Sterility*, vol. 88, no. 3, pp. 649–653, 2007.
- [13] A. Ferramosca, R. Focarelli, P. Piomboni, L. Coppola, and V. Zara, "Oxygen uptake by mitochondria in demembrated human spermatozoa: a reliable tool for the evaluation of sperm respiratory efficiency," *International Journal of Andrology*, vol. 31, no. 3, pp. 337–345, 2008.
- [14] S. Das, J. Das, A. Samadder, N. Boujedaini, and A. R. Khuda-Bukhsh, "Apigenin-induced apoptosis in A375 and A549 cells through selective action and dysfunction of mitochondria," *Experimental Biology and Medicine*, vol. 237, no. 12, pp. 1433–1448, 2012.
- [15] V. Chen, R. E. Staub, S. Baggett et al., "Identification and analysis of the active phytochemicals from the anti-cancer botanical extract Bezielle," *PLoS ONE*, vol. 7, no. 1, Article ID e30107, 2012.
- [16] R. Lagoa, I. Graziani, C. Lopez-Sanchez, V. Garcia-Martinez, and C. Gutierrez-Merino, "Complex I and cytochrome *c* are molecular targets of flavonoids that inhibit hydrogen peroxide production by mitochondria," *Biochimica et Biophysica Acta*, vol. 1807, no. 12, pp. 1562–1572, 2011.
- [17] R. D. Yeh, J. C. Chen, T. Y. Lai et al., "Gallic acid induces G₀/G₁ phase arrest and apoptosis in human leukemia HL-60 cells through inhibiting cyclin D and E, and activating mitochondria-dependent pathway," *Anticancer Research*, vol. 31, no. 9, pp. 2821–2832, 2011.
- [18] J. S. Bonvehí and A. L. Gutiérrez, "The antimicrobial effects of propolis collected in different regions in the Basque Country (Northern Spain)," *World Journal of Microbiology and Biotechnology*, vol. 28, no. 4, pp. 1351–1358, 2012.
- [19] M. Barbarić, K. Mišković, M. Bojić et al., "Chemical composition of the ethanolic propolis extracts and its effect on HeLa cells," *Journal of Ethnopharmacology*, vol. 135, no. 3, pp. 772–778, 2011.
- [20] WHO, "WHO laboratory manual for the examination and processing of human semen," 2010, <http://www.who.int/reproductivehealth/publications/infertility/9789241547789/en/>.
- [21] E. Gnaiger, G. Méndez, and S. C. Hand, "High phosphorylation efficiency and depression of uncoupled respiration in mitochondria under hypoxia," *Proceedings of the National Academy of Sciences of the United States of America*, vol. 97, no. 20, pp. 11080–11085, 2000.
- [22] A. V. Kuznetsov, D. Strobl, E. Ruttman, A. Königsrainer, R. Margreiter, and E. Gnaiger, "Evaluation of mitochondrial respiratory function in small biopsies of liver," *Analytical Biochemistry*, vol. 305, no. 2, pp. 186–194, 2002.
- [23] S. Larsen, J. Nielsen, C. N. Hansen et al., "Biomarkers of mitochondrial content in skeletal muscle of healthy young human subjects," *The Journal of Physiology*, vol. 590, no. 14, pp. 3349–3360, 2012.
- [24] G. Barroso, S. Taylor, M. Morshedi, F. Manzur, F. Gaviño, and S. Oehninger, "Mitochondrial membrane potential integrity and plasma membrane translocation of phosphatidylserine as early apoptotic markers: a comparison of two different sperm subpopulations," *Fertility and Sterility*, vol. 85, no. 1, pp. 149–154, 2006.
- [25] Č. R. Lesy, s. p., <http://www.lesy.cz/ls229/charakteristika-lesni-spravy/Stranky/default.aspx>.
- [26] R. D. Wojtyczka, A. Dziedzic, D. Idzik et al., "Susceptibility of *Staphylococcus aureus* clinical isolates to propolis extract alone

- or in combination with antimicrobial drugs,” *Molecules*, vol. 18, no. 8, pp. 9623–9640, 2013.
- [27] G. Ozturk, Z. Ginis, S. Akyol, G. Erden, A. Gurel, and O. Akyol, “The anticancer mechanism of caffeic acid phenethyl ester (CAPE): review of melanomas, lung and prostate cancers,” *European Review for Medical and Pharmacological Sciences*, vol. 16, no. 15, pp. 2064–2068, 2012.
- [28] V. C. Toreti, H. H. Sato, G. M. Pastore, and Y. K. Park, “Recent progress of propolis for its biological and chemical compositions and its botanical origin,” *Evidence-Based Complementary and Alternative Medicine*, vol. 2013, Article ID 697390, 13 pages, 2013.
- [29] A. Kujungiev, I. Tsvetkova, Y. Serkedjieva, V. Bankova, R. Christov, and S. Popov, “Antibacterial, antifungal and antiviral activity of propolis of different geographic origin,” *Journal of Ethnopharmacology*, vol. 64, no. 3, pp. 235–240, 1999.
- [30] D. Pesta and E. Gnaiger, “High-resolution respirometry: OXPHOS protocols for human cells and permeabilized fibers from small biopsies of human muscle,” *Methods in Molecular Biology*, vol. 810, pp. 25–58, 2012.
- [31] M. Piasecka and J. Kawiak, “Sperm mitochondria of patients with normal sperm motility and with asthenozoospermia: Morphological and functional study,” *Folia Histochemica et Cytobiologica*, vol. 41, no. 3, pp. 125–139, 2003.
- [32] M. Piasecka, M. Laszczyńska, and D. Gaczarzewicz, “Morphological and functional evaluation of spermatozoa from patients with asthenoteratozoospermia,” *Folia Morphologica*, vol. 62, no. 4, pp. 479–481, 2003.
- [33] A. Stendardi, R. Focarelli, P. Piomboni et al., “Evaluation of mitochondrial respiratory efficiency during in vitro capacitation of human spermatozoa,” *International Journal of Andrology*, vol. 34, no. 3, pp. 247–255, 2011.
- [34] A. M. Petrunkina, R. A. P. Harrison, M. Tsoleva, E. Jebe, and E. Töpfer-Petersen, “Signalling pathways involved in the control of sperm cell volume,” *Reproduction*, vol. 133, no. 1, pp. 61–73, 2007.
- [35] R. Barros Silva, N. A. G. Santos, N. M. Martins et al., “Caffeic acid phenethyl ester protects against the dopaminergic neuronal loss induced by 6-hydroxydopamine in rats,” *Neuroscience*, vol. 233, pp. 86–94, 2013.
- [36] K. S. Kumaran and P. S. M. Prince, “Caffeic acid protects rat heart mitochondria against isoproterenol-induced oxidative damage,” *Cell Stress and Chaperones*, vol. 15, no. 6, pp. 791–806, 2010.
- [37] H. Cimen, M. J. Han, Y. Yang, Q. Tong, H. Koc, and E. C. Koc, “Regulation of succinate dehydrogenase activity by SIRT3 in mammalian mitochondria,” *Biochemistry*, vol. 49, no. 2, pp. 304–311, 2010.
- [38] M. I. Yousef and A. F. Salama, “Propolis protection from reproductive toxicity caused by aluminium chloride in male rats,” *Food and Chemical Toxicology*, vol. 47, no. 6, pp. 1168–1175, 2009.
- [39] M. I. Yousef, K. I. Kamel, M. S. Hassan, and A. M. A. El-Morsy, “Protective role of propolis against reproductive toxicity of triphenyltin in male rabbits,” *Food and Chemical Toxicology*, vol. 48, no. 7, pp. 1846–1852, 2010.
- [40] O. Ciftci, I. Ozdemir, M. Aydin, and A. Beytur, “Beneficial effects of chrysin on the reproductive system of adult male rats,” *Andrologia*, vol. 44, no. 3, pp. 181–186, 2012.
- [41] R. Zheng and H. Zhang, “Effects of ferulic acid on fertile and asthenozoospermic infertile human sperm motility, viability, lipid peroxidation, and cyclic nucleotides,” *Free Radical Biology and Medicine*, vol. 22, no. 4, pp. 581–586, 1997.
- [42] A. Ferramosca, S. P. Provenzano, L. Coppola, and V. Zara, “Mitochondrial respiratory efficiency is positively correlated with human sperm motility,” *Urology*, vol. 79, no. 4, pp. 809–814, 2012.

Identification of CMY-2-Type Cephalosporinases in Clinical Isolates of *Enterobacteriaceae* by MALDI-TOF MS

C. C. Papagiannitsis,^a S. D. Kotsakis,^b Z. Tuma,^c M. Gniadkowski,^d V. Miriagou,^b J. Hrabak^a

Department of Microbiology, Faculty of Medicine and University Hospital in Plzen, Charles University in Prague, Plzen, Czech Republic^a; Laboratory of Bacteriology, Hellenic Pasteur Institute, Athens, Greece^b; Proteomic Laboratory, Charles University Medical School, Plzen, Czech Republic^c; National Medicines Institute, Warsaw, Poland^d

This study exploited the possibility to detect *Citrobacter freundii*-derived CMY-2-like cephalosporinases in *Enterobacteriaceae* clinical isolates using matrix-assisted laser desorption ionization–time of flight mass spectrometry (MALDI-TOF MS). Periplasmic proteins were prepared using a modified sucrose method and analyzed by MALDI-TOF MS. A ca. 39,850-*m/z* peak, confirmed to represent a *C. freundii*-like β -lactamase by in-gel tryptic digestion followed by MALDI-TOF/TOF MS, was observed only in CMY-producing isolates. We have also shown the potential of the assay to detect ACC- and DHA-like AmpC-type β -lactamases.

Matrix-assisted laser desorption ionization–time of flight mass spectrometry (MALDI-TOF MS) is increasingly used as a procedure for identification of pathogenic bacteria and fungi due to its time- and cost-effectiveness (1, 2). Recently, further applications of MALDI-TOF MS focusing on antimicrobial resistance mechanisms, including detection of carbapenemase activity in *Enterobacteriaceae*, *Pseudomonas* spp., and *Acinetobacter* spp., have been described (3–7).

In 2007, Camara and Hays described for the first time the use of MALDI-TOF MS for differentiating wild-type *Escherichia coli* from ampicillin-resistant (Amp^r) plasmid-transformed *E. coli* strains by the direct visualization of a β -lactamase (8). In a recent MALDI-TOF MS study, Schaumann et al. were not able to distinguish *Enterobacteriaceae* and *P. aeruginosa* isolates producing extended-spectrum β -lactamases (ESBLs) or metallo- β -lactamases (MBLs) from nonproducers (9). Consequently, so far the attempts to visualize native β -lactamases by MALDI-TOF MS in wild-type bacteria have been mostly unsuccessful.

We describe here a new assay for the identification of CMY-2-like β -lactamases in clinical enterobacterial isolates by MALDI-TOF MS. These enzymes are the most prevalent acquired AmpC-type cephalosporinases in *Enterobacteriaceae* (10). The method is based on the extraction of periplasmic proteins and the detection of CMY-2-like β -lactamases by MALDI-TOF MS according to their molecular weight.

Thirty-eight characterized *Enterobacteriaceae* strains from collections of the Faculty of Medicine and University Hospital in Plzen, Czech Republic, the Hellenic Pasteur Institute in Athens, Greece, and the National Medicines Institute in Warsaw, Poland, were used (Table 1) (11, 12). The group included 29 CMY-2-positive clinical isolates, two *E. coli* transconjugants/transformants with CMY-2-like enzymes (*E. coli* A15 or DH5 α), and seven non-CMY-producing isolates (13–21). *E. coli* ATCC 25922 and *Klebsiella pneumoniae* ATCC 13883 were used as negative controls. Purified CMY-2 enzyme (13) was used as a positive control for MALDI-TOF MS measurements.

Isolates were inoculated into 50 ml of Mueller-Hinton broth (Oxoid Ltd.) and incubated at 35°C for 16 h. Cultures were centrifuged at 5,000 \times *g* for 20 min, and the cell pellet was used for the extraction of the periplasmic proteins, performed essentially as

described by Naglak and Wang (22). Briefly, the pellet was resuspended in 360 μ l of 40% sucrose and incubated for 2 h at 4°C. After centrifugation (5,000 \times *g*, 5 min), the supernatant was discarded and the cell pellet was resuspended in 360 μ l of ice-cold double-distilled water (ddH₂O). After a 30-min incubation at 4°C, 40 μ l of 1 M Tris-HCl buffer (pH 7.8) and 12 μ l of lysozyme (10 mg/liter) were added to the suspension, which was then incubated for 90 min at 35°C. Spheroplasts were removed by centrifugation (14,000 \times *g*, 5 min), leaving the periplasmic fraction in the supernatant.

A 200- μ l volume of the periplasmic proteins was added to 1 ml of ice-cold ethanol (95%) supplemented with trifluoroacetic acid (TFA; 0.1%). After 20 min of incubation at –20°C, the solution was centrifuged at 14,000 \times *g* for 20 min. The supernatant was removed, and the pellet was allowed to dry. The pellet was resuspended in 50 μ l of TFA-acetonitrile-water (0.1:50:49.9 [volume fraction]), using a vortex device for 1 min, and centrifuged (14,000 \times *g*, 2 min) to obtain the supernatant extract. Subsequently, 1 μ l of each supernatant was applied on a stainless steel MALDI target plate (MSP 96 Target; Bruker Daltonics). After air drying, each sample was overlaid with 1 μ l of matrix (sinapinic acid as a saturated solution in 50% ethanol). The matrix/sample spots were allowed to crystallize at room temperature. Each sample was spotted in triplicate. The MALDI-TOF mass spectra were obtained using a Microflex LT mass spectrometer with flexControl 3.3 software (Bruker Daltonics), operating in the positive linear ion mode within the *m/z* range 20,000 to 45,000. The parameters were set up as follows: ion source 1, 20 kV; ion source 2, 16.7 kV; lens, 7 kV; pulsed ion extraction, 170 ns; detection gain, 50 \times ; electronic gain, enhanced (100 mV); sample rate, 2.0 GS/s; mass

Received 5 November 2013 Returned for modification 1 December 2013

Accepted 15 February 2014

Published ahead of print 24 February 2014

Address correspondence to J. Hrabak, jaroslav.hrabak@lfp.cuni.cz.

Copyright © 2014, American Society for Microbiology. All Rights Reserved.

doi:10.1128/AAC.02418-13

TABLE 1 Summary of the MALDI-TOF MS analysis of the periplasmic extracts^a

Strain	Country	β -Lactamase(s) produced	Peak at m/z 39,850	Reference or source
<i>E. coli</i> pB-cmy2	Greece	Cloned CMY-2	+	13
<i>E. coli</i> S95	Greece	CMY-6	+	14
<i>E. coli</i> S208	Greece	LAT-1, SHV-5, TEM-1	+	14
<i>E. coli</i> T27	Greece	CMY-2, CTX-M-3, TEM-1	–	15
<i>E. coli</i> AK-3281	Greece	CMY-2, TEM-1	+	This study
<i>E. coli</i> AK-5231	Greece	CMY-2, TEM-1	+	This study
<i>E. coli</i> AK-5495	Greece	CMY-2, TEM-1	+	This study
<i>E. coli</i> PL 5143/09	Poland	CMY-2	+	16
<i>E. coli</i> PL 5138/09	Poland	CMY-4	+	16
<i>E. coli</i> PL 6691/10	Poland	CMY-42	+	16
<i>E. coli</i> Cz 9162	Czech Republic	CMY-2, CTX-M-15	+	This study
Trc <i>E. coli</i> Cz 9162	Czech Republic	CMY-2	+	This study
<i>E. coli</i> Cz 9178	Czech Republic	CMY-2	+	This study
<i>E. coli</i> Cz 9261	Czech Republic	CTX-M-14	–	This study
<i>E. coli</i> Cz 9309	Czech Republic	CTX-M-27	–	This study
<i>E. coli</i> Cz 9355	Czech Republic	CTX-M-15	–	This study
<i>E. coli</i> A15		NT	–	
<i>E. coli</i> ATCC 25922		NT	–	
<i>E. aerogenes</i> Y15	Greece	CMY-2	+	14
<i>E. aerogenes</i> Y25	Greece	CMY-2, SHV-5	+	14
<i>K. pneumoniae</i> P20	Greece	LAT-1, SHV-5	+	17
<i>K. pneumoniae</i> L67	Greece	CMY-2	–	14
<i>K. pneumoniae</i> N1	Greece	CMY-2, SHV-5, TEM-1	+	14
<i>K. pneumoniae</i> N2	Greece	CMY-2, SHV-5, TEM-1	+	14
<i>K. pneumoniae</i> T80	Greece	CMY-2	+	14
<i>K. pneumoniae</i> HP205	Greece	CMY-36, SHV-5, TEM-1	+	18
<i>K. pneumoniae</i> PL 7246/10	Poland	CMY-2	+	19
<i>K. pneumoniae</i> PL 6185/11	Poland	CMY-4, VIM-19	–	This study
<i>K. pneumoniae</i> Cz 1006	Czech Republic	CMY-2	+	This study
<i>K. pneumoniae</i> Cz 3602	Czech Republic	CMY-2, NDM-1	+	This study
<i>K. pneumoniae</i> Cz 431	Czech Republic	VIM-1, SHV-5	–	This study
<i>K. pneumoniae</i> Cz 597	Czech Republic	KPC-2, OXA-9, SHV-12, TEM-1	–	This study
<i>K. pneumoniae</i> Cz 163243	Czech Republic	SHV-5	–	This study
<i>K. pneumoniae</i> ATCC 13883		NT	–	
<i>P. mirabilis</i> PL 6735/99	Poland	CMY-14, TEM-1	–	20
<i>P. mirabilis</i> PL 27/00	Poland	CMY-12, TEM-2	+	20
<i>P. mirabilis</i> PL 1662/00	Poland	CMY-15, TEM-2	+	20
<i>P. mirabilis</i> PL 864/01	Poland	CMY-4, TEM-1	–	20
<i>P. mirabilis</i> PL 1376/01	Poland	CMY-45, TEM-1	–	20
<i>P. mirabilis</i> PL 1455/04	Poland	CMY-38, TEM-2	+	20
<i>P. mirabilis</i> PM91	Greece	VEB-1, VIM-1	–	21

^a +, peak at m/z 39,850 observed; –, peak at m/z 39,850 not observed. Trc, transconjugant; NT, not tested.

range selector, medium range; laser frequency, 30 Hz; digitizer trigger level, 2,500 mV; and laser range, 100%. Spectra were measured manually in at least 10 positions with 500 laser shots. Spectra were analyzed using flexAnalysis 3.0 software (Bruker Daltonics).

The MALDI-TOF MS measurement of the molecular mass of the purified CMY-2 detected one major peak with m/z of 39,852 (Fig. 1), slightly differing from the expected value for the mature CMY-2 protein (39,854 [23]). The presence of a peak with a m/z of ca. 39,850 was also observed in the mass spectrum of the CMY-2-producing *E. coli* DH5 α pB-cmy2 transformant. In the mass spectra of the tested isolates, the \sim 39,850- m/z peak was found in most of the *E. coli* isolates (11/12) and *K. pneumoniae* isolates (8/10) and in all *Enterobacter aerogenes* isolates (2/2) producing CMY-2-like

enzymes (Table 1). Of six *Proteus mirabilis* isolates, the peak was identified in three. The latter isolates carried two copies of the *bla*_{CMY-2}-like gene in their chromosomes, while the false-negative ones carried a single copy of the gene (20). The lack of the \sim 39,850- m/z peak was observed for *E. coli* and *K. pneumoniae* ATCC strains and for all of the non-CMY-producing isolates. Mass spectra of representative isolates are shown in Fig. 1.

The protein content of periplasmic extracts was characterized by sodium dodecyl sulfate polyacrylamide gel electrophoresis (SDS-PAGE) (8). Protein bands of around 40,000 g/mol were detected in extracts of all the CMY-producing strains that were positive in the MALDI-TOF MS assay. These bands comigrated with the purified CMY-2 β -lactamase and were not found in the non-CMY-producing strains and the CMY producers that were nega-

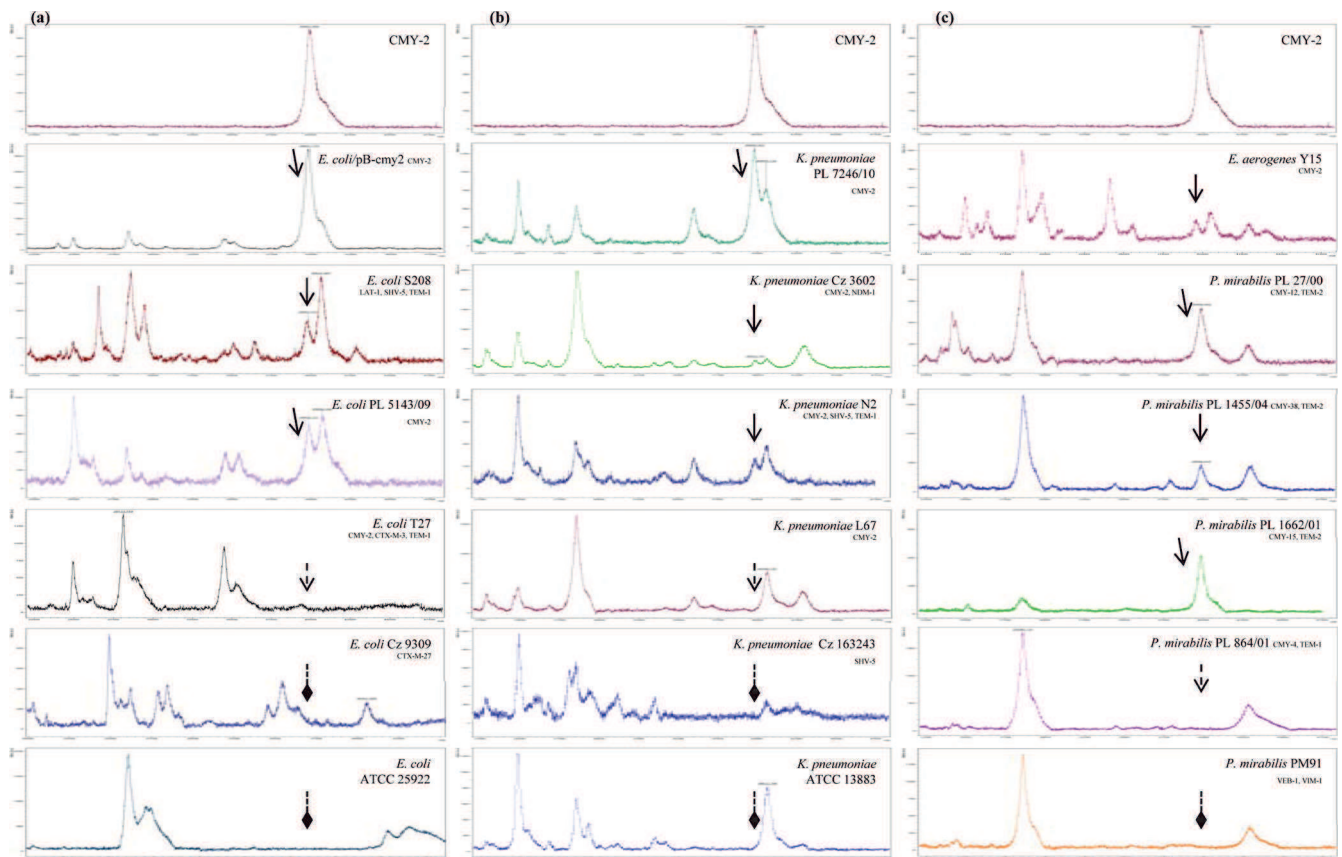


FIG 1 Mass spectra of the purified CMY-2 enzyme and the periplasmic extracts of representative CMY-2 and non-CMY-2-producing *E. coli* (a), *K. pneumoniae* (b), and *E. aerogenes* and *P. mirabilis* (c) isolates. Peaks corresponding to CMY β -lactamases are indicated with arrows with solid lines. The absence of the ca. 39,850- m/z peaks, representing CMY β -lactamases, is indicated with arrows with dotted lines for CMY producers and diamond-shaped arrows with dotted lines for non-CMY-producing isolates.

tive in the MALDI-TOF MS assay. Identification of proteins observed in SDS-PAGE at approximately 40,000 g/mol was performed by in-gel tryptic digestion followed by MALDI-TOF/TOF MS (24). The identification of the \sim 40,000-g/mol bands revealed multiple tryptic peptides, being fragments of CMY-2-like polypeptides, for all of the isolates that were positive in the MALDI-TOF MS assay (Table 2). Consistently, such peptides were not detected in extracts from the corresponding gel fragments for all the isolates that were negative by the MALDI-TOF MS assay. The absence of CMY-2-like tryptic peptides in the extracts of CMY

producers that were negative in the MALDI-TOF MS assay might be explained by a low concentration of CMY-2-like enzymes in the periplasmic extracts of the respective isolates. However, these results suggested that the presence of the \sim 39,850- m/z peak can be used as an indicator of the presence of the *C. freundii*-derived CMY-2-like group of acquired AmpC β -lactamases (10).

In the preliminary analysis of other AmpC-type β -lactamases, a ca. 39,670- m/z peak was observed in the mass spectra of the previously purified ACC-4 enzyme (theoretical relative molecular mass, 39,673 Da) and of the periplasmic extracts of the ACC-4-

TABLE 2 β -Lactamase peptides detected by in-gel tryptic and MALDI-TOF/TOF MS analysis

Observed m/z value	Expected m/z value	Calculated m/z value	ppm	Amino acid sequence ^a	Amino acid position ^b
930.4312	929.4239	929.4032	22.4	K-DYAWGYR-E	217–225
1,285.7499	1,284.7426	1,284.7150	21.5	K-TLQQGIALAQSR-Y	266–279
1,544.8279	1,543.8206	1,543.7895	20.1	K-SYPNPVVRVEAAWR-I	362–376
1,556.8695	1,555.8622	1,555.8318	19.6	-AAKTEQQIADIVNR-T	21–35
1,658.8035	1,657.7962	1,657.7518	26.8	R-WVQANMDASHVQEK-T	252–267
1,664.9054	1,663.8981	1,663.8682	18.0	K-LAHTWITVPQNEQK-D	203–218
1,827.1019	1,826.0946	1,826.0665	15.4	K-VALAALPAVEVNPAPAVK-A	310–330
2,081.1052	2,080.0979	2,080.0589	18.8	R-EGKPVHVSPGQLDAEAYGVK-S	224–245

^a Hyphens indicate tryptic restriction sites. Small capital letters correspond to amino acids found outside the restriction sites. Underlined residues were modified by oxidation.

^b CMY-2 peptide from *K. pneumoniae* HEL-1 (GenBank accession no. CAA62957) was used as a reference for the alignment of β -lactamase tryptic peptides.

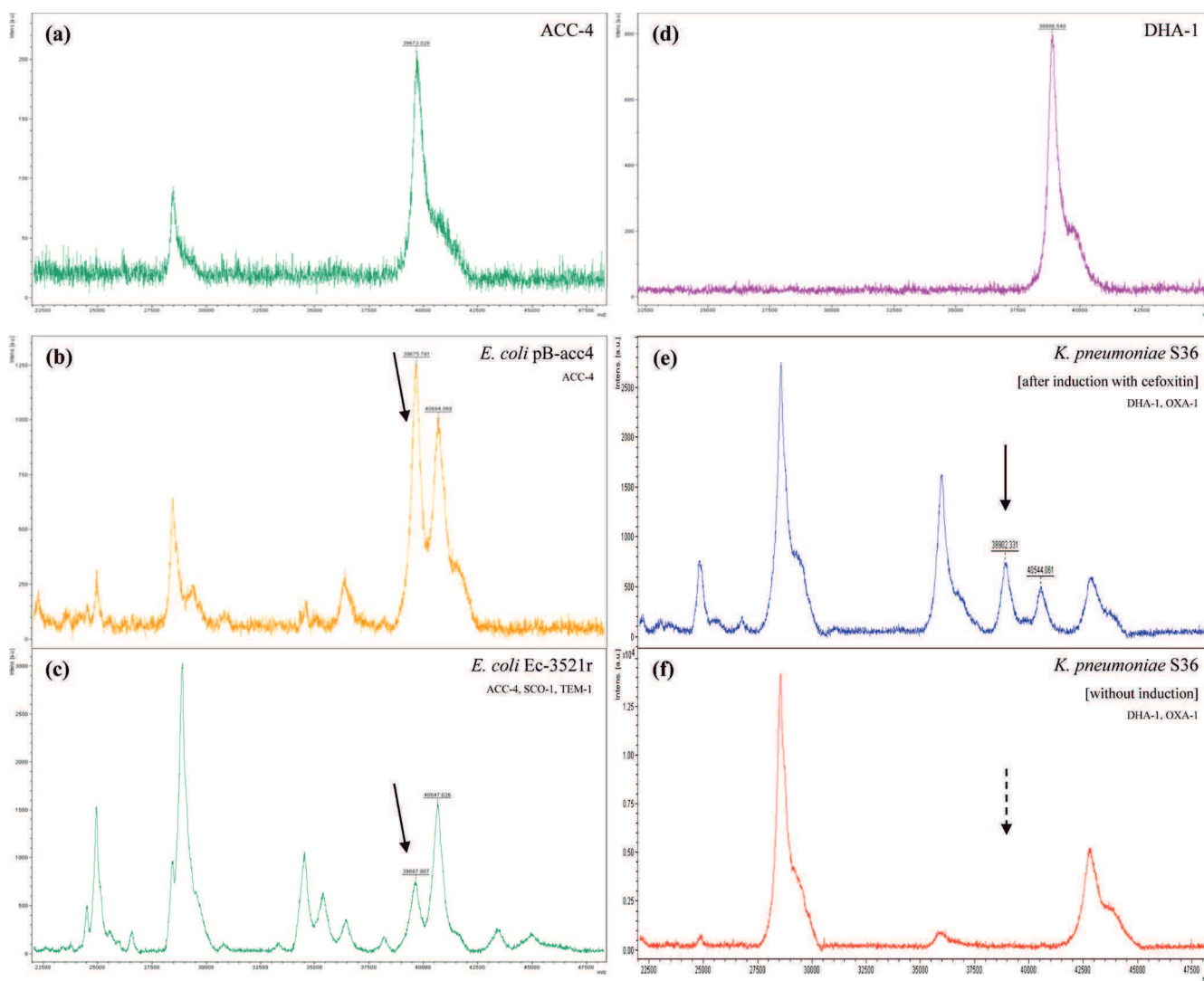


FIG 2 (a to c) Mass spectra of the purified ACC-4 enzyme (a) and the periplasmic extracts of ACC-producing *E. coli* pB-acc4 (b) and EC-3521r (c). (d to f) Mass spectra of the purified DHA-1 enzyme (d) and the periplasmic extracts of DHA-producing *K. pneumoniae* S36 after induction with cefoxitin (e) and without induction (f). Peaks corresponding to β -lactamases are indicated with arrows with solid lines. In the mass spectra of *K. pneumoniae* S36, the dotted arrow indicates the absence of the ca. 38,900- m/z peak, representing DHA-1 β -lactamase, in periplasmic extract prepared without adding cefoxitin in broth culture.

producing *E. coli* EC-3521r and pB-acc4/DH5 α strains (Fig. 2) (25). The MALDI-TOF MS measurement of the molecular mass of the purified DHA-1 β -lactamase detected a 38,887- m/z peak (theoretical relative molecular mass, 38,881 Da). In the DHA-1-producing isolate *K. pneumoniae* S36 strain (26) with the functional *ampC-ampR* system (10), a corresponding peak of ca. 38,900- m/z was observed but only when the AmpC production was induced by adding cefoxitin at 50 $\mu\text{g}/\text{ml}$ in broth cultures 3 h before harvesting the cells (Fig. 2). These data suggested that the assay can be used for the detection of other AmpC-type β -lactamases. Additionally, the observation of the 39,850- m/z , \sim 39,670- m/z , and \sim 38,900- m/z peaks for CMY-2-like, ACC-4, and DHA-1 enzymes, respectively, indicated that MALDI-TOF MS may discriminate the diverse groups of acquired AmpC-type cephalosporinases.

In this study, we showed for the first time that MALDI-TOF

MS has the potential to detect the most clinically important acquired AmpC β -lactamases, such as the CMY-2-like, ACC, and DHA types, in clinical isolates of *Enterobacteriaceae*. The described MALDI-TOF MS assay worked well with most of the CMY-producing isolates. However, the method performed poorly for *P. mirabilis*. It might be hypothesized that, in that case, increased production of a CMY-2-like enzyme upon gene duplication is important for the visualization of the \sim 39,850- m/z peak.

In agreement with previous studies illustrating that MALDI-TOF MS applications are quick and cheap procedures (3), the described protocol exhibits a 22-h turnaround time, which is comparable to that of molecular techniques only if considering PCR plus sequencing of the amplicon in order to identify the specific allelic variant of the β -lactamase gene. The use of classic PCR and real-time PCR (RT-PCR) assays in clinical settings is more expensive than the use of the described MALDI-TOF (not

considering the initial cost of investment for the equipment) but is less labor intensive and with a shorter turnaround time. Detection of β -lactamases by MALDI-TOF MS is a proteomic approach allowing the study of the behavior of the tested strains and should complement techniques already used for characterization of β -lactamases such as PCR and isoelectric focusing (IEF). The fact that MALDI-TOF MS can directly detect class A (9) and class C β -lactamases, as well as other mechanisms such as methylation of rRNA and cell wall components (3, 27), indicates the feasibility of establishing a MALDI-TOF supplementary database of resistance mechanisms that would promote research in this field. Notwithstanding the aforementioned problems, we strongly believe that proper modifications and validation of the described MALDI-TOF assay will easily lead to acceptance of its future application in diagnostic laboratories and reference centers.

ACKNOWLEDGMENTS

This work was supported by research project grants NT11032-6/2010 from the Ministry of Health of the Czech Republic and by the Charles University Research Fund (project number P36). C.C.P. was supported by the project. The establishment, development, and mobility of quality research teams at the Charles University, registration number CZ.1.07/2.3.00/30.0022, was financed by The Education for Competitiveness Operational Programme (ECOP) funded by the ESF and the government budget of the Czech Republic.

A patent application corresponding to this test has been sent on behalf of Charles University.

REFERENCES

- Seng P, Rolain JM, Fournier PE, La Scola B, Drancourt M, Raoult D. 2010. MALDI-TOF-mass spectrometry applications in clinical microbiology. *Future Microbiol.* 5:1733–1754. <http://dx.doi.org/10.2217/fmb.10.127>.
- Wieser A, Schneider L, Jung J, Schubert S. 2012. MALDI-TOF MS in microbiological diagnostics-identification of microorganisms and beyond (mini review). *Appl. Microbiol. Biotechnol.* 93:965–974. <http://dx.doi.org/10.1007/s00253-011-3783-4>.
- Hrabák J, Chudáková E, Walková R. 2013. Matrix-assisted laser desorption ionization-time of flight (MALDI-TOF) mass spectrometry for detection of antibiotic resistance mechanisms: from research to routine diagnosis. *Clin. Microbiol. Rev.* 26:103–114. <http://dx.doi.org/10.1128/CMR.00058-12>.
- Hrabák J, Walková R, Studentová V, Chudáková E, Bergerová T. 2011. Carbapenemase activity detection by matrix-assisted laser desorption ionization-time of flight mass spectrometry. *J. Clin. Microbiol.* 49:3222–3227. <http://dx.doi.org/10.1128/JCM.00984-11>.
- Burckhardt I, Zimmermann S. 2011. Using matrix-assisted laser desorption ionization-time of flight mass spectrometry to detect carbapenem resistance within 1 to 2.5 hours. *J. Clin. Microbiol.* 49:3321–3324. <http://dx.doi.org/10.1128/JCM.00287-11>.
- Kempf M, Bakour S, Flaudrops C, Berrazeg M, Brunnel JM, Drissi M, Mslí E, Touati A, Rolain JM. 2012. Rapid detection of carbapenem resistance in *Acinetobacter baumannii* using matrix-assisted laser desorption ionization-time of flight mass spectrometry. *PLoS One* 7:e31676. <http://dx.doi.org/10.1371/journal.pone.0031676>.
- Hrabák J, Studentová V, Walková R, Zemlicková H, Jakubu V, Chudáková E, Gniadkowski M, Pfeifer Y, Perry JD, Wilkinson K, Bergerová T. 2012. Detection of NDM-1, VIM-1, KPC, OXA-48, and OXA-162 carbapenemases by matrix-assisted laser desorption ionization-time of flight mass spectrometry. *J. Clin. Microbiol.* 50:2441–2443. <http://dx.doi.org/10.1128/JCM.01002-12>.
- Camara JE, Hays FA. 2007. Discrimination between wild-type and ampicillin-resistant *Escherichia coli* by matrix-assisted laser desorption/ionization time-of-flight mass spectrometry. *Anal. Bioanal. Chem.* 389:1633–1638. <http://dx.doi.org/10.1007/s00216-007-1558-7>.
- Schaumann R, Knoop N, Gnzel GH, Losensky K, Rosenkranz C, Stingu CS, Schellenberger W, Rodloff AC, Eschrich K. 2012. A step towards the discrimination of beta-lactamase-producing clinical isolates of Enterobacteriaceae and *Pseudomonas aeruginosa* by MALDI-TOF mass spectrometry. *Med. Sci. Monit.* 18:MT1–MT77. <http://dx.doi.org/10.12659/MSM.883339>.
- Jacoby GA. 2009. AmpC beta-lactamases. *Clin. Microbiol. Rev.* 22:161–182. <http://dx.doi.org/10.1128/CMR.00036-08>.
- Empel J, Baraniak A, Literacka E, Mrówka A, Fiett J, Sadowy E, Hryniewicz W, Gniadkowski M; Beta-PL Study Group. 2008. Molecular survey of beta-lactamases conferring resistance to newer beta-lactams in *Enterobacteriaceae* isolates from Polish hospitals. *Antimicrob. Agents Chemother.* 52:2449–2454. <http://dx.doi.org/10.1128/AAC.00043-08>.
- Pérez-Pérez FJ, Hanson ND. 2002. Detection of plasmid-mediated AmpC beta-lactamase genes in clinical isolates by using multiplex PCR. *J. Clin. Microbiol.* 40:2153–2162. <http://dx.doi.org/10.1128/JCM.40.6.2153-2162.2002>.
- Kotsakis SD, Papagiannitsis CC, Tzelepi EE, Tzouveleki LS, Miriagou V. 2009. Extended-spectrum properties of CMY-30, a Val211Gly mutant of CMY-2 cephalosporinase. *Antimicrob. Agents Chemother.* 53:3520–3523. <http://dx.doi.org/10.1128/AAC.00219-09>.
- Gazouli M, Tzouveleki LS, Prinarakis E, Miriagou V, Tzelepi E. 1996. Transferable cefoxitin resistance in enterobacteria from Greek hospitals and characterization of a plasmid-mediated group 1 beta-lactamase (LAT-2). *Antimicrob. Agents Chemother.* 40:1736–1740.
- Mavroidi A, Tzelepi E, Miriagou V, Gianneli D, Legakis NJ, Tzouveleki LS. 2002. CTX-M-3 beta-lactamase-producing *Escherichia coli* from Greece. *Microb. Drug Resist.* 8:35–37. <http://dx.doi.org/10.1089/10766290252913737>.
- Izdebski R, Baraniak A, Fiett J, Adler A, Kazma M, Salomon J, Lawrence C, Rossini A, Salvia A, Hryniewicz W, Brun-Buisson C, Carmeli Y, Gniadkowski M; MOSAR WP2 and WP5 Study Groups. 2013. Clonal structure, extended-spectrum β -lactamases, and acquired AmpC-type cephalosporinase of *Escherichia coli* populations colonizing patients in rehabilitation centers in four countries. *Antimicrob. Agents Chemother.* 57:309–316. <http://dx.doi.org/10.1128/AAC.01656-12>.
- Tzouveleki LS, Tzelepi E, Mentis AF. 1994. Nucleotide sequence of a plasmid-mediated cephalosporinase gene (*bla*_{LAT-1}) found in *Klebsiella pneumoniae*. *Antimicrob. Agents Chemother.* 38:2207–2209. <http://dx.doi.org/10.1128/AAC.38.9.2207>.
- Zioga A, Whichard JM, Kotsakis SD, Tzouveleki Tzelepi LS E, Miriagou V. 2009. CMY-31 and CMY-36 cephalosporinases encoded by ColE1-like plasmids. *Antimicrob. Agents Chemother.* 53:1256–1259. <http://dx.doi.org/10.1128/AAC.01284-08>.
- Baraniak A, Izdebski R, Fiett J, Sadowy E, Adler A, Kazma M, Salomon J, Lawrence C, Rossini A, Salvia A, Vidal Samsó J, Fierro J, Paul M, Lerman Y, Malhotra-Kumar S, Lammens C, Goossens H, Hryniewicz W, Brun-Buisson C, Carmeli Y, Gniadkowski M; MOSAR WP2 and WP5 Study Groups. 2013. Comparative population analysis of *Klebsiella pneumoniae* strains with extended-spectrum β -lactamases colonizing patients in rehabilitation centers in four countries. *Antimicrob. Agents Chemother.* 57:1992–1997. <http://dx.doi.org/10.1128/AAC.02571-12>.
- D'Andrea MM, Leteracka E, Zioga A, Giani T, Baraniak A, Fiett Sadowy JE, Tassios PT, Rossolini GM, Gniadkowski M, Miriagou V. 2011. Evolution and spread of a multidrug-resistant *Proteus mirabilis* clone with chromosomal AmpC-type cephalosporinase in Europe. *Antimicrob. Agents Chemother.* 55:2735–2742. <http://dx.doi.org/10.1128/AAC.01736-10>.
- Papagiannitsis CC, Miriagou V, Kotsakis SD, Tzelepi E, Vatopoulos AC, Petinaki E, Tzouveleki LS. 2012. Characterization of a transmissible plasmid encoding VEB-1 and VIM-1 in *Proteus mirabilis*. *Antimicrob. Agents Chemother.* 56:4024–4025. <http://dx.doi.org/10.1128/AAC.00470-12>.
- Naglak TJ, Wang HY. 1990. Recovery of a foreign protein from the periplasm of *Escherichia coli* by chemical permeabilization. *Enzyme Microb. Technol.* 12:603–611. [http://dx.doi.org/10.1016/0141-0229\(90\)90134-C](http://dx.doi.org/10.1016/0141-0229(90)90134-C).
- Kotsakis SD, Caselli E, Tzouveleki LS, Petinaki E, Prati F, Miriagou V. 2013. Interactions of oximino-substituted boronic acids and β -lactams with the CMY-2-derived extended-spectrum cephalosporinases CMY-30 and CMY-42. *Antimicrob. Agents Chemother.* 57:968–976. <http://dx.doi.org/10.1128/AAC.01620-12>.
- Mares J, Richtrova P, Hricinova A, Tuma Z, Moravec J, Jysak D, Matejovic M. 2010. Proteomic profiling of blood-dialyzer interactome reveals involvement of lectin complement pathway in hemodialysis-

- induced inflammatory response. *Proteomics Clin. Appl.* 4:829–838. <http://dx.doi.org/10.1002/prca.201000031>.
25. Papagiannitsis CC, Tzouveleki LS, Tzelepi E, Miriagou V. 2007. Plasmid encoded ACC-4, an extended-spectrum cephalosporinase variant from *Escherichia coli*. *Antimicrob. Agents Chemother.* 51:3763–3767. <http://dx.doi.org/10.1128/AAC.00389-07>.
26. Empel J, Hrabak J, Kozinska A, Bergerova T, Ubraskova P, Kern-
Zdanowicz I, Gniadkowski M. 2010. DHA-1-producing *Klebsiella pneumoniae* in a teaching hospital in the Czech Republic. *Microb. Drug Resist.* 16:291–295. <http://dx.doi.org/10.1089/mdr.2010.0030>.
27. Cai JC, Hu YY, Zhang R, Zhou HW, Chen GX. 2012. Detection of OMPK36 protein loss in *Klebsiella* spp. by matrix-assisted laser desorption ionization-time of flight mass spectrometry. *J. Clin. Microbiol.* 50:2179–2182. <http://dx.doi.org/10.1128/JCM.00503-12>.